

FINAL DEGREE THESIS

Bachelor's Degree in Mechanical Engineering

ESTUDIO Y DESARROLLO DE UN CUADRO DE DESCENSO

STUDY AND DEVELOPEMENT OF A DOWNHILL BICYCLE FRAME



Memory – Budget – Annexes

Author:	David Rey Escamilla
Supervisor:	Domingo Santos Espada
Department	FAB
Call:	2022, January

ABSTRACT

The objective of the present project is to study the development process of a downhill bicycle frame. The different stages involved are presented and then analysed in the course of the project. Material to use, a fundamental decision for the design because of its influence in resistance, durability, rigidity, and weight of the frame, is evaluated and different alternatives are balanced. Such fundamental aspect as geometry and suspension kinematics are discussed, as well as the procedure and tools used to define them. Design and development of a virtual model and testing as per ISO 4210, regarding safety requirement for bicycles, using a simulation method by finite elements is also covered in the following. Test reports on compliance with this standard have been issued, as well as a test sheet summarising the simulation results. An economic analysis of the costs involved to complete the project has also been conducted, concluding the cost for the manufacturing of a real prototype, as initially planned, is prohibitive. Nevertheless, all steps and considerations for prototyping have been considered and collected in this project.

Additionally, sustainability of current tendencies in the bicycle industry is analysed, and some alternatives are presented to reduce its environmental impact.

RESUMEN

El objetivo del presente proyecto es estudiar el proceso de desarrollo de un cuadro de bicicleta de descenso. Se presentan y se analizan a lo largo del proyecto las diferentes etapas. Se evalúa el material a utilizar, una decisión fundamental para el diseño, por su influencia en la resistencia, durabilidad, rigidez y peso del cuadro, y se sopesan diferentes alternativas. Se discuten aspectos tan fundamentales como la geometría y la cinemática de la suspensión, así como el procedimiento y las herramientas utilizadas para su definición. También se aborda el diseño y desarrollo de un modelo virtual y la realización de ensayos según la norma ISO 4210, relativa a los requisitos de seguridad para bicicletas, utilizando un método de simulación por elementos finitos. Se han emitido informes de ensayo sobre el cumplimiento de esta norma, así como una hoja de ensayo en la que se resumen los resultados de la simulación. También se ha realizado un análisis económico de los costes para llevar a cabo el proyecto, concluyendo que el coste para la fabricación de un prototipo real, tal y como estaba previsto inicialmente, es prohibitivo. No obstante, en este proyecto se han tenido en cuenta y recogido todos los pasos y consideraciones para la creación de un prototipo.

Además, se analiza la sostenibilidad de las tendencias actuales en la industria de la bicicleta, y se presentan algunas alternativas para reducir su impacto medioambiental.

RESUM

L'objectiu del present projecte és estudiar el procés de desenvolupament d'un quadre de bicicleta de descens. Es presenten i s'analitzen al llarg del projecte les diferents etapes. S'avalua el material a utilitzar, una decisió fonamental per al disseny, per la seva influència en la resistència, durabilitat, rigidesa i pes del quadre, i se sospesen diferents alternatives. Es discuteixen aspectes tan fonamentals com la geometria i la cinemàtica de la suspensió, així com el procediment i les eines utilitzades per a la seva definició. També s'aborda el disseny i desenvolupament d'un model virtual i la realització d'assajos segons la norma ISO 4210, relativa als requisits de seguretat per a bicicletes, utilitzant un mètode de simulació per elements finits. S'han emès informes d'assaig sobre el compliment d'aquesta norma, així com una fulla d'assaig en la qual es resumeixen els resultats de la simulació. També s'ha realitzat una anàlisi econòmica dels costos per a dur a terme el projecte, conclouent que el cost per a la fabricació d'un prototip real, tal com estava previst inicialment, és prohibitiu. No obstant això, en aquest projecte s'han tingut en compte i recollit tots els passos i consideracions per a la creació d'un prototip.

A més, s'analitza la sostenibilitat de les tendències actuals en la indústria de la bicicleta, i es presenten algunes alternatives per a reduir el seu impacte mediambiental.

ACKNOWLEDGEMENTS

I would like to acknowledge the help provided by Mr. Marc Urgell, whose support in the management of the intend of fabrication of a prototype has been greatly appreciated. For this, and for all the ideas and advice given in the process, thank you very much.

GLOSSARY

<u>Term:</u>	<u>Definition:</u>
<i>Reach</i>	<i>Horizontal distance from a vertical line that runs through the centre of the bottom bracket to the centre of the head tube.</i>
<i>Stack</i>	<i>Vertical distance from a vertical line that runs through the centre of the bottom bracket to the centre of the head tube.</i>
<i>Chainstay length</i>	<i>Horizontal distance from a vertical line that runs through the centre of the bottom bracket to the rear axle.</i>
<i>Wheelbase</i>	<i>Horizontal distance between front and rear axle.</i>
<i>Headtube angle</i>	<i>Angle of the steerer tube of the fork respect to a horizontal line.</i>
<i>Seat tube length</i>	<i>Distance between the centre of the bottom bracket and the centre top of the seat tube.</i>
<i>Seat tube angle</i>	<i>Effective angle of a line passing through the centre of bottom bracket and centre top of the seat tube respect to a horizontal line.</i>
<i>Instant centre</i>	<i>Point with instantaneous velocity equal to zero all moving parts rotate towards to.</i>
<i>Centre of curvature</i>	<i>centre of a circle passing through a curve at a given point which has the same instantaneous tangent and curvature.</i>
<i>Anti-squat</i>	<i>Measure of suspension independence from acceleration and chain forces.</i>
<i>Anti-rise</i>	<i>Measure of suspension independence from deceleration and braking forces.</i>
<i>CAD</i>	<i>Acronym for Computer Aided Design</i>
<i>CAE</i>	<i>Acronym for Computer Aided Engineering</i>

INDEX

ABSTRACT.....	2
RESUMEN	3
RESUM.....	4
ACKNOWLEDGEMENTS.....	5
GLOSARY	6
PREFACE	10
MOTIVATION.....	10
HISTORY	10
STATE OF THE ART.....	10
1. INTRODUCTION.....	13
1.1. OBJECTIVE	14
1.1.1. GENERAL CONSTRUCTIVE OBJECTIVES	14
1.1.2. PERFORMANCE OBJECTIVES	15
1.2. SCOPE.....	16
2. RESEARCH.....	17
2.1. INTERVIEW	17
2.2. APPLICABLE STANDARDS AND REGULATIONS	17
3. MATERIAL.....	19
3.1. MATERIAL OPTIONS	19
3.1.1. ALUMINIUM	19
3.1.2. STEEL	20
3.1.3. TITANIUM.....	21
3.1.4. CARBON FIBRE.....	22
3.2. MATERIAL CHOICE.....	24
4. GEOMETRY	25
4.1. INTRODUCTION TO BICYCLE GEOMETRY	25
4.2. DISCUSION OF GENERAL GEOMETRY.....	25
4.2.1. WHEEL SIZE	25
4.2.2. REACH	26
4.2.3. STACK	26
4.2.4. CHAINSTAY LENGTH	26
4.2.5. HEAD TUBE ANGLE	26
4.2.6. WHEELBASE.....	26
4.2.7. SEAT TUBE ANGLE	27

4.2.8.	SEAT TUBE LENGTH	27
4.3.	FINAL GEOMETRY	27
5.	KINEMATICS	28
5.1.	INTRODUCTION TO SUSPENSION KINEMATICS.....	28
5.2.	SUSPENSION SYSTEMS.....	28
5.2.1.	SINGLE PIVOT	28
5.2.2.	LINKAGE DRIVEN SINGLE PIVOT	28
5.2.3.	HORST-LINK	29
5.2.4.	TWIN-LINK	29
5.2.5.	SIX-BAR.....	30
5.3.	DISCUSION OF SUSPENSION SYSTEM CHOICE	30
5.4.	DISCUSION OF KINEMATICS	30
5.4.1.	INSTANT CENTRE.....	30
5.4.2.	CENTRE OF CURVATURE.....	32
5.4.3.	CHAIN GROWTH.....	32
5.4.4.	PEDAL KICKBACK	33
5.4.5.	ANTI-SQUAT	34
5.4.6.	ANTI-RISE.....	35
5.4.7.	AXLE PATH.....	37
5.4.8.	LEVERAGE RATIO.....	38
6.	COMPUTER AIDED DESIGN	43
6.1.	INTRODUCTION.....	43
6.2.	TWO-DIMENSIONAL MODEL.....	43
6.3.	THREE-DIMENSIONAL MODEL	49
6.3.1.	VERSION No.1.....	50
6.3.2.	VERSION No.2.....	56
6.3.3.	VERSION No.3.....	60
6.3.4.	VERSION No.4.....	63
7.	COMPUTER AIDED ENGINEERING	65
7.1.	CALCULATION MODEL.....	65
7.1.1.	TWO-DIMENSIONAL ANALYSIS	65
7.1.2.	THREE-DIMENSIONAL ANALYSIS	68
7.2.	SIMULATION METHOD.....	70
7.2.1.	STATIC ANALYSIS	71
7.2.2.	FATIGUE ANALYSIS.....	77
8.	PROTOTYPE MANUFACTURING	79

8.1. PROCESSING OF BASE MATERIAL.....	79
8.2. WELDING.....	79
8.3. ASSEMBLY	79
9. ENVIRONMENTAL IMPACT.....	81
CONCLUSION.....	84
BUDGET	85
SOFTWARE	85
PROTOTYPING	85
COMPONENTS.....	86
WORKING TIME.....	87
BIBLIOGRAPHY	88
ANNEX I: INTERVIEW TRANSCRIPTION	90
ANNEX II: MATERIAL SHEET	95
ANNEX III: ANALYTICAL EVALUATION OF CHAIN AND BRAKE FORCES INFLUENCE ON PERFORMANCE REAR SUSPENSION SYSTEMS	104
ANNEX IV: TEST REPORTS	109
ANNEX V: TEST SHEET	125
ANNEX VI: CALCULUS SHEET.....	175
ANNEX VII: DIMENSIONAL DRAWINGS	183

PREFACE

MOTIVATION

Having almost completed superior studies in mechanical engineering, for the final degree project the aim was to apply all the knowledge acquired in this period to an area of interest. For this, the most technical side of the own preferred ludic activity has decided to be the object of the project, which makes it a very personal work, boarding an area of interest and giving a deeper insight in the engineering behind the development of a downhill bicycle frame. This has been a great opportunity to get to know the stages, tools, and organisation involved in this particular process.

HISTORY

Mountain biking can be so considered a very young sport, having its origins in the mid last century. This was with the discipline cyclocross, which was used as a way of keeping fit in the winter season for road racers, and it was not until 1940 that the *Union Cycliste Internationale* (UCI) started its regulation making this a separate sport, and organising the first world championship in 1950, held in Paris.

However, it was in the 1970's decade that mountain biking and downhill as we know it nowadays had its origins, which can be attributed to different groups of riders from the United States of America, where old cruiser bicycles with drum or coaster brakes and wider tyres installed where ridden down fire roads and mountain trails. The first ever downhill race is deemed to have taken place in Fairfax, California, on October 21 of 1976 down a fire road known as *Repack Road*, this name is derivate from the necessity to repack the hub brakes after every run, which were filled with grease to prevent brake seizure, during intense use, the lubricant was overheated and drained, thus the assemblies had to be regreased.

Those adapted bicycles for all terrain use were known as *clunkers* and were the predecessors to the first purpose-built mountain bikes, the first of which was created in 1977 by frame manufacturer Joe Breeze. Tom Ritchey followed him in 1978, whom later would proportionate frames to businessman Charlie Kelly and cyclist Gary Fisher. In their frames, Kelly and Fisher would mount cyclocross and motorbike components and sold them through their company *MountainBikes*. In 1981 the first 125 exemplars of the *Specialized Stumpjumper* were sold only six days after being launched on the market, this model was revolutionary for bringing mountain biking to the masses, with a frame manufactured in Japan with TIG welding, a much more suitable technique for serial production than fillet-brazing, used for the handmade American frames. The *Stumpjumper* was completed with components from various disciplines due to the lack of specific ones for a sport that did not have even a name yet.

In the following years the mountain bicycle industry kept evolving, and downhill was definitively established in 1990 with its inclusion in the first ever UCI Mountain Bike Championship, held in Durango, Colorado. In this decade, purpose specific bicycles for this discipline started appearing, with innovations such as dual crown forks or disk brakes, standard to any current downhill bike.

STATE OF THE ART

Modern downhill bikes have come a long way from those early slightly modified cruiser bicycles to performance focused machines, for which every aspect in their design has been evolved and perfected for this purpose.

Use of materials for the construction of the frames has permitted great advancements for this type of bicycles. Steel, initially the standard option, was gradually replaced by the use of high resistance aluminium alloys and carbon fibre composites. Geometry of the tubes also play an important role when it comes to specific strength of a frame, some brands experimented with the use of diverse

section tubes which has evolved to variable section designs and the application of new manufacturing techniques, such as hydroformed aluminium tubes or Resin Transfer Moulding (RTM) for composite frames. These tendencies have helped to increase resistance of modern downhill bicycles while optimising weight. Currently, the peak for materials innovation could be deemed to be the method *Atherton Bikes* use to build their frames, which have a carbon fibre tubular design, joined with 3D printed titanium pieces.

Evolution of geometry has helped to push the sport forward making downhill bikes more capable. Wheel size has grown from the initial 26" standard, to 27.5", and finally 29" (which were used later than the 27.5 option, even being prior to this), being a mixed wheel size setup, with a 29" wheel in the front and 27.5" in the rear the most common configuration in World Cup races, at the moment. Geometry has also suffered great changes in conception from the first high and short designs, for good ground clearance and manoeuvrability, to the current trend of longer, lower, and slacker bicycles, for increased stability and control, pushed by brands like *Mondraker*, with their *forward geometry* concept. Changes in this direction have involved the increase of reach and wheelbase, and slackening of the headtube angle, for a more stable platform, while shortening the chainstay and stems used, to increase manoeuvrability and control.

Suspension is another area where great improvement has been made. Telescopic forks have always been, and still are the dominant option, the currently standard dual crown configuration was first seen in 1996 with the apparition of the first *RockShox Boxxer* prototype, featuring 150 millimetres of travel and 32 millimetres of diameter stanchions, this numbers have grown up to current standard 200 millimetres of travel, and up to 40 millimetres for stanchions diameter, even though there have been forks with up to 300 millimetres of travel, like the *Marzocchi Super monster*, these have never really succeeded. Improvements for the forks have been made mainly in sensibility and adjustability, being high and low speed for compression and rebound adjustments common to any high-end fork in the market. For rear suspension systems, there has also been a great improvement, overall, in the study of kinematics of the frames. Even though four bar systems, still very extended nowadays, were yet used in the first developments of rear suspension systems (see the *Gary Fisher RS-1*, from 1991), research for better control of the suspension characteristics, mainly the leverage ratio, has been performed, and there is a tendency of increase in complexity in suspension linkages, as every day six-bar systems are more common in production models.

In general, mountain bike specific components have been developed and improved during the evolution of the sport. Axels have changed significantly in this period, from 9 mm quick release system to different standards thru axles, being the current standard for downhill the *Superboost*, with a dimension (length per diameter) of 110x20 mm in the front and 157x12 mm in the rear. For brakes there have also been different options along history, finding coaster and drum brakes in the first mountain bikes, then cantilever style brakes actuating on the rim, and finally disk brakes, first mechanically actuated, and currently hydraulic actuated, with most common rotor sizes of 200 mm and 220 mm for downhill application. Transmission, unlike for other disciplines where great technical advances have been made, has evolved to be quite minimalistic, leading to standard one-by-seven speeds setups, as not many gears are required for this application. And for what components are concerned, the best improvement has arguably been in tyres, not only they have become wider (which has also required a major inner width for rims), being the most common sizes between 2.4 to 2.6 inches, which is the most obvious change, but there have been great improvements in casing (this is internal structure of the tyre), tyre tread pattern, and more importantly the compounds used, overall, this advancements have largely improved tyres performance and grip. With time, bicycle tyres have also gained the ability to install a tubeless setup, which has become increasingly popular.

Now, looking ahead to the future, electronics are deemed to be the next great revolution in mountain biking. While in other disciplines this has already underway, with the growth of electric mountain bikes market, the use of electronic transmissions, the recent apparition of electronically controlled suspension and some proposals for Anti-lock Brake Systems, for downhill mountain bicycles this has not arrived yet, at least to the general market. But observing this tendency, and the apparition of some suspiciously covered prototype shocks in World Cup races in the past years, it is not far-fetched to imagine some electronic suspension products might be in development. Letting debates about if this could take some part of the fun or skill required for the practise of this sport, the truth is that progress is already leading the mountain bike industry, and it is a matter of time it can be implemented in downhill bicycles. Notwithstanding nowadays these systems are not efficient enough, or even unable to bring any real benefit for this discipline, improvements in the use of this technology could led to a revolution in the conception and design of the frames, not only they will have to be compatible with these systems and provide space for extra hardware, which is the logical way of implementation for extra protection, but considerations on new possibilities shall be made, as this opens the door to a wide improvement for geometry and suspension design.

1. INTRODUCTION

The object of this project is to design a downhill specific double suspension bicycle frame. This process consists of different phases in which all the frame characteristics will be studied and defined.

Initially, the general geometry will be set to have a basis from which to start. All the important points will be given their coordinates to a reference point and doing so the main dimensions that define geometry will be defined. Having that, some different suspension systems will be discussed, deciding after that which one is the most suitable for the objectives of the project regarding their kinematics.

After having decided one option, an intensive kinematics study shall be done to define its final characteristics and adjust them to optimise its behaviour. With this study completed the geometry will be completely defined, with all the general dimensions established in the first phase and all the pivot points positions in the second one.

With that information it is enough to start with the next stage, the development of a 3D model using Computer Aided Design tools. The first utility of this model will be to transfer all the two dimensions points into a three-dimensional space, where it will be possible to study the constructive viability of the model, making sure there are no interference between the different parts in all the range of movement. Then modelling all the components that could also interfere with the frame parts will permit to study their compatibility, assembling them in the frame model and studying their movement and interactions.

Having that preliminary CAD model, the next step would be the Computer Aided Engineering stage, where the design shall be put under test by studying its resistance and durability. First of all, strength must be guaranteed, so the tensions generated when applying the forces that the frame shall withstand should not be high enough to produce a failure or even plastic deformation in any point. Apart from that, a study shall be carried out to evaluate durability of all elements susceptible to fatigue failure, for example axles and bearings, in order to choose them properly.

Those two last phases might have to be reciprocal, as maybe the CAE study concludes a change in dimensions is needed, those the CAD model shall be modified and analysed again and vice versa.

Once finalised and validated the computer 3D model, prototyping can start. This consists of the manufacturing of a real version of the frame, constructed by welding together sections of different standard profiles and machined parts. With the frame built, the full bicycle is put together by adding all the components, selected from specific manufacturers, those are: headset, suspension (fork and shock), cockpit, which includes stem, handlebar and grips, bottom bracket, transmission, brakes, those the discs, callipers, levers and housing, wheels and seat post and saddle.

1.1. OBJECTIVE

1.1.1. GENERAL CONSTRUCTIVE OBJECTIVES

The objective of this project is to create a custom-made downhill bicycle frame, adjusted to own likings and personal preferences. This implies that most of the design decisions made have a purely subjective justification, and do not necessarily be intended to improve performance in a unidirectional plane, for example, always looking for the fastest possible design optimisation. This gives a lot of freedom when designing the whole bike, as there is no need to sacrifice any other characteristic just for a minimum improvement in a unique specific feature. All decisions, however, will be justified and supported by calculus when applicable.

It is fundamentally important for the optimization of the design to categorize the relevance of all the aspects that may have an influence on it, as there will always be a compromise between some of them, so it is necessary to know which ones should be prioritized over the others.

For being a downhill specific bike, the most important aspect would be suspension performance, a correct support must be guaranteed (either in fast rough terrain, with several repeated impacts or in a single big hit situation, for example in the reception of a drop). Suspension independence of the braking forces has also to be considered, which is very important in this discipline as many situations (a vertical technical section, for example) will require a good performance of the suspension system under heavy braking. It will not be so important, however, the pedal efficiency, although it will be also taken into account because it may be necessary in some specific sections, especially in a race scenario, and this is affected by the same forces that influence pumping, a technique to gain speed by compressing the suspension.

Resistance and durability will also be a main concern because of the abuse a downhill bike suffers, and it may need to be overbuilt to resist situations out of normal use, as it could be a harsh landing or hard hits that may happen in a crash. The frame has to offer, however, a certain degree of compliance, as if it is way too stiff it may not be predictable enough, and traction could be abruptly compromised in certain situations.

Simplicity will be a well appreciated feature and will be weighed against suspension performance. The more complex a suspension system is, the most control of the kinematics through the travel can be achieved, but due to the high level of maintenance this kind of bikes requires, a very complex design with a lot of links, and therefor bearings and axles, would result in a great cost in the long term and a higher probability of failure in any element of the linkage. A good balance shall be found between these characteristics.

Finally, weight will not be a great concern, unlike in other disciplines. It is undeniable that the lighter the bike, the better for dealing with the least amount of inertia under heavy accelerations, for example, in a fast change of direction. A lighter bicycle is also easier to jump and manoeuvre in the air. However, to improve the control it is not so important the total weight but its distribution, for better handling, the bike centre of gravity must be as close as practicable to the bottom bracket, which is the lowest part of the frame and the nearest to the contact point with the foot, this means the weight will be directly controlled by the legs, which is the strongest part of the body. Notwithstanding this, the weight of the bicycle shall be within reasonable limits and when not strongly compromising other more relevant aspects, an attempt to reduce weight shall be made.

1.1.2. PERFORMANCE OBJECTIVES

Once defined the most relevant general characteristics for the kind of bike it is, some desirable traits for the intended use can be established depending on the desired behaviour when ridding in different situations.

Freeride bikes tend to be shorter and more agile, with a very progressive suspension system to make them easy to get to the air. In the other hand, more race-oriented bikes are longer for more stability, with a more linear suspension design for more predictability when going fast in rough terrain.

The intended use will mainly be for bike park laps, where a wide range of terrain and situations can be found, from blue flow trails all the way to double black technical tracks. The chosen design should be, far from being a purpose-built bike, quite polyvalent. The most consistent option to get this is to keep a neutral geometry, long enough to keep up speed in difficult terrain, but not falling in the excessive longer, lower, slacker trend set for nowadays market. Kinematics shall go in the same line, offering a reasonable degree of progressivity for having a supple initial part of the travel, a supportive middle stroke and a not easy to bottom out final part of the travel, but not so progressive that the force to compress it will ramp up so much that there's very little usable travel.

1.2. SCOPE

The phases of the project will be as described in the introduction, so the final scope is to manufacture a first prototype, which shall be rideable and serve as a test mule.

This however would be an early prototype, and in a project with the scope of getting a product into the market shall require further testing, as due to the complexity of the process of welding it is difficult to study all potential failure spots with a simulation. Apart from that, testing in the real world will help to improve kinematics and optimize the design in some relevant features such as weight distribution of the frame or less important details, like cable routing.

After that phase, testing with other materials more difficult to work with may start. This, for example, is very common in carbon fibre frames, as the fabrication of the moulds required is very expensive and prototyping directly with carbon fibre is not viable. In those cases, alloy frames are built instead for testing.

Then, every stage of the project will have its own scope, for general geometry it will be to define the main dimensions of the bicycle. In the kinematic analysis, a suspension system that fulfils the requirements set in the objective will be chosen and the characteristics of the suspension will be defined, in accordance with specifications for the behaviour and ride quality that is expected from the bike. With the use of CAD tools, a 3D model with complete geometry to ensure compatibility between all the parts shall be created, and then studied using CAE to guarantee resistance and durability of the frame. Finally, the scope of prototyping will be to create a physical version of the frame for testing and extracting some conclusions about the decisions taken along the design process.

2. RESEARCH

2.1. INTERVIEW

Any product design process is a very complex task that shall be correctly organised and planned. It is fundamental for this purpose to get to know all the project stages, what is necessary to cover all the aspects involved and how to correctly execute every part. With the aim to better cognize the specifics of a bicycle development process, an interview to a professional in the sector has been performed.

In this conversation, general aspects of the design process have been discussed. To start with, every stage has been defined and briefly explained, detailing all the activities to be carried out in each of them. Organization inside the design team and interaction with other departments has also been consulted to determine tasks and responsibilities of each group. Finally, more concrete doubts found during own research regarding the different phases have been solved by treating those details more in depth.

All relevant information for what this project is concerned has been included in the transcription (see annex I), nevertheless some parts of the interview have been omitted because of confidentiality reasons.

2.2. APPLICABLE STANDARDS AND REGULATIONS

The applicable regulation to the object of this project is the standard UNE-EN ISO 4210, regarding safety requirements for bicycles. The ISO 4210 standard, in which this regulation is based on, has been approved as a European standard by the CEN (European Committee for Standardization) and has been adopted as a national regulation by the publication of a text with no changes to the original versions by the national standardization authority, which in the case of Spain is AENOR (Spanish Association for Standardisation). Thus, the ISO 4210, EN ISO 4210, and UNE-EN ISO 4210 standards are deemed to be equivalent in content.

The scope of this regulation are young adult bicycles with maximum saddle height of 635 mm or more and less than 750 mm, city and trekking bicycles, mountain bicycles, and racing bicycles that have a maximum saddle height of 635 mm or more including folding bicycles. Thus, it applies to the object of this project, an adult downhill bike, which is a type of mountain bike with a maximum saddle height of 635 mm or more.

This ISO standard is divided in different parts regarding bicycles, its components, and sub-assemblies. In the case of a bicycle frame, are specifically applicable the following:

- ISO 4210-1:2014 – Terms and definitions
- ISO 4210-2:2015 – Requirements for young adult city and trekking bicycles, mountain bicycles and racing bicycles
- ISO 4210-3:2014 – Common test methods
- ISO 4210-6:2014 – Frame and fork test methods

It is important to note that these standards only cover security of bicycles, without consideration of aspects like weight limits, dimensions, or technical innovation. If the model is used in a competition it shall comply with its specific regulations and requirements (i.e., UCI accreditation).

For granting compliance with this standard a simulation method has been used. This is not considered in the standard itself, so no test procedure per simulation is stated. For being a self-certification process, thus any method for granting compliance can be used if it is correctly justified, and due to the lack of any standard on simulation in the industry, a procedure based on own criteria has been

used. The simulation has been based on a finite element analysis of an assembly of the frame as it would be physically built, with the pertinent union axles and bearings for granting a correct load transfer among different parts. Restrictions have been imposed to imitate as far as possible the layout described for every test, also granting equilibrium of the model in any scenario. The different parts of the frame have been tested independently to better evaluate possible inaccuracies of the main model. Application of forces as described in the standard assure all values for forces and its positioning are within tolerances laid and rigidity requirements for false components used in the test are deemed to be satisfied.

Test reports on compliance with the mentioned applicable parts of the ISO 4210 standard have been issued, as well as a test-sheet with detailed information on test procedure according to ISO 4210-6:2014 (see annexes IV and V).

3. MATERIAL

Material choice is very important for the whole design process because this decision has a great impact on the subsequent stages. This characteristic will not have only an impact on physical attributes of the frame but also in aspects such as the decision of the manufacturing process and final looks and finishing of the bicycle.

Characteristic physical properties of materials will be determinant for some traits. Density, on one hand, will determine the mass of the frame that shall be designed to be built with resistant enough sections for its purpose. On the other hand, yield strength will have an influence on minimum cross-section of every part of the frame. Combination of these two characteristics, not taking into account geometric considerations independent of the material to use, will determine a resistance to weight ratio, which shall be optimised to get enough strength of the frame with the minimum possible mass. Besides its impact on resistance, the characteristic stress-strain curve of the material and thickness chosen will also have an impact on ride quality, as the frame should be rigid enough to properly withstand loads, offering a good control, but also adequately compliant to admit minimum deformation for enough predictability in a traction breaking situation.

Attributes that make the materials more favourable towards different manufacturing processes, like machinability, ease of weldability, or the complexity of the moulds to be used, if any, may favour the use of a certain material over others. The ease of manipulation of raw material, or the nature of the manufacturing method itself, will admit more or less design features modifications like section variation of the frame tubes, or the finishing of union points between them. Finally, if the material is more prone to the use of moulds, this will mean a very good adaptability of the model to any design, including aesthetics of the frame, permitting for more complex lines and shapes.

Then some considerations shall be made for durability, as some materials are more prone to fatigue breaking, which might imply additional work for the design of stress concentration points or, depending on use, it shall be taken into account that some materials may be more suitable in more aggressive disciplines because of behaviour in an impact scenario. This may differ much from one material to another, as it can do consequences of said success, from minimal plastic deformation, usually seen in metals, to a potentially catastrophic failure, as it might happen in a composite frame. In this line, reparability is another important point to be contemplated. First of all, detection of potential failure points only with visual inspection is a great plus to facilitate the safety check that shall be periodically made on downhill bicycles. Then, in the event of finding a crack, some materials will permit an easier repair or a wider margin in which that failure can be or not critical for the frame integrity.

3.1. MATERIAL OPTIONS

For bicycle frame construction many materials with very different characteristics may be used, from metals to organic resources, passing through polymers and composites. The most usually used are listed and briefly discussed in the following.

3.1.1. ALUMINIUM

Aluminium is very widely used for bicycle frames construction, is commonly seen in entry level models for being cheaper than other options like carbon fibre but lighter than, for example, steel. Aluminium has also seen an increase of use in the most aggressive disciplines of mountain biking in the past years after popularisation of the use of composites, especially in downhill, as for freeride it has never been disused at all. The reason for the commitment to the use of this material may lie in its reasonable strength, considering its very low density, combined with good stiffness, and the fact it offers a good

behaviour on impacts, as for being a metal it can withstand plastic deformation before failing. Another benefit of this material is its resistance to corrosion, as when in contact with oxygen a hard film of alumina is created, protecting the rest of the material from oxidation.

Many manufacturing processes can be used with aluminium, but the most commonly used are laminating and hydroforming, which consists in the forming of tubes by permanent deformation with the use of a mould and the application of hydraulic pressure, whereas solid parts are easily machinable because of being a soft material. Weldability of this material is inferior to other metals, mainly because of the need of adding alloying agents to improve mechanical properties of pure aluminium. These properties can also be modified with cold work processes or many different heat treatments.

6061-T6 aluminium alloy is the most commonly used for bicycle frames construction, this numeration, *6061*, indicates this is an alloy containing magnesium and silicon as its main alloying elements, remarkable traits of this are its high weldability and corrosion resistance. The alphanumeric suffix *T6* indicates this alloy has been solution tempered and artificially aged, this provides the most precipitation hardening thus the highest yield strength for this aluminium alloy.



Figure 1: Aluminium bicycle frame (Source: pinkbike.com)

3.1.2. STEEL

Although this material has been very popular for frame construction in bicycle history, it has gradually fallen in disuse in favour of lighter and more flexible options when it comes to manufacturing methods. Steel is one of the strongest materials that can be used for this purpose, due to this characteristic, the section of the tubes can be so reduced to provide for a light enough frame. Steel's ductility is a valuable property as this characteristic can improve the ride comfort offering small bump damping and more compliance than aluminium. Downsides of this options are it is very susceptible to corrosion, so protective coats are needed for these frames, and they require periodic inspection to avoid local corrosion due to chips in the paint caused by little impacts, it is usually a more expensive option than aluminium because it is more difficult to process, and the beforementioned weight disadvantage.

Many processes can be used to create steel profiles, the above-mentioned hydroforming technique can be applied to steel sheets, but it is not so common owing the high cost of the moulds needed, which usually cannot be compensated by the production of a high volume of pieces because this

material is most commonly used for short series. This makes the most commonly used tubes are standard profiles obtained by hot rolling, that usually shall be reinforced with extra material in order to optimise weight considering the impossibility of getting variable section tubes. This gives steel mountain bikes a very particular look.

Usually, two types of steel are used for bicycle frame construction. High-tensile carbon steel is the cheaper option for a long-lasting product, but usually higher tech chrome molybdenum alloys are used because of its higher tensile strength, which permits to reduce frame section, thus final weight while maintaining its resistance. The most commonly used of those alloys is the 4130, these steel series present good weldability, and are much stronger and harder than standard 1020 steel, so the strength to weight ratio is much higher than the achievable with that option.

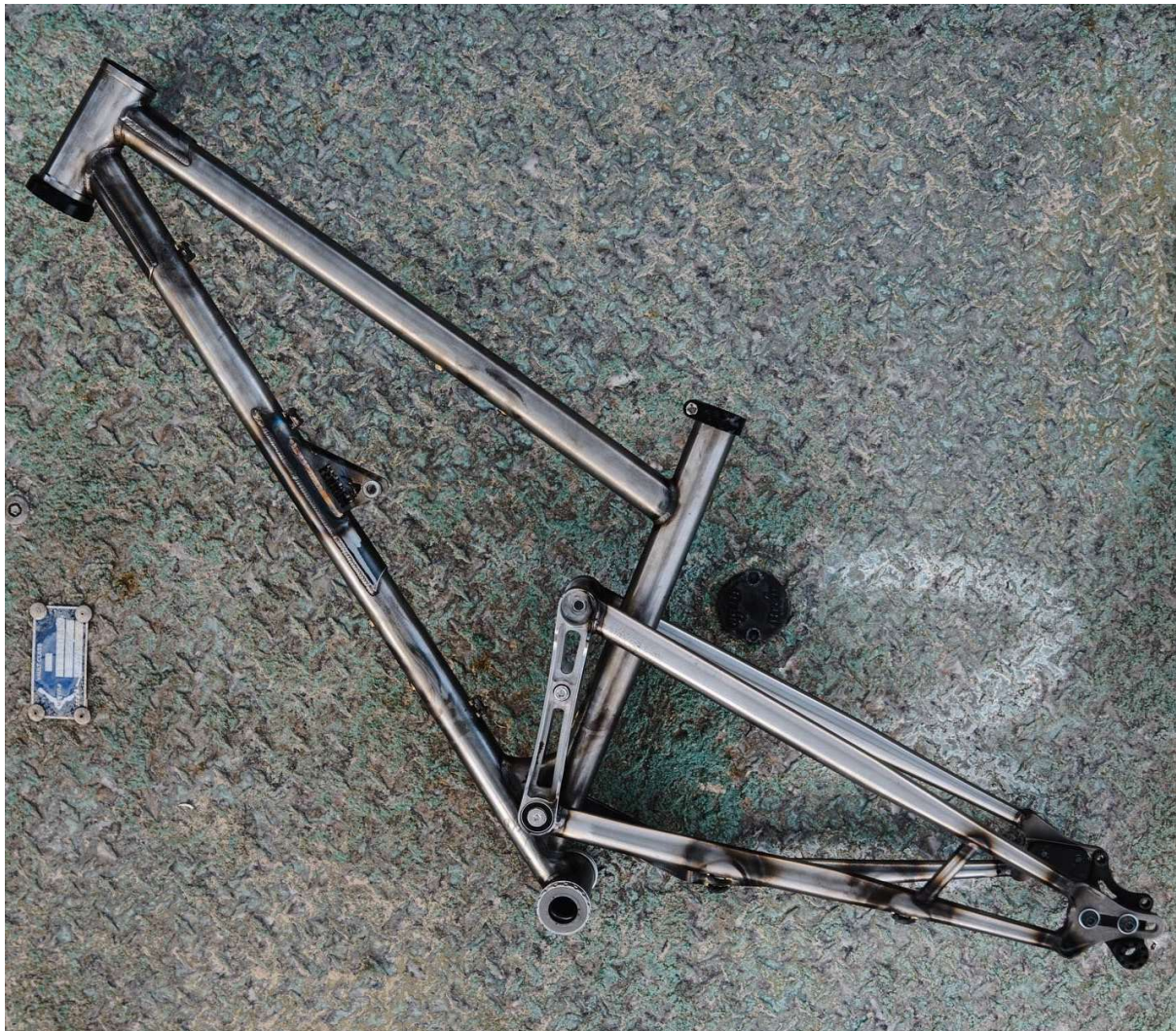


Figure 2: Steel bicycle frame (Source: pinterest.com)

3.1.3. TITANIUM

Titanium is a great material for bicycle frame construction, being as strong as steel but 45% lighter, it provides a great ratio between weight and resistance, enabling to create very thin tube frames still strong enough to withstand any stress under hard use. Its elasticity provides for vibration damping characteristics better than steel, ensuring compliance for great traction still being stiff enough. Titanium also shows great corrosion resistance, as just as aluminium, oxidation of this material creates a strongly adherent oxide film that protects inner layers from this process. In spite of objectively being

the best metallic material option for bicycle's frame construction, it is not widely used because of the high cost of raw material and its processing.

Pure titanium obtention require a very specific method known as the *Kroll Process*, in which several chemical reactions are required for isolating this material, and then it shall be alloyed via a vacuum arc remelting method, which usually occurs in various stages. In addition to these difficulties in its obtention, all the positive attributes that make this a great option for the purpose of frame building also difficult to work with it, for example the high temperatures required and high reactivity when hot working it, and its hardness regarding its machinability make those manufacturing methods more expensive than they can be on other materials.

The most commonly used titanium alloy for industrial applications is Ti-6Al-4V (Grade 5), in which this material is combined with aluminium and vanadium, this makes this composition significantly stronger than pure titanium while maintaining its stiffness and corrosion resistance. Grade 5 titanium is an alpha-beta alloy, heat treatable (which not all titanium alloys are) and that presents good weldability and relatively good fabricability. The option to temper and artificially age this alloy makes it possible to further improve its already excellent properties.



Figure 3: Titanium bicycle frame (Source: pinkbike.com)

3.1.4. CARBON FIBRE

Although referred as carbon fibre, this is just one constituent material of the composite material used for bicycle frames manufacturing, consisting in a polymeric epoxy resin matrix with those fibres as the reinforcement. Carbon fibres are crystalline filaments made out of carbon atoms which present a very high tensile strength, great stiffness, very low density, chemical resistance, and other good thermic properties, like tolerance to excessive heat and little thermal expansion, that are not so relevant for this application. On the other hand, epoxy resin is a thermoset polymer that presents a rigid phase after being cured, in this state it has good mechanical properties and present high chemical and

thermal resistance, it actuates as a conglomerating agent for the carbon fibres, fragile and prone to spreading and cracking on their own. Derivate from its individual constituent's properties, carbon fibre composite is a very strong and stiff yet extremely light material, that has great chemical resistance and is thermal stable. Nevertheless, properties of this material cannot be directly compared to the previously seen, as those were all isotropic. This composite instead outlines its benefits directionally, as the fibres are the ones that contribute the most to its excellent characteristics, parts made of this composite will show better behaviour in the longitudinal direction in which the fibres are disposed.

So, disposition of the carbon filaments will have a great impact on carbon fibre parts performance, to better understand this particularity, it is important to get to know the manufacturing process. Carbon fibres as raw material can be woven in different patterns, these can be unidirectional or multidirectional, create two-dimensional layers, or even three-dimensional structures, even though those last ones are not so common for this application. Taking into account the directionality of the threads, an analysis on the stresses the part that is being designed shall withstand must be performed, and carbon fibre layers shall be so placed to optimise alignment with the forces applied. Many layers, with the same or different dispositions, or relatively rotated ones towards others, can be piled to get the most optimal structure. There are many manufacturing methods to create carbon fibre parts, for all of them it is necessary to use an autoclave to cure the epoxy resin, but they differ in how it is applied to the carbon reinforcement. Epoxy can be applied to the mould and in between carbon layers by hand, it can be prepreg in the carbon sheets, or a Resin Transfer Moulding (RTM) method can be used, in which resin is injected in the closed mould. For whichever method is used, carbon layers shall be cut and mounted on a set of preforms and plastic bags, which permit to apply pressure on the interior of the carbon tubes. Pressure and temperature to cure the epoxy resin shall then be applied as required by the method used.

Once seen the manufacturing process of carbon fibre parts, it follows the main thread of the layers used mark a preferred direction, notwithstanding directionality of the material properties offers a great flexibility when designing and permits for a better grade of optimisation for the quantity of material to use, it makes the tubes unable to stand stress on directions that they are not designed for, this combined with carbon fibres fragility, makes frames made of this material vulnerable to impacts transversal to main thread direction, which may occur in an event of a fall, however, if the impact is not critical, carbon fibre can be repaired with the addition of new material. To solve this fragility issue would imply to obtain an isotropic material, which can be achieved by the use of other manufacturing methods, like forged carbon in which carbon fibres are not woven but put in a random disposition, but this would also eliminate all benefits related with directionality, as for example weight optimisation.

The other great problem with carbon fibre is it is a high tech material so its performances comes to an expense, although its price has been democratised over the past twenty years, a great part of this reduction comes from a higher volume of sales, as fabrication of the moulds required plays an important role on the high cost of frames constructed in carbon fibre, thus it might not be the best option for short series and in fact prototypes in the industry are usually developed using aluminium versions.

Properties of carbon fibre composites will come from, as seen above, its disposition, but also from the modulus, this is the number of threads per fibre. The most common modulus used for bicycle frame construction are 1000, 3000, 6000 and 12000 filaments, referred as 1K, 3K, 6K and 12K respectively.



Figure 4: Carbon fibre bicycle frame (Source: pinkbike.com)

3.2. MATERIAL CHOICE

In this case the material selection will be determined mainly by cost efficiency and the manufacturing process, being those the limiting factors, the best possible option is the use of steel profiles, the fact those are standardised and the ease of welding of low carbon steel make this material to meet the requirements regarding these considerations. Resistance and weight optimisation will be treated during the design process in which knowing the material to work with will make it possible to choose the correct thickness of the profiles conforming the frame. The downside to this option will be impossibility of variation in tube's shape, either in their section nor their lines, so these restrictions must be considered in the development of the frame.

Specifically, steel used for tubes is Spanish structural steel graded S-235J (equivalent to 1.0039 according to EN 10027-2 standard), and for solid pieces F-1110 (no equivalent in EN 10027-2 standard). Both alloys are similar to AISI 1015 steel, a low carbon alloy that presents a good equilibrium between machinability and weldability.

Aluminium will also be used for the link, due to the increased difficulty of welding this material, this part will be composed of solid parts bounded mechanically. The different material choice for this specific part is made in order to reduce weight of the complete assembly, and because the better machinability aluminium offers over steel, as manufacturing of this part requires a considerable amount of this process. The alloy to use is aluminium 5083, with magnesium as main alloying agent and traces of manganese and chromium, this alloy offers great machinability and high corrosion resistances, apart from being the strongest among non-heat treatable aluminium alloys.

4. GEOMETRY

4.1. INTRODUCTION TO BICYCLE GEOMETRY

Considering this will be a custom-built frame, just one size will be defined. There are many aspects that shall be considered when defining the geometry, so it will be set according to different parameters discussed below.

The most obvious is physiognomic features, in general the main trait used to determine bicycle's size is height, which gives a range of dimensions suitable for a rider based on standard proportions of the human body. In more pedalling focused bikes leg inseam is also used to determine sizing, but in a downhill bike is not so important, as this measurement affects the seat post length, which is fairly standard for all bike's brands and ranges (it usually is maintained from the smallest to the largest sizes).

Another important factor that will determine if the dimensions of a bike are suitable for a certain rider is riding position. Considering the most stable possible position is to be centred in the bike, this means, if an imaginary triangle would be drawn taking the front and rear axles and the centre of gravity of the combination rider-bike as the vertex, this last point shall fall in the middle of the base, generating an isosceles triangle. This means if there is a tendency to lean forward, a longer reach will help to put the weight more centred, as a longer front end will set the front wheel further from the centre of mass. If there is a propensity to get weight over the rear wheel, the shortening of the front end would have the same effect of bringing the centre of gravity to the middle of the wheelbase.

Finally, there is a subjective factor when deciding geometry depending on personal preference and riding style. An aggressive conduction may get a benefit from a longer bike due to the extra stability and not be so affected by the loss of manoeuvrability because of sharper reactions. Nevertheless, a more playful style could be better suited to a shorter bike that permits more agile movements and make continuous corrections a lot easier.

4.2. DISCUSION OF GENERAL GEOMETRY

4.2.1. WHEEL SIZE

Wheel size is a very important factor when stablishing geometry, as it directly conditionate most of the bicycle dimensions. There are many standards in the industry, being the most used for mountain biking 29" and 27.5" sizes. The standard some years ago was 26", but it is currently used only in young adult bikes and very specific applications.

Generally, a bigger wheel brings more roll-over capability and has more inertia when rolling, thus it permits to maintain speed more easily, it also has a greater contact patch which means it offers more grip. A smaller wheel is, on the other hand, stronger and stiffer than its bigger counterpart, and is easier to accelerate and maneuverer.

In an attempt to get the best of both worlds, the option chosen for this project is to use a mixed wheel configuration, this is, having a 29" wheel up front and a 27.5" wheel in the rear. The bigger front wheel gives more traction where it is more important, as grip break in the front is much more difficult to correct than in the rear, where in some conditions is even desirable. This also permits for a better control, and more ease of carrying speed because of the greater rolling-over capability. This characteristic is much more important in the front than in the rear, as the front wheel receive direct impacts from upcoming obstacles, while the rear tyre is dragged over them, and its trajectory in those situations may be compensated via linkage geometry.

A smaller rear wheel permits for more clearance and offers more movement freedom towards the rear end. It geometrically makes it possible to shorten the chainstay length, which enables to get a more manoeuvrable and reactive platform. Benefits also come from an easier acceleration when pedalling and higher torque because of the minor radius.

4.2.2. REACH

This is the horizontal distance between the bottom bracket and the top of the headtube, it is the most important dimension for sizing bikes. With the stack, this measurement defines the leverage that the rider has between the pedals and the handlebar, because of that, it is strongly related to height of the person riding the bike. In this case, rider's height is 1,72 meters, which would fall in the M size in most size charts of manufacturers in the market, where measurements for the reach from 420 up to 460 millimetres can be found, being the most common those in the range between 430 and 450 millimetres. In ridding position there is a tendency to lean backwards, so going for the lower values in the defined range should be considered. On the other hand, riding style is quite aggressive, so a longer bike may be more suitable. Taking all this into account, a reach that falls just in the middle of the range seems the correct option. Apart from that, according to personal experience 440 mm for the reach is the sweet spot for this measurement, so this will be the value for it.

4.2.3. STACK

Stack will result from the subtraction of bottom bracket height from the total height of the top section of the headtube. This last term is a function of front wheel size, fork length, and chosen headtube angle. With the geometry as stablished, the resulting stack height is 608 millimetres. This will be the design measurement, as for being a dual crown setup this height will be slightly adjustable in the final setup.

4.2.4. CHAINSTAY LENGTH

This dimension will determine how far the rear wheel is from the bottom bracket, those it has a direct impact on wheelbase, and handling. For the intended use and considering balance between the rear and front end, the best option is to choose a neutral length, that offers good manoeuvrability in thigh corners but still stable when going fast. Considering a 27.5" rear wheel, 435 millimetres is a fairly standard measure for this dimension which meets all the requirements specified above.

4.2.5. HEAD TUBE ANGLE

In accordance with the philosophy of keeping a neutral geometry, the head tube angle will be 63°, which is a value that offers a perfect balance between control and stability. A slacker angle would elongate the front end too much pushing weight forward. If it would be steeper, it may not be enough for dealing with steep terrain, increasing the probability of falling over the handlebar.

4.2.6. WHEELBASE

Having defined the reach, chainstay length, headtube angle, and knowing the fork offset, the wheelbase can be deduced as follows:

$$WB = R + CS + S \cdot \cos(HA) + FO \cdot \sin(HA) \quad (\text{Equation 1})$$

Where:

WB = Wheelbase, in mm

R = Reach, in mm

CS = Chainstay length, in mm

S = Stack, in mm

FO = Fork Offset, in mm

4.2.7. SEAT TUBE ANGLE

This angle has the least importance in a downhill bike, as it is directly related with pedalling position and efficiency. In the case of this kind of mountain bikes, this angle must permit good mobility and put the seat in a comfortable position. A value of 73° , which is quite common in the industry, situates the saddle far enough to allow maneuverers but still in a position that gives positive feedback of its situation in space and bicycle's orientation.

4.2.8. SEAT TUBE LENGTH

Seat tube for a downhill application shall be as short as practicable, still permitting control by pushing with the interior part of the legs, so the saddle should set just over the knees, for this purpose, a seat post height of 400 millimetres offers a correct balance and permits the correct adjustment of saddle height.

4.3. FINAL GEOMETRY

With all dimensions defined, it is possible to establish a two-dimensional sketch of general geometry. This model will be the basis for the following project stages as it is the framework for designing the frame. This will facilitate the points to input in the kinematics calculator and will be the first draft of the CAD model.

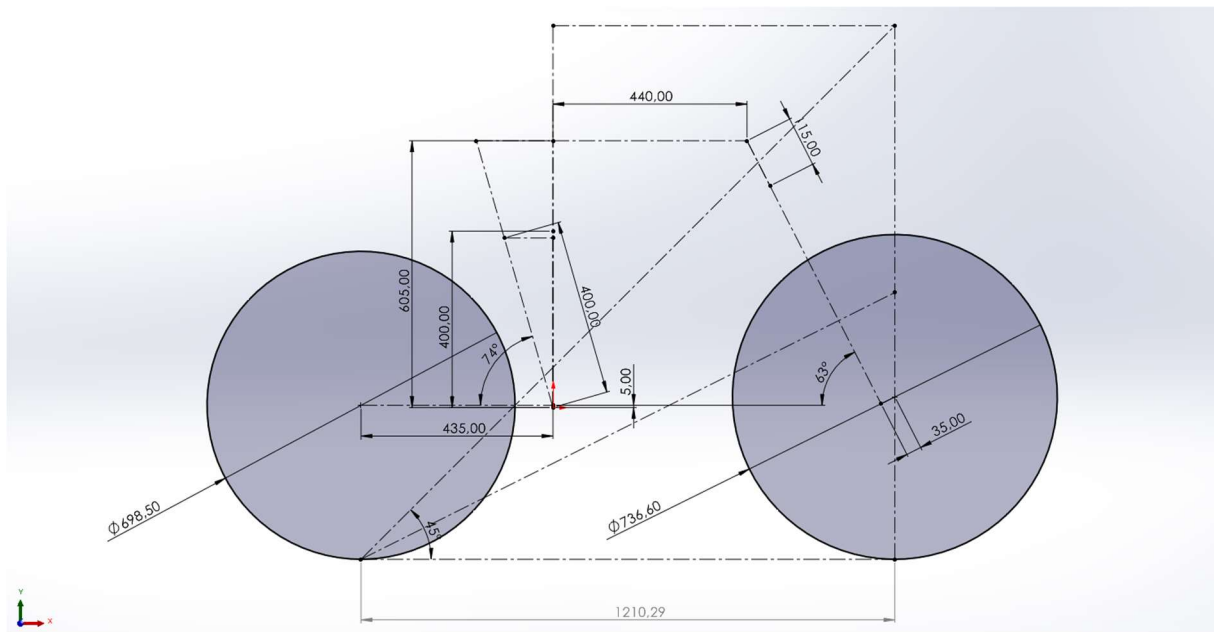


Figure 5: Bicycle geometry

5. KINEMATICS

5.1. INTRODUCTION TO SUSPENSION KINEMATICS

There are many different options for the suspension system, the layout of which will provide for some generic inherent traits and characteristics depending on basic geometry of every kind of system. Some of the most common of these are analysed and discussed in the following.

5.2. SUSPENSION SYSTEMS

5.2.1. SINGLE PIVOT

This comprises any system consisting in a swingarm that rotates around a fix pivot point, compressing the shock, directly mounted in the main frame, with this movement. This fix pivot is the instant centre of the whole trajectory of the rear wheel along its travel.

The main advantages of this system are its simplicity and low maintenance, but it offers very limited control on the leverage curve, and results in very linear designs that give very little end of the stroke support. This system also provides quite bad anti-rise values, which translates into little independence of suspension performance and braking forces.

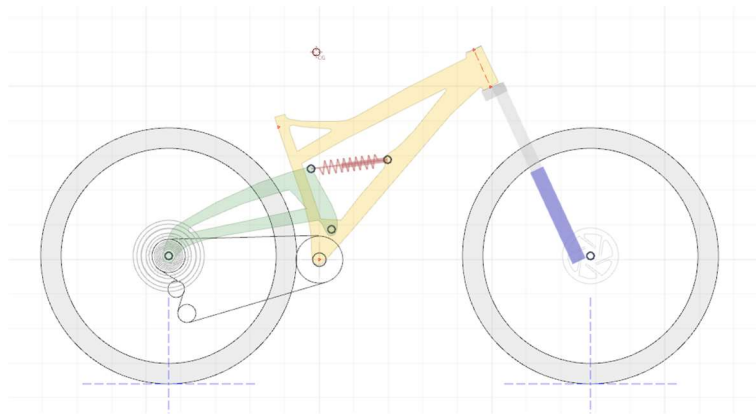


Figure 6: Example of a single pivot design

5.2.2. LINKAGE DRIVEN SINGLE PIVOT

In this case, the wheel also rotates towards a fix point in the main frame, but the shock is compressed by a linkage system. This offers more tunability of the leverage curve, enabling for more progressive designs. If the brake caliper is mounted in the swingarm, this linkage driven system will have the same anti-rise problem as a single pivot arrangement, however, there are options in the market that solve this problem by mounting the caliper in the seatstay, which is a component of the linkage system.

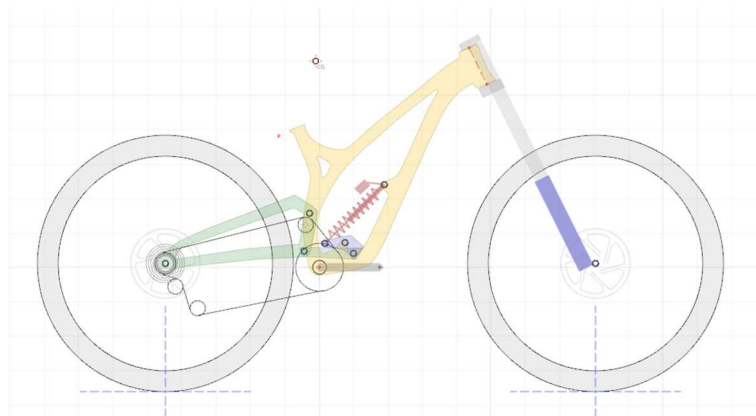


Figure 7: Example of a linkage driven single pivot design

5.2.3. HORST-LINK

This is a four-bar virtual pivot design where the chainstay connects the main frame with the seatstay. Then the seatstay, where the rear wheel is affixed, is connected to another link that attaches to the main frame. This layout creates a deformable parallelogram that compresses the shock. This system makes it possible to have better control of all the kinematics, not just making it possible to adjust anti-rise but also the anti-squat.

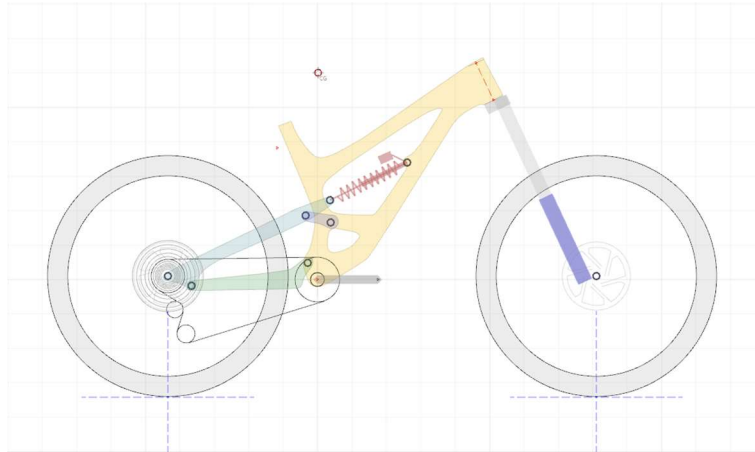


Figure 8: Example of a horst-link design

5.2.4. TWIN-LINK

In a twin-link driven system, there is a rigid rear triangle that rotates towards the main triangle by two short linkages. This also uses a four-bar virtual pivot layout, so there is no geometric difference with a horst-link design other than the length of the links and the impact in progression of the characteristics their rotation may have.

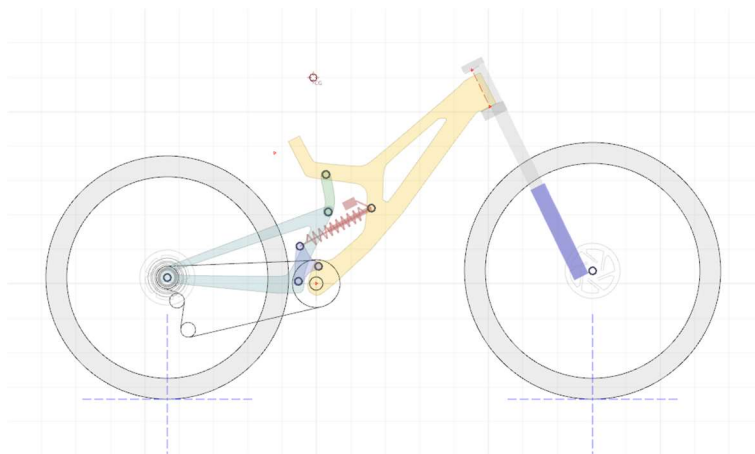


Figure 9: Example of a twin-link design

For the two four-bar virtual pivot layouts mentioned above, it is important to point out that it has much more impact on their behaviour if they are co-rotating or counter-rotating systems, rather than being a horst-link or a twin-link. In a co-rotating setup, anti-squat values tend to be more similar to a single pivot, so in general they are less pedal efficient but offer greater sensibility, on the other hand, counter-rotating designs have more support for mid stroke anti-squat values, making them more pedal efficient but giving a harsher suspension feeling.

5.2.5. SIX-BAR

This system consists of a deformable parallelogram assembly plus two extra bars that compress the shock. This involves an increase in complexity, in return for greater tunability of suspension kinematics and finer control of its characteristics. As the shock has its own linkage system, it does not depend on the movement of the four-bar mechanism directly, so there is more freedom when establishing anti-rise and anti-squat values, as well as defining the leverage ratio curve.

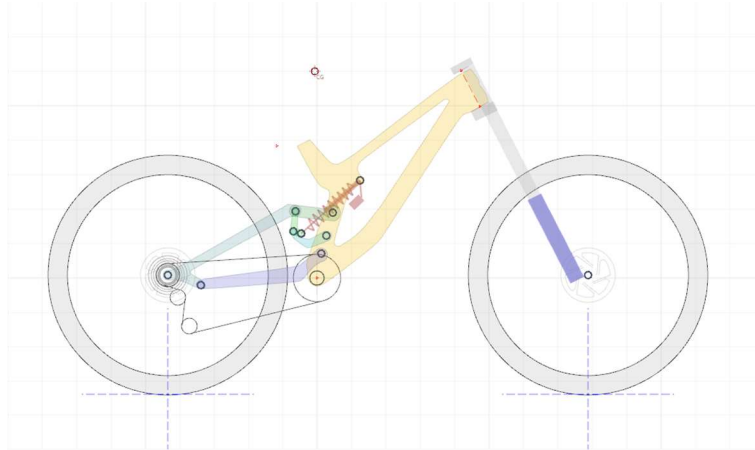


Figure 10: Example of a six-bar design

5.3. DISCUSION OF SUSPENSION SYSTEM CHOICE

Once seen the most common options for rear suspension systems, it is time to decide which one will be chosen for this project.

We can observe a general trend in the exposed options above, the most complex a system is, the finer control of suspension kinematics it permits. The designs discussed have been listed from the simplest to the most complex, thus, the one that offers the least tunability to the one that offers the most.

At first sight, suspension performance in downhill is the preferent trait any design would have to put ahead other characteristics, but due to the use conditions this kind of bicycles must withstand, ease of maintenance is a very important factor. In the same line, reliability is another great concern, a layout with more linkages means the need for more axles and bearing susceptible of failing.

Taking all that into account, one of the four-bar systems seen, those are the linkage driven single pivot, horst-link, and twin-link, seems the best option for a good balance between performance and tunability. From those, a virtual pivot system benefits from better anti-rise values, with no prejudice at all against any other characteristic, so the single pivot option may be excluded. For downhill application, a co-rotating layout has many advantages over a counter-rotating mechanism, anti-squat values tend to be lower which causes more pedal bob, but also makes the suspension more sensitive, enabling the rear wheel for better traction, and as pedal efficiency is not a great concern in this case, lower anti-squat values will only benefit suspension performance. For this scenario, a horst-link facilitates the design and manufacturing, as the rear triangle is made of two bars instead of a single rigid piece.

5.4. DISCUSION OF KINEMATICS

5.4.1. INSTANT CENTRE

The instant centre is that point with an instantaneous velocity equal to zero, that all moving parts rotate towards to, with a velocity perpendicular to an imaginary line passing through the point of application of that velocity vector and the instant centre.

It is very important to find the instant centre when designing any mechanism because that is the reference point to which every part of the assembly moves, so it will permit to determine other magnitudes necessary for kinematics analysis.

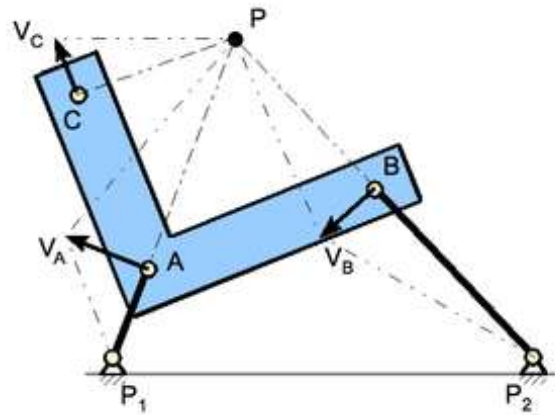


Figure 11: Example of the instant centre of a rotating body (Source: wikipedia.com)

The easiest way to determine the instant centre for what it is concerned in this project is using a graphic method.

In a single pivot bicycle, including the linkage driven ones, the instant centre is very easy to find, as it is the main pivot point. This is the fix point in the main frame where the chainstay is attached and it does not change its position along the travel.

In a virtual pivot design, as its name indicates, the instant centre is not a singular point but a virtual point that moves along the travel. To find the instant centre in a virtual pivot system, a line must be drawn passing through both attachment points of the links with the main frame and the bar holding the rear wheel. If those points are drawn all along the travel, we will get the instant centre trajectory.

For this project the chosen system is a virtual pivot design, so the instant centre will be an instantaneous virtual point and will follow a trajectory:

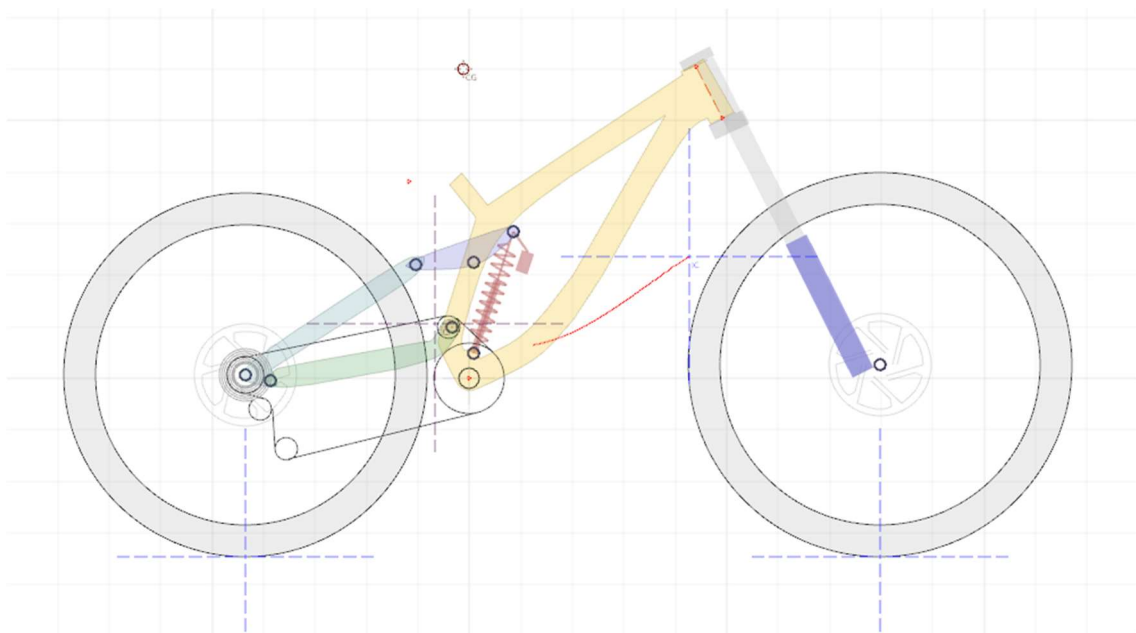


Figure 12: In red, instant centre of the suspension system

5.4.2. CENTRE OF CURVATURE

In a virtual pivot design, this is the effective point the rear wheel rotates towards to at any instant of its trajectory. It is not a fix point, and either is the rotation radii. By definition, a line passing through the rear axle to the instant centre passes also through the centre of curvature, which can be graphically found by the union of the intersection between consecutive rear axle-to-instant centre lines.

The chosen system is co-rotating so the centre of curvature may be expected not to change much along the travel. In a counter-rotating linkage system, the position change would be much more noticeable and is this fact that gives those systems its particular characteristics.

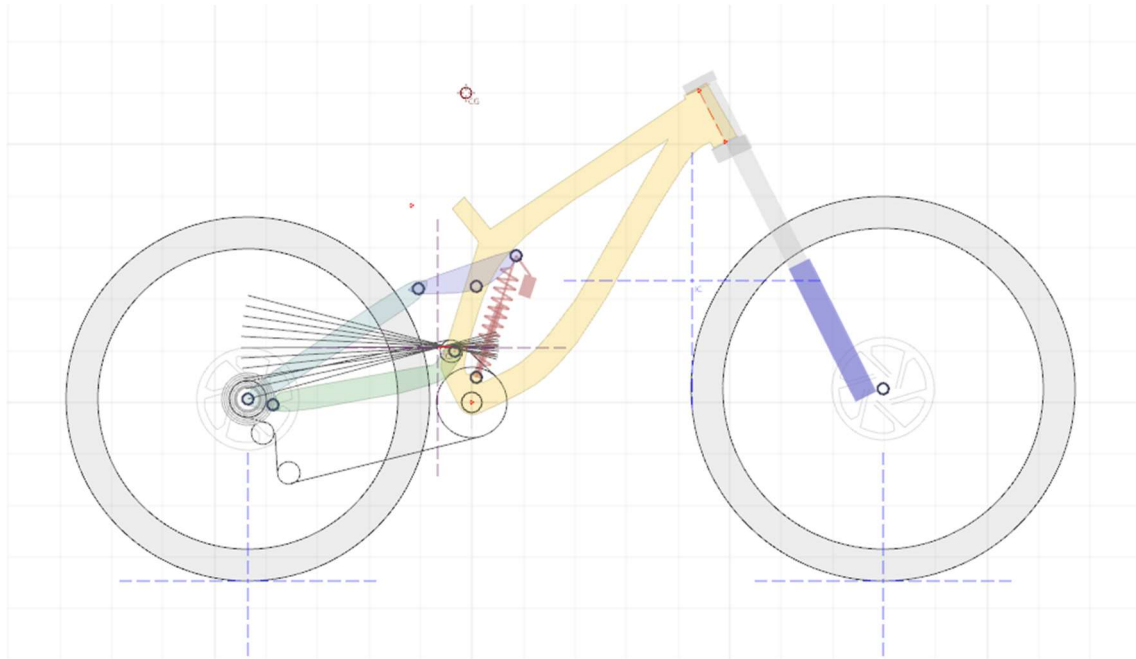


Figure 13: In red, centre of curvature of the suspension system

5.4.3. CHAIN GROWTH

This is a consequence of relative movement between different parts of the transmission. The most common configuration, although there are some exceptions, is to put the bottom bracket, thus the cranks and chainring assembly, in the main triangle, whereas gears and derailleur are mounted in the rearmost part of the rear triangle. Thus, when suspension is compressed, longitudinal distance between these parts change (the only configuration where this would not happen is in a single pivot system with the main pivot located in the bottom bracket, which would result in negative or very low anti-squat values depending on the gear). This geometric variation generates an alteration of chain-line length, usually increasing this distance.

In some designs, this elongation is so critical that a conventional transmission would result in ridiculous values for chain growth. That is the case of high pivot systems, which situate the pivot point far above the chainring. In a lower pivot suspension, the pivot point remains close to the bottom bracket, so when suspension compresses, there is a difference in height between transmission parts, but longitudinal distance decreases because of the arch described by the axle path, this compensates for the vertical distance increase and results in acceptable chain growth values. In a high pivot system, however, not only increases vertical distance between bottom bracket and rear axle but also horizontal distance, as the axle path shows a rearwards trajectory in this kind of layout. The design

solution in these cases is to add an idler pulley that guides the chain near the pivot point, getting practically null values of chain growth.

The bicycle design has a high pivot point, so an idler pulley has been used to reduce chain growth. In the next graphic, upper, and total chain growth are represented. The first one is the most important of both, as it is the responsible for the effects described above, whereas the second one tends to be compensated by derailleur elongation and will be reduced, however, by the use of an inferior chain guide (option not available in the program if there is already an idler pulley).

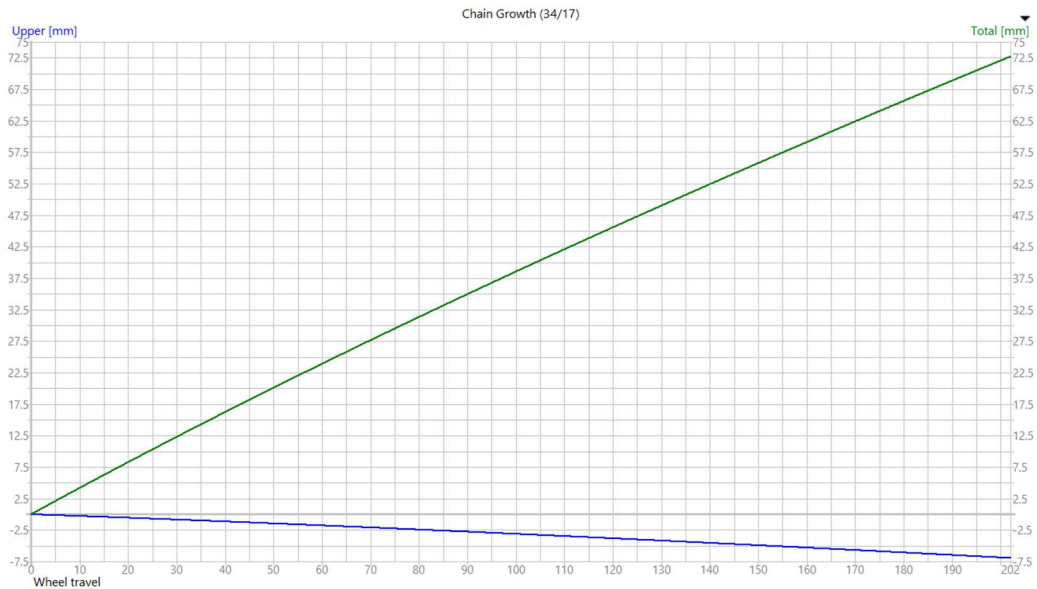


Figure 14: Chain growth of the suspension system

5.4.4. PEDAL KICKBACK

As chains and belts are very limitedly elastic, chain growth as the extension of the chain or belt in its physical dimension is obviously not possible, then pedal kickback appears because of that change in length. This phenomenon consists in backwards rotation of the chainring to compensate that elongation of the chain line generated in suspension compression.

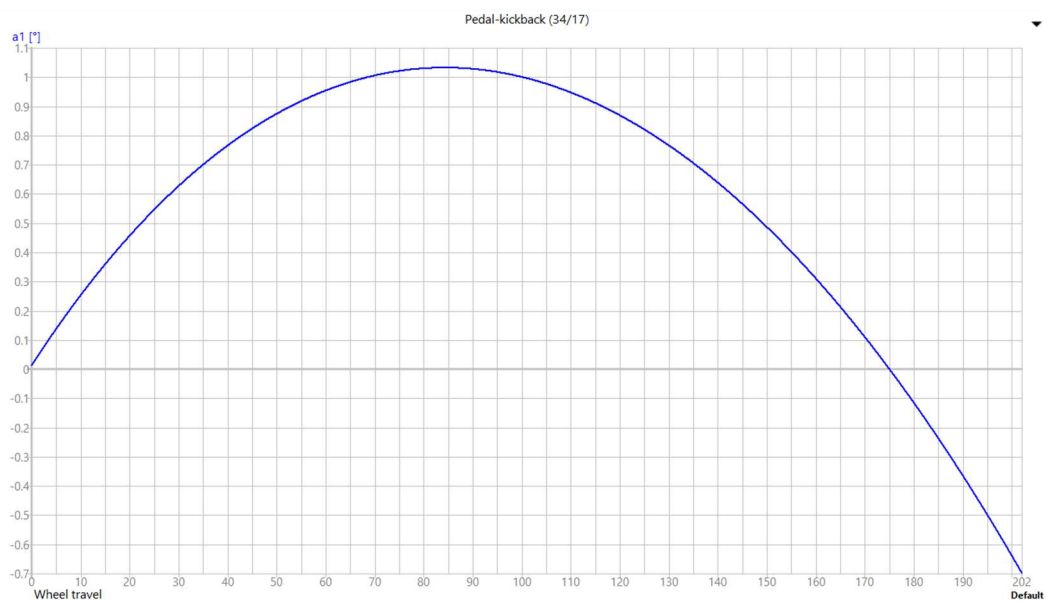


Figure 15: Pedal kickback of the suspension system

5.4.5. ANTI-SQUAT

For deducing anti-squat, a graphic method may be used. First of all, we have to take the 100% anti-squat reference point, this will be the intersection of a vertical line from the front contact patch and a horizontal line at the centre of gravity of the bike and rider combination. If we do not know where the centre of gravity sits, a line at 45° may be drawn from the rear contact patch, and the cut with the first line will determine approximately that height. Then, two more lines must be drawn, one from the rear axle to the instant centre (this line will pass through the centre of curvature or main pivot point, depending on suspension layout), and another one tangential to the gear enabled to the chainring, following the chain line. The intersection of these two lines now has to be marked, and a line passing through this point, from the rear contact patch, shall be extended to the vertical line from the front contact patch that was drawn in first place. The ratio between the height this line marks and the height of the centre of gravity multiplied by one hundred will give back the anti-squat percentage.

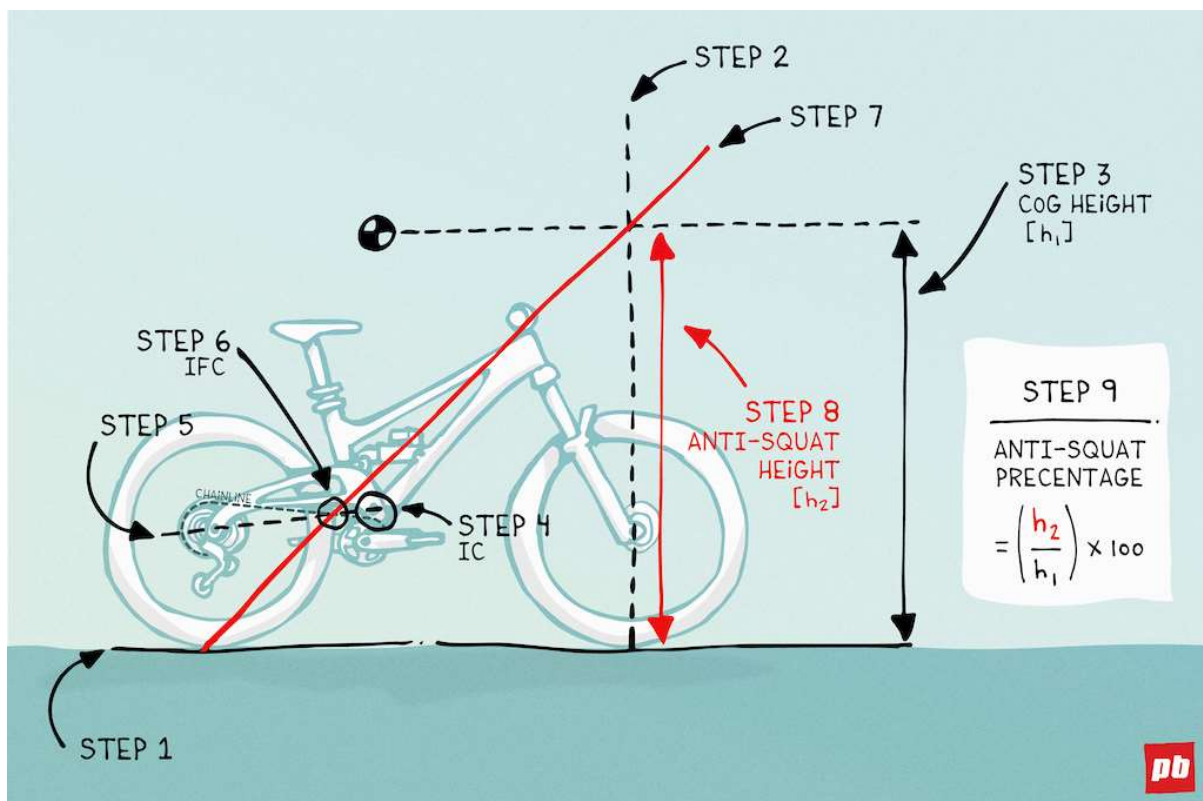


Figure 16: Example of anti-squat graphic method calculation (Source: pinkbike.com)

The anti-squat is the capacity of a suspension system to resist compression generated by chain forces and weight transfer. This value gives us an idea on how suspension will react under the action of those forces, for values under 100% suspension will compress and for values over that it will extend.

This characteristic is usually used to define pedal efficiency, as near 100% anti-squat values will prevent the loss of energy because of pedal bob. However, in the case of a downhill bicycle this trait is rather useless, and it has much more interest the possibility of isolating suspension performance from chain forces. Riding in rough terrain makes the wheel to move along its travel as it tracks the ground, and we have already seen that this causes tension in the chain, which prevents the system from moving freely. Low anti-squat values will reduce the counter force that the suspension makes when chain tension is applied, making it much more sensitive.

However too low anti-squat values are not desirable either, as it will make the bike to feel not lively at all and too stuck to the ground, rider inputs such as pumping or pushing in a turn will be absorbed by the suspension instead of generating the expected response.

The best approach has been found to be a decreasing anti-squat curve, with values near 100% at sag for a great response when the main forces applied are by the rider, and descending values from here when going deeper in the travel, for more sensitivity when compression will be produced by impacts.



Figure 17: Anti-squat curve of the suspension system

5.4.6. ANTI-RISE

For determining anti-rise, a graphic method may be used. In a similar way to how the anti-squat value is found, a vertical line from the front contact patch and a horizontal line passing through the centre of gravity must be drawn. Again, if this height is unknown, it can be approximated by a segment at 45° from the rear contact point of the wheel with the ground to the first vertical line. Now, a line starting at the rear contact patch and passing through the instant centre shall be extended to the front vertical line first drawn, and this will give us the anti-rise height, the ratio between this value and the height of the centre of gravity, multiplied by a hundred, will give the anti-rise percentage.

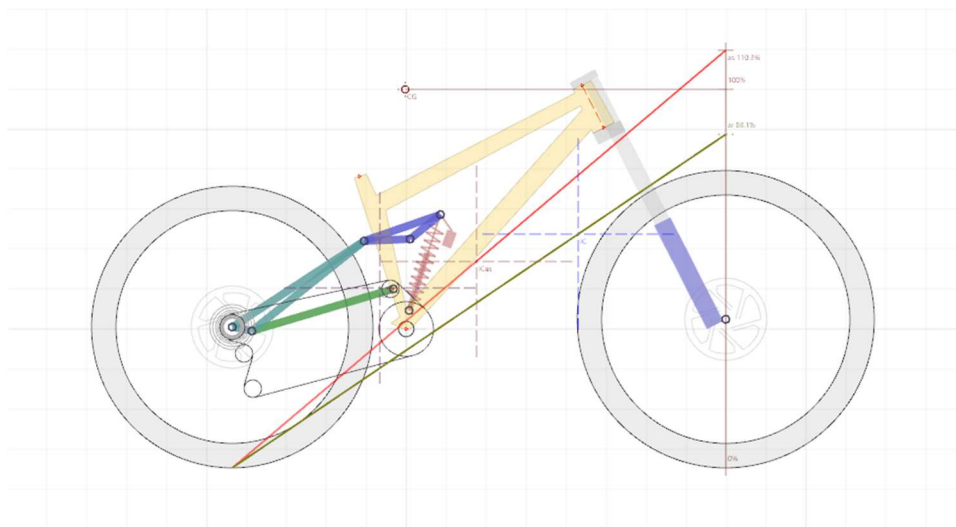


Figure 18: In yellow, example of anti-rise graphic method calculation

Anti-rise gives an idea on suspension performance under braking, thus the effect of weight transfer during heavy deceleration and the force applied by the brake caliper. Theoretically, the rear brake action would cause the suspension to compress for values over 100% anti-rise, and to extend for values under that.

In a deceleration scenario, weight transfers towards the front, so the rear axle would be unladen and suspension may lose traction. To compensate for that, the system should extend to maintain the contact patch of the wheel stuck to the ground and with sufficient load to effectively brake. This reaction is achieved with values for anti-rise under 100%.

To understand how anti-rise affects suspension performance it is very important to comprehend the forces involved under braking. Weight transfer is easily understandable and has already been explained, but caliper force influence may not be so intuitive. It is necessary to point out that during compression the contact patch remains horizontal, so because of swingarm movement describing an arch respect to the centre of curvature, there is a rotation of the caliper around the brake disk which causes a torque that resists movement if the brake is actuating. That is the reason single pivot designs with the caliper mounted in the chainstay tend to present very high anti-rise values, as the angle followed by this part of the braking system along the travel is the same as the described by the swingarm. Virtual pivot layouts can be so designed to minimise that relative rotation, thus they make it possible for a much lower anti-rise, if the brake caliper is mounted in the floating bar, this will be driven by the linkage system, and the angle variation with respect to the disk will be much smaller than the corresponding rotation of the virtual swingarm. An historical solution for braking forces interference in single pivot configurations has been to use a floating brake, mounted in a separate linkage system that drives the brake caliper independently through suspension travel, minimising its relative rotation respect to the disk.

The chosen design has been a co-rotating virtual pivot system as we have seen before, so low anti-rise values are to be expected. In this case, anti-rise presents decreasing values from around 80% at sag to 60% at full compression.

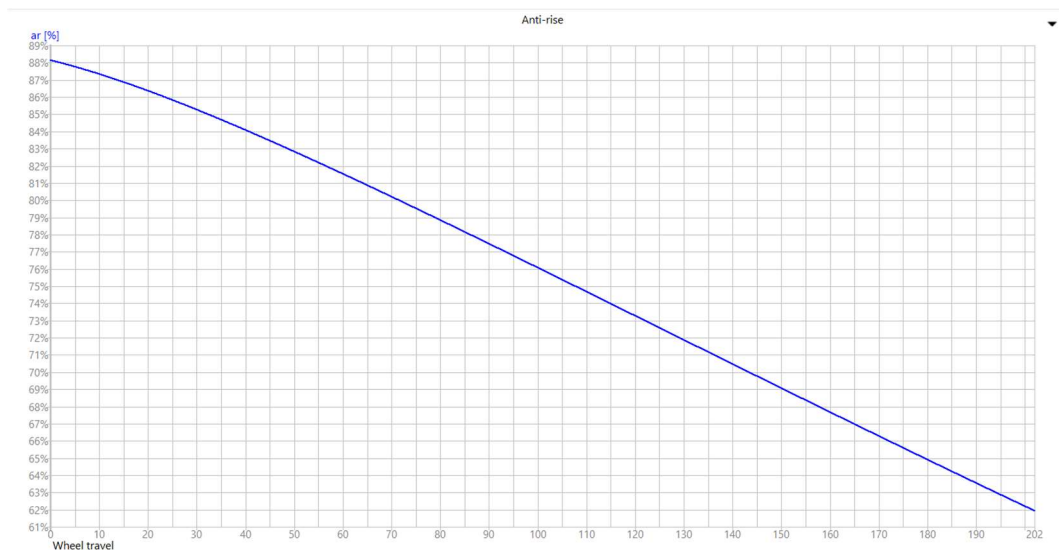


Figure 19: Anti-rise curve of the suspension system

Note: For an analytical evaluation of anti-squat and anti-rise parameters see annex III.

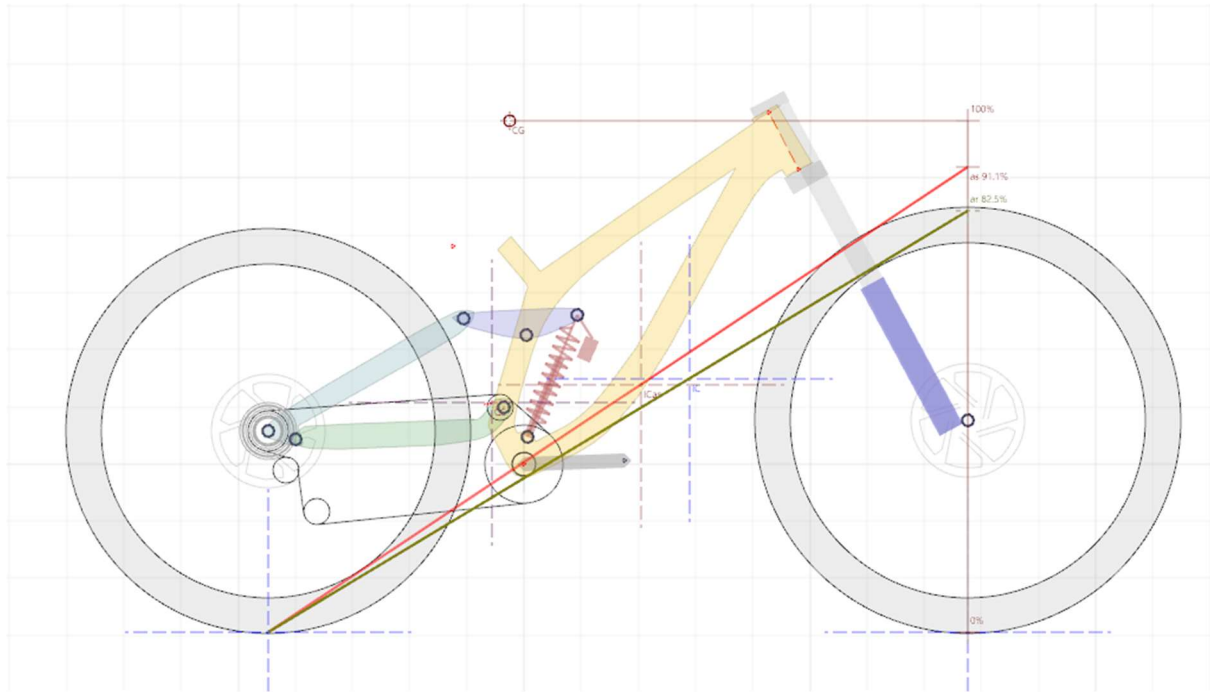


Figure 20: Anti-squat and anti-rise values at sag (20% front, 30% rear)

5.4.7. AXLE PATH

Axle path is the trajectory that the rear wheel axle follows during compression. This is an arch drawn from the centre of curvature. This geometric characteristic may give an idea on suspension performance, the steeper it is, the most efficiently energy absorbed during an impact is used to compress the shock. That is because force effectively actuating in the suspension will be the component tangent to this trajectory, however, the horizontal forward component of this vector is not helping to compress suspension in its vertical dimension. Thus, this horizontal force is counterproductive and reduces kinetic energy of the bicycle when hitting an obstacle.

It is important to notice that in a high pivot design this axle path shows a backwards trajectory, when a bump is hit there is a horizontal component in this direction, so more force of the impact is used for suspension compression, making this kind of systems more efficient for keeping speed.

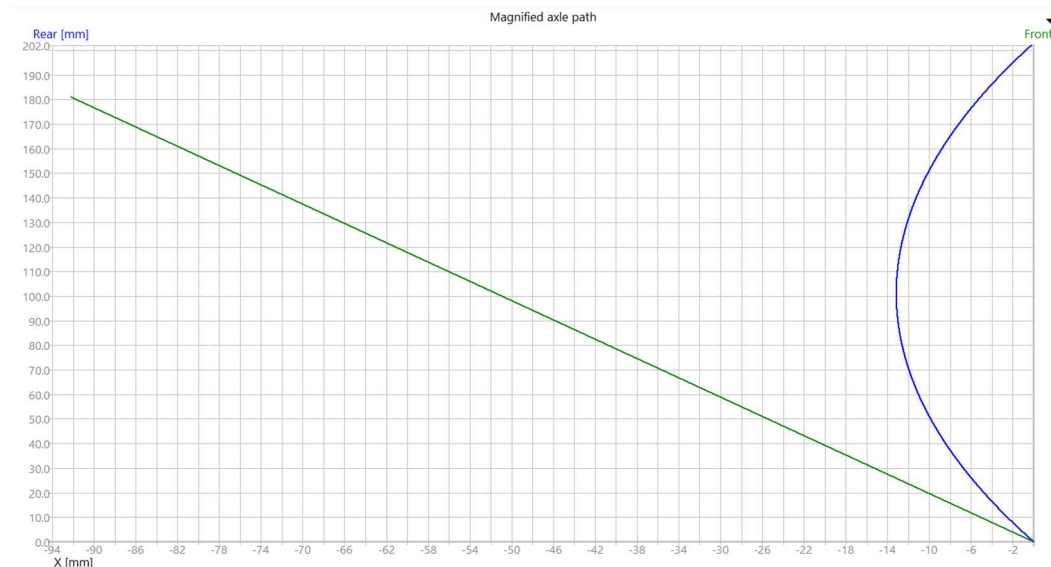


Figure 21: Magnified axle path

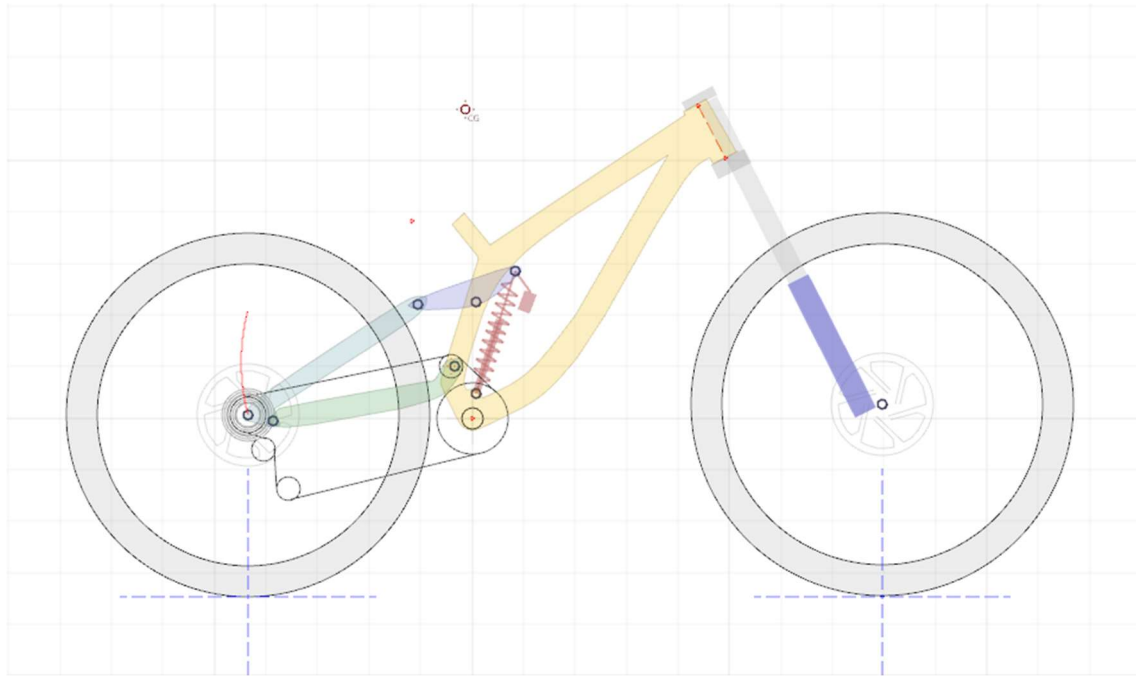


Figure 22: In red, rear axle path of the suspension system

5.4.8. LEVERAGE RATIO

This is the most important trait when speaking about suspension kinematics. It is the ratio between rear axle and shock leverage, so it gives us an idea on how much force applied in the rear wheel is required to compress the shock.

Instantaneous values of leverage ratio may be useful, for example leverage ratio at sag, to choose if rather a softer or stiffer spring shall be used in the case of a coil shock. However, when it comes to defining suspension kinematics, leverage ratio variation along the travel is what really matters. If leverage ratio for every differential portion of travel is plotted, this will give the leverage ratio curve, from which it is possible to deduce the suspension system progressivity.

The total amount of progressivity is calculated using only extreme values of leverage ratio, this is at full extension and full compression. To determine the general behaviour of the system a ratio between those values difference and the initial leverage ratio, multiplied by a hundred to get a percentage, is used. Speaking in general terms, if that percentage is negative, that means the suspension system is regressive, so the force increment required to compress the shock a certain amount at the initial part of the travel will be greater than the one needed to compress the same portion at the end of the travel. This characteristic does not have any advantage at all and might only be found in some cross-country bikes as a consequence of compact packaging or weight reduction in the suspension system. For values of overall progression near 0% that is a linear system, this means the amount of force increments to compress the shock do not differ much along the travel. This provides for a very predictable behaviour and great capability of ground tracking, but this might be a problem in heavy impact scenarios, where suspension could be too easily bottomed out, to solve this problem spring ratio shall be increased, making the suspension feel too harsh and little sensitive in the first part of the stroke. As a solution to this mismatch, a more progressive system could be used, as leverage ratio decreases at the end of the stroke, it is possible to have a very sensitive first part of the travel while getting bottom out support by the effective stiffening of the suspension. Notwithstanding the benefits of a progressive linkage, those are less intuitive than more linear systems, and they may feel harsher and even reduce useful travel if leverage ratio decrease is too accused.

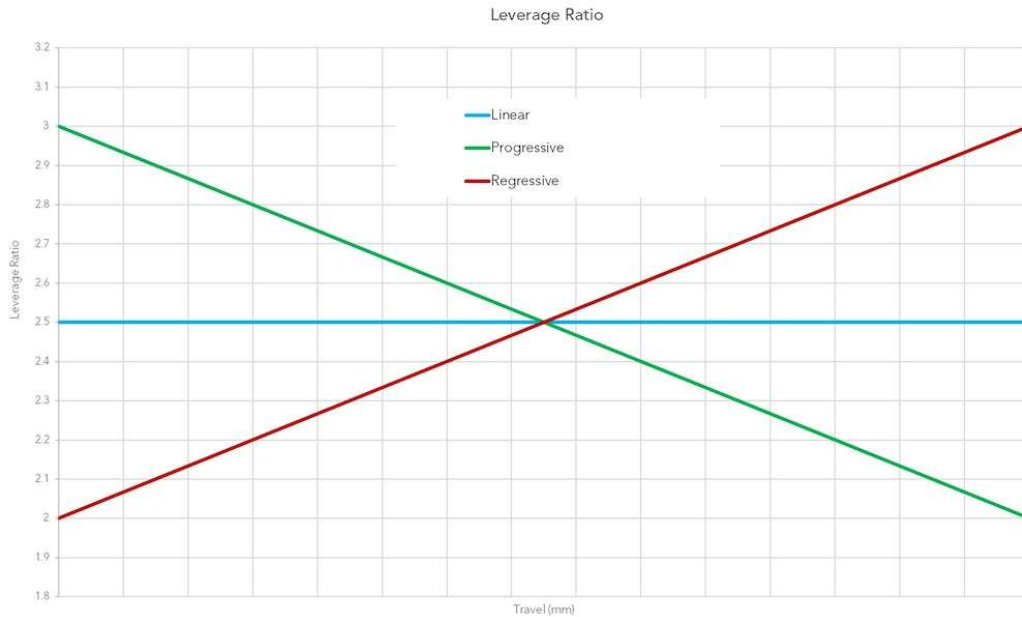


Figure 23: Example of a linear, a progressive, and a regressive leverage curve (Source: pinkbike.com)

Now, going more in depth into this subject, it is essential for suspension fine tuning to analyse the variation of the leverage curve along the travel. Two different linkages with the same average ratio could give very different feelings, depending on the shape of the curve they describe. To explain this an example will be used, see the following case where three designs with different leverage curves are represented.

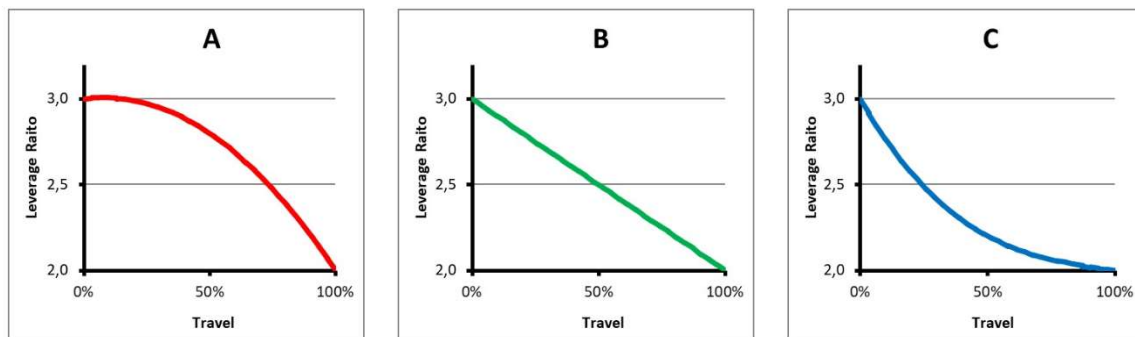


Figure 24: Examples of progressive curves (Source: youtube.com)

Either A, B or C have the same average progressivity:

$$\overline{LR} = \frac{3,0-2,0}{3,0} \cdot 100 = 33,3\% \quad (\text{Equation 2})$$

This means both the force required to start compressing the suspension and to bottom it out (considering they are using the same spring rate) will be the same, however, this is not true for any point in between. For model A leverage ratio keeps in the higher end of the range for the most part of the initial travel, then it starts to slowly decrease in the middle and at the end it falls drastically to its ultimate value, this provides for a very progressive suspension where the first part of the stroke will be very sensitive, there is a noticeable hardening in the mid-stroke and it ramps up in the end. This profile, typically found in coil-sprung frames, offers great bottom out support and a lot of traction

until the middle part of the travel but might lack a bit of support in this zone and feel too harsh under heavy repeated impacts.

In model *B* leverage ratio decreases linearly along the travel, there is a softer start of the travel, and good support in the middle and final part. This layout is the most predictable and polyvalent of the three cases, but might not be optimized for any specific application, whether if a design to work specifically with coil or air shocks is wanted or if it is a very purpose focused bicycle.

For *C*, the graphic presents a decreasing leverage ratio that stabilizes by the end of the travel, this means suspension firms up more quickly at the beginning of the stroke, and then it progresses more linearly until full compression. This curve might be used in air suspension specifically designed frames to overcome the greater initial friction this kind of shocks have due to extra sealings, and then get quickly into standard leverage ratio values. This progression curve should give great middle of the stroke support, and good control under heavy repeated compressions, but might feel too harsh in mellow trails and lack a bit of bottom out support.



Figure 25: "Flip-chip" for adjusting suspension progressivity (Source: trekbikes.com)

In the discussion above, some models have been mentioned to work better with a specific type of shock. This is because those elements have its own characteristics when it comes to progressivity during compression. In general, coil springs are linear by nature, as their constant define the amount of force per distance needed to compress them, in application of Hooke's law.

$$F = k \cdot x \quad (\text{Equation 3})$$

Where:

F = Force to compress the shock (lbf)

k = Spring constant $\left(\frac{\text{lbf}}{\text{in}}\right)$

x = Distance compressed (in)

Note: Units typically used in the industry.

On the other hand, air shocks are inherently progressive, this is because their action is based on a fluid compression as its name indicate, then, the equation of the force needed to actuate them can be approximated using the ideal gas equation:

$$P \cdot V = n \cdot R \cdot T ; \frac{P \cdot V}{n \cdot T} = R \quad (\text{Equation 4})$$

Where:

P = Pressure (Pa)

V = Volume (m^3)

n = number of mols

R = universal gas constant

If we consider the air volume is perfectly sealed, now we can compare the state for the uncompressed (1) and compressed (2) volume:

$$\frac{P_1 \cdot V_1}{n \cdot T_1} = \frac{P_2 \cdot V_2}{n \cdot T_2} = R \quad (\text{Equation 5})$$

Now, although this process is not isotherm, we can consider so for simplification, as temperature increments in a single compression of the suspension can be neglected. Thus, in application of Boyle-Mariotte law:

$$\frac{P_1 \cdot V_1}{T} = \frac{P_2 \cdot V_2}{T} ; \frac{F_1}{S} \cdot V_1 = \frac{F_2}{S} \cdot V_2 \quad (\text{Equation 6})$$

Surface application of the force in both cases will be the same, this is the piston surface, we can now see that force is inversely proportional to volume, from where we can deduce progressive nature of air shocks.

This inherent characteristic of both types of shocks is what makes them more suitable for certain progression curves, ideally with a highly progressive frame a coil shock shall be used, using an air option might reduce usable travel, disabling the final part of the stroke. Contrary, if a coil is used in a very linear layout, suspension could dive too much into the travel, making it too easy to bottom out. It is worth mentioning that there are options for progressive or dual ratio coils springs, and larger volume air shocks are less progressive than their reduced counterparts, however, if a certain frame needs an increased progression, using an air shock is still the best option, as this characteristic is easily tunable by using volume reducers.



Figure 26: An air (left) and a coil (right) shock (Source: ridefox.com)

For this project, a progressive design has been chosen, with an average progressivity of 36,8%, that decreases almost linearly from a 3,44 to a 2,18 leverage-ratio from the beginning of the stroke to full compression, respectively. This layout is more suitable for use with a coil shock, due to the great amount of progression inherent to the frame.

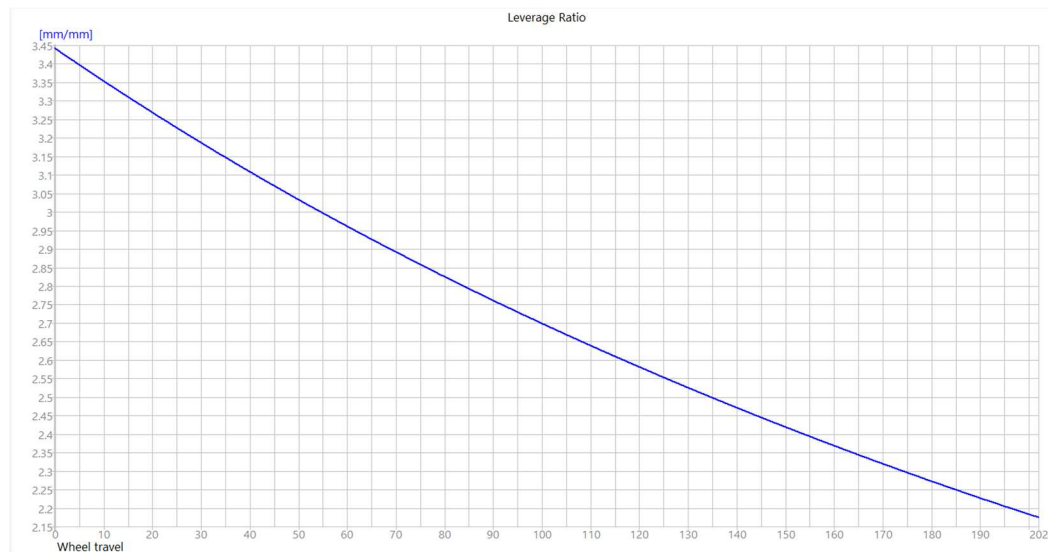


Figure 27: Leverage curve of the suspension system

"Horst-link" 4-Bar (202/203 mm)			"Horst-link" 4-Bar (202/203 mm)	
Vertical rear travel	60.0 mm		Vertical rear travel	201.0 mm
Rear travel on axle path	61.1 mm		Rear travel on axle path	203.2 mm
Front wheel travel	40.0 mm		Front wheel travel	203.0 mm
Vertical Front wheel travel	35.3 mm		Vertical Front wheel travel	179.2 mm
Shock Compression	18.8 mm		Shock Compression	74.8 mm
Max shock compression	75.3 mm		Max shock compression	75.3 mm
Progressivity (Lev.Ratio)	36.8%		Progressivity (Lev.Ratio)	36.8%
Gear ratio	2.00		Gear ratio	2.00
Rollout (gear metre)	4436 mm		Rollout (gear metre)	4436 mm
Instant center	293.6 ; 143.9 mm		Instant center	123.0 ; 64.6 mm
Center of curvature	-54.3 ; 107.7 mm		Center of curvature	-43.0 ; 107.2 mm
Chain Growth	-1.8 mm		Chain Growth	-6.9 mm
Total chain growth	+23.9 mm		Total chain growth	+72.4 mm
Minimal required chain length	1250.5 mm		Minimal required chain length	1298.9 mm
	99 Chain eyes			103 Chain eyes
Pedal-kickback	+2.19°		Pedal-kickback	+0.64°
Wheel rot. (BB dist.change)	+2.02°		Wheel rot. (BB dist.change)	+0.69°
Force to wheel	446.1 N		Force to wheel	2408.3 N
Current anti-squat (a1)	91.1%		Current anti-squat (a1)	35.6%
A(x)	261.04 N		A(x)	92.19 N
Anti-rise (ar)	82.5%		Anti-rise (ar)	59.3%

Figure 28: Kinematics comparison between values at sag (left) and full compression (right)

6. COMPUTER AIDED DESIGN

6.1. INTRODUCTION

Fabrication of a product, due to processes like machining, the need of specific tools, or moulds for the parts needed, might be a very expensive process. Fortunately, there are many tools that permit us to create a virtual model to work with before bringing anything to the real world, which are highly valuable for making it possible to solve issues that may arise during the development of the product or get a reasonable grade of optimisation for the design, without need of creating any real prototype.

Virtual models can be generated to study almost any aspect that can be considered for any object or system. For this project, two different programmes have been used for the design of the frame. First of all, a geometry calculator has been used to generate a two-dimensional model for establishing a general silhouette of the bicycle, by placing all the characteristic points that will define it. Then, using this layout as a template, a three-dimensional model has been developed for the study of compatibility between all its components and constructive viability.

6.2. TWO-DIMENSIONAL MODEL

The programme *Linkage X3* has been used to study bicycle's kinematics and to define its geometry. Having decided the general dimensions of the bicycle and knowing which suspension system will be used, we have everything necessary to create a first draft. Having entered those as an input, the programme will ask for different pivot and interaction points, the coordinates of some of which have not been defined yet. These will be set arbitrarily in a coherent disposition for the linkage type chosen, and then relocated in an iterative optimisation process.

When creating a new project we have two options, to start from a side picture of the frame we want to characterise or to use a predefined template for the suspension system to use. As the frame design start from a blank sheet with no specific geometry, this second option is the most reasonable.

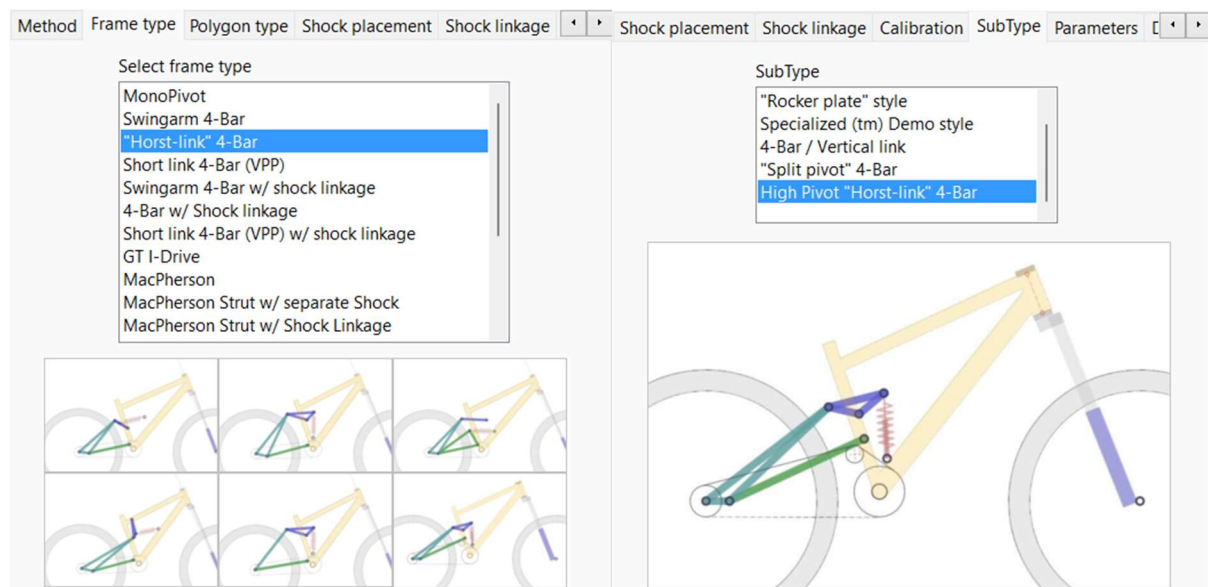


Figure 29: Suspension system choice in the program's interface

Now, the new model has to be configured with general geometry parameters, already discussed above. As some of them are co-dependent, in case of interference the most important of them (those are reach, stack, chainstay length and head angle) have been introduced as the input and the rest are automatically calculated.

Shock linkage	Calibration	SubType	Parameters	Drivetrain	Titles
Wheels - Rear Size	27x2.4				
Front Size	29x2.4				
Rear Travel					
Shock Length	250.0				
Shock Stroke	75.0				
Front Travel	203.0				
Fork Axle To Crown	563.5				
Head Angle	63.0°				
BB height / BB drop	348.0 / 5.0				
Chainstay Length	435.0				
Top tube length	625.9				
Wheelbase	1234.3				
Reach / Stack	440.0 / 608.0				
Head Tube Length	120.0				
Seat tube Angle	73.0°				
Seat tube Length	400.0				
Seat tube offset	0.0				
<input checked="" type="checkbox"/> Create frame polygons					
Top tube thickness	35.0				
Down tube thickness	50.0				
Seat tube thickness	32.0				
Head Tube	Tapered (50-60mm)				

Refresh

Figure 30: General geometry definition in the program's interface

With all this information, a generic model will be generated. Pivot points are set automatically in an editable configuration, so they can be modified as desired. The interface to work with is the following:

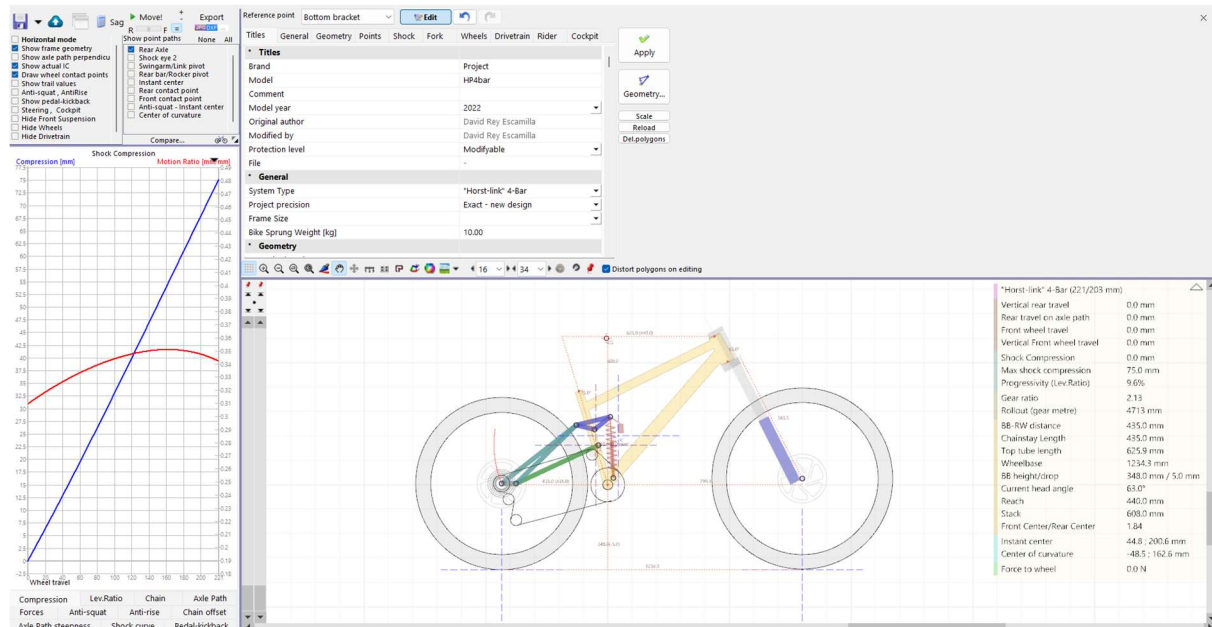


Figure 31: Interface for the study of a bicycle model

Four different working spaces in the interface can be distinguished. The two windows in the upper part are for settings, whereas in the lower part of the screen graphic information is shown.

Going from top to bottom, and right to left, the first window consists in check lists of information to show in the graphic output. The boxes in the left column refer to graphical information regarding

suspension characteristics or which components are shown in the model. For example, anti-squat and anti-rise lines, pedal kickback, or the instant centre in real time can be enabled, or the main frame can be isolated by hiding the wheels, front suspension, and drivetrain, independently. In the second column, showing the path along the travel for all relevant points can be enabled. This is especially useful for virtual points like the instant centre or centre of curvature, or points which trajectory has a considerable importance, for example the rear axle path.

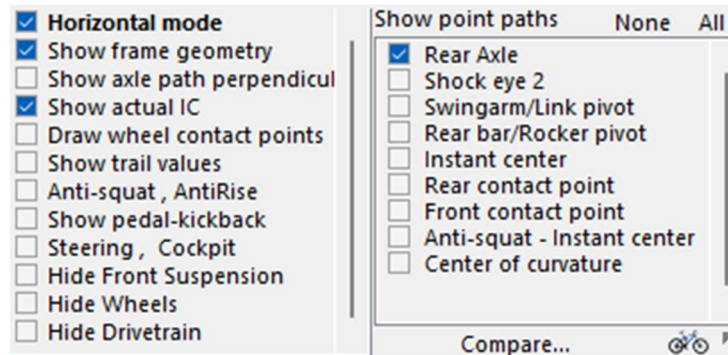


Figure 32: Checklist for displayed information

Now, moving to the left, the next box is an editable interface where all parameters of the bicycle can be modified, from editing the general geo and specific coordinates, to all component's characteristics, including suspension elements (both fork and shock), wheels, drivetrain, brakes, and cockpit. This is the main workspace where the model can be precisely edited to fine tune suspension kinematics, or easily experiment with alternative components, like using a coil or an air shock, or changes introduced by using different wheel sizes.

Reference point

Bottom bracket

Edit

↶

↷

Titles

General

Geometry

Points

Shock

Fork

Wheels

Drivetrain

Rider

Cockpit

Points

Rear Axle

-435.0

5.0

Bottom bracket

0.0 ; 0.0

Front Axle

799.3 ; 24.0

Shock eye 1

24.2 ; 27.7

Shock eye 2

10.7 ; 277.3

First link fix pivot

-38.4 ; 161.8

Swingarm/Link pivot

-374.9 ; 4.9

Rear bar/Rocker pivot

-127.9 ; 243.3

Rocker fix pivot

-51.9 ; 224.5

Head tube Bottom

493.6 ; 502.9

Head tube Top

440.0 ; 608.0

Center of Gravity

-3.0 ; 600.0

Seat tube Bottom

0.0 ; 0.0

Seat tube Top

-116.9 ; 382.5

Chain guide roller center

-62.1 ; 123.4

Figure 33: Parameter adjuster

In the bottom left-hand corner of the screen, dynamic and kinematic characteristics are plotted against rear wheel travel. A total of eleven different graphs are available in this section, including some already discussed (see point 5.3.) as leverage curve, chain growth, axle path and axle path steepness, pedal kickback, anti-squat, and anti-rise, but also some extra information that could be useful. It is possible to plot shock compression and motion ratio along the travel, this second term is the instantaneous ratio between wheel travel and shock stroke, and it is the inverse of leverage ratio. Another option available is chain offset, which is the distance between the chain line and the centre

of curvature, which can be an indicative if an idler pulley is required for the design. Finally, we have two dynamic characteristics plotted, that depend not only in geometry but also in parameters set for the shock. We can find the shock curve, that defines inherent progressivity of this component, and forces to apply on the rear wheel to compress the suspension, with an additional curve for this graph representing rate of force per millimetre required.

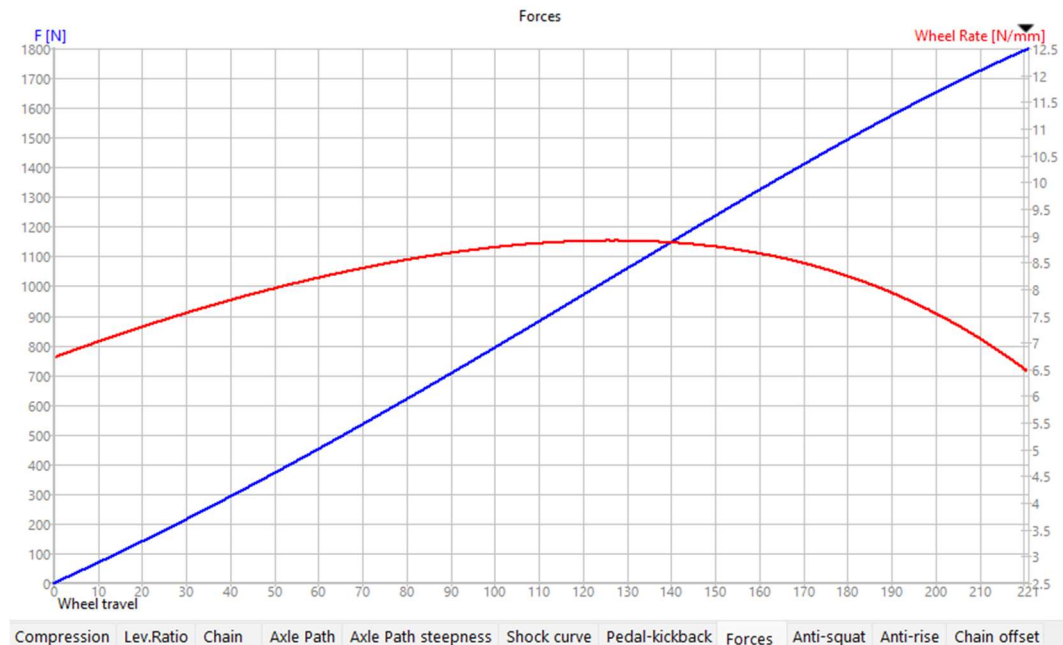


Figure 34: Example of a characteristic plotted and at the bottom all different graph options

At the right-hand of the bottom part of the interface, we can find a two-dimensional drawing of the bicycle, with a table showing different instantaneous values for geometrical, kinematic, and dynamic characteristics for a given front and rear suspension compression. The information here displayed will be the selected in the first window, this permits for a very intuitive comprehension of what is exactly happening during compression, and this helps to better understand the graphs above mentioned. Then, as this two-dimensional model situates all the main points in the frame, it makes it possible to study the viability of the design, taking into account interferences between different parts of the structure or the components that complete the bicycle.

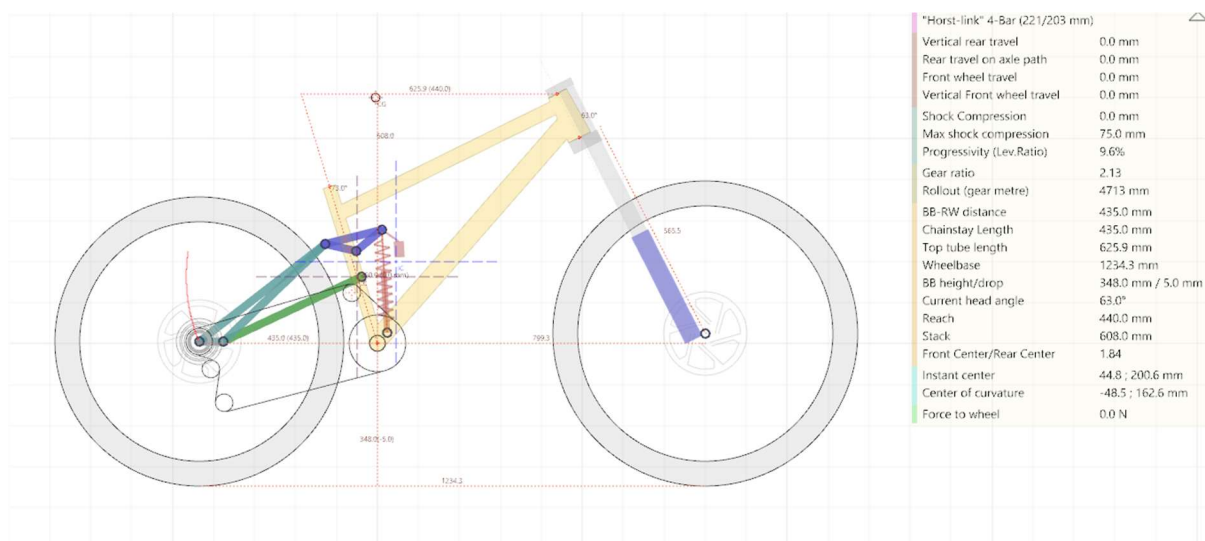


Figure 35: Two-dimensional bicycle model and its instantaneous characteristics

Now, with all this information available, pivot points in the linkage shall be relocated to get the aimed kinematics for the suspension system. This is a complex process where every point location does not just affect one aspect but many of the suspension characteristics, so the best approach to it is an iterative method to readjust pivots positioning continuously. The starting point of the generated template is the following.

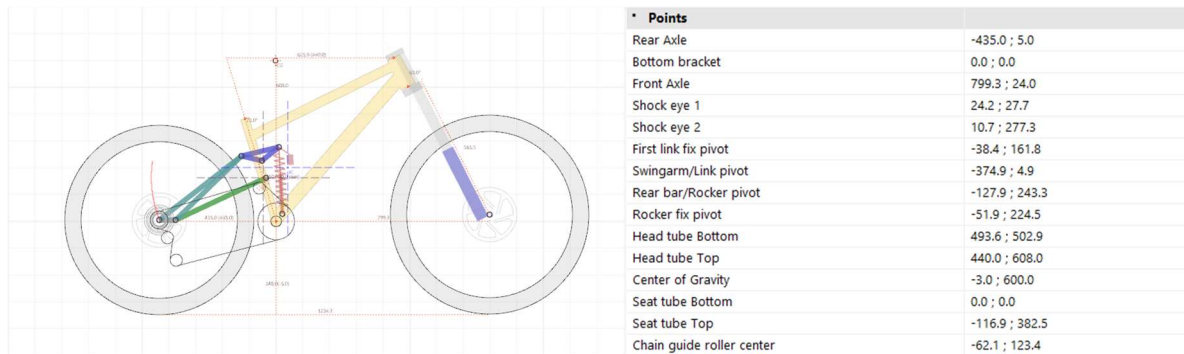
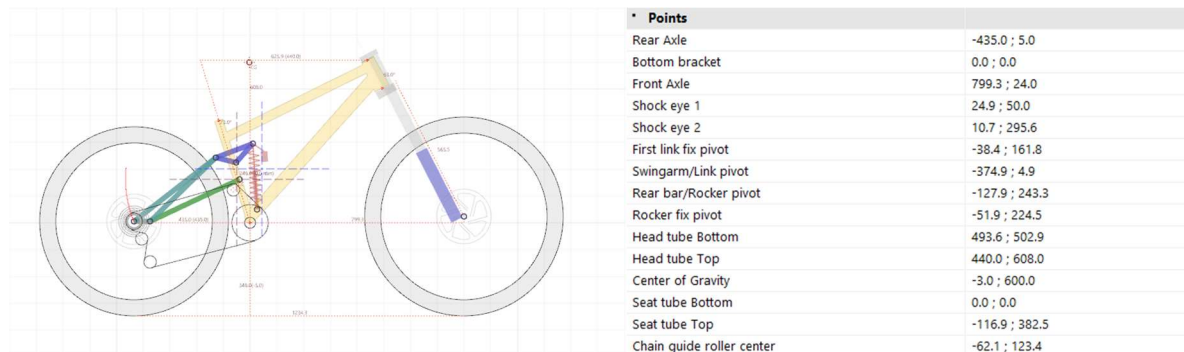
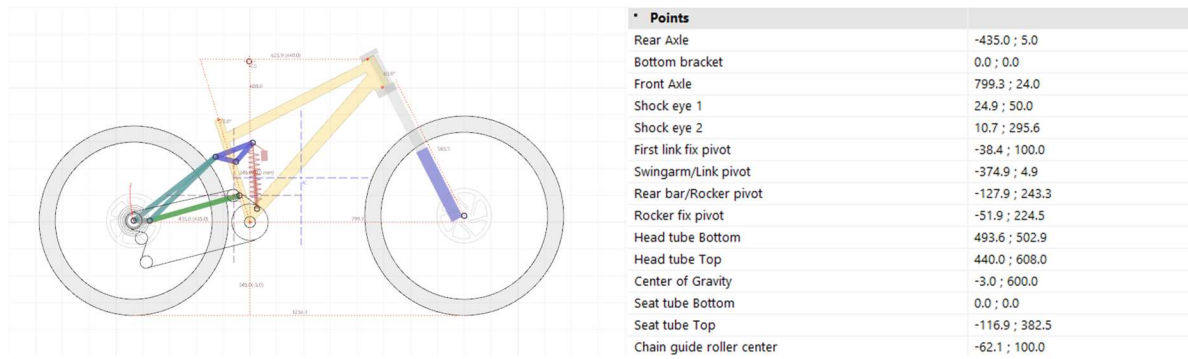


Figure 36: Coordinates of general geometry defining points

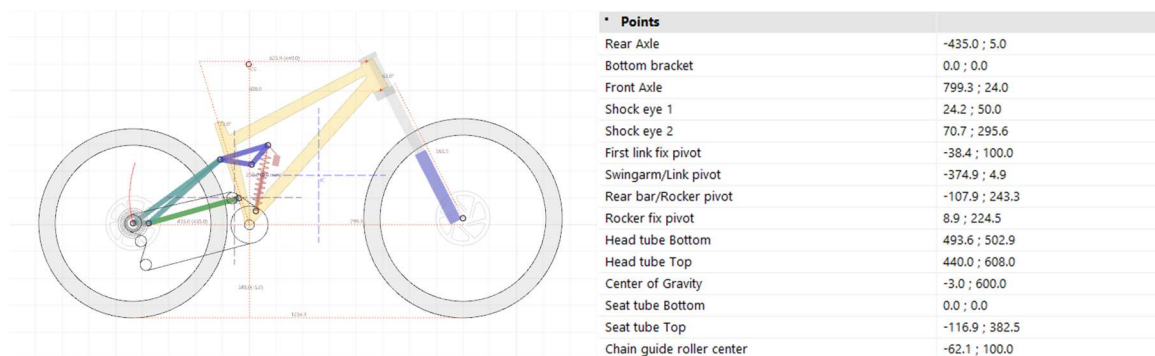
The most effective way to start with is location of points we can actually foresee. First of all, points that provide for a non-constructively viable solution shall be modified, in this case, we can see the shock attachment to the main frame interferes with the frame, although this might be possible by cutting the downtube, it is not optimal because it would reduce strength in this part, which is the most critical of the frame. The attachment point shall be raised as per be mounted over the bottom bracket, vertical distance with respect to this point will provisionally be fifty millimetres, this will also rise shock attachment point with the rocker link to keep the same shock length.



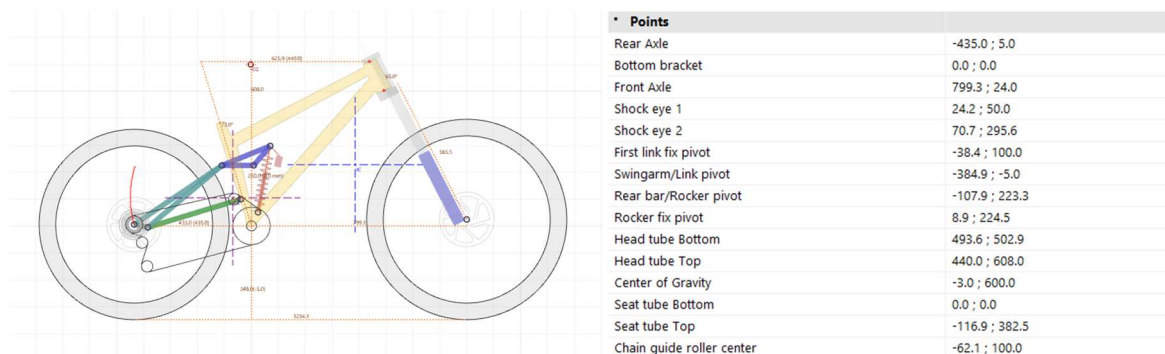
Now, knowing this is a horst-link design, it is known that centre of curvature will be located near the chainstay attachment point with the main frame, so this will approximately be the origin of the radius that describes rear axle path, which is aimed to have a rearwards trajectory, but not a too exaggerated elongation in order to not alter handling during compression. This requirement shall be deemed to be fulfilled if the longitudinal position of the uncompressed and full compression longitudinal location of the rear axle is the same, for this geometric condition the centre of curvature shall be located in the half of the vertical travel, which can be approximated to two hundred millimetres, thus height of the chainstay pivot shall be one hundred millimetres. The idler pulley has to be also relocated consequently, as this element shall guide the chain line as near as practicable to the centre of curvature for minimising chain growth, its height is also modified to meet the new y coordinate of the chainstay pivot.



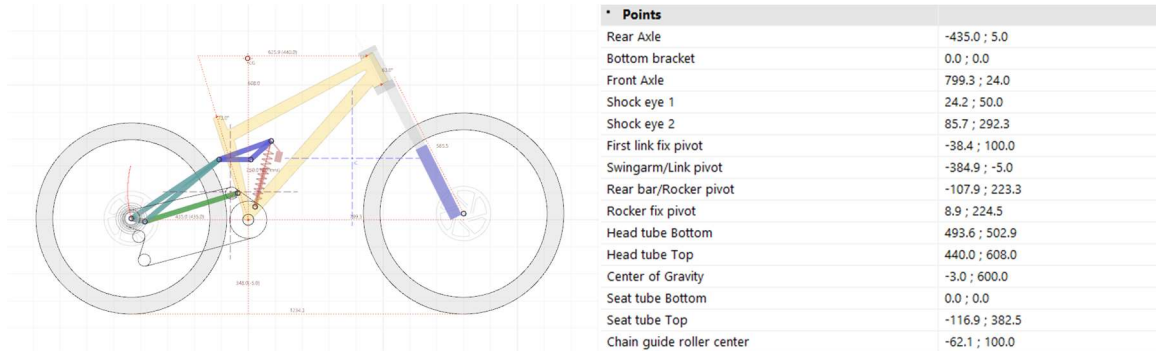
These modifications introduced in the system elongate the rocker link lever on the shock, providing for a shorter travel than desirable of 144 millimetres. To fix this, rear bar leverage on the rocker link shall be increased, but the attachment point of these two elements is too close to the rear wheel already, so the other two points that define the rocker links shall be shifted to the left. Apart from that, the distance of the rear bar attachment point with the rocker link makes it impossible to build the union for the rear bar left and right side, so the entire rocker link shall be shifted forward. A relative displacement of the rear pivot point, and a forward shifting will provide for longer travel and enough clearance for all constructive elements.



Now, anti-squat and anti-rise values are not optimal for this design. Anti-squat is too low, starting at 76,6% and falling to 35,4% at full compression, these values can be increased by lowering the instant centre position, which will raise the cutting point of the swingarm with the chain line. Anti-rise on the other hand, show a bit higher initial values than desired, from a 99,6% to 62,6%, and raising the instant centre will further increase those, as a solution instant centre can be longitudinally separated, which will generate a slacker anti-rise line. The rear bar attachment's height shall be modified, lowering the chainstay and the rocker link attachment points will have the aimed effect on anti-rise, and shifting the chainstay pivot to the rear will affect positively the anti-rise.



Looking at the leverage curve, this is a too progressive linkage, with a total leverage ratio decrease of 45,2%. To reduce this value, leverage on the shock can be increased by enlarging the arm of the rocker link that pushes this component, this action will decrease overall leverage ratio values. Leverage curve can be easily adjusted by relatively rotating the shock, this positioning defines distance perpendicular to the shock stroke to the main pivot of the rocker link, which is effectively the leverage of this arm, this is in fact the principle on how progressivity adjustment systems are based on (see point 5.3.8.).



The process of geometry adjustment may follow until optimisation is achieved. Some changes will be conditioned by constructive restrictions, which shall be analysed in a three-dimensional model, as described in the following (see point 6.2.). In the process described above some solutions have been presented to adjust different aspects of suspension kinematics, after every change these characteristics shall be revised and may be readjusted as applicable. The final geometry of the bicycle after this iterative analysis will be as follows.

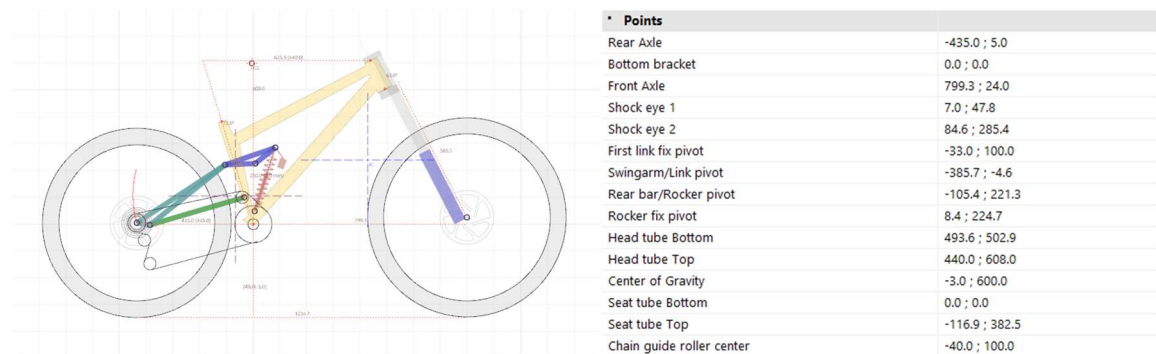


Figure 37: Final geometry of the frame

6.3. THREE-DIMENSIONAL MODEL

For the development of a three-dimensional model, Computer Aided Design software *SolidWorks* has been used.

The different parts that form the frame are to be created separately and then assembled together. Then, the first step is to create the pieces that conform the frame individually, for this, a new document must be created, selecting the option *part*.

Once a new part has been opened, the software interface will show a taskbar at the top of the window, of which relevant tabs as far as design is concerned are *croquis* and *operations*. With the first, a new *croquis* can be created and edited, either in a defined plane with the *croquis* option, or directly in the three-dimensional space, with the *3D croquis* alternative. The *Features* tab, on the other hand, permits to generate new solids from the *croquis* created by extruding, cutting, etc. These new elements generated using the mentioned tools will be listed in the *Feature Manager*, shown at the left side of the screen, where all the steps to create the part will be registered, including reference geometry,

croquis, and operations. Finally, in the central part of the screen, the main workspace is displayed as a three-dimensional space where the part that is being created will be shown.

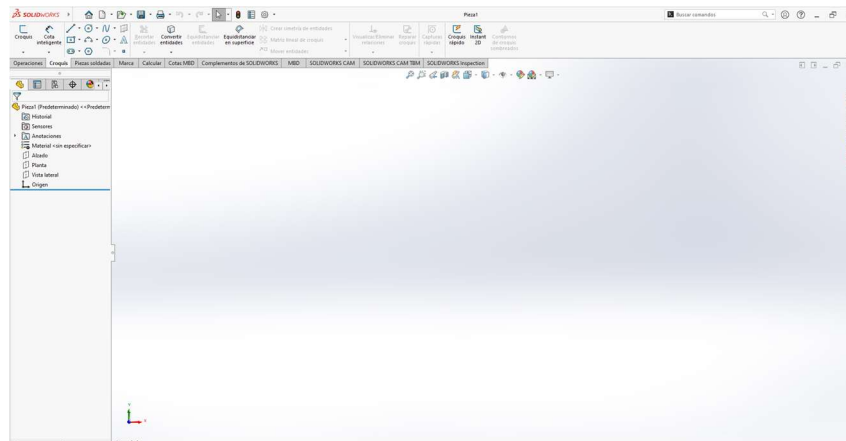


Figure 38: SolidWorks interface

This software offers a wide range of possibilities when creating solids, the correct choice of proper operations depending on the geometry and nature of the part we want to model might reduce considerably the number of steps and the time spent in creating the part. In this case, solids and routed tubing will be used, so the best approach possible is a combination of extrusion of solid parts with material subtraction for pieces that shall be machined, and sweep features over a defined trajectory for tubes. This working method will permit to easily modify the frame structure by adjusting the croquis used for tubes routing, this is important because the creation of the two-dimensional and three-dimensional models are not sequential, but parallel processes, and as they are interdependent one from each other, they shall evolve side by side.

6.3.1. VERSION No.1

Once decided the design method to use, modelling of the frame shall start. The first version of the model will be a prove of concept that will have the objective of preliminarily analysing viability of the design. To start with, the first part to be created is the front triangle, for being the most relevant when it comes to frame geometry, and the one containing the bottom bracket, which is the main reference point for everything else. It seems a good strategy to draw general dimensions of the bicycle for reference (see point 4.3.) and then create a template for general lines of the frame, considering all important points found in the two-dimensional model.

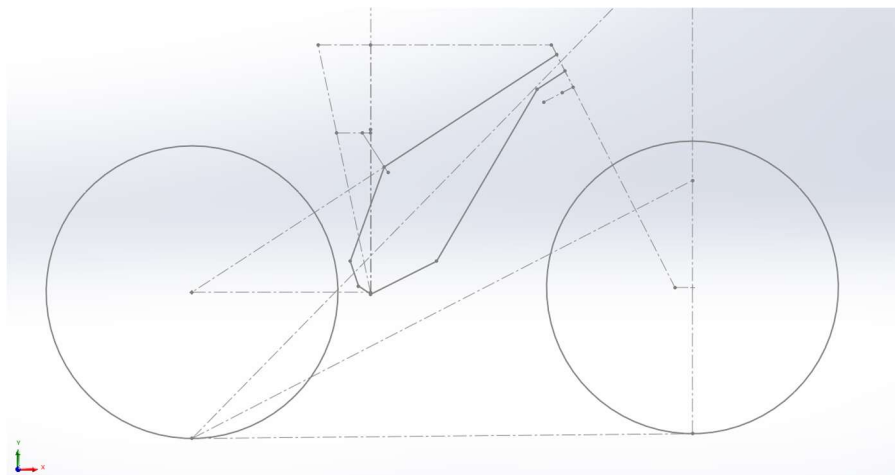


Figure 39: General lines of the main frame

This croquis will define the shape of the main frame and can be used as the extrusion path for the tubes conforming it. For this purpose, the tool *Swept Boss/Base* that permits variability of the extruded cross-section along the path and adaptation to trajectory curves is usually used. However, as per constructive restrictions standard profiles will be used for the construction of the frame, following straight lines and being of a constant section in any segment, structural members might be used for this construction. This option will not be found in the *Features* tab, but in *Weldments*, and enables to sweep a standard profile predefined in a standard library, or whatever area that may be created and added here, over a drawn croquis trajectory. This procedure has the advantage that no drawings in the transversal plane are needed in the model, and adjustment is fairly easy because of the *Trim/Extend* option, which will automatically make a union between two adjacent beams. Disadvantages are that it is not so flexible nor adaptable as the *Swept Boss/Base* option and will only allow to create segments with a well-defined and constant shape.

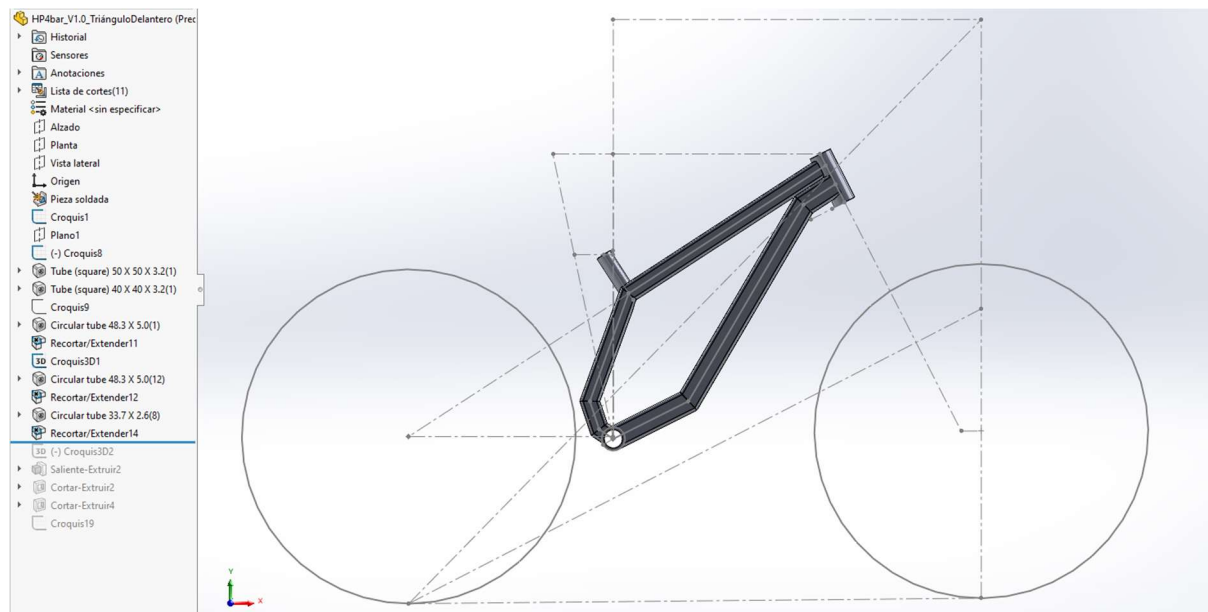


Figure 40: Profiles conforming the main frame

Once the main structure has been created, it is necessary to generate the solids that complete the structure of the front triangle, those are just the shock supports. Aforesaid pieces are to be two metal plates welded near the bottom bracket, so they will have a double function, to reinforce this part of the frame, and they shall be suitable for correct shock positioning to ensure correct suspension functioning. Now with all the parts created, holes will be made on the frame where axles are to be fitted, those are for reference only when assembling all the frame parts, so no extra material will be added for bearing housing in this phase.

For marking the geometry defining points in the main triangle, a new croquis shall be created, this will be a construction of the lines characterising the other parts of the frame, situating the pivot points as defined in the two-dimensional model. On the other hand, dimensions for the rest of the models can be directly taken from these segments, with no need of using trigonometry comparing different point's coordinates. Then, the mentioned holes are situated in those position, in this case, two are made for the chainstay pivot, to analyse a normal and a high pivot solution in both the two-dimensional and three-dimensional model, to get to know its influence in kinematics and evaluate its constructive difficulties of each.

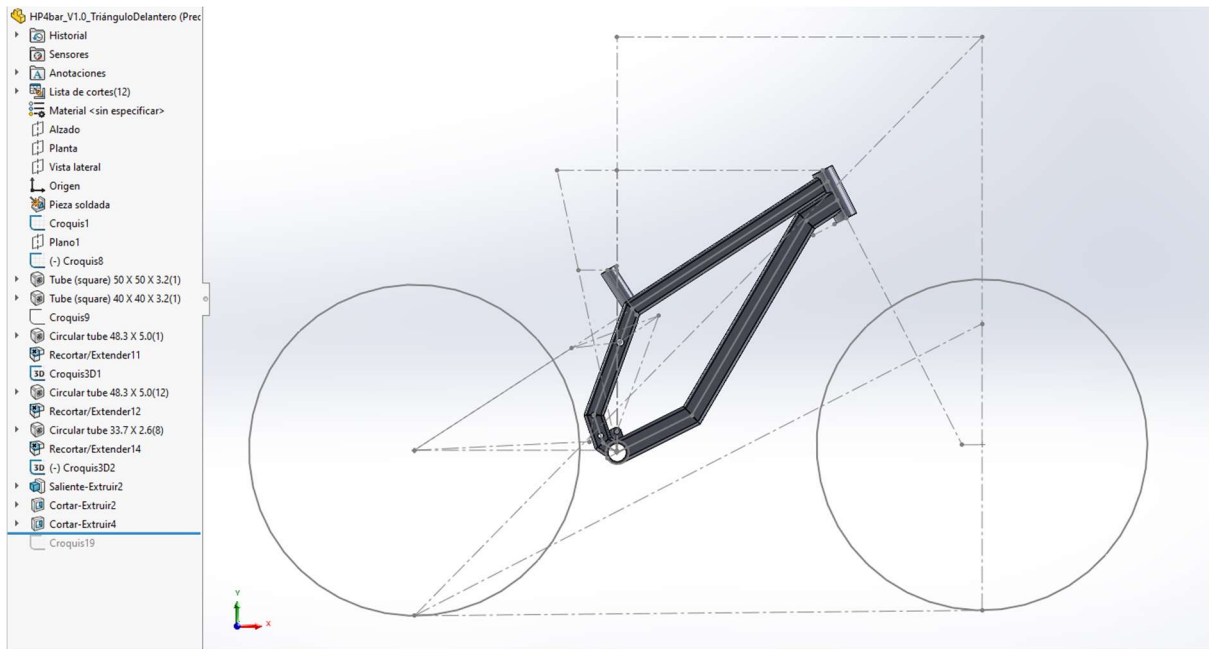


Figure 41: Version No.1 of the main frame

The next part to be created is the chainstay. In this case, a very different approach will be taken, this is a bar that connects two different parts, so both extremes shall be constituted by machined pieces. As these will be the ones delimiting the model, thinking of more flexibility for an easy modification of the part when changing geometric references, these pieces shall be the first to be created. The origin for reference will be in the main pivot point of the attachment fork with the main frame. To create the model of this machined component, a block with the outline of the cross-section is extruded and then cut to size to obtain its shape. For this version one of the model, machined parts will be square cut, no rounding radius because of the tool used in the process nor finishes to avoid edges are to be considered yet.

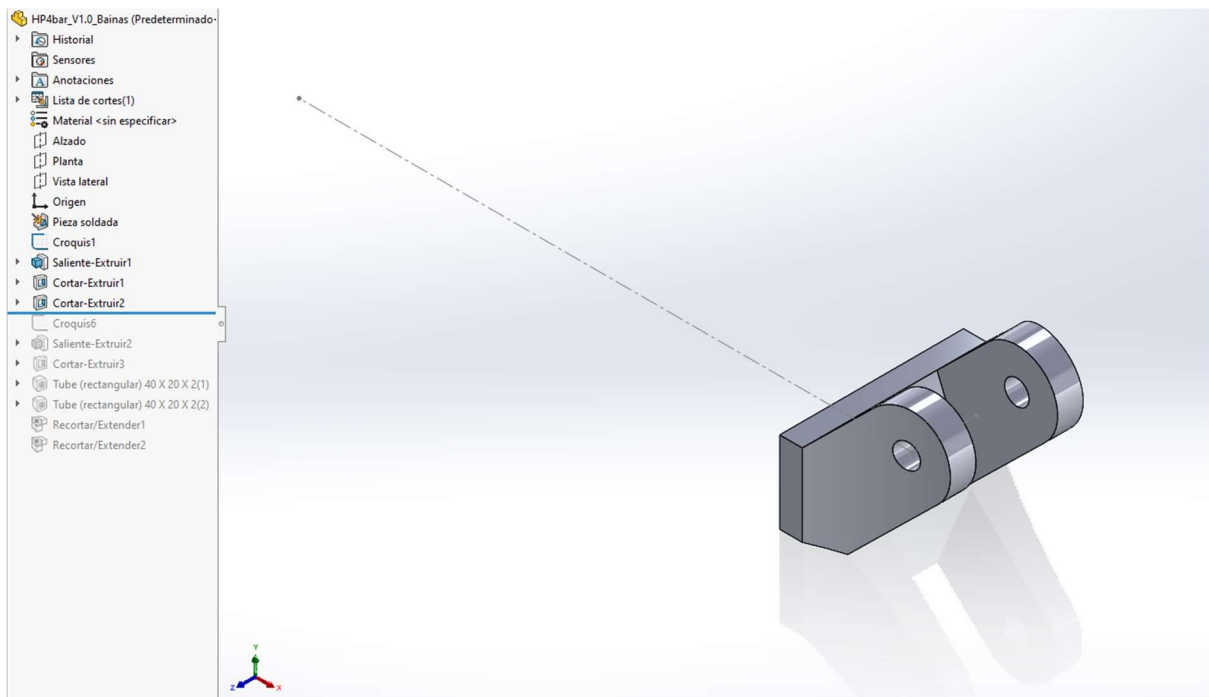


Figure 42: Attachment piece of the chainstay with the main frame

With this piece defined, the solids for the rear attachments shall be created. These will be two separate symmetrical pieces, one for each side union point with the rear bar. Being this version a test purpose model, just a solid piece with a hole situated in the linking axle will be modelled, this hole is the reference for the interaction in the assembly, this piece will later be modified in order to avoid any interference with other parts.

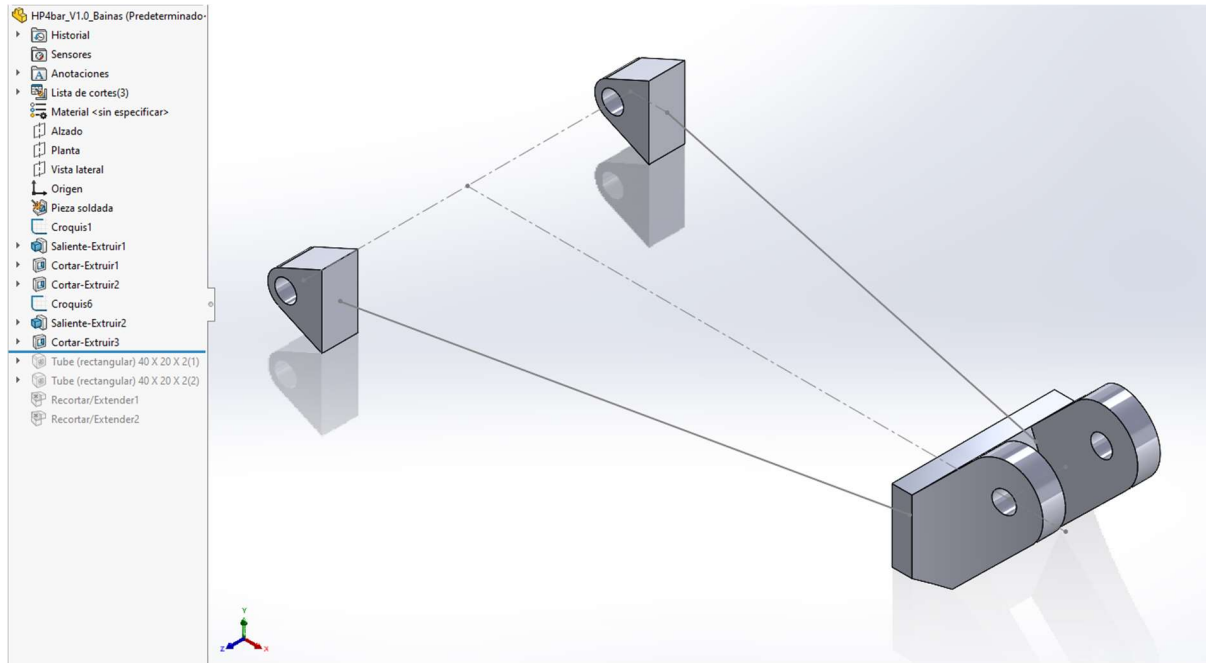


Figure 43: Solid parts of the chainstay

To complete this part's model, the tubes connecting the solid elements shall be extruded. The croquis to guide the chainstay tubes may be the same used to situate the rear attachments, in order to reduce the number of elements in the operation tree and facilitate further modifications of the part.

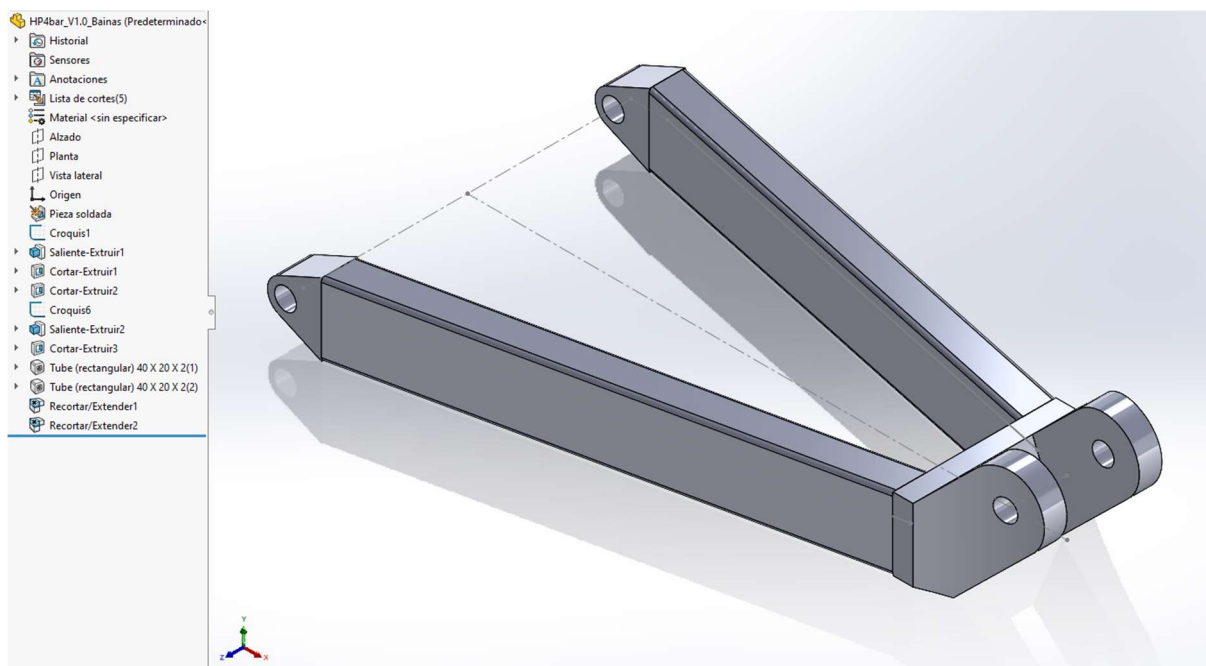


Figure 44: Version No.1 of the chainstay

The same process for the modelling of the chainstay will be reproduced to create the rear bar, which has fundamentally the same structure of solid extreme pieces bonded with intermediate tubes. In this case holes shall be made for the attachment points with the chainstay and the rocker link, and two extra perforations for the rear wheel axle. It is important to note that this part will have to have a rear brake mount in the right side and a space for the correct placement of the mech hanger in the left side, those will be added in further versions of the model.

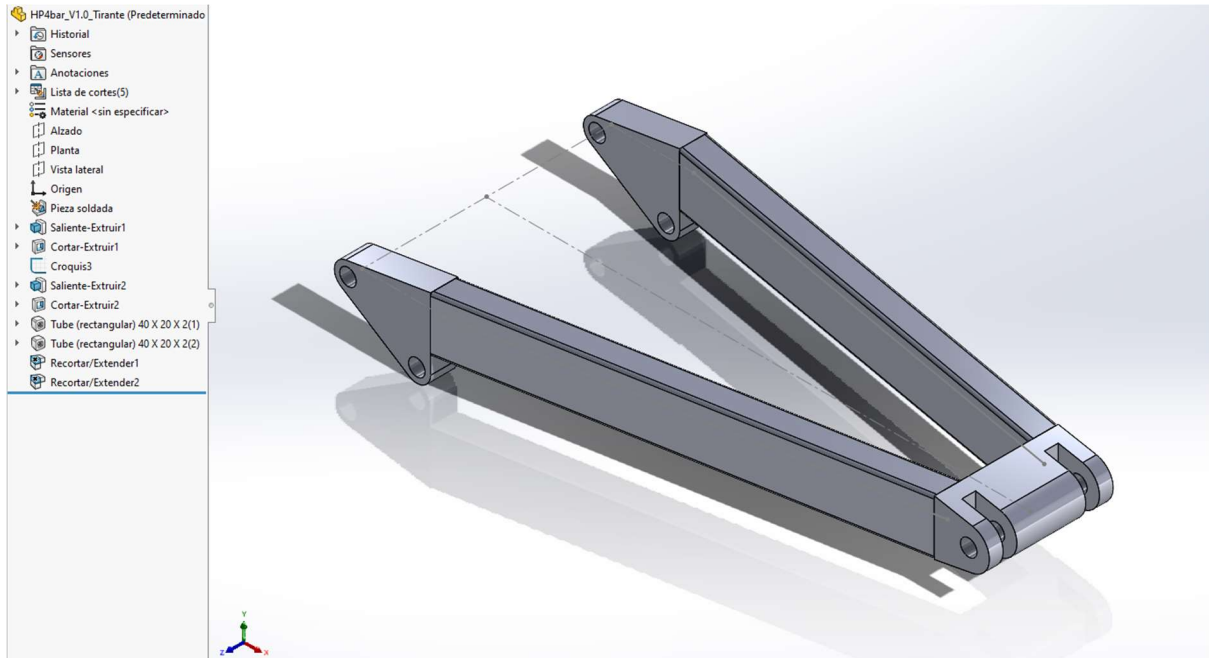


Figure 45: Version No.1 of the rear bar

The final part of the assembly is the rocker link, which is quite particular with respect all the other parts for being a solid piece with no tubes, so in this case all operations are made on a solid block of material. This part has a triangular shape defined by the attaching points with the main frame, rear bar, and shock eye mount. To reduce the number of operations to do, the initial shape extruded will have the triangular profile with rounded edges and the pertinent holes for the attachments in place.

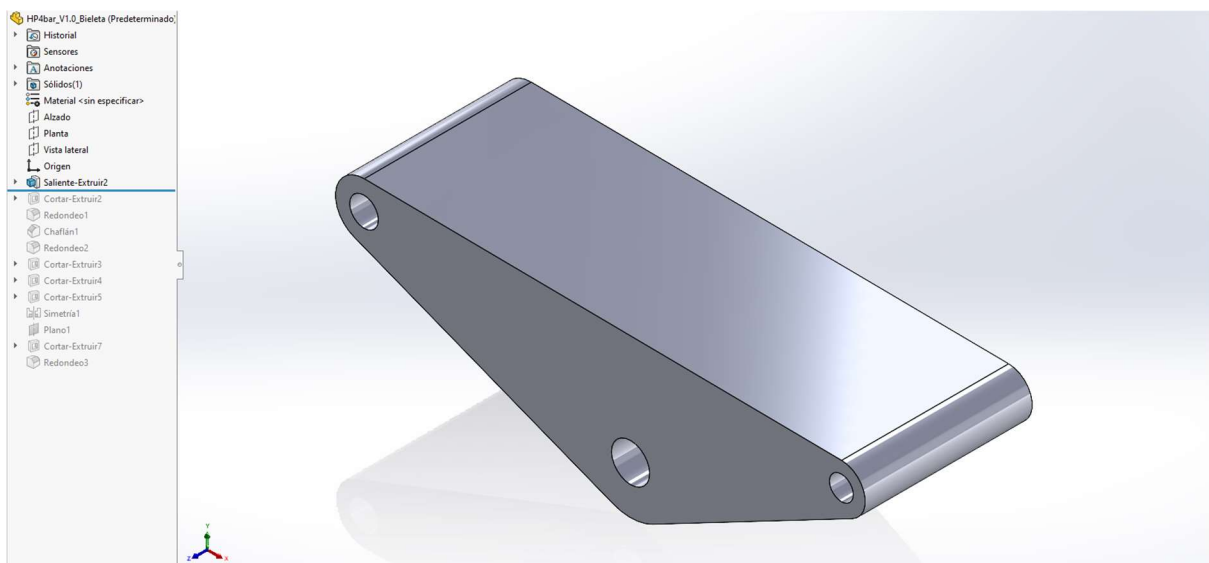


Figure 46: Initial material block for the link

In this preliminary version, for lack of data on rigidity and resistance of the part, the union between the right and left part of this piece will be arbitrarily situated behind the main frame union point, thus in the rear end of the part. A cut to permit installation of the link in the main frame shall be done, enough space so no contact in any inclination angle with the main frame is observed shall be cleared. This must be done in this iteration, even though clearance will be treated in the following, to ensure the desired geometry does not present any essential inconsistency for construction.

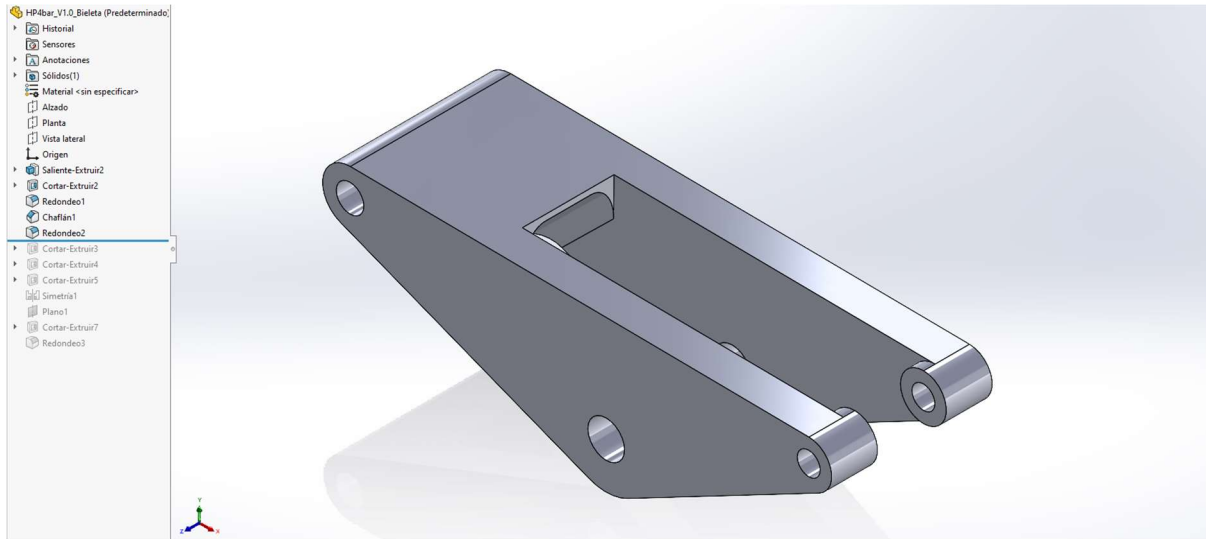


Figure 47: Extrusion of the main shape of the rocker link

Now some finishing details to enlighten the part can be cut to better visualize how a more advanced version could look, and that some material can be easily removed with the said purpose without compromising the main structure of the part. Then, to finalise this part's model, another cut is required in the rearmost section of the link, this will generate the protrusions for the attachments with the rear bar, which have to be wide enough to sit a bearing as these parts will be the housing for those in this particular interaction point.

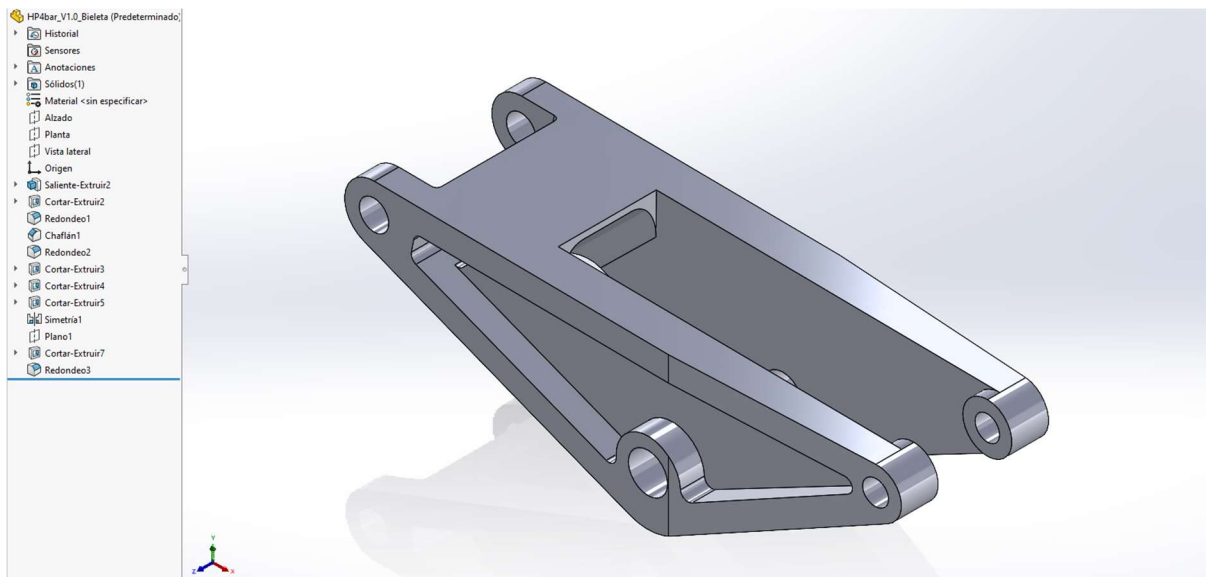


Figure 48: Version No.1 of the link

With all the individual parts modelled, an assembly of the frame concept can be constructed. To better analyse behaviour of the complete frame, the rear shock is modelled with the characteristic length

and stroke to be installed in order to give the desired rear suspension travel. For part interactions, the bottom bracket is aligned with the assembly origin point to be able to take direct measures on the model to facilitate modifications on the individual parts. Then, the main frame is fixed in the space and the rest of parts are to be floating objects restricted only by relative positioning.

Noy chainstay and rocker link are mounted in the main frame with a *concentric* relationship between the corresponding holes in the respective interaction points, then these parts are centred with the *width* option. Once those parts are situated, the rear suspension deformable parallelogram can be completed by setting interactions of the rear bar with these two last parts, again, using *concentric* and *width* interactions.

The shock is formed by two pieces, the main body, and the shaft, those shall be put together with a concentric relation, and then the stroke is restrained indicating a distance variation equal to maximum stroke between two parallel faces perpendicular to the movement direction. Then the shock can be mounted in its position adding the respective mates with the main body and rocker link.

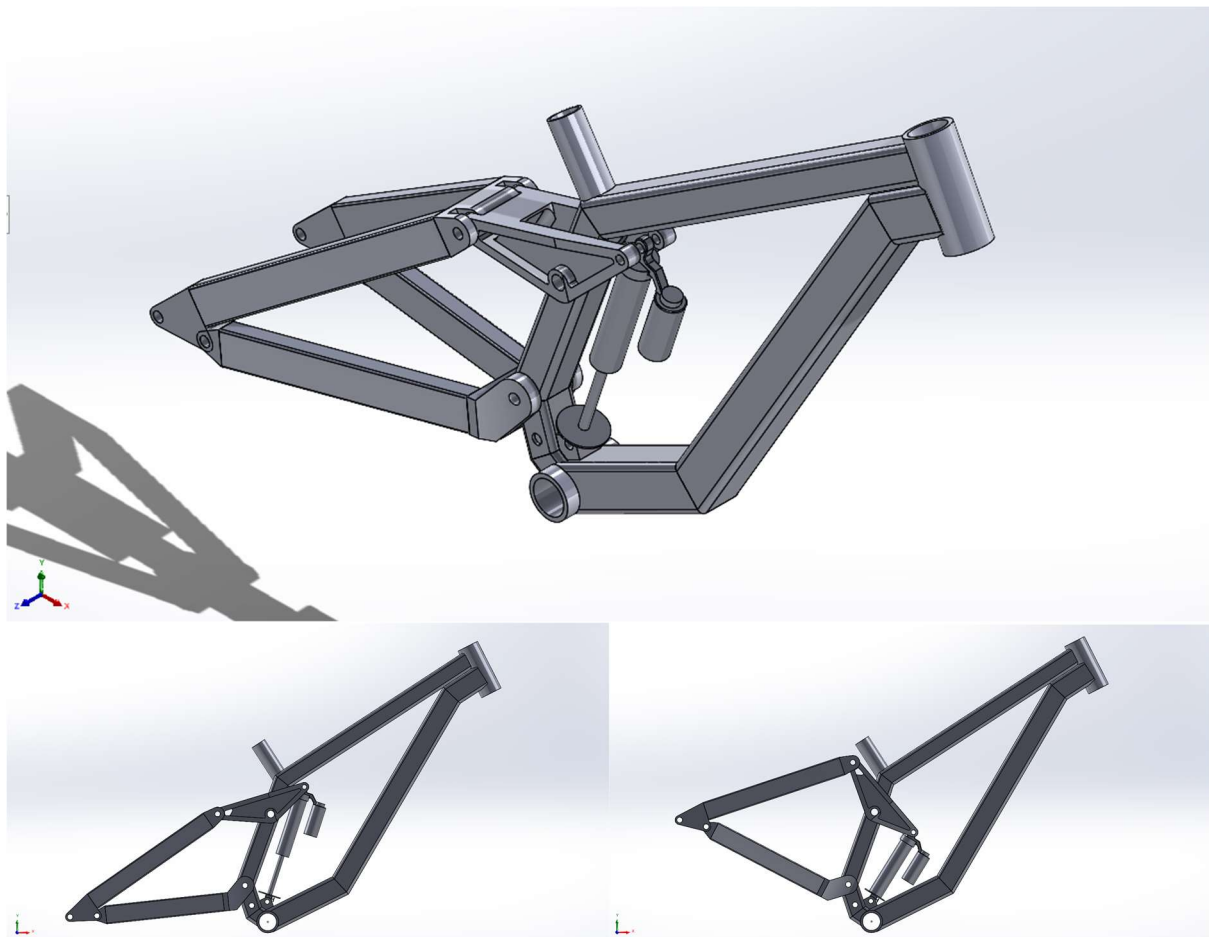


Figure 49: Version No.1 of the frame

6.3.2. VERSION No.2

At this point, having used the version No.1 as support, the two-dimensional model is deemed to be concluded thus final geometry is definitively set. This can be brought to the version No.2 of the three-dimensional model by modifying the characteristic cotes of every frame part, these modifications will not be mentioned in the following for being a general procedure common to all components. Every part has had its material associated in this version to get an approximation of frame weight for further stages. The main objective of this second version is to guarantee all bicycle components clearance.

Notwithstanding the scope of this iteration, some necessary modifications have been incorporated to each part in order to get a product with a higher grade of refinement. To start with, the main frame has seen little change from its previous version, extra tubes for bearing housing in the attachment points of the chainstay and link have been added, and the shock mount has been modified to create the two plates separated at a proper distance for the shock eye.



Figure 50: Version No.2 of the main frame

For the chainstay, all its parts have undergone some modification. The main solid piece being the attachment to the main frame has been reduced in width because of chainring interference, the tubes have been split in two sections, the first of which is now thrown back in a straight line, this is because cranks would hit this part in the first version of the chainstay, the rear section have been given more angle to reach the same width in spite of the shorter distance, and finally the rear attachments to the seatstay have been cut to fit with its counterpart of this bar.

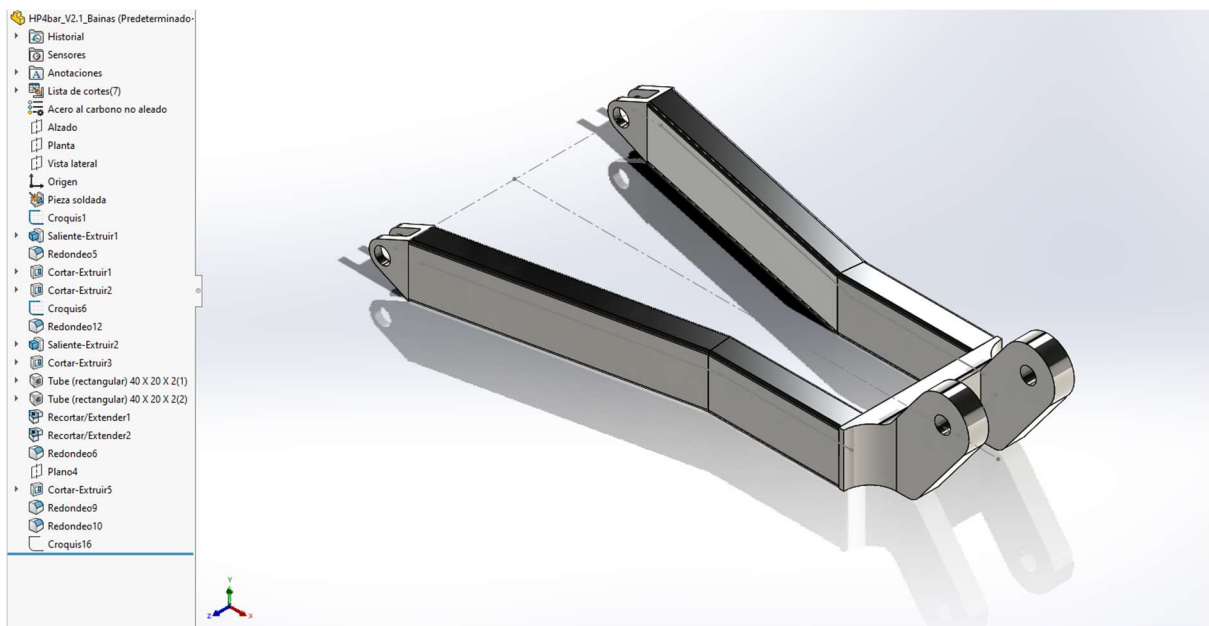


Figure 51: Version No.2 of the chainstay

The only modification other than the general ones for the seatstay is the adaptation of the attachment to the chainstay to fit this beforementioned piece. The thickness of the inferior part of the solid pieces in the rear has been reduced, at this point no further modification is deemed to be necessary for correct fitting.



Figure 52: Version No.2 of the rear bar

The link has been the part that has seen the most change in this version No.2 of the frame, as it has been completely reconceptualised. Instead of getting this piece from a single aluminium block, it has now been split in three parts, the right and left sides, and a reinforcement, which will be bonded mechanically using bolts. This new design is much more efficient with the use of raw material, much less machining is required thus the waste is very inferior using this configuration. Apart from that, this design permits to modify the stiffness of the link by changing the dimension of the reinforcement, so it can be reduced for more traction or increased for less flex in the rear end to gain control.

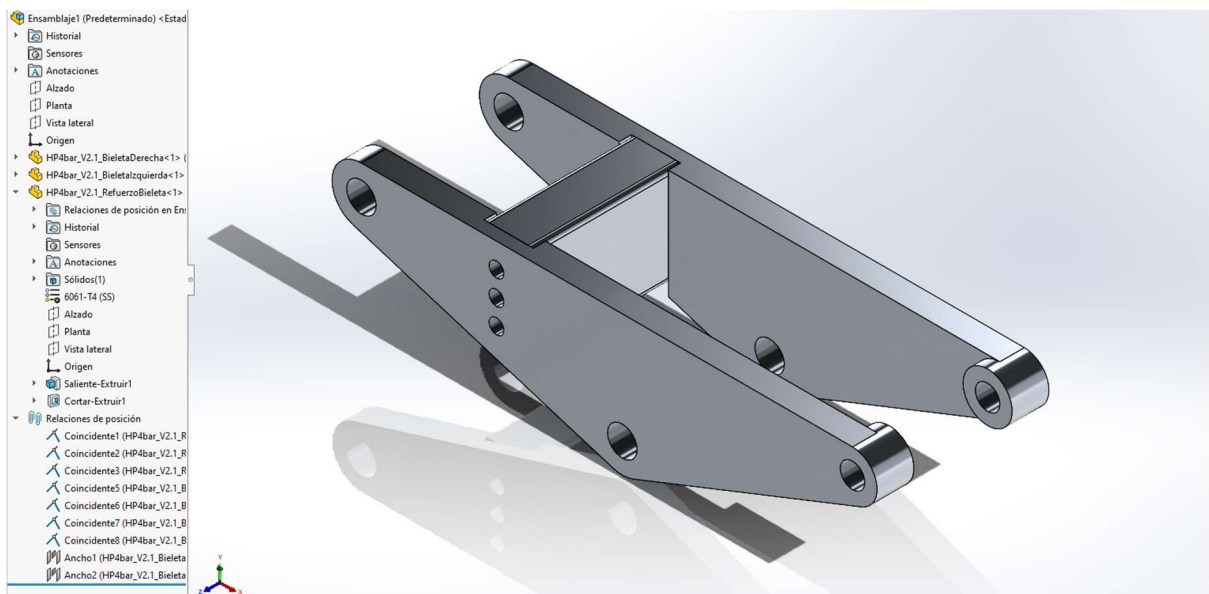


Figure 53: Version No.2 of the link

For the version No.2 of the frame's complete assembly, some extra components have been modelled to prevent any interference between them and any part of the frame at any given travel position of the rear suspension. These figures are basic, oversized models of the real components to install which unique function is to permit to analyse its compatibility with the frame and guarantee enough clearance at any position of the linkage system. The extra parts added to the frame are the previously mentioned shock, cranks assembly with the chainring, and rear wheel. The seat and seat post combination has not been added because of the high variability of its installation position, however there is enough space for it at full compression, which is the worst possible case.

Having defined every part's material, this is steel for the main frame, the chainstay, and the seatstay, and aluminium for all the pieces conforming the link, an approximation can be obtained for the frame weight, without any hardware that would compete the assembly, like bolts or bearing. This version's mass is approximately thirteen kilograms, which is way over acceptable values for a frame solo, the standard weight for a complete downhill bike would be around eighteen kilograms, being a metallic frame on four to six kilograms. Considering the material to use is mostly steel, and restrictions on design for the use of constant section tubes, which means some sections will have extra material not necessary for the frame integrity under load, the aimed weight for the frame is set around eight kilograms.



Figure 54: Version No.2 of the frame

6.3.3. VERSION No.3

In this third iteration of the frame, constructive issues will be approached, dimensions of all parts will be adapted to fit standard components and more detailed pieces will be moulded as per a near to production model. The aforesaid weight reduction needed will also be considered and measures to enlighten the frame will be taken.

The main frame has been simplified, compared to its previous version, the near to the bottom bracket section of the upper frame tube has been unified in just one piece instead of two, this facilitates the construction of this part of the frame as well as collocation of the shock supports, and will provide a more resistant structure because an additional welding will be required in the intersection of the upper and lower tubes. This will need more work for this concrete section but will benefit load transfer in the bottom bracket zone, which is the most critical of the frame.

Headtube diameter has been increased to fit a standard downhill headset, and this tube, the bottom bracket, and housings for bearings have been made a cut to standard diameter of the components to be fit up to a proper depth for correct installation. These insertion diameters are fifty-six millimetres for the headset, forty-one millimetres for a standard press-fit bottom bracket for downhill application, and thirty millimetres for external bearing diameter.



Figure 55: Version No.3 of the main frame

In the third version of the chainstay, the solid clamping piece with the main frame has been redesigned with a thinner profile, and its curves have been better aligned with the direction of the main stresses this piece will suffer to optimise its resistance to weight ratio, permitting to eliminate material not contributing to strengthen the structure.

Chainstay tubes have been again separated and a third section has been added to let enough room for the brake disc.

Finally, all bolt placements have been countersunk to hide the heads once put in place, this is to get a cleaner look but also to avoid any protrusion that could damage the user, in the same line, all sharp edges susceptible to come into contact with any part of the body during normal use or in the event of a fall have been rounded.

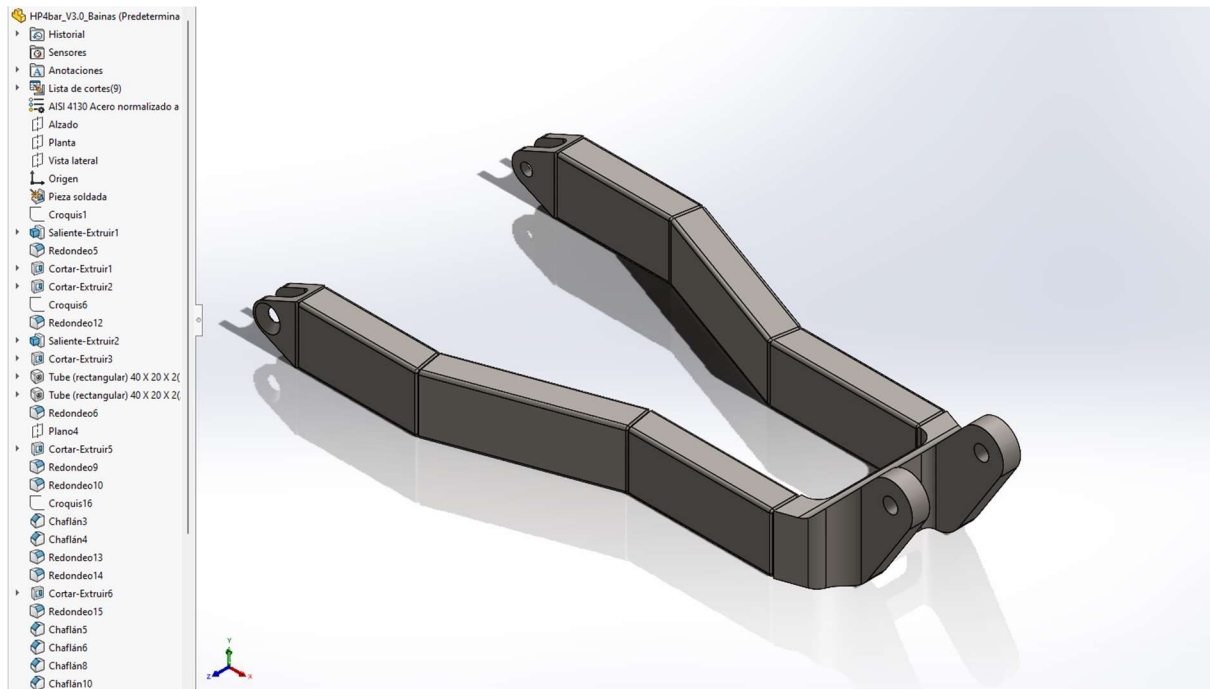


Figure 56: Version No.3 of the chainstay

The focus on rear bar modifications has been put in weight reduction, this is the part that has the most room for improvement from its last version, and the one in which lightening will have the greatest effect because of having the most and furthest unsprung mass, so this will not only reduce the frame's weight but will also enhance suspension performance and facilitate the rear end rotation. For this purpose, material used for the attachment with the link has been significantly reduced, letting two protrusions to let for a much thinner transversal section. The rear solid pieces have been overall reduced in thickness and hollowed to eliminate unnecessary mass.



Figure 57: Version No.3 of the rear bar

Finally, the link has also been highly modified in this version. The modular concept from the last iteration is maintained, but position of the union reinforcement has been brought to the front to avoid issues with shock performance because of possible relative movement and deflection of the plates. With this modification, raw material for the construction of the parts is reduced because the reinforcement itself will now be the support for the shock, and no extra thickness will be required in the lateral pieces for this purpose. The plates have been hollowed to reduce its weight while maintaining a good resistance thanks to the ribs generated.

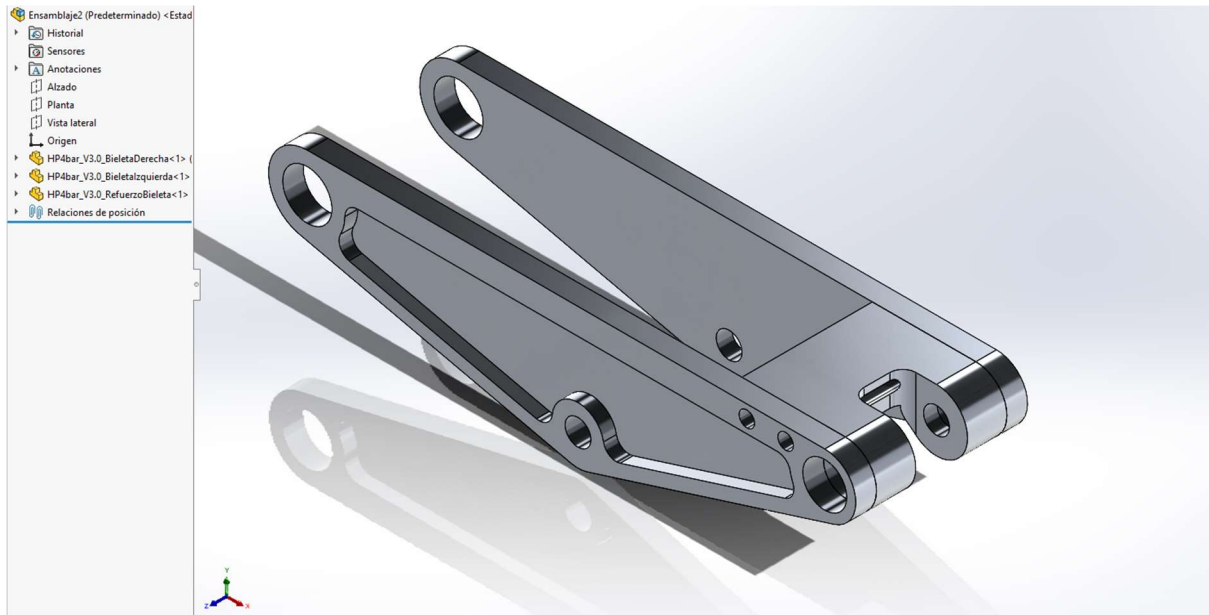


Figure 58: Version No.3 of the link

The assembly of this frame version will be created adding all the necessary hardware to complete the frame, thus all the bolts and bearings required for all the pivot points are included. This version comes at a hypothetic mass of ten and a half kilograms, which is already an improvement on the last version, moreover, considering all the extra parts that have been included, but it is still far from the weight objective for the frame.

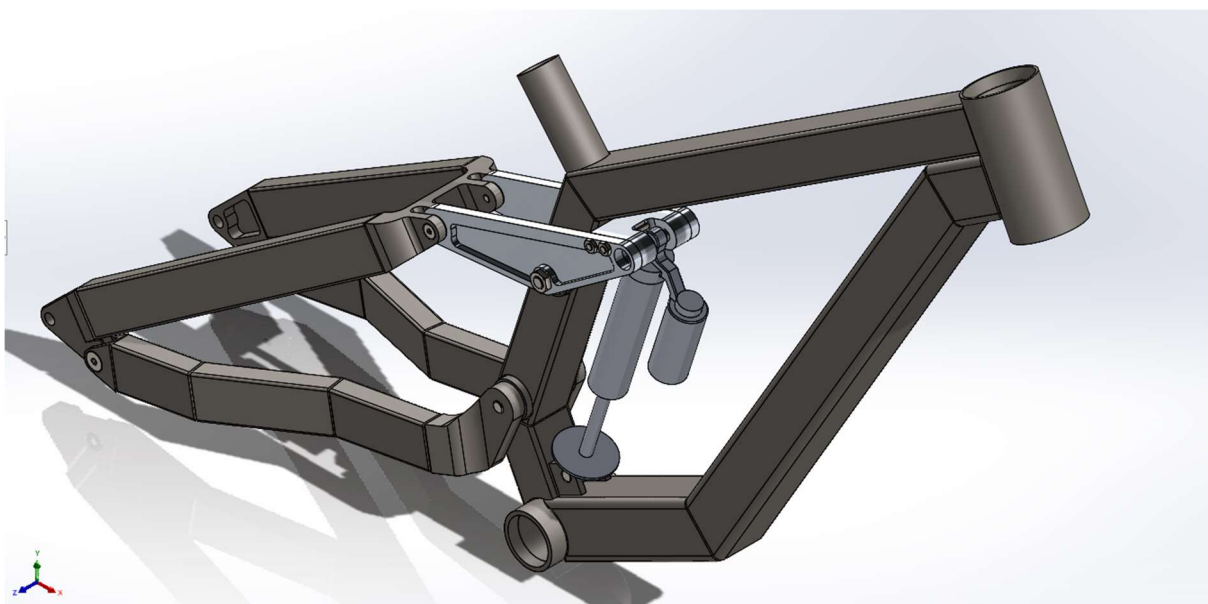


Figure 59: Version No.3 of the frame

6.3.4. VERSION No.4

This is an improvement on the last frame version by the use of the data obtained in the study of frame resistance via simulation method as described in the next section (see point 7.2.). Changes have been added for both, to increase structural resistance as required and to optimise weigh.

Modifications on the main triangle have been made mainly in the seat tube area. The previous design was not resistant enough to withstand forces applied on the seat, so the insertion tube has been extended to be welded to the inferior face of the frame tube, and a rib has been added as a reinforcement. Initial thickness of the inferior tube, which had been set arbitrarily, has been reduced for offering enough resistance.

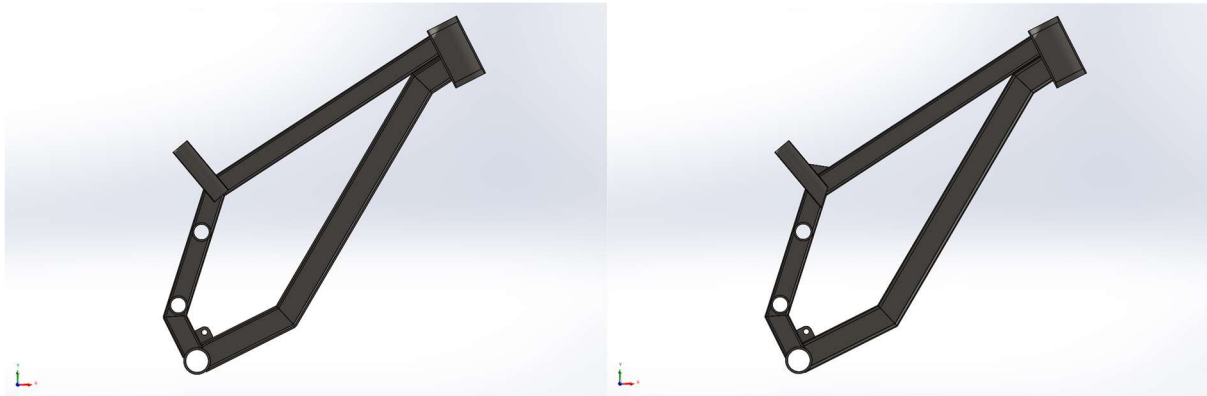


Figure 60: Comparison of cut section of version No.3 (left) and No.4 (right) of the main frame

The chainstay have not been changed in this version, the tubes of this part have an appropriate section and all modifications introduced in last version for weight reduction provide for a resistant enough design with all the benefits of being now a lighter piece.

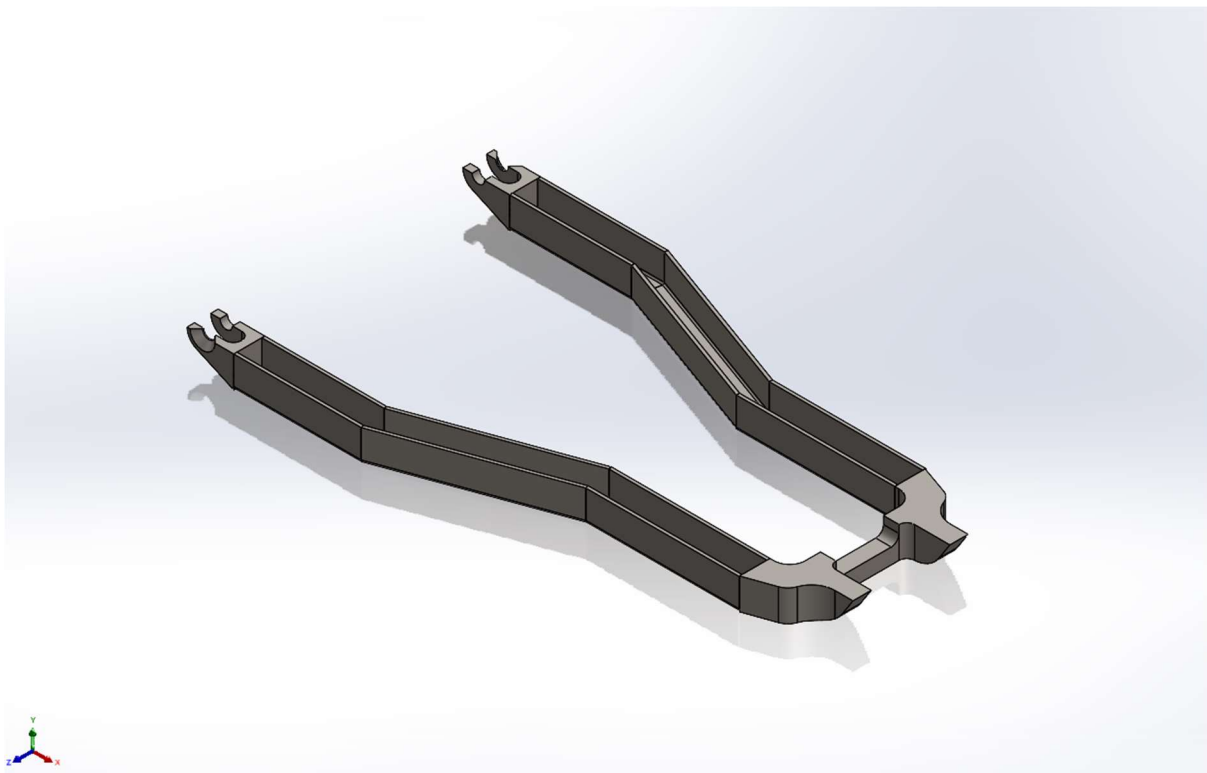


Figure 61: Cut section of the chainstay

The rear solid pieces of the seatstay have been modified to permit to install all the hardware needed to build a complete bicycle, a brake mount has been extruded in the left side and the right part has been adapted to fit a mech hanger. It has been possible in this case to reduce the thickness of the tubes of this part to reduce weight and still maintain resistance and enough rigidity.

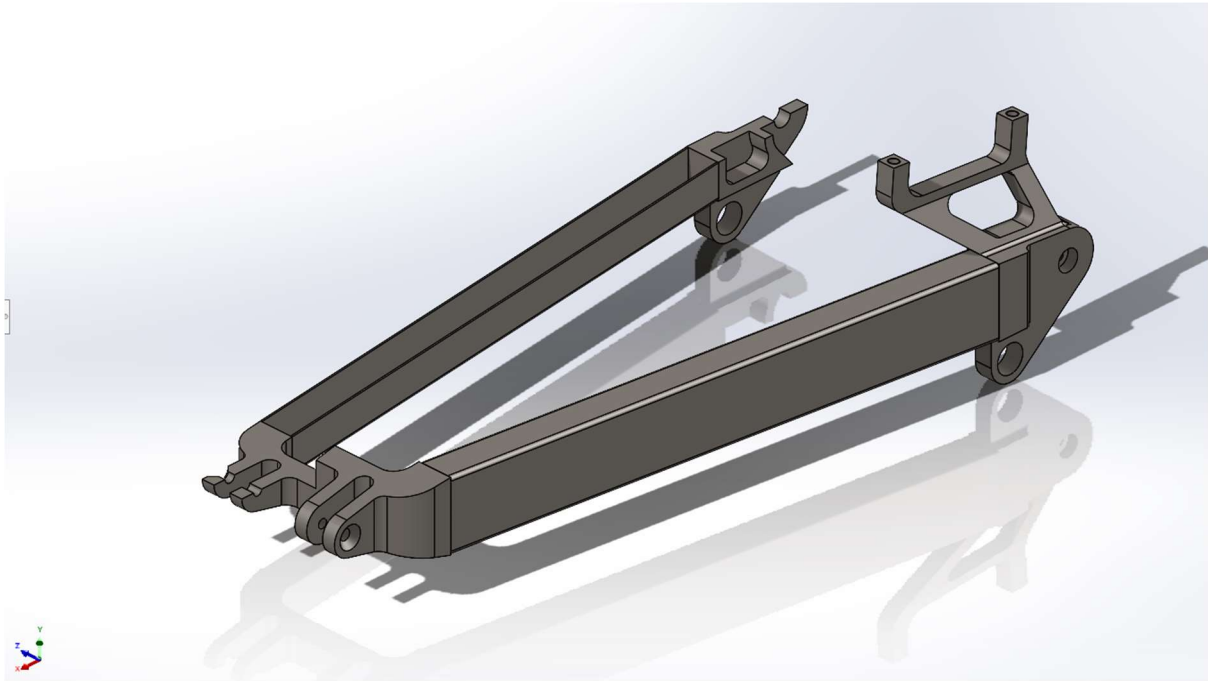


Figure 62: Changes introduced in version No.4 of the chainstay

The link design also remains unchanged, and in this version, it has only been proven that modifications introduced in the latest iteration provide for a properly resistant part and deflection of the plates is in under acceptable values.

For the complete assembly of the version No.4 of the frame, the shock has been substituted by a rigid part that sits the suspension in sag position as described in ISO 4120 for the conduct of test.

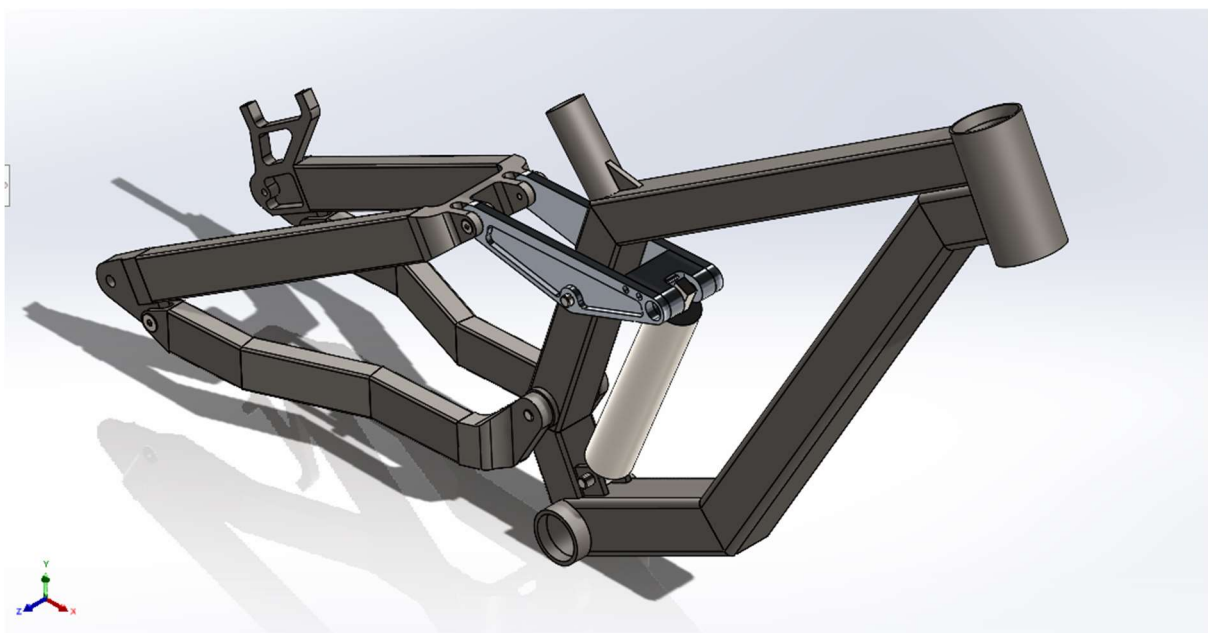


Figure 63: Version No.4 of the frame

7. COMPUTER AIDED ENGINEERING

7.1. CALCULATION MODEL

To get more accurate results of the resistance and durability of frame components, the model has been spread in subassemblies and every part has been tested independently. Those separately studied parts have been the main frame, the chainstay, the seatstay, and the link.

To correctly analyse every one of those parts, it is necessary to know actions and reactions between them when a force is applied in any point of the bicycle, so a calculus model must be developed to get to know these interactions. This will be made assuming solid rigid parts, which is justified by the little deformations observed in the complete assembly (see annex V).

7.1.1. TWO-DIMENSIONAL ANALYSIS

For the purpose of getting component interactions, a two-dimensional analysis of the assembly may be used. Reactions can then be extrapolated to a three-dimensional model because of constructive symmetry of the frame (see point 7.2.). This simplification provides for a much simpler equilibrium equations system, easier to work with than a three-dimensional model. The equation system is obtained by considering six elements, those are the four frame subassemblies, the shock, and the fork, and using eight nodes: upper and lower attaching points of the fork in the headtube, chainstay and link unions with the main frame, rear bar attaching points with the chainstay and link, and the two mounting points of the shock in the main frame and in the link.

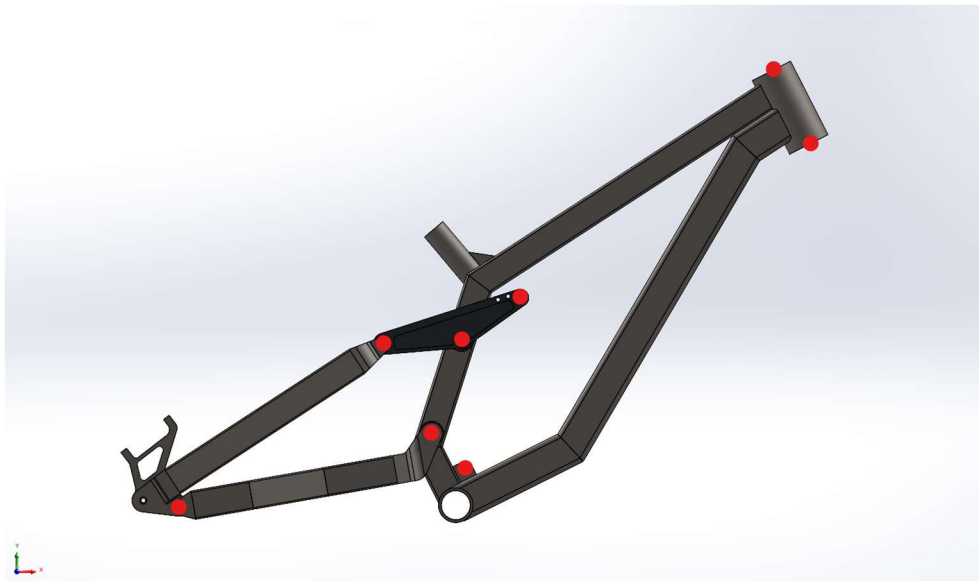


Figure 64: In red, nodes for the two-dimensional calculus model

For abbreviation purpose, from now on the following notation will be used. Every component will have its index, these will be:

F: Fork

1: Main frame

2: Chainstay

3: Rear bar

4: Link

S: Shock

And every variable will be given two subindexes in the form:

$$x_{ij}$$

Where:

i = index of the bar where the force is applied

j = index of the bar applying the force

Note: For the particular case of the fork and main frame interaction, a third subindex will be added, noting if it is the interaction produced on top (t) or bottom (b) of the headtube.

So, for example, the force applied in the shock mount to the main frame will be F_{1s} , and the reaction generated by this in the shock will be F_{s1} , being F_{1s} and F_{s1} forces of equal modulus and direction but contrary sense.

In a similar way, nodal coordinates with respect to the bottom bracket as the reference point, will also be expressed with the same subindex notation.

For external forces, its subindex will indicate the exact point of application, which will be defined in the respective equations.

Now, equations for equilibrium of forces in the x and y axis, and momentums in the z axis for every element can be written. Starting with the fork, those would be: (Equation 7)

$$\left\{ \begin{array}{l} \sum F_x = 0; Fx_{F1t} + Fx_{F1b} + Fx_{FW} = 0 \\ \sum F_y = 0; (Fy_{F1t} \vee Fy_{F1b}) + Fy_{FW} = 0 \\ \sum M_{F1t} = 0; -Fx_{F1b} \cdot (y_{F1b} - y_{F1t}) - Fx_{FW} \cdot (y_{FW} - y_{F1t}) + Fy_{F1b} \cdot (x_{F1b} - x_{F1t}) \\ \quad + Fy_{FW} \cdot (x_{FW} - x_{F1t}) = 0 \end{array} \right.$$

Where:

FW = subindex for Front Wheel axle

Note: $Fy_{F1t} \vee Fy_{F1b}$ are in an "or" function, this is because the headset uses angular contact ball bearings, so they can absorb only compression forces. Depending on the sense of the vertical force applied on the wheel, the reaction in this direction will be produced by the top or bottom bearing.

For the main frame, which is the element with the most interactions, equilibrium is defined as follows: (Equation 8)

$$\left\{ \begin{array}{l} \sum F_x = 0; Fx_{1Ft} + Fx_{1Fb} + Fx_{1s} + Fx_{12} + Fx_{14} + Fx_{BB} + Fx_{HT} + Fx_{SP} = 0 \\ \sum F_y = 0; Fy_{1Ft} + Fy_{1Fb} + Fy_{1s} + Fy_{12} + Fy_{14} + Fy_{BB} + Fy_{HT} + Fy_{SP} = 0 \\ \sum M_{BB} = 0; -Fx_{1Ft} \cdot y_{1Ft} - Fx_{1Fb} \cdot y_{1Fb} - Fx_{1s} \cdot y_{1s} - Fx_{12} \cdot y_{12} - Fx_{14} \cdot y_{14} - Fx_{HT} \cdot y_{HT} - Fx_{SP} \cdot y_{SP} \\ \quad + Fy_{1Ft} \cdot x_{1Ft} + Fy_{1Fb} \cdot x_{1Fb} + Fy_{1s} \cdot x_{1s} + Fy_{12} \cdot x_{12} + Fy_{14} \cdot x_{14} + Fy_{HT} \cdot x_{HT} + Fy_{SP} \cdot x_{SP} = 0 \end{array} \right.$$

Where:

BB = subindex for Bottom Bracket

HT = subindex for Head Tube

SP = subindex for Seat Post

The next subassembly to study is the chainstay, which being a simple bar, effectively just defines interaction between the main frame and the rear bar: (Equation 9)

$$\left\{ \begin{array}{l} \sum F_x = 0 ; Fx_{21} + Fx_{23} = 0 \\ \sum F_y = 0 ; Fy_{21} + Fy_{23} = 0 \\ \sum M_{23} = 0 ; -Fx_{21} \cdot (y_{21} - y_{23}) + Fy_{21} \cdot (x_{21} - x_{23}) = 0 \end{array} \right.$$

For the rear bar equations, we have to take into account that the rear wheel is attached to this component: (Equation 10)

$$\left\{ \begin{array}{l} \sum F_x = 0 ; Fx_{32} + Fx_{34} + Fx_{RW} = 0 \\ \sum F_y = 0 ; Fy_{32} + Fy_{34} + Fy_{RW} = 0 \\ \sum M_{32} = 0 ; -Fx_{34} \cdot (y_{34} - y_{32}) - Fx_{RW} \cdot (y_{RW} - y_{32}) + Fy_{34} \cdot (x_{34} - x_{32}) + Fy_{RW} \cdot (x_{RW} - x_{32}) = 0 \end{array} \right.$$

Where:

RW = subindex for Rear Wheel axle

Then, the forces applied in the linkage have to accomplish: (Equation 11)

$$\left\{ \begin{array}{l} \sum F_x = 0 ; Fx_{41} + Fx_{43} + Fx_{4S} = 0 \\ \sum F_y = 0 ; Fy_{41} + Fy_{43} + Fy_{4S} = 0 \\ \sum M_{43} = 0 ; -Fx_{41} \cdot (y_{41} - y_{43}) - Fx_{4S} \cdot (y_{4S} - y_{43}) + Fy_{41} \cdot (x_{41} - x_{43}) + Fy_{4S} \cdot (x_{4S} - x_{43}) = 0 \end{array} \right.$$

Finally, equilibrium equations for the shock are the following: (Equation 12)

$$\left\{ \begin{array}{l} \sum F_x = 0 ; Fx_{S1} + Fx_{S4} = 0 \\ \sum F_y = 0 ; Fy_{S1} + Fy_{S4} = 0 \\ \sum M_{S1} = 0 ; -Fx_{S4} \cdot (y_{S4} - y_{S1}) + Fy_{S4} \cdot (x_{S4} - x_{S1}) = 0 \end{array} \right.$$

However, using the summatory in x and y axis for the shock would result in a redundant system, it is import though the momentum equation for the z axis, because the shock is a simple bar, so this will define the only direction in which forces can be applied to this component.

Once defined, the system can be solved with any resolution method. In this case, a matrix method has been used (see annex VI) for ease of adaptation to any load condition. All the mentioned equations have been indexed in a matrix which product with the variables vector equals to the external nodal inputs vector. Thus, the system resolution is as follows:

$$M \cdot x = f ; x = M^{-1} \cdot f \quad \text{(Equation 13)}$$

Where:

M = equation matrix

x = variables vector

f = external loads vector

7.1.2. THREE-DIMENSIONAL ANALYSIS

A nodal analysis of the three-dimensional structure would be the most precise option. For this calculus a system with 6 elements, those are the four mentioned subassemblies plus the fork and the shock, and 12 nodes: upper and lower parts of the headtube (those are the contact points between the main frame and the fork), left and right contact points of the main frame with both, the chainstay, and the link, left and right unions of the rear bar with the chainstay and the link, and two shock attachment points, one in the main frame and the other in the link.

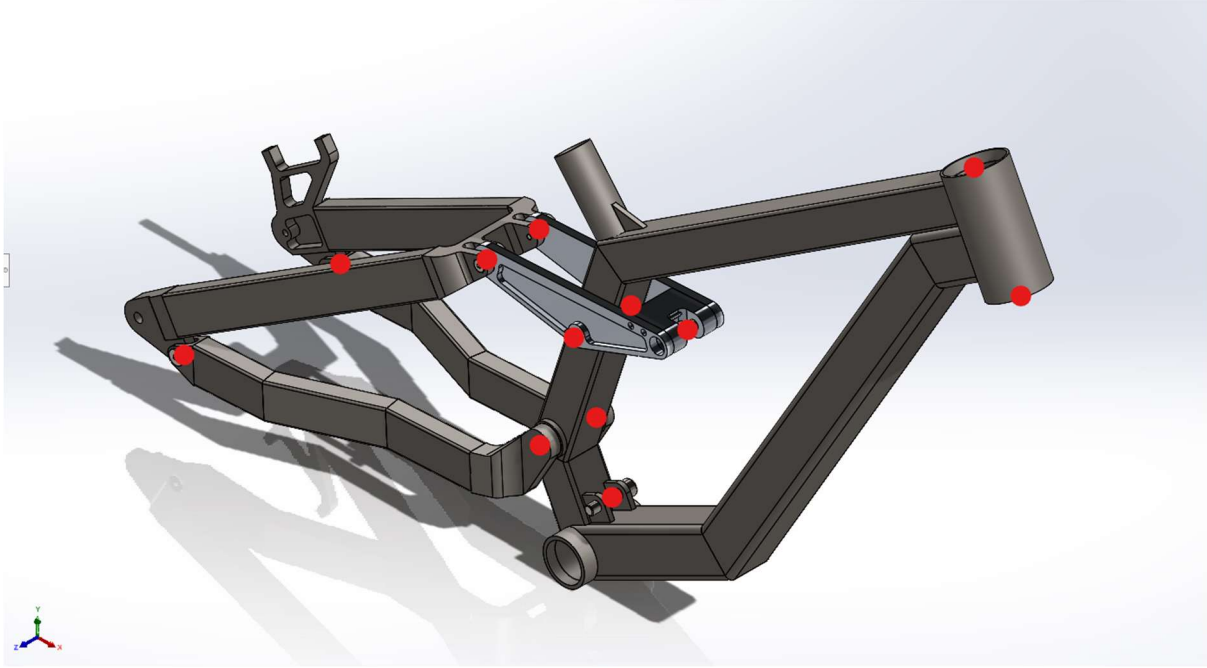


Figure 65: In red, nodes for the three-dimensional calculus model

This configuration provides for six equilibrium equations (forces and momentums in every axis) for every element, and three variables for each node, thus a thirty-six equations system with thirty-six variables.

Just like for the two-dimensional model, a subindex nomenclature system will be used, apart from the forementioned two indexes referring the parts connected in the referred node, where applicable, a third index will be added, this will refer to respective position of said point in the Z axle, being *L* (left) for negative and *R* (right) for positive coordinates.

Starting with the fork, equilibrium equations are:

(Equation 14)

$$\left\{ \begin{array}{l} \sum F_x = 0; Fx_{F1t} + Fx_{F1b} + Fx_{FW} = 0 \\ \sum F_y = 0; (Fy_{F1t} \vee Fy_{F1b}) + Fy_{FW} = 0 \\ \sum F_z = 0; Fz_{F1t} + Fz_{F1b} + Fz_{FW} = 0 \\ \sum Mx_{F1t} = 0; +Fz_{F1b} \cdot (y_{F1b} - y_{F1t}) + Fz_{FW} \cdot (y_{FW} - y_{F1t}) = 0 \\ \sum My_{F1t} = 0; -Fz_{F1b} \cdot (x_{F1b} - x_{F1t}) - Fz_{FW} \cdot (x_{FW} - x_{F1t}) = 0 \\ \sum Mz_{F1t} = 0; -Fx_{F1b} \cdot (y_{F1b} - y_{F1t}) - Fx_{FW} \cdot (y_{FW} - y_{F1t}) + Fy_{F1b} \cdot (x_{F1b} - x_{F1t}) \\ \quad + Fy_{FW} \cdot (x_{FW} - x_{F1t}) = 0 \end{array} \right.$$

Thus, for the main frame it can be written:

(Equation 15)

$$\left\{ \begin{array}{l} \sum F_x = 0; Fx_{1Ft} + Fx_{1Fb} + Fx_{1S} + Fx_{12} + Fx_{12L} + Fx_{14R} + Fx_{14} + Fx_{BB} + Fx_{HT} + Fx_{SP} = 0 \\ \sum F_y = 0; Fy_{1F} + Fy_{1Fb} + Fy_{1S} + Fy_{12R} + Fy_{12L} + Fy_{14R} + Fy_{14L} + Fy_{BB} + Fy_{HT} + Fy_{SP} = 0 \\ \sum F_z = 0; Fz_{1Ft} + Fz_{1Fb} + Fz_{12} + Fz_{12L} + Fz_{14R} + Fz_{14L} + Fz_{BB} + Fz_{HT} + Fz_{SP} = 0 \\ \sum Mx_{BB} = 0; -Fy_{12} \cdot z_{12R} - Fy_{12L} \cdot z_{12L} - Fy_{14} \cdot z_{14} - Fy_{14} \cdot z_{14} - Fz_{1Ft} \cdot y_{1Ft} + Fz_{1Fb} \cdot y_{1F} \\ \quad + Fz_{12} \cdot y_{12} + Fz_{12} \cdot y_{12} + Fz_{14} \cdot y_{14} + Fz_{14} \cdot y_{14} + Fz_{HT} \cdot y_{HT} + Fz_{SP} \cdot y_{SP} = 0 \\ \sum My_{BB} = 0; +Fx_{12} \cdot z_{12} + Fx_{12} \cdot z_{12L} + Fx_{14} \cdot z_{14} + Fx_{14} \cdot z_{14} - Fz_{1F} \cdot x_{1Ft} - Fz_{1Fb} \cdot x_{1Fb} \\ \quad - Fz_{12} \cdot x_{12} - Fz_{12} \cdot x_{12} - Fz_{14} \cdot x_{14} - Fz_{14} \cdot x_{14} - Fz_{HT} \cdot x_{HT} - Fz_{SP} \cdot x_{SP} = 0 \\ \sum Mz_{BB} = 0; -Fx_{1Ft} \cdot y_{1Ft} - Fx_{1Fb} \cdot y_{1Fb} - Fx_{1S} \cdot y_{1S} - (Fx_{12R} + Fx_{12}) \cdot y_{12} - (Fx_{14} + Fx_{14L}) \cdot y_{14} \\ \quad - Fx_{HT} \cdot y_{HT} - Fx_{SP} \cdot y_{SP} + Fy_{1Ft} \cdot x_{1Ft} + Fy_{1Fb} \cdot x_{1Fb} + Fy_{1S} \cdot x_{1S} + (Fy_{12} + Fy_{12L}) \cdot x_{12} \\ \quad + (Fy_{14R} + Fy_{14L}) \cdot x_{14} + Fy_{HT} \cdot x_{HT} + Fy_{SP} \cdot x_{SP} = 0 \end{array} \right.$$

Equations for the chainstay are as follows:

(Equation 16)

$$\left\{ \begin{array}{l} \sum F_x = 0; Fx_{21R} + Fx_{21} + Fx_{23R} + Fx_{23} = 0 \\ \sum F_y = 0; Fy_{21R} + Fy_{21L} + Fy_{23R} + Fy_{23} = 0 \\ \sum F_z = 0; Fz_{21} + Fz_{21} + Fz_{23} + Fz_{23L} = 0 \\ \sum Mx_{23L} = 0; -Fy_{21} \cdot (z_{21} - z_{23L}) - Fy_{21} \cdot (z_{21L} - z_{23}) - Fy_{23} \cdot (z_{23} - z_{23L}) \\ \quad + (Fz_{21R} + Fz_{21}) \cdot (y_{21} - y_{23}) = 0 \\ \sum My_{23} = 0; +Fx_{21R} \cdot (z_{21R} - z_{23}) + Fx_{21} \cdot (z_{21L} - z_{23L}) + Fx_{23} \cdot (z_{23} - z_{23}) \\ \quad - (Fz_{21R} + Fz_{21L}) \cdot (x_{21} - x_{23}) = 0 \\ \sum Mz_{23L} = 0; -(Fx_{21R} + Fx_{21}) \cdot (y_{21} - y_{23}) + (Fy_{21} + Fy_{21L}) \cdot (x_{21} - x_{23}) = 0 \end{array} \right.$$

Then, for the chainstay, equilibrium will be acquired if:

(Equation 17)

$$\left\{ \begin{array}{l} \sum F_x = 0; Fx_{32R} + Fx_{32L} + Fx_{34} + Fx_{34} + Fx_{RWR} + Fx_{RWL} = 0 \\ \sum F_y = 0; Fy_{32} + Fy_{32L} + Fy_{34R} + Fy_{34} + Fy_{RWR} + Fy_{RWL} = 0 \\ \sum F_z = 0; Fz_{32} + Fz_{32L} + Fz_{34R} + Fz_{34} + Fz_{RWR} + Fz_{RWL} = 0 \\ \sum Mx_{32} = 0; -Fy_{34R} \cdot (z_{34} - z_{32}) - Fy_{34L} \cdot (z_{34L} - z_{32}) - Fy_{32R} \cdot (z_{32R} - z_{32}) \\ \quad - Fy_{RWR} \cdot (z_{RWR} - z_{32L}) - Fy_{RWL} \cdot (z_{RWL} - z_{32L}) + (Fz_{34} + Fz_{34}) \cdot (y_{34} - y_{32}) \\ \quad + (Fz_{RWR} + Fz_{RWL}) \cdot (y_{RW} - y_{32}) = 0 \\ \sum My_{32} = 0; +Fx_{34R} \cdot (z_{34R} - z_{32}) + Fx_{34} \cdot (z_{34} - z_{32}) + Fx_{32R} \cdot (z_{32} - z_{32L}) \\ \quad + Fx_{RWR} \cdot (z_{RWR} - z_{32}) + Fx_{RWL} \cdot (z_{RWL} - z_{32}) - (Fz_{34} + Fz_{34L}) \cdot (x_{34} - x_{32}) \\ \quad - (Fz_{RWR} + Fz_{RWL}) \cdot (x_{RW} - x_{32}) = 0 \\ \sum Mz_{32} = 0; -(Fx_{34R} - Fx_{34L}) \cdot (y_{34} - y_{32}) - (Fx_{RWR} + Fx_{RWL}) \cdot (y_{RW} - y_{32}) \\ \quad + (Fy_{34R} + Fy_{34L}) \cdot (x_{34} - x_{32}) + (Fy_{RWR} + Fy_{RWL}) \cdot (x_{RW} - x_{32}) = 0 \end{array} \right.$$

Equations for the link are:

(Equation 18)

$$\left\{ \begin{array}{l} \sum F_x = 0; Fx_{41R} + Fx_{41L} + Fx_{43R} + Fx_{43L} + Fx_{4S} = 0 \\ \sum F_y = 0; Fy_{41} + Fy_{41L} + Fy_{43R} + Fy_{43L} + Fy_{4S} = 0 \\ \sum F_z = 0; Fz_{41R} + Fz_{41} + Fz_{43R} + Fz_{43} + Fz_{4S} = 0 \\ \sum M_{x_{43L}} = 0; -Fy_{41R} \cdot (z_{41R} - z_{43L}) - Fy_{41} \cdot (z_{41L} - z_{43}) - Fy_{43} \cdot (z_{43} - z_{43}) \\ \quad - Fy_{4S} \cdot (z_{4S} - z_{43}) + (Fz_{41R} + Fz_{41L}) \cdot (y_{41} - y_{43}) + Fz_{4S} \cdot (y_{4S} - y_{43}) = 0 \\ \sum M_{y_{43}} = 0; +Fx_{41R} \cdot (z_{41R} - z_{43L}) + Fx_{41L} \cdot (z_{41} - z_{43}) + Fx_{43R} \cdot (z_{43R} - z_{43}) \\ \quad + Fx_{4S} \cdot (z_{4S} - z_{43}) - (Fz_{41R} + Fz_{41}) \cdot (x_{41} - x_{43}) - Fz_{4S} \cdot (x_{4S} - x_{43}) = 0 \\ \sum M_{z_{43}} = 0; -(Fx_{41R} - Fx_{41L}) \cdot (y_{41} - y_{43}) - Fx_{4S} \cdot (y_{4S} - y_{43}) \\ \quad + (Fy_{41R} + Fy_{41L}) \cdot (x_{41} - x_{43}) + Fy_{4S} \cdot (x_{4S} - x_{43}) = 0 \end{array} \right.$$

And finally, for the shock:

(Equation 19)

$$\left\{ \begin{array}{l} \sum F_x = 0; Fx_{S1} + Fx_{S4} = 0 \\ \sum F_y = 0; Fy_{S1} + Fy_{S4} = 0 \\ \sum F_z = 0; Fz_{S1} + Fz_{S4} = 0 \\ \sum M_{x_{S1}} = 0; +Fz_{S4} \cdot (y_{S4} - y_{S1}) = 0 \\ \sum M_{y_{S1}} = 0; -Fz_{S4} \cdot (x_{S4} - x_{S1}) = 0 \\ \sum M_{z_{S1}} = 0; -Fx_{S4} \cdot (y_{S4} - y_{S1}) + Fy_{S4} \cdot (x_{S4} - x_{S1}) = 0 \end{array} \right.$$

Note: Extra symmetry in the XY plane could be exploded with this particular geometry, but for generalisation purpose, as unlike symmetry in the other planes this is not required for correct functioning of the pivots, this will not be considered for this calculation.

This is a compatible system, but the main problem with this model is its element configuration, as there are two bars mounted in only two supports, those are the fork and the shock, each of the rest of the elements interact in four different nodes, making them hyperstatic. This provides for an undetermined system, that should be solved using a hyperstatic structures resolution methods like the virtual work principle, or a numerical approximation. This extra complexity makes this model less optimum than the two-dimensional analysis, and because the solution of this last one is good enough for the purpose of this calculation (being used as a verification complement to the complete frame simulation), the three-dimensional analysis will not be used. It is important to remark that for both models, other inputs can be added to simulate different load conditions, for this it is necessary to add the corresponding values for the force and momentum to the appropriate equations, as applicable.

7.2. SIMULATION METHOD

Test methods to be simulated are those described in ISO 4210 (see point 2.2.). The test simulations have been conducted in version No.4 of the CAD model of the frame, which has been especially developed for this purpose. The first step to adapt the three-dimensional model to make it suitable for the simulation is to convert the tubes of every part of the frame (main triangle, chainstay, and rear bar) to solids, this is because for being extruded welded profiles, they are treated as beams for

structural analysis by default, being substituted by an extreme-to-extreme central nerve for simplification in the model and not permitting to study in detail stress produced in the external surface of the beam, thus potential fracture points of the frame. This conversion can be easily done with the operation *Save solids*, with this it is possible to separate all pieces that form the part and save them individually, as well as an assembly featuring all those parts as solids. This shall be made with all specified above parts and a new assembly must be created utilising the new assemblies instead of the original parts. From now on, those will be referred as subassemblies.

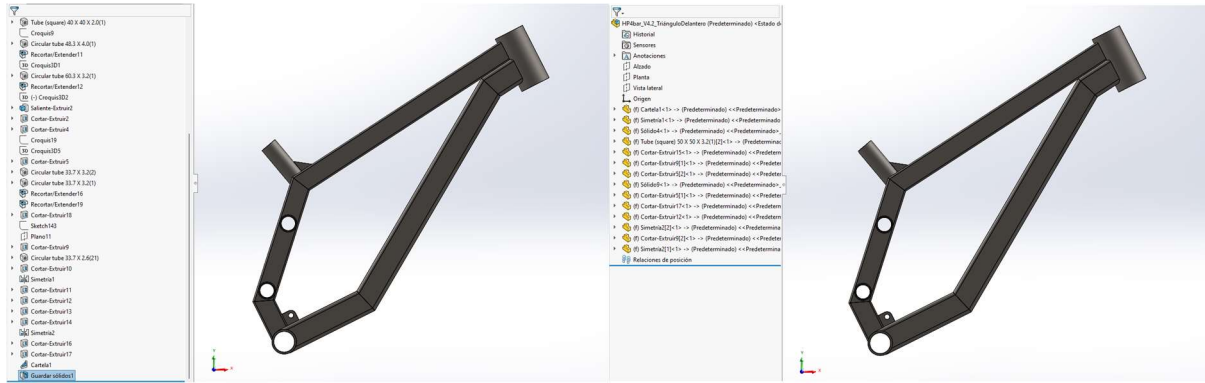


Figure 66: Comparison between operation tree of the original part and the solids assembly generated

7.2.1. STATIC ANALYSIS

The simulation tool utilised for this is the *Simulation* module from *SolidWorks*, the same software used to develop the CAD model. This provides for a finite element analysis method to evaluate many different aspects related to mechanical design of the parts created. Basic analysis options consist in a static analysis, to know tensions, displacements, and deformation produced in the part by a certain load condition, and a frequency study, for analysing natural frequencies and associated modal forms of the geometry designed. Then, tools for design optimisation are provided, those are a topology iterative study with different objectives available (maximum rigidity, minimum displacement, and minimum weight) and a design study for correct dimensioning of elements. For more specific applications, advanced simulation options permit for thermal, buckling, fatigue, non-linear, and linear dynamics analysis while specialized simulation offers fall analysis and pressure vessel design tools.



Figure 67: Example of available study options from SOLIDWORKS Simulation

From the range of studies available, static and fatigue analysis are to be used. The fatigue analysis is carried for the specified number of cycles under a certain load condition, defined by a static study, so for both cases, the first step is to open a new static analysis. Now, every part shall have its material assigned, for those being part of the subassemblies it will be already defined, those will be marked with a green tick on the part's icon. Instead, elements from the toolbox (bearings and bolts) will not be so marked, for those alloy steel will be selected as a representative material due to lack of information on exact steel grade of these parts. For the complete parts list, see test sheet in annex V.

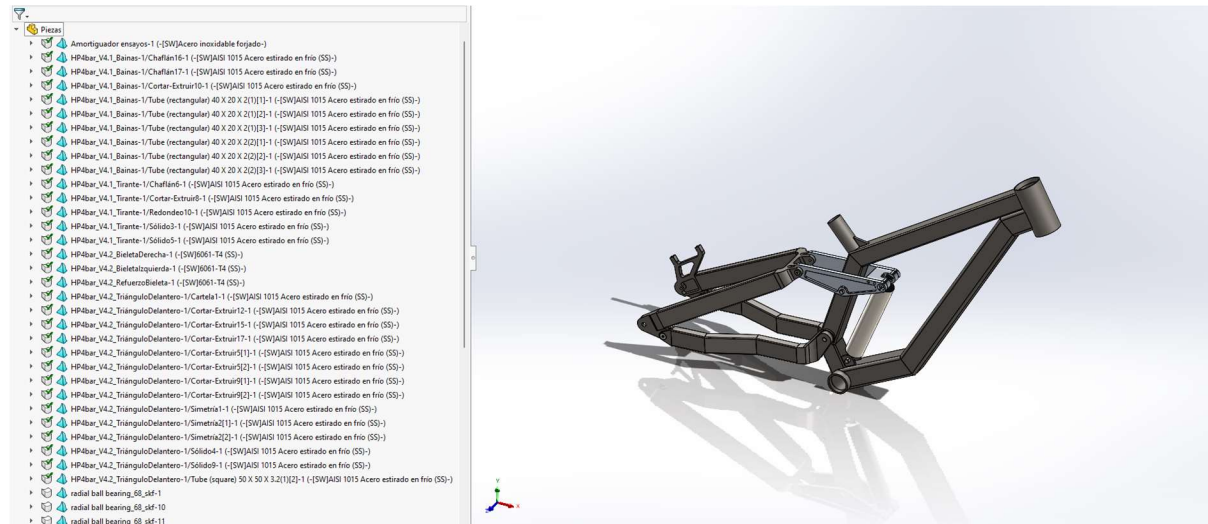


Figure 68: Example of assigned and unassigned material parts

Next, interaction between components shall be defined. By default, global interaction between components is set to rigid union, which is not the case for this assembly. The global interaction shall be changed to *contact* type. This is important because even though the complete assembly is restricted enough to avoid movement, there will be relative displacements because of deformation, and in those cases where relative movement is permitted, for example, a bearing, if this is to be a rigid union excessive local stress could appear because of the torsion generated as a reaction to avoid rotation. Then, individual *rigid union* interactions between parts in each subassembly shall be set. Welds are deemed to be more rigid than its locally surrounding sections, so for general frame stress analysis this kind of interaction is a valid approximation.

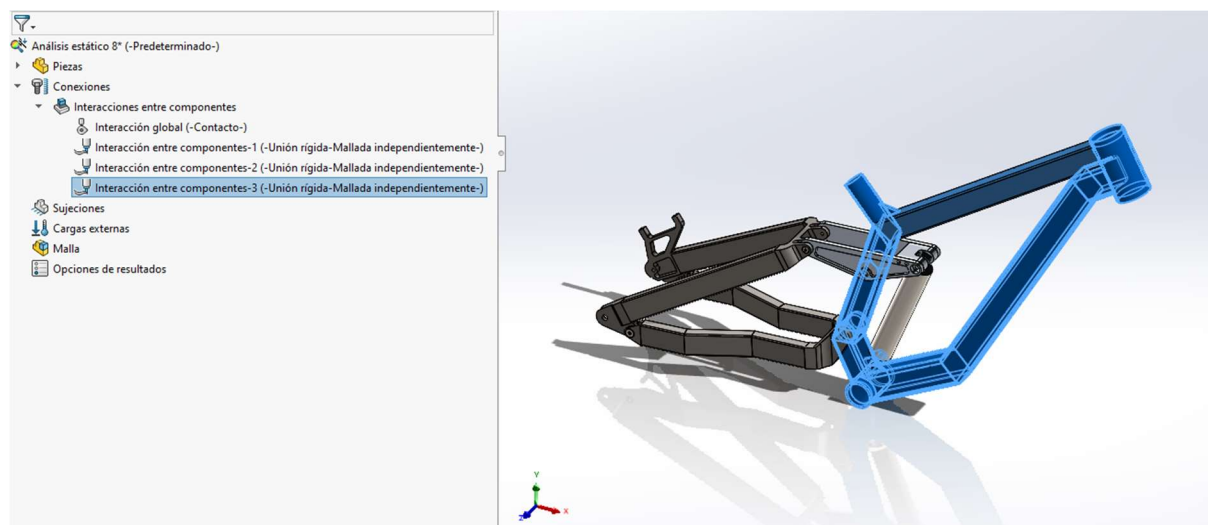


Figure 69: Interactions between components

Then, for fixing the model in the space, restraints shall be defined. This part might be problematic, because an equilibrium between exact characterisation of the real restraint as defined for the test and enough restriction to get a stable model shall be found. For balancing these concepts, chosen criteria for simulations has been to input forces exactly as described in the test procedure and reactions, if applicable, as extra forces to get the best balance possible. Then, some fix geometry is defined to avoid instability in the model. With this layout, for the tests where a horizontal force is applied in the front wheel, for example, a torsion appears in the fixed rear axle attachment points for not being at the same height than the front axle, thus this is necessary to avoid rotation of the frame. These characterisation errors can be identified as unusual stress concentrations in a spiral gradient form around the fix point. To help to better study these sections more accurately and not disturb the overall model, individual part's simulations have been used as a support for local evaluation.

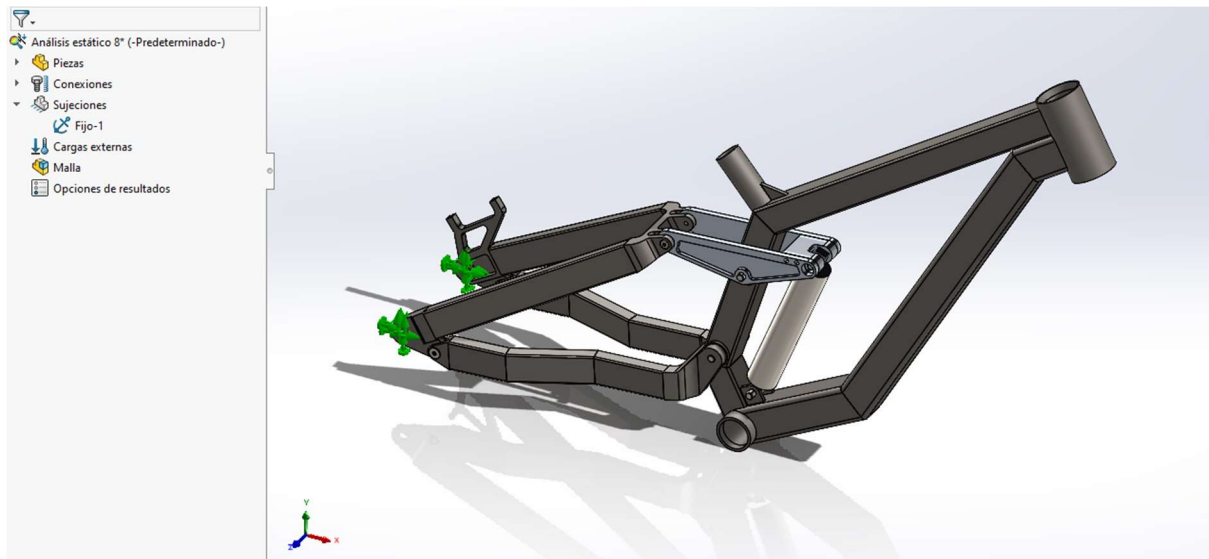


Figure 70: Example of a fix geometry restraint

Having fixed the model, it is time to set the forces actuating on the frame. There are many different actions to be chosen from, in this case only forces and remote loads are needed to characterise all stresses described in the test methods to simulate. This second option will be used for all those forces applied on a mechanical device, being this method of implementation an idealisation of any physical object with this function, thus ensuring requirements for rigidity are met.

For the tests where actions are described as free-falling masses, these have been transformed to equivalent forces equal to product of mass and acceleration. The second term of the equation is obtained by calculating local deceleration of the point of application in an instantaneous impact (time considered for this event is $t = 0,1$ s).

$$F = m \cdot a$$

$$a = \frac{v}{t} = \frac{v}{0,1}$$

Where:

m = mass, in kg

a = acceleration, in m/s^2

v = instantaneous velocity in the impact, in m/s

$t = \text{time, in } s$

Now, instantaneous velocity of a given point of the model can be deduced by mechanical energy conservation, knowing initial height (if it is not explicitly known, it can be found by similarity of triangles) and assuming velocity in this point is equal to zero, final velocity will be as follows:

$$E_m = U + K = m \cdot g \cdot h + \frac{1}{2} \cdot m \cdot v^2 \quad (\text{Equation 20})$$

$$E_m = E'_m; m \cdot g \cdot h + \frac{1}{2} \cdot m \cdot v^2 = m \cdot g \cdot h' + \frac{1}{2} \cdot m \cdot v'^2; \quad (\text{Equation 21})$$

$$v' = \sqrt{2 \cdot g \cdot (h - h')} = \sqrt{2 \cdot g \cdot \Delta h} \quad (\text{Equation 22})$$

Where:

$E_m = \text{mechanical energy, in } J$

$U = \text{potential energy, in } J$

$K = \text{Kinnetic energy, in } J$

$h = \text{heigth, in } m$

$g = \text{gravity, in } m/s^2$



Figure 71: Example of a force applied in the fork

With this, all inputs for the simulation are finally defined. Now, to run the finite element analysis, a mesh of elements for which equilibrium equations will be solved must be constructed. The mesh can be parameterised in three steps to optimally fit the model. First parameter is average size of the triangular elements conforming the mesh. Then, the algorithm to generate the mesh can be selected, three options are here given, a *standard mesh*, this is optimal for simple geometry, *curvature-based mesh*, where size of fundamental constituents of the mesh generated will be automatically fit to the geometry, so in those areas where there is a drastic change the mesh will be denser, and *blend curvature-based mesh*, a similar algorithm than the curvature-based, but where it is possible to calculate minimum element size required to capture small geometric features. Then, the *mesh control* option is a tool that permits to locally control mesh element size for focusing on a specific region. All

mesh parameters are focused on the size of the triangles conforming the mesh, this is because average element size will have a direct impact on how accurate the analysis is, but also in computational requirements, as the more elements a mesh has, the better it can characterise the element being studied, but the more equations will be added to the calculus.

A good balance between accuracy and computation time has been found in a medium average size for the triangular elements of the mesh, this offers good enough resolution to correctly discern problematic stress concentration points in a reasonable time per simulation.

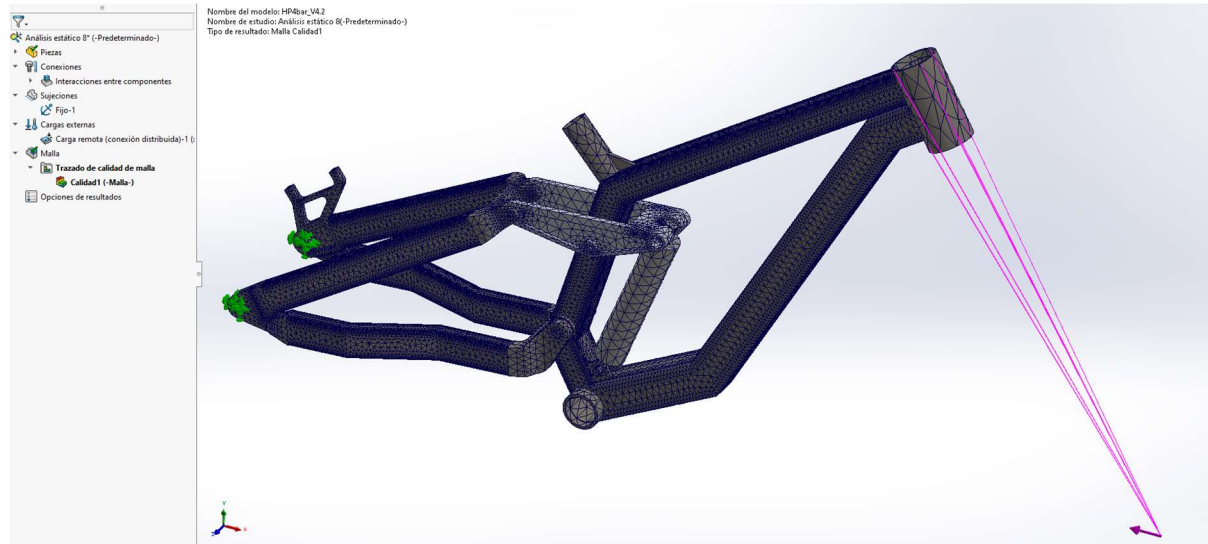


Figure 72: Triangular mesh for the finite element analysis

Finally, for fine tuning the simulation, some more setups can be done from the properties tab of the analysis. From here, the solver to use can also be chosen, this software offers different options, which can be more or less suitable depending on the problem characteristics and available RAM memory.

FFEPlus is an iterative solver, this means a solution is assumed and then evaluated using the error, then the solution is estimated again, and this process is repeated until the error is small enough. This solver is particularly good for large problems, requiring 1 GB of RAM memory for every two million degrees of freedom. However, it can fail if components have largely different stiffnesses, which difficult the obtention of a numerical solution, or if connectors, node to surface contact, virtual walls, or soft springs, for example, are used in the model.

Direct Sparse solvers use instead, as its name indicate, a more direct solution to the stiffness matrix method equation ($F=K \cdot x$). These are less efficient than the *FFEPlus* solver, thus they usually require more RAM memory, and these can fail on resolution of problems between 1,5 and 4 million degrees of freedom (thereafter use of numeric solutions is highly recommendable), but they offer more accurate solutions and some stability advantages over the iterative method for small and medium systems. Different options are offered for this type of solvers, the Intel Direct Sparse uses RAM memory more efficiently and improves multi-core processing, it permits to exploit all memory available and when it is exceeded it can use available disk space to run the simulation, which makes this suitable for resolution of linear and nonlinear problems with more than four million equations. A *Large Problem Direct Sparse* is also available, with limited improvement on performance especially optimised for over a million degrees of freedom problem resolution.

Solver selection can be made manually or automatically, this second option is the most optimal because an algorithm chooses the most optimal option (*FFEPlus* or *Intel Direct Sparse*) depending on

the number of equations to solve, type of loads, specific geometry, mesh type, contacts defined, and connectors used. In addition, this automatic selection is not definitively set at the first iteration but is dynamically adaptable at every step of the iterative resolution process. In any case, which solver is being used at any given point of the simulation is available, so if an error happens and is susceptible due to solver choice it will be easily identifiable.

Then, some options to stabilize the model can be chosen from the property manager. In-plane effect can be activated to consider the effects of compressive and tensile stresses on resistance to blending of the structure, which is respectively reduced and increased by stress softening and stress stiffening. To consider these effects an additional geometric stiffness matrix is added to the model, function of both static loads and deformation. Since this additional matrix is dependent on the displacements, the static analysis is performed in two stages, in the first, displacements are calculated using the standard stiffness matrix, in the following, the geometric stiffness matrix is computed based on these and using this, new displacements are calculated. The equation for this method can be written as:

$$([K] + [K_G(u_i)]) \cdot \{u_{i+1}\} = \{F\} \quad (\text{Equation 23})$$

Where:

$[K]$ = Stiffness matrix

$[K_G]$ = Geometric stiffness matrix

$\{u_i\}$ = Displacement vector for a given "i" iteration

$\{F\}$ = Force vector

The use of soft spring to stabilize the model can be enabled to add a diagonal component to the stiffness matrix. This is to avoid instability of the model due to an unbalance in the model for deformation of the parts, which may make them to rotate, this is susceptible to happen for example when reactions for equilibrium are added as forces, thus the modification of the point of application can lead to an unstable model. The addition of this term in the rigidity matrix can solve this issue and permit to give a solution for the model, however it is highly recommendable to use this option to identify where the error may be given and reevaluate the system when properly restrained, and with this option not activated, as it can increase global stiffness of the model. The equation for the stiffness matrix used in this method can be written:

$$[K_{ss}] = [K] + k_{ss} \cdot [I] \quad (\text{Equation 24})$$

Where:

$[K_{ss}]$ = Stiffness matrix using the soft spring option

k_{ss} = Stiffness added due to the soft spring option

In those cases where accelerating bodies are being analysed, the inertial relief option can be selected, as systems can be unstable if restraints are not well defined, or even if they are, an unbalancing force can result from numerical approximations. This option permits to automatically establish inertial forces for an equivalent state of static equilibrium, this operation is defined as follows:

$$\{F\}_t + \int \{a\}_t \cdot \rho dV = 0 \quad (\text{Equation 25})$$

Where:

$\{F\}_t$: external forces vector

$\{a\}_t$: translational acceleration vector

ρ : material density

V : volume

This equation is represented as:

$$\begin{Bmatrix} F_x \\ F_y \\ F_z \end{Bmatrix} + \begin{bmatrix} M_{xx} & 0 & 0 \\ 0 & M_{yy} & 0 \\ 0 & 0 & M_{zz} \end{bmatrix} \cdot \begin{Bmatrix} a_x \\ a_y \\ a_z \end{Bmatrix} = \begin{Bmatrix} 0 \\ 0 \\ 0 \end{Bmatrix} \quad (\text{Equation 26})$$

Where:

$[M_{ij}]$: total mass in every axle

This option can be used to stabilise other effects than inertial forces, however this is not recommended for balancing gravity, centrifugal, or thermal loads as it could induce an error in the system and there are additional load options to better characterise those.

For the present simulation, only soft spring option has been enabled to find errors in the model's restrictions. Once those have been correctly defined, this option has been disabled to reevaluate the assembly.

Results obtained in a static analysis will be by default three three-dimensional heat maps on the model being studied: equivalent Von-Mises stress, absolute displacements, and unitary deformations.

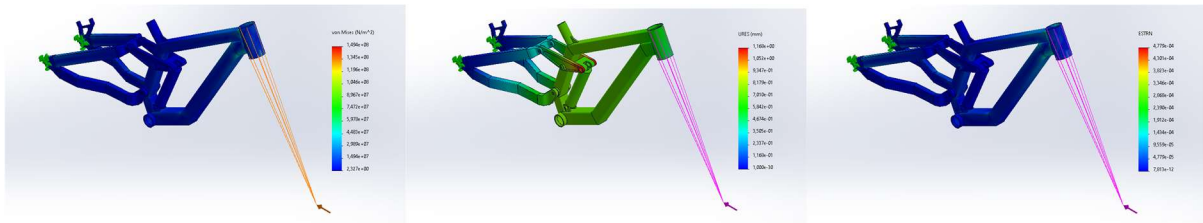


Figure 73: Examples of results of a static analysis

7.2.2. FATIGUE ANALYSIS

Fatigue analysis setup is much simpler than the static analysis. On this has been created applying the load condition to evaluate, a preliminary study can be done, the result of which is whether further analysis is required or not. This is made on the static analysis and indicates where the part is liable to fail because of fatigue, these areas are marked in red.

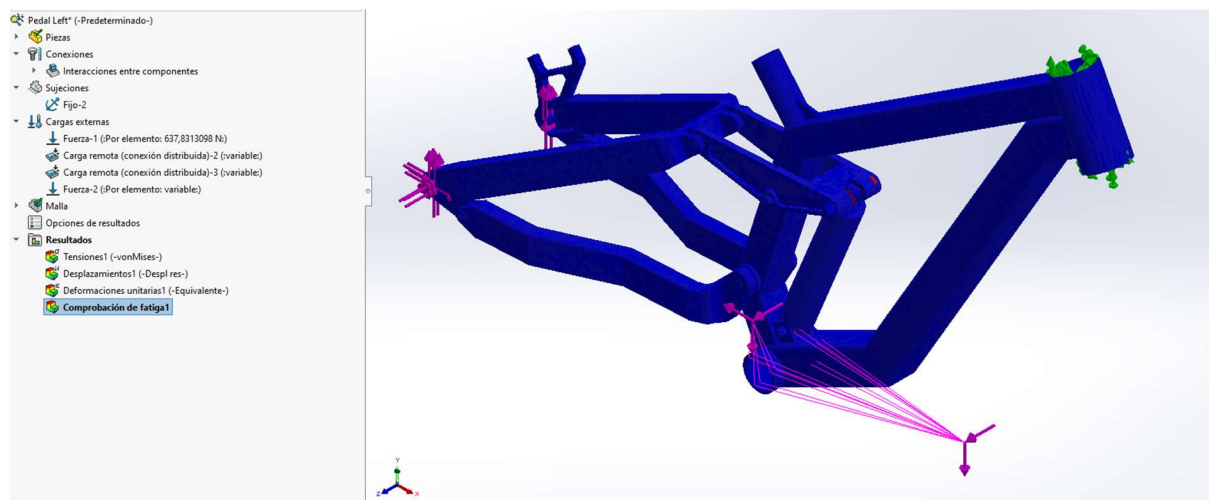


Figure 74: Example of preliminary fatigue study on static analysis

If this analysis concludes a deeper analysis is required, or various loads states are applied simultaneously or alternatively in a test, a fatigue study shall be performed.

The input for a fatigue analysis will be the loads in the form of static analysis. Then the number of cycles must be specified. Finally, the cycles must be characterised, depending on if the stress is applied in just the determined sense, thus cycles are load and unload as determined by the static model, or if the cycles consist in a change in sense of application of the load, alternatively with a positive and negative sign in the direction defined in the static model.

Then, fatigue data for all the solids shall be defined, this depends on the material and is got experimentally. Alternatively, the software offers the possibility to derivate these from the elastic modulus of the material based on American Society of Mechanical Engineers (ASME) steel curves. Due to lack of a better approximation this option will be used for the fatigue study.

From the property manager of this studies, further setup can be defined. First option is interaction of constant amplitude events, two possibilities are displayed here, *random interaction*, which will simulate the worst possible sequence of the selected events, and *no interaction*, for which events will be applied sequentially. In all cases, *random interaction* will be selected here, as all test cycles are described as alternative application of different events, the defined events will be simulated this way for being this the mode with the widest amplitude. Then, the choice of the alternating stress calculation method sets the type of stresses to be used for extracting the number of cycles from the S-N curve, options here laid are *Stress intensity (P1-P3)*, *Equivalent stress (von Mises)* and *Max. absolute principal (P1)*. The mean stress correction method permits to choose the correction applied to this stress, if any, options given here are *None* (if no correction is required), *Goodman method* (suitable for brittle materials), *Gerber method* (suitable for ductile materials) and *Soderberg method* (Generally the most conservative). Finally, some additional options can be defined, a K_f factor can be set to characterise real world conditions versus laboratory conditions for the fatigue study, and a number of cycles can be defined to be deemed as infinite life, this value will substitute the last number of cycles of the S-N curve in those cases where alternating stress is inferior to endurance limit.

The result obtained with the fatigue analysis is a three-dimensional heat map with damage observed on the model after all cycles prescribed.

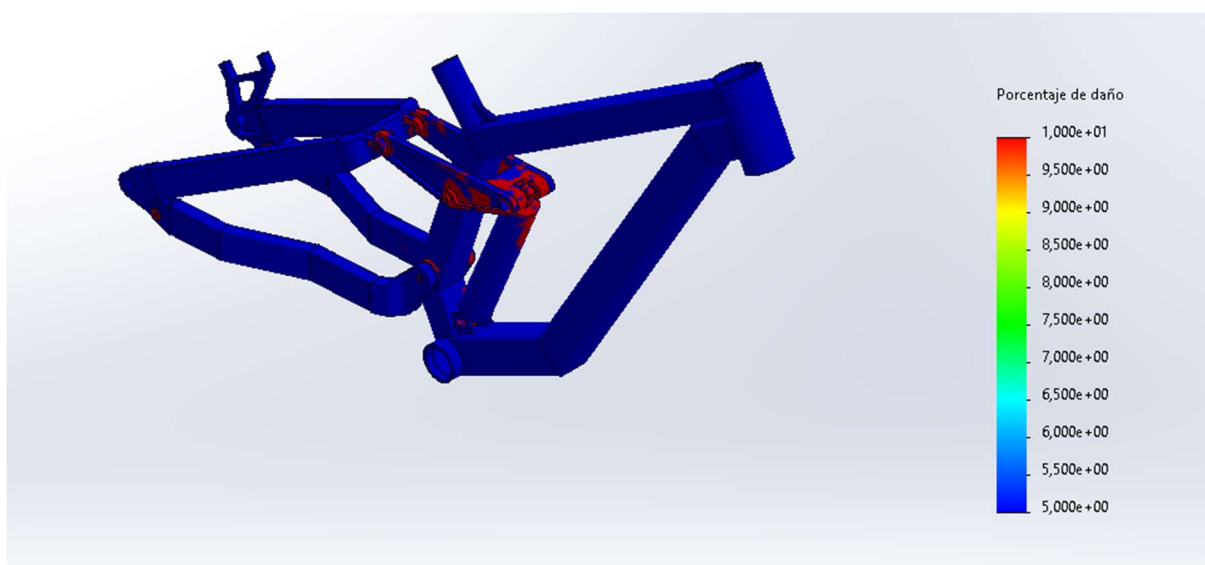


Figure 75: Example of the result of a fatigue analysis

8. PROTOTYPE MANUFACTURING

The prototype to build will be based on the three-dimensional model. From this, all dimensional drawings for the different pieces conforming the frame will be obtained (see annex VII). Then, different stages for the construction of the frame are discussed in the following.

8.1. PROCESSING OF BASE MATERIAL

Base material to start with will be standard steel profiles and solid steel and aluminium blocks (see point 3.2.). To conform the tubes, the standard profiles shall be cut to measure and prepared for welding, this is all sections to be welded shall be chamfered for better penetration of the filler material, and specifically those facing a round area shall be machined to get a good covering of the curved surface. The solid pieces shall be machined from the solid blocks, these will be cut to an appropriate dimension and shape in order to reduce milling time.

All pieces obtained in this stage will be measured to ensure they are within fabrication tolerances.

8.2. WELDING

An arc welding process is then used to conform the parts of the frame. For arc welding, a power supply unit is used to generate an electric arc between the electrode and the material to weld, which melts the filling material. The most commonly used methods are gas metal arc welding (GMAW) and gas tungsten arc welding (GTAW), most commonly known as metallic inert gas (MIG) and tungsten inert gas (TIG), respectively. MIG welding consists in a continuous feed of filling material, which is also a consumable electrode, and application of a protective atmosphere generated by an inert gas. For TIG welding, a non-consumable tungsten electrode is used, and filling material is added apart, a protective inert gas protective atmosphere is also required for this method. Generally, TIG welding is considered to be a more difficult process than MIG welding because of the closer tolerance between the electrode, filling material stick, and working part, but usually welds obtained are of a higher quality and more corrosion resistant. In this case, the selected method is MIG welding because this is the option available in the workshop where the frame is to be built, although for all the exposed above TIG welding would be a more appropriate choice for bicycle frame manufacturing.

Once welded, the frame, the chainstay, and the rear bar shall be straightened and measured to ensure they are within fabrication tolerances and the heat applied in the process has not excessively deformed the pieces conforming those parts.

8.3. ASSEMBLY

Then, headset, bottom bracket, and all bearing housings and axle fitments shall be machined again to ensure they have a proper dimension and circularity tolerance for a correct adjustment, after they may have deformed under heat application in the welding process. All parts to fit bolts shall be threaded, this includes all threaded axles and fittings for the screws in the brake mount.

All the steel parts shall then be painted with a corrosion resistant product to prevent the frame from rusting, all the beforementioned fitting areas shall be correctly covered to not be painted in this process. Then all bearings shall be installed in the frame and the different parts shall be assembled with the corresponding axles. Now all components shall be installed in the frame to complete the bicycle, first of all, the shock can be fitted to lock the linkage and make working in the bicycle easier, then the bottom bracket and headset can be pressed in their respective housings. As internal cable routing has not been considered, threaded rivets can be installed in the frame to install guides for the rear brake line and shifting actuator cable. The cranks and chainring assembly can be fit in the bottom bracket. Now the fork and the cockpit can be installed as well as the brakes. The mech hanger shall be

put in place to install the derailleur, and the wheels with the brake discs, cassette (in the rear) and tyres can be fit, and finally the chain can be guided by all the transmission elements. The seat post can be inserted in place and secured, to which the saddle can now be fit. Once all parts are in place, everything must be adjusted, this includes brake callipers, transmission, and suspension setup.

9. ENVIRONMENTAL IMPACT

The cycling industry is usually seen as green and environmentally friendly for offering a non-pollutant mobility alternative to cars, motorcycles, or collective transport, all of them generating certain emissions when being used. But just like any industry, bicycle manufacturing has its emissions and generates waste, and there is currently a great issue with this second factor because of the increasing use of composites in bicycle frames and components construction.

Carbon fibre is a really good material for frames construction (see point 3.1.4.) which has been increasingly used in the bicycle industry over the last two decades. Its democratisation has brought great benefits to the general public, as the most it has been used, the most affordable it has become, making available this excellent material from the mid-range and even entry level models, in those cases where an aluminium option is not offered.

This, however, has had very negative consequences for the environment, as recycling of carbon fibre composites is a difficult process that comes at a high environmental and economic cost. The main issue encountered when it comes to recycling this material is it is not a single material but a composite, obtained by the combination of the carbon fibres and epoxy resin. To effectively recycle it, both materials should be able to be separated and reused individually, and as epoxy is a thermoset polymer, this means it cannot be melted and utilized again as its properties will be lost in the process. Now, separation of the carbon fibres is possible by different methods, however, all of them result in a damage to the carbon fibres. Thermal degradation can be used, but this process reduces the mechanical properties of the fibres, which are responsible for the excellent characteristics of carbon fibre composites, and produce high grades of contamination, which difficult its reutilisation. Chemical degradation may also be used to eliminate the epoxy resin, even though this will lead to less degraded and cleaner fibres, it will cause a waste that shall be treated and will still limit recycled fibres application. In addition, notwithstanding which method is used, carbon parts to recycle are usually shredded and crushed to facilitate the separation, this makes it impossible to reutilise them for the application they were first used, as the strength and stiffness of carbon parts come from the use of long fibres, thus resultant material after a mechanical treatment could be used in other applications as reinforced plastic parts, but not be given a structural function.

Later studies have aborded this problem by modifying the epoxy hardeners with acid-cleavable groups, those are designed with a polyamine structure in which amino end groups are bonded together by the forementioned cleavable molecules, this makes the thermoset polymer to transform into a usable thermoplastic by the application of temperature (70 to 100°C) and an acidic environment. This method permits an easy separation of the undamaged carbon fibres and a different than the initially used, but still usable polymer. Although very promising, this method is not yet stablished at an industrial scale, and it would need for a standardisation in the carbon fibre composite industry for being realistically a green option for the use of this material. Carbon fibre parts should not undergo any mechanical process susceptible of reducing the fibres length if those are to be used in a structural application, this will highly increase the recycling process complexity, and will make fibres not infinitely reusable, because of the processing they shall undergo (for example, be cut to a new measure) for its reutilisation.

With the increase of carbon fibre composites application in this and other industries, it is sure enough that in the future there will be methods to easily recycle this material, but by the moment, recycled carbon fibres are more expensive and of less quality than new raw material. Current recycling processes are highly costly and environmentally intensive, and there is not an immediate solution for this problem, neither a developed industry nor logistics around this theme. Although the bicycle

industry is highly conscious about the problem, and some brands are working in projects that help to solve his issue, the reality is most of the carbon parts produced to date will end its life in a landfill.

Obviously, further research is required to solve the problem in the long term, but some action could be taken in the short term to minimise negative consequences in the future. This measure, in the case of manufacturing of downhill bicycle frames, could be to take a step back in materials to use. It is undeniable for other more pedal focused disciplines that carbon offers great advantages over all the other options available, but for freeride and downhill applications those benefits are not so obvious. In a nutshell, weight loss for carbon fibre options is not so noticeable nor critical, in competition, the short runs characteristic of these disciplines make no difference in fatigue levels during a race or exhibition, and even considering a lighter bicycle has less inertia, this might be a disadvantage in some scenarios and for control of the bicycle what does really matter is the situation of the centre of gravity. Required rigidity levels can be perfectly achieved with other materials, as a too stiff frame can give an uncomfortable and unpredictable feel, so neither is a distinctive advantage the higher levels of rigidity that can be obtained by using carbon fibre.

On the other hand, metallic alternatives do offer a set of advantages over the composite. First of all, the cost of a carbon fibre frame is higher than its aluminium equivalent, if both options are available, this is very significative because a lot of consumers have these as a secondary bicycle, for being of a very specific application. Then, while carbon fibre is a high resistant material, this property is directional and it is fragile when an impact is transversal to the fibre's direction, metals instead admit elastic and plastic deformation, this gives them a higher energy absorption capacity before a critical failure may happen. Finally, and most important for what this section is concerned, metals are much easier to recycle and currently there is a developed industry for this purpose.

Starting with aluminium, which is the most widely used of the metallic options for mountain bicycle frames and components manufacturing, this is a 100% recyclable material, which can be reused infinitely without losing any of its properties. The use of recycled instead of primary aluminium reduces the energetic cost by 88%, this is because a great part of aluminium obtention process is invested in molten-salt electrolysis of alumina, rising energy consumption to 174 GJ/tonne versus the 20 GJ/tonne required to process recycled aluminium, primarily for melting it. Solid waste is estimated to be reduced in a 90% when recycling aluminium, even though solid residues are generated in the remelting in the form of dross and salts, volume of those is much lower than the produced in the alumina refinement process. Primary aluminium obtention also generates over 90% more emissions in the form of hazardous and non-hazardous gasses when compared to the recycling process, which also has its emissions, but much reduced. Economically, recycling of aluminium is profitable, while it is true that it presents its challenges, cost reduction per tonne for processing of recycled aluminium instead of generating primary material is estimated to be over an 80%.

Steel is another good example of a 100% recyclable material that can be used for bicycle frames construction. In this case, obtention of primary steel is easier and less energy intensive than the process for aluminium, but using recycled steel is still a better option environmentally speaking. The estimated energy to produce austenitic stainless steel (not the used for bicycle construction, but this can be used for reference) is 79 GJ/tonne for primary material whereas for recycled steel this value is reduced to 26 GJ/tonne, thus a 67% difference between both sources. Carbon dioxide emissions are also reduced by this amount when the two methods are compared. Steel recycling processes are not just economically profitable but necessary, as the demand of this material increases for a wide variety of industrial applications, it will be more and more necessary to use secondary steel to satisfy it in the future.

Titanium is the worst example of recyclability of the here shown metals, with a post-consumer reuse of less than 1%. This value, however, does not reflect real recyclability of this material, as it is usually used for very long-lasting applications, this makes for a very low availability of titanium scrap. Being a so expensive material makes recyclability percentage in manufacturing, this is material discarded in machining processes, for example, grows to estimated values over 90%. Titanium recycling is mainly achieved by remelting the material, which is applied to high grade alloys, taking the required measured for the forementioned high reactivity of this material when heated. There are currently open investigations to facilitate separation of highly contaminated titanium alloys with iron and oxygen, produced for example in the smelting process (it is important to consider the volume produced in-house in this stage is significantly bigger than post-consumer titanium products), but to date these cannot be utilised for the obtention of raw material and are instead used as ferro-titanium for steel alloys production.

In conclusion, the use of new materials such as carbon fibre composites can bring a lot of benefits for its mechanical and chemical properties, but when scaling the use of those to an industrial scale, post-treatment in the end-of-life of those products must be considered and a proper structure to guarantee this is made efficiently must be developed. While it is important to keep working on procedures to recycle this material which predictably will see its use highly increased in the following years in various industries, including bicycle manufacturing, a good step to avoid the generation of waste which will not be processed by the moment could be to avoid its use for applications in which it is not highly necessary and it could be easily substituted by other more environmentally friendly alternatives.

CONCLUSION

The design and development of a bicycle frame is a complex process which requires knowledge in a wide variety of engineering areas to cover all the stages involved in it, apart from some experience to take decisions based on difficult to quantify parameters, such as sensations or feelings associated.

It is important to know applicable standards and regulations for the purpose for which the bicycle is being designed, these can also serve as a guide for the development of a model that fits requirements of those applications.

Material to use for the manufacturing of the frame is a basic yet very important decision, different materials will have distinct properties thus this will result in certain characteristics, and considerations that shall be made during the design process. Manufacturing methods compatible with each material will also play an important role in those decisions, as this can bring a lot of flexibility in the design.

It is fundamental to know the basics of the specific knowledge applicable to bicycle design, this is geometry and suspension kinematics. Those aspects will define overall feeling and performance of a bicycle, and its study is indispensable to get the expected qualities of a frame. These decisions are based on a theoretical basis but also have a subjective component to them, as some traits can be achieved by different ways, and there will always be a balance between characteristics, as a certain modification will not make an absolute improvement or worsen to the design but will point it towards a specific overall performance.

To help to implement this theory in the design of a frame, a specific CAD tool for geometry and kinematics calculation has been used, with this, a two-dimensional model has been created with which all the important point and pivots of the frame have been situated in the plane. Then, this has been translated to a three-dimensional space to create a virtual model of the frame, in which different production aspects such as compatibility with all components have been evaluated. This model has also been used to simulate tests on the frame to grant safety of the bicycle in a CAE process.

Finally, the fabrication of a prototype has not been possible because machining of the solid parts of the frame in the university laboratory could not be managed, as it was initially proposed. This made the manufacture of a real model to be economically not viable. However, the project has been approached as if this was to be made, and everything necessary to make a prototype has been considered and covered in this project.

So even if the initial objective has not been achieved, the project is deemed to be completed successfully as far as engineering is concerned, all stages involved in the design have been treated and necessary tools for the development of the frame have been used to create a virtual model that could be brought to the real world.

BUDGET

For the realisation of this project, an analysis on budget has been brought to term, different activities involved in the process have a cost associated to them, this will be analysed in the following.

For every item involved in the development of the project, a table showing the total amount and partial cost of the deductible concepts will be displayed.

SOFTWARE

First of all, for earlier stages of the project, there is a software cost associated with the design of the frame. For the kinematics analysis, the personal use version of the *Linkage X3* software has been used, which cost is 25,00€. However, there is a professional version which is allowed for industrial or for-profit use, and that extends possibilities for dynamics analysis and offers more exporting options, aside from permitting to work in more projects simultaneously.

For *SolidWorks* software, an annual student's license has been considered for being the option that best fits the usage this programme has been given for the development of the project. A professional license price is difficult to estimate, as this is not available to the public in its official site, instead it has to be consulted with a reseller who also offers formation and technical support, so services other than software value would be included for this option. Annual price for the *SOLIDWORKS Student Edition* license is 99,00€.

Then, some software has been used not for designing itself but as tools to facilitate the realization of the project. *Microsoft Office* includes programmes like *Excel*, a calculus sheet used for development and resolution of the calculus model used to analyse forces in the individual parts of the frame, or *Word*, a text processing software utilised for the present redaction. The annual cost for a personal license is 69,00€.

Software	193,00€
Linkage X3	25,00€
SolidWorks	99,00€
Microsoft Office	69,00€

PROTOTYPING

Then, manufacturing of the frame makes the greatest part of the cost of the project. For its prototype condition, elaboration of an accurate budget is difficult, but assuming the materials and fabrication methods to be used an approximation can be calculated. In the following, an overview of the expected cost related to both materials and labour costs involved in the frame prototyping will be given.

For the material, all frame constituents shall be acquired, those are standardised steel tubes and steel and aluminium block for the solid parts to machine. Antioxidant paint is also considered in this section as it is completely necessary to avoid corrosion of the steel parts.

Labour costs are divided in the different operations required. Machining has been considered with a cost of 36,00€ per hour, and a total of 48 hours of work has been estimated for machining of the solid parts and surfaces to weld, and for the bearing housings, that shall be made after welding, which cost is 1.440€ and 288,00€ respectively. Welding and straightening cost of this specific design has been estimated in 200,00€. Other activities cost has been considered at 32,00€ per hour, and predictably 6 hours will be required for assembling and adjusting the complete frame and two extra hours are considered to be needed for painting all the steel parts.

Materials	220,00€
Steel tubes	80,00€
Aluminium blocks	80,00€
Steel blocks	50,00€
Antioxidant paint	10,00€
Labour costs	2.184,00€
Machining	1.440,00€
Welding + Straightening	200,00€
Machining of bearing housings	288,00€
Assembly + Adjustment	192,00€
Painting	64,00€
Total	2.404€

COMPONENTS

The frame must be completed with appropriate components, in this case, those are to be reutilised, so they will not make an extra cost for the project itself. Component's price is very variable depending on the range, so market price for the exact components to install will be here discussed, if they had to be acquired for the complete bicycle cost associated would be as follows.

Time spent for complete assembly and set-up of the bicycle is considered to be four hours, this includes greasing, components fitting and adjustment, brakes bleeding, and set-up. Gross cost for this activity is deemed to be 10,00€ per hour.

Components	4.322,14€
Shock	630,00€
Fork	1.569,95€
Brakes	334,50€
Brake discs	42,00€
Front wheel (Hub + Rim)	240,00€
Rear wheel (Hub + Rim)	330,00€
Headset	57,80€
Bottom bracket	50,00€
Cranks	167,00€
Cassette	41,00€
Gearshift lever	56,00€
Deraillleur	139,00€
Chain	16,00€
Saddle	67,00€
Seat post	55,00€
Stem	45,00€
Handlebar	45,00€
Grips	25,00€
Pedals	179,99€
Tyres	224,00€
Tubes	7,90€
Labour costs	40,00€
Total	4.362,14€

WORKING TIME

Finally, time spent for the realisation of the project has an associate cost, every activity will be given an adequate price per hour depending on required formation for its realisation. Time spent on design and development will be counted as engineering hours at a price of 12,00€ per hour for being a qualified work. This will include drawings and sketching for initial conception (20 hours), geometry definition (4 hours), kinematic study of the rear suspension (48 hours), development of calculation method (60 hours), computer aided design of the virtual model (216 hours), virtual tests by simulation (72 hours), and test report issue (10 hours).

Then, other activities that do not require any specific formation will be considered at a price of 10,00€ per hour. Those are research of general information (40 hours), interview preparation (12 hours), redaction (120 hours), and communication and management (20 hours).

Engineering	5.160,00€
Sketching	240,00€
Geometry definition	48,00€
Kinematic study	576,00€
Calculation	720,00€
Computer Aided Design	2.592,00€
Computer Aided Engineering	864,00€
Report issuing	120,00€
Other activities	1.920,00€
Research	400,00€
Interview	120,00€
Redaction	1.200,00€
Communication and Management	200,00€
Total	7.080,00€

BIBLIOGRAPHY

- Andy Barlow. Do you need to re-learn how to ride on a modern mountain bike?. *MBR* [online]. 21 February 2020. [Accessed: 27 September 2022]. Available at: <https://www.mbr.co.uk/news/how-to-ride-a-modern-mountain-bike-339281>>
- Asociación Española de Normalización y Certificación. *UNE-EN ISO 4210-1: Ciclos. Requisitos de seguridad para bicicletas – Parte 1: Términos y definiciones*. Madrid: AENOR, June 2014.
- Asociación Española de Normalización y Certificación. *UNE-EN ISO 4210-2: Ciclos. Requisitos de seguridad para bicicletas – Parte 2: Requisitos para bicicletas de paseo, para adultos jóvenes, de montaña y de carreras*. Madrid: AENOR, August 2015.
- Asociación Española de Normalización y Certificación. *UNE-EN ISO 4210-3: Ciclos. Requisitos de seguridad para bicicletas – Parte 3: Métodos de ensayo comunes*. Madrid: AENOR, June 2014.
- Asociación Española de Normalización y Certificación. *UNE-EN ISO 4210-6: Ciclos. Requisitos de seguridad para bicicletas – Parte 6: Métodos de ensayo del cuadro y la horquilla*. Madrid: AENOR, June 2014.
- Dan Roberts. Engineering: What Is Anti-Squat & How Does It Actually Affect Mountain Bike Performance?. *Pinkbike* [online]. 14 February 2020. [Accessed: 28 September 2022]. Available at: <https://www.pinkbike.com/u/dan-roberts/blog/definitions-what-is-anti-squat.html>>
- Dassault Systèmes SE. *SOLIDWORKS Web Help* [online]. [Accessed: 22 December 2022]. Available at: <https://help.solidworks.com/HelpProducts.aspx>>
- Derek Covill; Steven Begg; Eddy Elton; Mark Milne; Richard Morris; Tim Katz. Parametric Finite Element Analysis of Bicycle Frame Geometries. *Procedia Engineering* [online]. 2014, No. 72, p. 441-446. DOI <https://doi.org/10.1016/j.proeng.2014.06.077>. [Accessed: 19 November 2022]. Available at: <https://www.sciencedirect.com/science/article/pii/S1877705814005931>>
- Gerth, M.; Haecker, M.; Kohmann, P. Influence of mountain bike riding velocity, braking and rider action on pedal kickback. *Sports Engineering* [online]. 27 November 2019, No.23. DOI <https://doi.org/10.1007/s12283-019-0315-4>. [Accessed: 17 November 2022]. Available at: <https://link.springer.com/article/10.1007/s12283-019-0315-4>>
- Jody Muelaner; Tom Knight; Joss Darling. Kinematic Analysis and Optimization of Bicycle Suspension. *InImpact: The Journal of Innovation Impact* [online]. May 02, 2016, No. 8, p. 29-38. ISSN 2051-6002. [Accessed: September 30, 2022]. Available at: <http://nimbusvault.net/publications/koala/inimpact/papers/sdm15-009.pdf>>
- Johnson, Jeremiah; Reck, B. K.; Wang, T.; Graedel, T. E. The energy benefit of stainless steel recycling. *Energy Policy* [online]. 01 January 2008, No. 36, p. 181-192. ISSN 0301-4215. [Accessed: 08 December 2022]. Available at: <https://www.sciencedirect.com/science/article/abs/pii/S0301421507003655>>
- K. Weman. *Welding Processes Handbook* [online]. 2nd Edition. Elsevier, 08 November 2011. ISBN 9780857095183. [Accessed: 15 October 2022]. Available at: https://books.google.es/books?hl=es&lr=&id=oaNgAgAAQBAJ&oi=fnd&pg=PP1&dq=welding&ots=xbVI_OnM20&sig=iaW1b6bwU-ZtfDq_5gF1yyUNeSU#v=onepage&q=welding&f=false>

Larry Jeffus. *Welding* [online]. 7th Edition. Cengage Learning, 12 May 2011. ISBN 9781133714422. [Accessed: 15 October 2022]. Available at:
<<https://books.google.es/books?hl=es&lr=&id=pUcKAAAQBAJ&oi=fnd&pg=PR4&dq=welding&ots=XNG5ovwuav&sig=6Yy1y5QFPsaJBSok9tCZqSz62y4#v=onepage&q=welding&f=false>>

L.H.Lang; Z.R.Wang; D.C.Kang; S.J.Yuan; S.H.Zhang; J.Danckert; K.B.Nielsen. Hydroforming highlights: sheet hydroforming and tube hydroforming. *Journal of Materials Processing Technology* [online]. 01 September 2004, No. 151, P. 165-177. [Accessed: 04 October 2022]. Available at:
<<https://www.sciencedirect.com/science/article/abs/pii/S0924013604003371>>

Mark E. Schlesinger. *Aluminum Recycling* [online]. 1st Edition. Boca Raton: CRC Press, 01 November 2006. ISBN 9780429122897. [Accessed: 08 December 2022]. Available at:
<<https://www.taylorfrancis.com/books/mono/10.1201/9781420006247/aluminum-recycling-mark-schlesinger>>

MatWeb, LLC. MatWeb [online]. [Accessed: 28 December 2022]. Available at:
<<https://www.matweb.com/index.aspx>>

Peter Suci. The not so green bike: carbon fiber's carbon footprint. *BikeRadar* [online]. 17 December 2011. [Accessed 09 December 2022]. Available at: <<https://www.bikeradar.com/features/the-not-so-green-bike-carbon-fibers-carbon-footprint/>>

Seb Stott. The ultimate guide to bike geometry and handling. *BikeRadar* [online]. 11 September 2020. [Accessed: 26 September 2022]. Available at: <<https://www.bikeradar.com/features/the-ultimate-guide-to-bike-geometry-and-handling/>>

Seb Stott. The ultimate guide to mountain bike rear suspension systems. *BikeRadar* [online]. 02 October 2018. [Accessed: 26 September 2022]. Available at:
<<https://www.bikeradar.com/features/the-ultimate-guide-to-mountain-bike-rear-suspension-systems/>>

ZEP MTB camps. Zep's How-To Mythbusters: Body Position for Descending and Corners. *Pinkbike* [online]. 09 February 2016. [Accessed: 27 September 2022]. Available at:
<<https://www.pinkbike.com/news/zeps-how-to-body-position-descending-cornering-braking-2016.html>>

Takeda, O.; Ouchi, T.; Okabe, T.H. Recent Progress in Titanium Extraction and Recycling. *Metallurgical and Materials Transactions B* [online]. 07 July 2020, No. 51, p. 1315-1328. DOI <https://doi.org/10.1007/s11663-020-01898-6>. [Accessed 10 December 2022]. Available at:
<<https://link.springer.com/article/10.1007/s11663-020-01898-6>>

Tempia, A., Subic, A., Pagliarella, R.M. *The Engineering of Sport 6* [online]. 1st Edition. New York: Springer, 10 May 2010. ISBN 978-0-387-46050-5. [Accessed: 02 October 2022]. Available at:
<https://link.springer.com/chapter/10.1007/978-0-387-46050-5_17>

A.D.La Rosa; D.R.Banatao; S.J.Pastine; A.Latter; G.Cicala. Recycling treatment of carbon fibre/epoxy composites: Materials recovery and characterization and environmental impacts through life cycle assessment. *Composites Part B: Engineering* [Online]. 01 November 2016, No. 104, p. 17-25. DOI 10.1016/J.COMPOSITESB.2016.08.015. [Accessed: 09 December 2022]. Available at:
<<https://www.sciencedirect.com/science/article/abs/pii/S1359836816306898>>

ANNEX I: INTRVIEW TRANSCRIPTION

Hello, good afternoon!

Hello David, nice to meet you!

Nice to meet you too! As we have been speaking, I am currently working on the design of a downhill bike frame, and as you are a professional working in the sector, I would like to ask you some questions if you don't mind.

Of course, no problem!

Perfect! So, as far as I know, you are working on the design of the bicycles at Commencal, is that correct?

Exactly, design and development. Do you have an idea on how the design of a bicycle works? Just to put you in context, so you can ask anything of your interest later.

Yes, I have a slight idea. I guess the first step would be the definition of general geometry and to design the suspension system, depending on the desired behaviour. Then I would imagine that a three-dimensional model is created and modified using design and simulation tools, until getting something that can be prototyped. Am I too far wrong?

That is right, first of all the team leader defines the geometry and kinematics using the program *Linkage*. Having those points, it is time for the designer to propose various solutions in two-dimensional sketches and some three-dimensional drawings to help visualise the shapes of the tubes, rockets, etc., in a better way. Those are given to the engineer/product designer, who is the responsible of bringing those sketches to life by modelling with Computer Aided Design tools, and once finalised, simulations are carried out on that model which is modified to reduce weight or solving excessive stress.

In parallel, during all the design process, three-dimension models of the different pieces are printed to get conscious of the volumes and surfaces.

Then, to make sure everything we have been developing virtually works in real life, a prototype is made. This is usually constructed using tubes and pieces from older models, so not new moulds are required. Different tests are carried out in the prototype, making sure everything works as it should and that kinematics are correct, if some changes need to be made this is the moment. Once approved the prototype, drafts are sent to the suppliers to check the design is suitable for production, looking for the best balance between performance, reliability, and cost.

Yes, it is more less what I imagined it to be according to what I have found in my research, I skipped the optimisation, test, and cost balance, but obviously those are very important parts of the process.

They are, and they are very present during the design and development. Production process and cost reduction are very heavily considered.

Starting with some generic questions, how much people is involved in the design process? You mentioned the project manager, designer and engineer, but I guess there is a larger team behind.

Well, I can tell you how we work at Commencal. In the design process of a specific bike model there are four people involved. As you said an engineer (in this case the team leader) who is responsible for the geometries, the designer, the design engineer, and the engineer in charge of the simulations.

Of course, before and after this process there are different teams who work on accountancy, bike SPECs (those are responsible for deciding which components are mounted in production bicycles), a team in charge of production (who are the ones in contact with suppliers), a marketing team, etc. But those are personnel you can find in any company, those who work specifically in designing are 4 people for bicycle.

Obviously, you need different areas to give support to the productive process, but I am quite impressed there is only four people for the design... I thought you would be more people. You say there is four people per bicycle, every team is specialised in a model or discipline? Or different teams my work in different projects?

We really are just one team. The team leader, designer and simulation engineer are the same for all the projects, the only one that changes is the engineer who develops the bicycle.

Then, here at Commencal we also have a team of engineers working in parallel with us, who are in charge for the upgrade and adaptation of the production models for racing application. We are always in contact with them so we can improve and learn from the feedback of professional riders.

That is a very interesting point! I have some more questions about organisation, then we may go more in depth into technical aspects, if you do not care. One of the biggest issues I am having is going back and forth in the design stages. In your case, design decisions on modifications are taken in a consolidated way by all the team or once closed a phase it remains unmodified, and work goes on from that?

It is always sought, during the briefing of the project, to consolidate the design with all the team, but it is almost impossible to get it right from the start. During the evolution of the project there are always some issues not considered at first, and as they come out, we try to look for a solution with all the team. For example, today I have had a problem due to tolerances, which resulted in a complete change of a piece, so I have met with the team leader and designer and presented two different solutions and all together we have chosen the one we considered to be the most suitable for the design and our necessities. Although we are a little team it is very important to work all together.

Also, along the development of the project there are checkpoints (meetings with the rest of the team, SPECs, production, etc.) to see the evolution of the project, if we are on-time in the Gantt, show the changes made from the original idea and more.

I guess it will make it a lot easier for you the fact you are so little people involved in the design, it would be much more difficult to coordinate a larger team considering all the issues that may appear during the project. I will not ask more in depth about project monitoring because it is a common part to any kind of project, but as you mentioned the Gantt, may I ask how much time does it take the whole design process? And individual duration of every phase?

That is a very relative factor, it depends a lot on deadlines of course, but also on the kind of bike we are developing, if it is a rigid or double suspension model, a downhill bike, or a city one, etc. But development stages are conceptually the same for all the bicycles, from conception, development (design plus simulation), to prototyping, test and manufacture.

Now, going back into the racing focused team you mentioned earlier, competition bikes are much different from production models? It is very frequent to see, for example, custom

linkages, but has the main frame any difference? For example, longer rear ends for increased stability are used or it is not that common?

And how much impact has competition when it comes to designing a bike? Because for the average user, an entire bike park day in a racing bike, well... let's say it must not be very comfortable.

Our philosophy here at Commencal for production bikes is to be the same than the racing version. In this way, the frame is always the same, although there may be some modifications for finer control of chassis rigidity.

[...]

That is amazing, because in the end we are riding the same bike which are racing at world cups, this would be inconceivable in other racing disciplines. So, what are the desired characteristics of a downhill bike? For example, you have changed a lot your philosophy in sizing over the last years, what would be the most important part of the design for this application?

Overall, the most important part is to get a good progression curve. In general, you would like to look for a leverage ratio decrease along the travel, to get a good mid-stroke and bottom out support, but progression must be smooth to have a still predictable design. However, kinematics is a very complex aspect, and getting to understand it all along and knowing how to play with all the values to get the behaviour you want is a universe itself.

Regarding the Computer Aided Design and Engineering, what studies are done on the model? I would imagine a stress analysis using Von Mises or a similar method, and limit deformations. Anything else? And how do you define forces and load conditions for those tests?

Regarding simulations, the ISO 4210 regulation is a good reference to start with. It describes general requirements in safety for bicycles and some tests are described to ensure this very important aspect of the product design. However, extra testing may be carried out under own criteria to ensure the suitability for the intended use.

And for the simulations, is it a good approximation to consider a continuous solid regardless the welds, supposing they are oversized thus they are more rigid than the tubes, or they are also studied? If so, how do you do it? As welding may be difficult to analyse using simulations.

We simulate them, in the sense that we consider every tube partition to be an individual solid and then, using the respective CAD tools we assemble the full piece, selecting the kind of union we want in every case. There is not a standard for simulation in the industry, so every maker does it its own way.

[...]

Now going into the manufacturing process, with which tolerances do you work? For general dimensions and more specifically for bearing housing and axles?

As we manufacture in Taiwan, we work with general tolerances of plus or minus a value to a dimension. For tolerances we generally move between the tenths and hundreds of millimetre range. If the product is sent to Europe instead, we follow European standards.

Finally, how do you manage the quality assurance? In the case of series production and in the case of prototypes, this second is the one I am more interested in, as it is the one applicable for me.

Prototypes do not have to accomplish any ISO standard, so we make our own checks to make sure they are manufactured properly. All production frames or parts, however, go through an ISO quality test.

[...]

Okey, that is all for me! Before closing the interview, have you got anything important worth mentioning or that we missed?

Yes, when simulating, if you have some problems with excessive stress in welded edges, you may try to round them, this is very helpful to solve those issues!

Nice to know, thank you very much for the interview!

No worries! See you!

ANNEX II: MATERIAL SHEET

6061-T6 ALUMINIUM ALLOY

Physical Properties	Metric	Comments
Density	2.70 g/cc	AA; Typical

Mechanical Properties	Metric	Comments
Hardness, Brinell	95	AA; Typical; 500 g load; 10 mm ball
Hardness, Knoop	120	Converted from Brinell Hardness Value
Hardness, Rockwell A	40	Converted from Brinell Hardness Value
Hardness, Rockwell B	60	Converted from Brinell Hardness Value
Hardness, Vickers	107	Converted from Brinell Hardness Value
Tensile Strength, Ultimate	310 MPa	AA; Typical
Tensile Strength, Yield	276 MPa	AA; Typical
Elongation at Break	12 % @Thickness 1.59 mm	AA; Typical
	17 % @Diameter 12.7 mm	AA; Typical
Modulus of Elasticity	68.9 GPa	AA; Typical; Average of tension and compression. Compression modulus is about 2% greater than tensile modulus.
Poissons Ratio	0.33	Estimated from trends in similar Al alloys.
Fatigue Strength	96.5 MPa @# of Cycles 5.00e+8	completely reversed stress; RR Moore machine/specimen
Fracture Toughness	29.0 MPa-m ^{1/2}	K _{IC} ; TL orientation.
Machinability	50 %	0-100 Scale of Aluminum Alloys
Shear Modulus	26.0 GPa	Estimated from similar Al alloys.
Shear Strength	207 MPa	AA; Typical

Thermal Properties	Metric	Comments
CTE, linear	23.6 µm/m-°C @Temperature 20.0 - 100 °C	AA; Typical; average over range
	25.2 µm/m-°C @Temperature 20.0 - 300 °C	
Specific Heat Capacity	0.896 J/g-°C	
Thermal Conductivity	167 W/m-K	AA; Typical at 77°F
Melting Point	582 - 651.7 °C	AA; Typical range based on typical composition for wrought products >= 1/4 in. thickness. Eutectic melting can be eliminated by homogenization.
Solidus	582 °C	AA; Typical
Liquidus	651.7 °C	AA; Typical

Processing Properties	Metric	Comments
Solution Temperature	529 °C	
Aging Temperature	160 °C	Rolled or drawn products; hold at temperature for 18 hr

177 °C

Extrusions or forgings; hold at temperature for 8 hr

Component Elements Properties	Metric	Comments
Aluminum, Al	95.8 - 98.6 %	As remainder
Chromium, Cr	0.04 - 0.35 %	
Copper, Cu	0.15 - 0.40 %	
Iron, Fe	<= 0.70 %	
Magnesium, Mg	0.80 - 1.2 %	
Manganese, Mn	<= 0.15 %	
Other, each	<= 0.05 %	
Other, total	<= 0.15 %	
Silicon, Si	0.40 - 0.80 %	
Titanium, Ti	<= 0.15 %	
Zinc, Zn	<= 0.25 %	

5083 ALUMINIUM ALLOY

Physical Properties	Metric	Comments
Density	2.66 g/cc	AA; Typical

Mechanical Properties	Metric	Comments
Hardness, Brinell	81	500 kg load with 10 mm ball. Calculated value.
Hardness, Knoop	104	Converted from Brinell Hardness Value
Hardness, Rockwell B	50	Converted from Brinell Hardness Value
Hardness, Vickers	91	Converted from Brinell Hardness Value

Tensile Strength, Ultimate	300 MPa	
	>= 270 MPa	
	@Thickness 38.13 - 76.2 mm	
	>= 275 MPa	
	@Thickness 6.35 - 38.1 mm	

Tensile Strength, Yield	190 MPa	
	>= 115 MPa	
	@Thickness 38.13 - 76.2 mm	
	>= 125 MPa	
	@Thickness 6.35 - 38.1 mm	

Elongation at Break	>= 12 %	
	@Thickness 6.35 - 38.1 mm	
	>= 12 %	
	@Thickness 38.13 - 76.2 mm	
	16 %	In 5 cm
	@Thickness 1.60 mm	

Tensile Modulus	70.3 GPa	
-----------------	----------	--

Compressive Modulus	71.7 GPa	
---------------------	----------	--

Poissons Ratio	0.33	Estimated from trends in similar Al alloys.
----------------	------	--

Shear Modulus	26.4 GPa	
---------------	----------	--

Shear Strength	180 MPa	Calculated value.
----------------	---------	-------------------

Thermal Properties	Metric	Comments
CTE, linear	22.3 $\mu\text{m/m}\cdot^\circ\text{C}$	
	@Temperature -50.0 - 20.0 $^\circ\text{C}$	
	23.8 $\mu\text{m/m}\cdot^\circ\text{C}$	AA; Typical; average over range
	@Temperature 20.0 - 100 $^\circ\text{C}$	
	24.2 $\mu\text{m/m}\cdot^\circ\text{C}$	
	@Temperature 20.0 - 100 $^\circ\text{C}$	
	25.0 $\mu\text{m/m}\cdot^\circ\text{C}$	
	@Temperature 20.0 - 200 $^\circ\text{C}$	
	26.0 $\mu\text{m/m}\cdot^\circ\text{C}$	
	@Temperature 20.0 - 300 $^\circ\text{C}$	

Specific Heat Capacity	0.900 J/g- $^\circ\text{C}$	
------------------------	-----------------------------	--

Thermal Conductivity	117 W/m-K	
----------------------	-----------	--

Melting Point	590.6 - 638 $^\circ\text{C}$	AA; Typical range based on typical composition for wrought products >= 1/4 in. thickness
---------------	------------------------------	---

Solidus	590.6 $^\circ\text{C}$	AA; Typical
---------	------------------------	-------------

Liquidus	638 $^\circ\text{C}$	AA; Typical
----------	----------------------	-------------

Processing Properties	Metric	Comments
Annealing Temperature	413 °C	holding at temperature not required
Hot-Working Temperature	316 - 482 °C	

Component Elements Properties	Metric	Comments
Aluminum, Al	92.4 - 95.6 %	As remainder
Chromium, Cr	0.05 - 0.25 %	
Copper, Cu	<= 0.10 %	
Iron, Fe	<= 0.40 %	
Magnesium, Mg	4.0 - 4.9 %	
Manganese, Mn	0.40 - 1.0 %	
Other, each	<= 0.05 %	
Other, total	<= 0.15 %	
Silicon, Si	<= 0.40 %	
Titanium, Ti	<= 0.15 %	
Zinc, Zn	<= 0.25 %	

AISI 4130 STEEL ALLOY

Physical Properties	Metric	Comments
Density	7.85 g/cc	

Mechanical Properties	Metric	Comments
Hardness, Brinell	197	
Hardness, Knoop	219	Converted from Brinell
Hardness, Rockwell B		Converted from Brinell
Hardness, Rockwell C	13	Converted from Brinell hardness. Value below normal HRC range, for comparison purposes only.
Hardness, Vickers	207	Converted from Brinell
Tensile Strength, Ultimate	670 MPa	
Tensile Strength, Yield	435 MPa	
Elongation at Break	25.5 %	in 50 mm
Reduction of Area	60 %	
Modulus of Elasticity	205 GPa	Typical for steel
Bulk Modulus	160 GPa	Typical for steel
Poissons Ratio	0.29	Calculated
Machinability	70 %	Annealed and cold drawn. Based on 100% machinability for AISI 1212 steel.
Shear Modulus	80.0 GPa	Typical for steel
Izod Impact	87.0 J	

Thermal Properties	Metric	Comments
Specific Heat Capacity	0.477 J/g-°C	@Temperature >=100 °C
	0.523 J/g-°C	@Temperature 150 - 200 °C
	0.837 J/g-°C	@Temperature 750 - 800 °C
Thermal Conductivity	30.1 W/m-K	@Temperature 1200 °C
	40.7 W/m-K	@Temperature 300 °C
	42.7 W/m-K	@Temperature 100 °C

Component Elements Properties	Metric	Comments
Carbon, C	0.28 - 0.33 %	
Chromium, Cr	0.80 - 1.1 %	
Iron, Fe	97.03 - 98.22 %	As remainder
Manganese, Mn	0.40 - 0.60 %	
Molybdenum, Mo	0.15 - 0.25 %	
Phosphorus, P	<= 0.035 %	
Silicon, Si	0.15 - 0.30 %	
Sulfur, S	<= 0.040 %	

AISI 1015 STEEL ALLOY

Physical Properties	Metric	Comments
Density	7.87 g/cc	

Mechanical Properties	Metric	Comments
Hardness, Brinell	111	
Hardness, Knoop	129	
Hardness, Rockwell B	64	Converted from Brinell
Hardness, Vickers	115	Converted from Brinell
Tensile Strength, Ultimate	385 MPa	
Tensile Strength, Yield	325 MPa	
Elongation at Break	18 %	In 50 mm
Reduction of Area	40 %	
Modulus of Elasticity	205 GPa	Typical for steel
Bulk Modulus	160 GPa	Typical for steel
Poissons Ratio	0.29	Typical For Steel
Machinability	60 %	Based on 100% machinability for AISI 1212 steel.
Shear Modulus	80.0 GPa	Typical for steel

Thermal Properties	Metric	Comments
CTE, linear	11.9 $\mu\text{m/m-}^\circ\text{C}$	
	@Temperature 0.000 - 100 $^\circ\text{C}$	
	13.0 $\mu\text{m/m-}^\circ\text{C}$	
	@Temperature 0.000 - 300 $^\circ\text{C}$	
	14.2 $\mu\text{m/m-}^\circ\text{C}$	
	@Temperature 0.000 - 500 $^\circ\text{C}$	
Specific Heat Capacity	0.486 J/g- $^\circ\text{C}$	annealed
	@Temperature ≥ 100 $^\circ\text{C}$	
Thermal Conductivity	51.9 W/m-K	estimated based on similar materials

Component Properties	Elements	Metric	Comments
Carbon, C		0.13 - 0.18 %	
Iron, Fe		99.13 - 99.57 %	As remainder
Manganese, Mn		0.30 - 0.60 %	
Phosphorus, P		≤ 0.040 %	
Sulfur, S		≤ 0.050 %	

Ti-6Al-4V (Grade 5) TITANIUM ALLOY

Physical Properties	Metric	Comments
Density	4.43 g/cc	
Mechanical Properties	Metric	Comments
Hardness, Brinell	334	Estimated from Rockwell C.
Hardness, Knoop	363	Estimated from Rockwell C.
Hardness, Rockwell C	36	
Hardness, Vickers	349	Estimated from Rockwell C.
Tensile Strength, Ultimate	950 MPa	
Tensile Strength, Yield	880 MPa	
Elongation at Break	14 %	
Reduction of Area	25 %	
	36 %	
Creep Strength	150 MPa @Temperature 455 °C, Time >=360000 sec	strain 1%
	290 MPa @Temperature 455 °C, Time >=252000 sec	strain 0.1%
	395 MPa @Temperature 400 °C, Time >=108000 sec	strain 1%
	500 MPa @Temperature 400 °C, Time >=540000 sec	strain 0.1%
Rupture Strength	400 MPa @Temperature 455 °C, Time 1.80e+6 sec	
Modulus of Elasticity	113.8 GPa	
Modulus of Rigidity	42.1 GPa	
Compressive Yield Strength	970 MPa	
Notched Tensile Strength	1450 MPa	K _t (stress concentration factor) = 6.7
Ultimate Bearing Strength	1860 MPa	e/D = 2
Bearing Yield Strength	1480 MPa	e/D = 2
Poissons Ratio	0.342	
Fatigue Strength	240 MPa @# of Cycles 1.00e+7	K _t (stress concentration factor) = 3.3
	250 MPa @# of Cycles 1.00e+7	notched bar
	300 MPa @# of Cycles 100000	notched bar
	510 MPa @# of Cycles 1.00e+7	smooth bar
	510 MPa @# of Cycles 1.00e+7	Unnotched
	600 MPa @# of Cycles 100000	smooth bar
Fracture Toughness	74.6 MPa-m ^{1/2} 75.0 MPa-m ^{1/2}	Annealed plate
Shear Modulus	44.0 GPa	
Shear Strength	550 MPa	Ultimate shear strength
Charpy Impact	17.0 J	V-notch
Bend Radius, Minimum	5.0 t @Thickness >=1.80 mm	
Thermal Properties	Metric	Comments
CTE, linear	8.60 µm/m-°C @Temperature 20.0 - 100 °C	

	9.20 $\mu\text{m/m}\cdot^\circ\text{C}$ @Temperature 20.0 - 315 $^\circ\text{C}$	average
	9.70 $\mu\text{m/m}\cdot^\circ\text{C}$ @Temperature 20.0 - 650 $^\circ\text{C}$	average
Specific Heat Capacity	0.5263 J/g- $^\circ\text{C}$	
Thermal Conductivity	6.70 W/m-K	
Melting Point	1604 - 1660 $^\circ\text{C}$	
Solidus	1604 $^\circ\text{C}$	
Liquidus	1660 $^\circ\text{C}$	
Beta Transus	980 $^\circ\text{C}$	

Component Elements	Metric	Comments
Properties		
Aluminum, Al	5.5 - 6.75 %	
Carbon, C	≤ 0.080 %	
Hydrogen, H	≤ 0.015 %	
Iron, Fe	≤ 0.40 %	
Nitrogen, N	≤ 0.030 %	
Other, each	≤ 0.050 %	
Other, total	≤ 0.30 %	
Oxygen, O	≤ 0.20 %	
Titanium, Ti	87.725 - 91 %	As Balance; Elemental Composition per ASTM B265
Vanadium, V	3.5 - 4.5 %	

ANNEX III: ANALYTICAL EVALUATION OF CHAIN AND BRAKE FORCES INFLUENCE ON PERFORMANCE REAR SUSPENSION SYSTEMS

CHAIN AND BRAKE FORCES INFLUENCE ON PERFORMANCE OF A BICYCLE REAR SUSPENSION SYSTEM

ABSTRACT

During the design process of a bicycle rear suspension system, different parameters are studied to evaluate its performance. Particularly, anti-squat and anti-rise are used to characterise linkage independence from forces different than those deemed to compress the shock, induced by weight transfer because of accelerations and decelerations, or influence of systems external to the suspension that may have an effect on its operation.

ANALYTICAL EVALUATION OF ANTI-RISE AND ANTI-SQUAT

Usually, for simplicity reasons, graphic methods are used to characterise anti-rise and anti-squat. In the following, an analytical evaluation on these parameters will be performed to better understand influence of external systems to suspension in its performance. Effects of weight transfer and accelerations will not be treated due to the great complexity of the different cases that may have an influence in this, briefly, if the centre of gravity is globally retarded towards its normal position, lever of the rear wheel contact patch will be reduced, which will result in an effectively higher load, and vice versa for the opposite case.

ANTI-RISE

Anti-rise gives an idea on the effect of braking in suspension performance. Conceptually, this depends on relative rotation of the rear brake calliper with the rear wheel. The force to compress the suspension applied on the rear wheel is always perpendicular to the contact patch, thus with the wheel in a stationary state, if the linkage is to be compressed, a relative rotation can be observed between the force line and the bars conforming the suspension system. If the rear wheel is locked by the action of the brake, this will prevent any relative rotation between it and the calliper, which could effectively lock the suspension system.

For the demonstration, a *split pivot* layout will be used, this is a specific type of single pivot linkage driven design, in which the attachment point of the chainstay (AB) with the rear bar (BC) is coincident with the rear axle (B). This particularity permits to evaluate the same layout with the calliper mounted either on the chainstay or in the rear bar, which will change the position of its instant centre. See figure below:

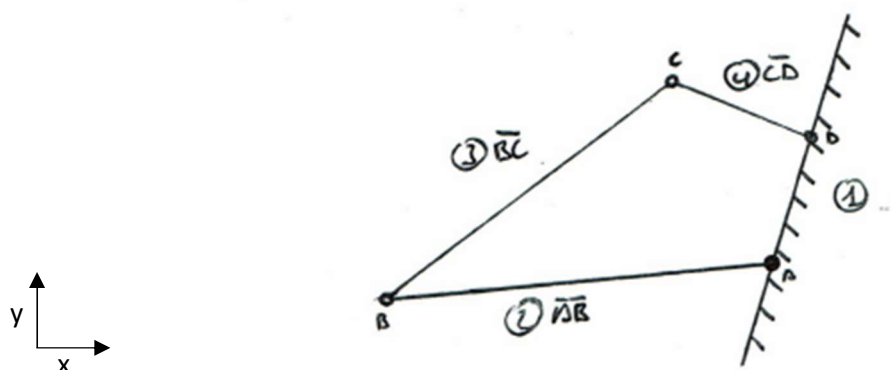


Figure 3.1: Split pivot layout model

Two different scenarios will be here presented, in which the brake calliper, represented by a new point "E", will be situated in the AB segment, this is the bar number 2, which represents the chainstay, or it was in the BC segment, which is bar number 3, representing the rear bar.

In the following, longitude of every bar will be the length in which segment they are contained, and their rotation will be notated as φ with the corresponding subindex.

Setting the angular velocity for either *bar no.2* or *bar no.4*, for any given geometry it is possible to find linear and angular velocity for all given points and bars, respectively.

$$\vec{v}_B = \vec{\omega}_2 \times \overline{AB} = \omega_2 \cdot (-\overline{AB} \cdot \sin \varphi_2 \hat{i} + \overline{AB} \cdot \cos \varphi_2 \hat{j}) \quad (\text{Equation 3.1})$$

$$\vec{v}_C = \vec{\omega}_4 \times \overline{CD} = \omega_4 \cdot (-\overline{CD} \cdot \sin \varphi_4 \hat{i} + \overline{CD} \cdot \cos \varphi_4 \hat{j}) \quad (\text{Equation 3.2})$$

Considering these two points are united by a rigid bar, thus relative velocity is equal to 0, we can write:

$$\begin{aligned} \vec{v}_C &= \vec{v}_B + \vec{\omega}_3 \times \overline{BC} + \vec{v}_{rel} \\ &= \omega_2 \cdot (-\overline{AB} \cdot \sin \varphi_2 \hat{i} + \overline{AB} \cdot \cos \varphi_2 \hat{j}) + \omega_3 \cdot (-\overline{BC} \cdot \sin \varphi_3 \hat{i} + \overline{BC} \cdot \cos \varphi_3 \hat{j}) \end{aligned} \quad (\text{Equation 3.3})$$

Now, equalizing both equations for \vec{v}_C :

$$\begin{aligned} \omega_4 \cdot (-\overline{CD} \cdot \sin \varphi_4 \hat{i} + \overline{CD} \cdot \cos \varphi_4 \hat{j}) &= \omega_2 \cdot (-\overline{AB} \cdot \sin \varphi_2 \hat{i} + \overline{AB} \cdot \cos \varphi_2 \hat{j}) + \omega_3 \cdot (-\overline{BC} \cdot \sin \varphi_3 \hat{i} + \overline{BC} \cdot \cos \varphi_3 \hat{j}) \\ \begin{cases} \omega_4 \cdot (-\overline{CD} \cdot \sin \varphi_4) = \omega_2 \cdot (-\overline{AB} \cdot \sin \varphi_2) + \omega_3 \cdot (-\overline{BC} \cdot \sin \varphi_3) \\ \omega_4 \cdot (\overline{CD} \cdot \cos \varphi_4) = \omega_2 \cdot (\overline{AB} \cdot \cos \varphi_2) + \omega_3 \cdot (\overline{BC} \cdot \cos \varphi_3) \end{cases} \\ \omega_3 = \frac{\omega_4 \cdot (-\overline{CD} \cdot \sin \varphi_4) - \omega_2 \cdot (-\overline{AB} \cdot \sin \varphi_2)}{(-\overline{BC} \cdot \sin \varphi_3)} \end{aligned} \quad (\text{Equation 3.4})$$

Having obtained this relation, some considerations shall be made. Knowing both sinus for bars 2 and 4 are positive for any given point of the travel, and this is a corotating system, thus ω_2 and ω_4 will have the same sign, we can conclude absolute value of ω_3 will always be minor than absolute value of ω_2 , as those cases where sinus for φ_4 is equal to zero are not part of the useful travel range. As a consequence, any given point a certain distance from *B* (this will be defined by the rotor size and will be equal notwithstanding the calliper is mounted in bar 2 or 3) will rotate more relatively to the wheel if it is mounted in bar 2 than if its mounted in bar number 4, for this reason, the second option will provide more independence for the suspension system from braking forces.

However, there is another factor considered in the graphical method, to better understand this, movement and velocity equations for point *E* shall be written for both cases. This is made by defining the equation of the trajectory of the calliper with respect the bench (bar 1), and then finding its first derivative.

Writing movement equations for point *E* if it was situated in bar 2: (Equation 3.5)

$$\begin{aligned} \vec{r} &= \overline{AE} \cdot \cos(\varphi_{2o} + \omega_{2o} \cdot t + \frac{1}{2} \cdot \varepsilon_{2o} \cdot t^2) \hat{i} + \overline{AE} \cdot \sin(\varphi_{2o} + \omega_{2o} \cdot t + \frac{1}{2} \cdot \varepsilon_{2o} \cdot t^2) \hat{j} \\ \vec{v} = \frac{d\vec{r}}{dt} &= \overline{AE} \cdot \left(-\sin\left(\varphi_{2o} + \omega_{2o} \cdot t + \frac{1}{2} \cdot \varepsilon_{2o} \cdot t^2\right) \cdot (\omega_{2o} + \varepsilon_{2o} \cdot t) \right) \hat{i} + \overline{AE} \\ &\quad \cdot \left(\cos\left(\varphi_{2o} + \omega_{2o} \cdot t + \frac{1}{2} \cdot \varepsilon_{2o} \cdot t^2\right) \cdot (\omega_{2o} + \varepsilon_{2o} \cdot t) \right) \hat{j} \end{aligned} \quad (\text{Equation 3.6})$$

Instead, if E was mounted in bar no.3, its equations would be:

(Equation 3.7)

$$\vec{r} = \overline{AB} \cdot \cos\left(\varphi_{2o} + \omega_{2o} \cdot t + \frac{1}{2} \cdot \varepsilon_{2o} \cdot t^2\right) + \overline{BE} \cdot \cos\left(\varphi_{3o} + \omega_{3o} \cdot t + \frac{1}{2} \cdot \varepsilon_{3o} \cdot t^2\right) \hat{i} + \overline{AB} \cdot \sin\left(\varphi_{2o} + \omega_{2o} \cdot t + \frac{1}{2} \cdot \varepsilon_{2o} \cdot t^2\right) + \overline{BE} \cdot \sin\left(\varphi_{3o} + \omega_{3o} \cdot t + \frac{1}{2} \cdot \varepsilon_{3o} \cdot t^2\right) \hat{j}$$

(Equation 3.8)

$$\vec{v} = \frac{d\vec{r}}{dt} = \left(\overline{AB} \cdot \left(-\sin\left(\varphi_{2o} + \omega_{2o} \cdot t + \frac{1}{2} \cdot \varepsilon_{2o} \cdot t^2\right) \cdot (\omega_{2o} + \varepsilon_{2o} \cdot t) \right) + \overline{BE} \cdot \left(-\sin\left(\varphi_{3o} + \omega_{3o} \cdot t + \frac{1}{2} \cdot \varepsilon_{3o} \cdot t^2\right) \cdot (\omega_{3o} + \varepsilon_{3o} \cdot t) \right) \right) \hat{i} + \left(\overline{AB} \cdot \left(\cos\left(\varphi_{2o} + \omega_{2o} \cdot t + \frac{1}{2} \cdot \varepsilon_{2o} \cdot t^2\right) \cdot (\omega_{2o} + \varepsilon_{2o} \cdot t) \right) + \overline{BE} \cdot \left(\cos\left(\varphi_{3o} + \omega_{3o} \cdot t + \frac{1}{2} \cdot \varepsilon_{3o} \cdot t^2\right) \cdot (\omega_{3o} + \varepsilon_{3o} \cdot t) \right) \right) \hat{j}$$

Now, considering the force on the wheel to compress the suspension must necessarily be in the form:

$$F_{whe} = 0 \hat{i} + x \hat{j}$$

This only has component in the y axle as this is the normal force considered in a flat horizontal ground. Velocity in the y axis, this is component \hat{j} of the velocity vector, will be in line with this force vector, so this will not cause any interference in the functioning of the suspension. Component \hat{i} instead, is perpendicular to the direction of movement of the wheel, this is, it will cause the calliper to rotate towards the wheel, being the responsible of the braking forces interference on suspension performance. Looking at *figure 3.1* it can be observed that \overline{AB} and \overline{BC} vectors have an opposite sense, thus we can deduce that the terms corresponding to position and velocity in the x axis will be minor in the case where the calliper sits in bar 3.

These two ideas are exploited in the graphical method, where the instant centre, point towards all moving parts are moving at a given instant, is used to mark a line which will categorize in an intuitive scale how in-line the direction of the velocity vector of any component, including the calliper, is towards the normal force on the wheel.

ANTI-SQUAT

A part of determining anti-squat is to analyse influence of chain forces in suspension performance. This is made by drawing the contact point between the chain line and the effective swingarm. Forces applied by the chain will be in the form of tension, as this is the only stress this component can transfer. Effective swingarm is a measurement defined by the segment passing through the rear axle and the centre of curvature.

The effect of the chain forces \vec{F}_c on the suspension is determined by the momentum it generates with respect to the centre of curvature (cc). We can write:

$$\sum \vec{M}_{cc} = \vec{r}_c \times \vec{F}_c = \begin{vmatrix} \hat{i} & \hat{j} & \hat{k} \\ r_x & r_y & 0 \\ F_x & F_y & 0 \end{vmatrix} = +r_x \cdot F_y - r_y \cdot F_x \quad (\text{Equation 3.9})$$

Note: Forces on z axis or momentums in x or y axis will be absorbed by the bearings.

Looking at *figure 3.1*, in this case the effective swingarm is the chainstay (bar 2), for being a single pivot design. The line of application of the chain force on the rear wheel is defined by the point of tangency of the chain with the chosen gear of the cassette and the chainring, or the redirection pulley, if any. If the momentum this tension generates is positive, thus tending to rotate the swingarm counterclockwise, this will extend the suspension, instead, if the force generates a negative momentum, inducing a clockwise rotation, this will compress the suspension.

To better analyse these interactions, the whole system can be rotated, situating the effective swingarm along the x axis. Being θ_2 the angle the chainstay forms with the ground, all coordinates can be transformed to the new reference system:

$$\begin{pmatrix} x' \\ y' \end{pmatrix} = \begin{pmatrix} \cos \theta_2 & \sin \theta_2 \\ -\sin \theta_2 & \cos \theta_2 \end{pmatrix} \cdot \begin{pmatrix} x \\ y \end{pmatrix} \quad (\text{Equation 3.10})$$

The direction of the chain tension \vec{d}_c will be obtained with the new coordinates of the beforementioned tangency points:

$$\vec{d}_c = (x'_{t,chainring} - x'_{t,cassette})\hat{i} + (y'_{t,chainring} - y'_{t,cassette})\hat{j} \quad (\text{Equation 3.11})$$

Now, for any given modulus of this tension $|\vec{F}_c|$, the force of the chain can be defined:

$$\vec{F}_c = |\vec{F}_c| \cdot \vec{d}_c = |\vec{F}_c| \cdot (x'_{t,chainring} - x'_{t,cassette})\hat{i} + |\vec{F}_c| \cdot (y'_{t,chainring} - y'_{t,cassette})\hat{j} \quad (\text{Equation 3.12})$$

And being the point of application for this force the cassette tangency point, for what its effect on the swingarm is concerned, it is obtained:

$$\vec{r}_c = \vec{r}_{t,cassette} - \vec{r}_{cc} = (x'_{t,cassette} - x'_{cc})\hat{i} + (y'_{t,cassette} - y'_{cc})\hat{j} \quad (\text{Equation 3.13})$$

Analysing the graphical method, it uses this idea by finding the intersection between the chain line and the effective swingarm line, which shall necessarily pass through the instant centre. Depending on the position of this intersection, a value in an intuitive scale is given for determining anti-squat. The centre of curvature will usually be situated in the near to 100% anti-squat range, so for systems with a chain-line passing through this point, minimal effect of chain force on suspension performance can be deduce and demonstrated by the minimal momentum towards cc this will generate. Instead, if the chain line intercepts the swingarm line retarded, or advanced towards the cc, this will tend to extend or compress the suspension by the generation of a positive and negative momentum, respectively.

CONCLUSION

Effects of systems exterior to suspension do affect its performance, and this can be analytically demonstrated. However, the use of graphical methods is largely extended in the industry because of being much more immediate and intuitive, notwithstanding this is not so precise, those methods characterise the interferences of braking and chain forces well enough to permit to qualitatively analyse a suspension system.

ANNEX IV: TEST REPORTS

Campus Diagonal Besòs, Building A (EEBE)
Avda. Eduard Maristany, 16
08019 Barcelona (SPAIN)

Standard: ISO 4210-1:2014
Report No.: 42100101

Phone +34 93 413 74 00
Fax +34 93 413 74 01

TEST REPORT No. 42100101

TEST ACCORDING TO ISO 4210-1:2014 CONCERNING SAFETY REQUIREMENTS FOR BICYCLES WITH REGARD TO TERMS AND DEFINITIONS

Applicant	:	Campus Diagonal Besòs, Building A (EEBE) Avda. Eduard Maristany, 16 08019 Barcelona (SPAIN)
Manufacturer	:	Campus Diagonal Besòs, Building A (EEBE) Avda. Eduard Maristany, 16 08019 Barcelona (SPAIN)
Commercial description	:	HP4bar
Type	:	Mountain bike
Category	:	Suspension-frame
Complete bicycle	:	No
Component	:	Bicycle frame
Place and date	:	Vilafranca del Penedès, 03/12/2022

CONCLUSIONS: The sample described above has been verified to meet ISO 4210-1:2014 prescriptions and is suitable to be tested as per ISO 4210 standard.

Test responsible:

David Rey Escamilla

ANNEX TO THE REPORT

1. SAMPLE DESCRIPTION

- 1.1. Applicant : Campus Diagonal Besòs, Building A (EEBE)
Avda. Eduard Maristany, 16
08019 Barcelona (SPAIN)
- 1.2. Manufacturer : Campus Diagonal Besòs, Building A (EEBE)
Avda. Eduard Maristany, 16
08019 Barcelona (SPAIN)
- 1.3. Commercial description : HP4bar
- 1.4. Type : Mountain bike
- 1.5. Category : Suspension-frame
- 1.6. Component : Bicycle frame
- 1.7. Material : F-1110 steel / S-235J steel / 5083 aluminium alloy
- 1.8. Method of construction : MIG welding (only steel structures)

2. TEST RESULTS

2.1. SCOPE

FULFILLS

- 2.1.1. The tested sample is considered in the scope of this standard:
Yes / ~~No~~
- 2.1.2. Type of bicycle:
Mountain bicycle.
- 2.1.3. Maximum saddle height:
1.030 mm.

Place: Vilafranca del Penedès, Barcelona
Date: 03/12/2022



David Rey Escamilla

TEST REPORT No. 42100201

TEST ACCORDING TO ISO 4210-2:2015 CONCERNING SAFETY REQUIREMENTS FOR BICYCLES WITH REGARD TO REQUIREMENTS FOR CITY AND TREKKING, YOUNG ADULT, MOUNTAIN AND RACING BICYCLES

Applicant	:	Campus Diagonal Besòs, Building A (EEBE) Avda. Eduard Maristany, 16 08019 Barcelona (SPAIN)
Manufacturer	:	Campus Diagonal Besòs, Building A (EEBE) Avda. Eduard Maristany, 16 08019 Barcelona (SPAIN)
Commercial description	:	HP4bar
Type	:	Mountain bike
Category	:	Suspension-frame
Complete bicycle	:	No
Component	:	Bicycle frame
Place and date	:	Vilafranca del Penedès, 03/12/2022

CONCLUSIONS: The sample described above has been tested by simulation according to ISO 4210-2:2015 and does meet the requirements of this standard as described in the annex to this report.

Test responsible:

David Rey Escamilla

ANNEX TO THE REPORT

1. SAMPLE DESCRIPTION

- | | | | |
|------|------------------------|---|---|
| 1.1. | Applicant | : | Campus Diagonal Besòs, Building A (EEBE)
Avda. Eduard Maristany, 16
08019 Barcelona (SPAIN) |
| 1.2. | Manufacturer | : | Campus Diagonal Besòs, Building A (EEBE)
Avda. Eduard Maristany, 16
08019 Barcelona (SPAIN) |
| 1.3. | Commercial description | : | HP4bar |
| 1.4. | Type | : | Mountain bike |
| 1.5. | Category | : | Suspension-frame |
| 1.6. | Component | : | Bicycle frame |
| 1.7. | Material | : | F-1110 steel / S-235J steel / 5083 aluminium alloy |
| 1.8. | Method of construction | : | MIG welding (only steel structures) |

2. TEST RESULTS

2.1. REQUIREMENTS

- | | | |
|----------|---|----------------|
| 2.1. | REQUIREMENTS | FULFILLS |
| 2.1.1. | Requirements regarding toxicity: | FULFILLS |
| 2.1.2. | Requirements regarding sharp edges: | FULFILLS |
| 2.1.3. | Requirements regarding security and strength of safety-related fasteners: | FULFILLS |
| 2.1.3.1. | Security of screws: | FULFILLS |
| 2.1.3.2. | Minimum failure torque: | FULFILLS |
| 2.1.3.3. | Folding bicycle mechanism: | NOT APPLICABLE |
| 2.1.4. | Requirements regarding crack detection methods: | NOT APPLICABLE |
| 2.1.5. | Requirements regarding protrusions: | FULFILLS |

2.1.6. Requirements regarding brakes:

NOT APPLICABLE

Remark: The bicycle will be equipped with two independently actuated braking systems, one operating in the front wheel and one operating in the rear wheel, complying the specific component requirements described in this standard.

2.1.7. Requirements regarding steering:

NOT APPLICABLE

Remark: The bicycle will be equipped with suitable handlebar, grips, and stem complying the specific component requirements described in this standard.

2.1.8. Requirements regarding the frame:

FULFILLS

2.1.8.1. Special requirements for suspension frames:

FULFILLS

2.1.8.2. Falling mass impact test:

FULFILLS

Remark: See test report No. 42100601.

2.1.8.3. Falling frame impact test:

FULFILLS

Remark: See test report No. 42100601.

2.1.8.4. Fatigue test with pedalling forces:

FULFILLS

Remark: See test report No. 42100601.

2.1.8.5. Fatigue test with horizontal forces:

FULFILLS

Remark: See test report No. 42100601.

2.1.8.6. Fatigue test with a vertical force:

FULFILLS

Remark: See test report No. 42100601.

2.1.9. Requirements regarding front fork:

NOT APPLICABLE

Remark: The bicycle will be equipped with a suspension fork complying the specific component requirements described in this standard.

2.1.10. Requirements regarding wheels and wheel/tyre assembly:

NOT APPLICABLE

Remark: The bicycle will be equipped with proper wheels complying the specific component requirements described in this standard. The frame is suitable for a tyre up to 2.6" wide.

2.1.11. Requirements regarding rims, tyres, and tubes:

NOT APPLICABLE

Remark: The bicycle will be equipped with aluminium rims which are not deemed to be part of the braking system. Tubes and/or tyre inflation pressure shall be as specified by the manufacturer.

2.1.12. Requirements regarding front mudguard:

NOT APPLICABLE

Remark: If front mudguard is fitted it shall comply with fork manufacturer specifications.

2.1.13. Requirements regarding pedals and pedal/crank drive system:

NOT APPLICABLE

Remark: The bicycle will be equipped with suitable pedals and cranks complying the specific component requirements described in this standard.

2.1.14. Requirements regarding drive-chain and drive belt:

NOT APPLICABLE

Remark: The bicycle will be equipped with a suitable chain-drive system complying the specific component requirements described in this standard.

2.1.15. Requirements regarding chain-wheel and belt-drive protective device:

NOT APPLICABLE

2.1.16. Requirements regarding saddles and seat-posts:

NOT APPLICABLE

Remark: The bicycle will be equipped with a suitable saddle and seat-post complying the specific component requirements described in this standard.

2.1.17. Requirements regarding spoke protector:

NOT APPLICABLE

2.1.18. Requirements regarding luggage carriers:

NOT APPLICABLE

2.1.19. Road test of a fully assembled bicycle:

NOT APPLICABLE

Remark: See test report No. 42100301

2.1.20. Requirements regarding lighting systems and reflectors:

NOT APPLICABLE

Remark: No retroreflectors nor lighting systems will be installed because the bicycle is not intended for public road use. If it is used in public roads suitable devices shall be so installed to meet national regulation requirements.

2.1.21. Requirements regarding warning device:

NOT APPLICABLE

Remark: No warning device will be installed because the bicycle is not intended for public road use. If it is used in public roads a warning device shall be so installed to meet national regulation requirements.

2.2. MANUFACTURER'S INSTRUCTIONS

FULFILLS

Remark: The bicycle will be provided with an information document covering all points required in part 5 of ISO 4210-2:2015 standard.

2.3. MARKING

FULFILLS

2.3.1. Method of marking:

Serial number stamped, see test report No. 42100301.

FULFILLS

2.3.2. Location of that marking:

Lower part of bottom bracket.

FULFILLS

Place: Vilafranca del Penedès, Barcelona
Date: 03/12/2022



David Rey Escamilla

Campus Diagonal Besòs, Building A (EEBE)
Avda. Eduard Maristany, 16
08019 Barcelona (SPAIN)

Standard: ISO 4210-3:2014
Report No.: 42100301

Phone +34 93 413 74 00
Fax +34 93 413 74 01

TEST REPORT No. 42100301

TEST ACCORDING TO ISO 4210-3:2014 CONCERNING SAFETY REQUIREMENTS FOR BICYCLES WITH REGARD TO COMMON TEST METHODS

Applicant	:	Campus Diagonal Besòs, Building A (EEBE) Avda. Eduard Maristany, 16 08019 Barcelona (SPAIN)
Manufacturer	:	Campus Diagonal Besòs, Building A (EEBE) Avda. Eduard Maristany, 16 08019 Barcelona (SPAIN)
Commercial description	:	HP4bar
Type	:	Mountain bike
Category	:	Suspension-frame
Complete bicycle	:	No
Component	:	Bicycle frame
Place and date	:	Vilafranca del Penedès, 03/12/2022

CONCLUSIONS: The sample described above has been tested by simulation according to ISO 4210-3:2014 and does meet the requirements of this standard as described in the annex to this report.

Test responsible:

David Rey Escamilla

ANNEX TO THE REPORT

1. SAMPLE DESCRIPTION

- | | | | |
|------|------------------------|---|---|
| 1.1. | Applicant | : | Campus Diagonal Besòs, Building A (EEBE)
Avda. Eduard Maristany, 16
08019 Barcelona (SPAIN) |
| 1.2. | Manufacturer | : | Campus Diagonal Besòs, Building A (EEBE)
Avda. Eduard Maristany, 16
08019 Barcelona (SPAIN) |
| 1.3. | Commercial description | : | HP4bar |
| 1.4. | Type | : | Mountain bike |
| 1.5. | Category | : | Suspension-frame |
| 1.6. | Component | : | Bicycle frame |
| 1.7. | Material | : | F-1110 steel / S-235J steel / 5083 aluminium alloy |
| 1.8. | Method of construction | : | MIG welding (only steel structures) |

2. TEST RESULTS

2.1. TEST PROCEDURES

FULFILLS

2.1.1. Braking and endurance tests:

FULFILLS

2.1.1.1. Definition of braking tests:

NOT APPLICABLE

2.1.1.2. Definition of endurance tests:

APPLICABLE

2.1.1.3. Number of samples for endurance tests:

FULFILLS

Remark: Simulations will be made on undamaged samples.

2.1.1.4. Tolerances for precision of test procedures:

FULFILLS

Remark: Simulations will be made as described in the applicable standard, using the values given for loads and dimensions and not considering any induced error.

2.1.2. Test methods for front mudguard:

NOT APPLICABLE

Remark: If a front mudguard is fitted it shall be fitted according to fork manufacturer instructions.

2.1.3. On road test method for a complete bicycle:

NOT APPLICABLE

Remark: Not considered as per simulation test. CAD model has been so designed to avoid interference between parts that should not come into contact in normal use of the bicycle.

2.1.4. Endurance test for bicycle marking:

FULFILLS

Remark: Bicycle serial number stamped in the inferior part of the bottom bracket. This marking method ensures resistance against abrasion and chemical attack.

2.1.5. Fatigue tests:

FULFILLS

Remark: Assembly restrictions ensures no loosening of mechanical bonding.

2.1.6. Fatigue test for composite components:

NOT APPLICABLE

2.1.7. Impact test:

FULFILLS

Remark: Impact test simulations are made at 100% of the speed specified in the direction of application.

2.1.8. Tests on plastic materials at ambient temperature:

NOT APPLICABLE

Place: Vilafranca del Penedès, Barcelona
Date: 03/12/2022



David Rey Escamilla

Campus Diagonal Besòs, Building A (EEBE)
Avda. Eduard Maristany, 16
08019 Barcelona (SPAIN)

Standard: ISO 4210-6:2014
Report No.: 42100601

Phone +34 93 413 74 00
Fax +34 93 413 74 01

TEST REPORT No. 42100601

TEST ACCORDING TO ISO 4210-6:2014 CONCERNING SAFETY REQUIREMENTS FOR BICYCLES WITH REGARD TO REQUIREMENTS FOR CITY AND TREKKING, YOUNG ADULT, MOUNTAIN AND RACING BICYCLES

Applicant	:	Campus Diagonal Besòs, Building A (EEBE) Avda. Eduard Maristany, 16 08019 Barcelona (SPAIN)
Manufacturer	:	Campus Diagonal Besòs, Building A (EEBE) Avda. Eduard Maristany, 16 08019 Barcelona (SPAIN)
Commercial description	:	HP4bar
Type	:	Mountain bike
Category	:	Suspension-frame
Complete bicycle	:	No
Component	:	Bicycle frame
Place and date	:	Vilafranca del Penedès, 03/12/2022

CONCLUSIONS: The sample described above has been tested by simulation according to ISO 4210-6:2014 and does meet the requirements of this standard as described in the annex to this report.

Test responsible:

David Rey Escamilla

ANNEX TO THE REPORT

1. SAMPLE DESCRIPTION

- 1.1. Applicant : Campus Diagonal Besòs, Building A (EEBE)
Avda. Eduard Maristany, 16
08019 Barcelona (SPAIN)
- 1.2. Manufacturer : Campus Diagonal Besòs, Building A (EEBE)
Avda. Eduard Maristany, 16
08019 Barcelona (SPAIN)
- 1.3. Commercial description : HP4bar
- 1.4. Type : Mountain bike
- 1.5. Category : Suspension-frame
- 1.6. Component : Bicycle frame
- 1.7. Material : F-1110 steel / S-235J steel / 5083 aluminium alloy
- 1.8. Method of construction : MIG welding (only steel structures)

2. TEST RESULTS

2.1. FRAME TEST METHODS

APPLICABLE

Remark: The forces in the front fork have been applied as a remote load, simulating a solid rigid fork, thus meeting requirements for a false fork as described in annex A of this standard.
Bicycle equipped with a non-lockable rear suspension system. A rigid union with a dimension that permits a 30% SAG position with similar fittings as a real suspension system has been installed.

- 1.1. Falling mass impact test:
 - 1.1.1. Test conditions:
 - 1.1.1.1. Force applied: 603,74 N
 - 1.1.1.2. Time considered for the impact: 0,1 s
 - 1.1.1.3. Calculated deceleration of the mass: 26,83 m/s²
 - 1.1.2. Test results:
 - 1.1.2.1. Maximum stress: 117,0 MPa
 - 1.1.2.2. Maximum displacement: 0,376 mm

1.1.2.3. Maximum unitary deformation: $0,368 \times 10^{-3}$

Remark: Highest stress values on the frame are observed in the headtube union. Maximum stress values are lower than yield strength thus no plastic deformation is observed after the test simulation. No visible cracks or fractures are deemed to occur.

1.2. Falling frame impact test:

1.2.1. Test conditions:

1.2.1.1. Force applied:

1 – Seat tube:	285,14 N
2 – Headtube:	208,02 N
3 – Bottom bracket:	738,10 N

1.2.1.2. Time considered for the impact: 0,1 s

1.2.1.3. Calculated deceleration of the mass:

1 – Seat tube:	9,50 m/s ²
2 – Headtube:	20,80 m/s ²
3 – Bottom bracket:	14,76 m/s ²

1.2.2. Test results:

1.2.2.1. Maximum stress: 631,8 MPa

1.2.2.2. Maximum displacement: 4,825 mm

1.2.2.3. Maximum unitary deformation: $3,581 \times 10^{-3}$

Remark: Highest stress values on the frame are observed in the rear wheel axle attaching points. Maximum stress values are lower than yield strength thus no plastic deformation is observed after the test simulation. No visible cracks or fractures are deemed to occur.

1.3. Fatigue test with pedalling forces:

1.3.1. Test conditions:

1.3.1.1. Force applied: 1.200 N

1.3.1.2. Number of cycles: 100.000

1.3.2. Static analysis results:

1.3.2.1. Maximum stress: 730,9 MPa

1.3.2.2. Maximum displacement: 7,268 mm

1.3.2.3. Maximum unitary deformation: $1,923 \times 10^{-3}$

1.3.2.4. Further testing required: Yes / ~~No~~

1.3.3. Test results:

1.3.3.1. Damage percentage: 10%

Remark: Damage observed after the test simulation will not cause a critical failure. No visible cracks or fractures are deemed to occur, however, further testing on a real sample should be made.

1.4. Fatigue test with horizontal forces:

1.4.1. Test conditions:

1.4.1.1. Force applied:

Compression: 600 N
Traction: 1.200 N

1.4.1.2. Number of cycles: 50.000

1.4.2. Static analysis results:

1.4.2.1. Maximum stress:

Compression: 112,2 MPa
Traction: 249,5 MPa

1.4.2.2. Maximum displacement:

Compression: 0,344 mm
Traction: 0,885 mm

1.4.2.3. Maximum unitary deformation:

Compression: $0,355 \times 10^{-3}$
Traction: $0,807 \times 10^{-3}$

1.4.2.4. Further testing required: Yes / ~~No~~

1.4.3. Test results:

1.4.3.1. Damage percentage: 10%

Remark: Damage observed after the test simulation will not cause a critical failure. No visible cracks or fractures are deemed to occur, however, further testing on a real sample should be made.

1.5. Fatigue test with a vertical force:

1.5.1. Test conditions:

1.5.1.1. Force applied:

1.200 N

1.5.1.2. Number of cycles: 50.000

1.5.2. Static analysis results:

1.5.2.1. Maximum stress: 494,3 MPa

1.5.2.2. Maximum displacement: 2,466 mm

1.5.2.3. Maximum unitary deformation: $2,866 \times 10^{-3}$

1.5.2.4. Further testing required: Yes / ~~No~~

1.5.3. Test results:

1.5.3.1. Damage percentage: 5%

Remark: Damage observed after the test simulation will not cause a critical failure. No visible cracks or fractures are deemed to occur, however, further testing on a real sample should be made.

2.2. FORK TEST METHODS

NOT APPLICABLE

Place: Vilafranca del Penedès, Barcelona
Date: 03/12/2022



David Rey Escamilla

ANNEX V: TEST SHEET

TEST SHEET No. 42100601

TEST ACCORDING TO ISO 4210-6:2014 CONCERNING SAFETY REQUIREMENTS FOR BICYCLES WITH REGARD TO REQUIREMENTS FOR CITY AND TREKKING, YOUNG ADULT, MOUNTAIN AND RACING BICYCLES

1. SAMPLE DESCRIPTION

- 1.1. Applicant : Campus Diagonal Besòs, Building A (EEBE)
Avda. Eduard Maristany, 16
08019 Barcelona (SPAIN)
- 1.2. Manufacturer : Campus Diagonal Besòs, Building A (EEBE)
Avda. Eduard Maristany, 16
08019 Barcelona (SPAIN)
- 1.3. Commercial description : HP4bar
- 1.4. Type : Mountain bike
- 1.5. Category : Suspension-frame
- 1.6. Component : Bicycle frame
- 1.7. Material : F-1110 steel / S-235J steel / 5083 aluminium alloy
- 1.8. Method of construction : MIG welding (only steel structures)

2. TEST RESULTS

2.1. Applicable tests:

- Falling mass impact test
- Falling frame impact test
- Fatigue test with pedalling forces
- Fatigue test with horizontal forces
- Fatigue test with vertical forces

2.2. Use of false fork as described in annex 1: Yes / ~~No~~ / ~~Not applicable~~

2.3. Suspension frame: Yes / ~~No~~ / ~~Not applicable~~







































2.4. Lockable suspension system: ~~Yes~~ / No / ~~Not applicable~~

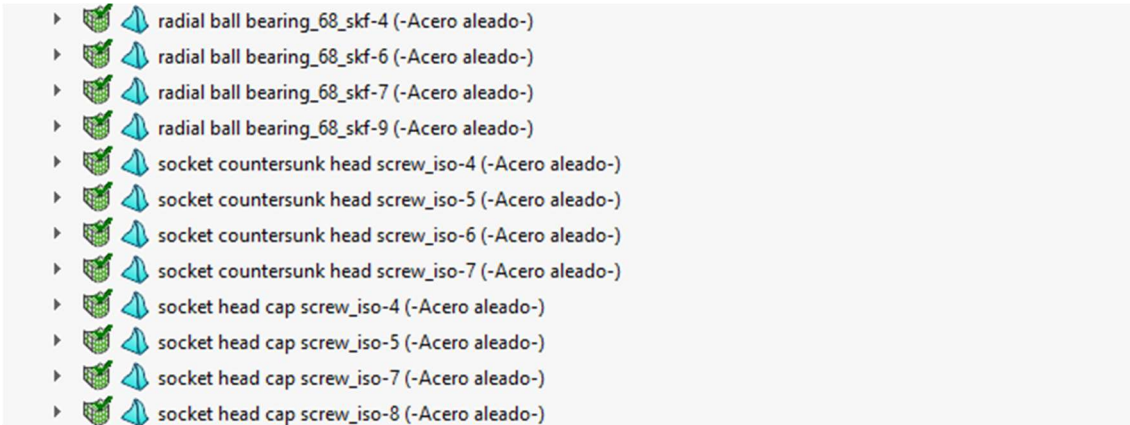
2.5. Remarks:

Tests on individual components have been made considering all reactions and interactions as loads. Restraints have been considered as fixed hinges in union points with other parts to allow for free rotation of those points due to deformation.

3. SIMULATION MODEL

3.1. List of materials:

Piezas	
	Amortiguador ensayos-1 (-[SW]Acero inoxidable forjado-)
	HP4bar_V4.1_Bainas-1/Chaflán16-1 (-[SW]AISI 1015 Acero estirado en frío (SS)-)
	HP4bar_V4.1_Bainas-1/Chaflán17-1 (-[SW]AISI 1015 Acero estirado en frío (SS)-)
	HP4bar_V4.1_Bainas-1/Cortar-Extruir10-1 (-[SW]AISI 1015 Acero estirado en frío (SS)-)
	HP4bar_V4.1_Bainas-1/Tube (rectangular) 40 X 20 X 2(1)[1]-1 (-[SW]AISI 1015 Acero estirado en frío (SS)-)
	HP4bar_V4.1_Bainas-1/Tube (rectangular) 40 X 20 X 2(1)[2]-1 (-[SW]AISI 1015 Acero estirado en frío (SS)-)
	HP4bar_V4.1_Bainas-1/Tube (rectangular) 40 X 20 X 2(1)[3]-1 (-[SW]AISI 1015 Acero estirado en frío (SS)-)
	HP4bar_V4.1_Bainas-1/Tube (rectangular) 40 X 20 X 2(2)[1]-1 (-[SW]AISI 1015 Acero estirado en frío (SS)-)
	HP4bar_V4.1_Bainas-1/Tube (rectangular) 40 X 20 X 2(2)[2]-1 (-[SW]AISI 1015 Acero estirado en frío (SS)-)
	HP4bar_V4.1_Bainas-1/Tube (rectangular) 40 X 20 X 2(2)[3]-1 (-[SW]AISI 1015 Acero estirado en frío (SS)-)
	HP4bar_V4.1_Tirante-1/Chaflán6-1 (-[SW]AISI 1015 Acero estirado en frío (SS)-)
	HP4bar_V4.1_Tirante-1/Cortar-Extruir8-1 (-[SW]AISI 1015 Acero estirado en frío (SS)-)
	HP4bar_V4.1_Tirante-1/Redondeo10-1 (-[SW]AISI 1015 Acero estirado en frío (SS)-)
	HP4bar_V4.1_Tirante-1/Sólido3-1 (-[SW]AISI 1015 Acero estirado en frío (SS)-)
	HP4bar_V4.1_Tirante-1/Sólido5-1 (-[SW]AISI 1015 Acero estirado en frío (SS)-)
	HP4bar_V4.2_BieletaDerecha-1 (-[SW]6061-T4 (SS)-)
	HP4bar_V4.2_BieletaIzquierda-1 (-[SW]6061-T4 (SS)-)
	HP4bar_V4.2_RefuerzoBieleta-1 (-[SW]6061-T4 (SS)-)
	HP4bar_V4.2_TriánguloDelantero-1/Cartela1-1 (-[SW]AISI 1015 Acero estirado en frío (SS)-)
	HP4bar_V4.2_TriánguloDelantero-1/Cortar-Extruir12-1 (-[SW]AISI 1015 Acero estirado en frío (SS)-)
	HP4bar_V4.2_TriánguloDelantero-1/Cortar-Extruir15-1 (-[SW]AISI 1015 Acero estirado en frío (SS)-)
	HP4bar_V4.2_TriánguloDelantero-1/Cortar-Extruir17-1 (-[SW]AISI 1015 Acero estirado en frío (SS)-)
	HP4bar_V4.2_TriánguloDelantero-1/Cortar-Extruir5[1]-1 (-[SW]AISI 1015 Acero estirado en frío (SS)-)
	HP4bar_V4.2_TriánguloDelantero-1/Cortar-Extruir5[2]-1 (-[SW]AISI 1015 Acero estirado en frío (SS)-)
	HP4bar_V4.2_TriánguloDelantero-1/Cortar-Extruir9[1]-1 (-[SW]AISI 1015 Acero estirado en frío (SS)-)
	HP4bar_V4.2_TriánguloDelantero-1/Cortar-Extruir9[2]-1 (-[SW]AISI 1015 Acero estirado en frío (SS)-)
	HP4bar_V4.2_TriánguloDelantero-1/Simetría1-1 (-[SW]AISI 1015 Acero estirado en frío (SS)-)
	HP4bar_V4.2_TriánguloDelantero-1/Simetría2[1]-1 (-[SW]AISI 1015 Acero estirado en frío (SS)-)
	HP4bar_V4.2_TriánguloDelantero-1/Simetría2[2]-1 (-[SW]AISI 1015 Acero estirado en frío (SS)-)
	HP4bar_V4.2_TriánguloDelantero-1/Sólido4-1 (-[SW]AISI 1015 Acero estirado en frío (SS)-)
	HP4bar_V4.2_TriánguloDelantero-1/Sólido9-1 (-[SW]AISI 1015 Acero estirado en frío (SS)-)
	HP4bar_V4.2_TriánguloDelantero-1/Tube (square) 50 X 50 X 3.2(1)[2]-1 (-[SW]AISI 1015 Acero estirado en frío (SS)-)
	radial ball bearing_68_skf-1 (-Acero aleado-)
	radial ball bearing_68_skf-10 (-Acero aleado-)
	radial ball bearing_68_skf-11 (-Acero aleado-)
	radial ball bearing_68_skf-12 (-Acero aleado-)
	radial ball bearing_68_skf-2 (-Acero aleado-)
	radial ball bearing_68_skf-3 (-Acero aleado-)



3.2. Interaction between components:



Remark: A contact interaction has been globally defined for all the components in the model.

A rigid interaction has been defined for welded sub-assemblies:

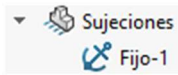
- Rigid union No. 1: Chainstay
- Rigid union No. 2: Seatstay
- Rigid union No. 3: Main frame

1. FALLING MASS IMPACT TEST

SIMULATION OF FALLING MASS IMPACT TEST AS PER ISO 4210-6:2014

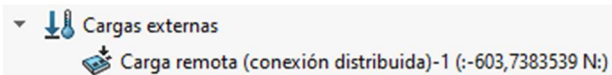
1.1. Simulation preparation

1.1.1. Restraints:

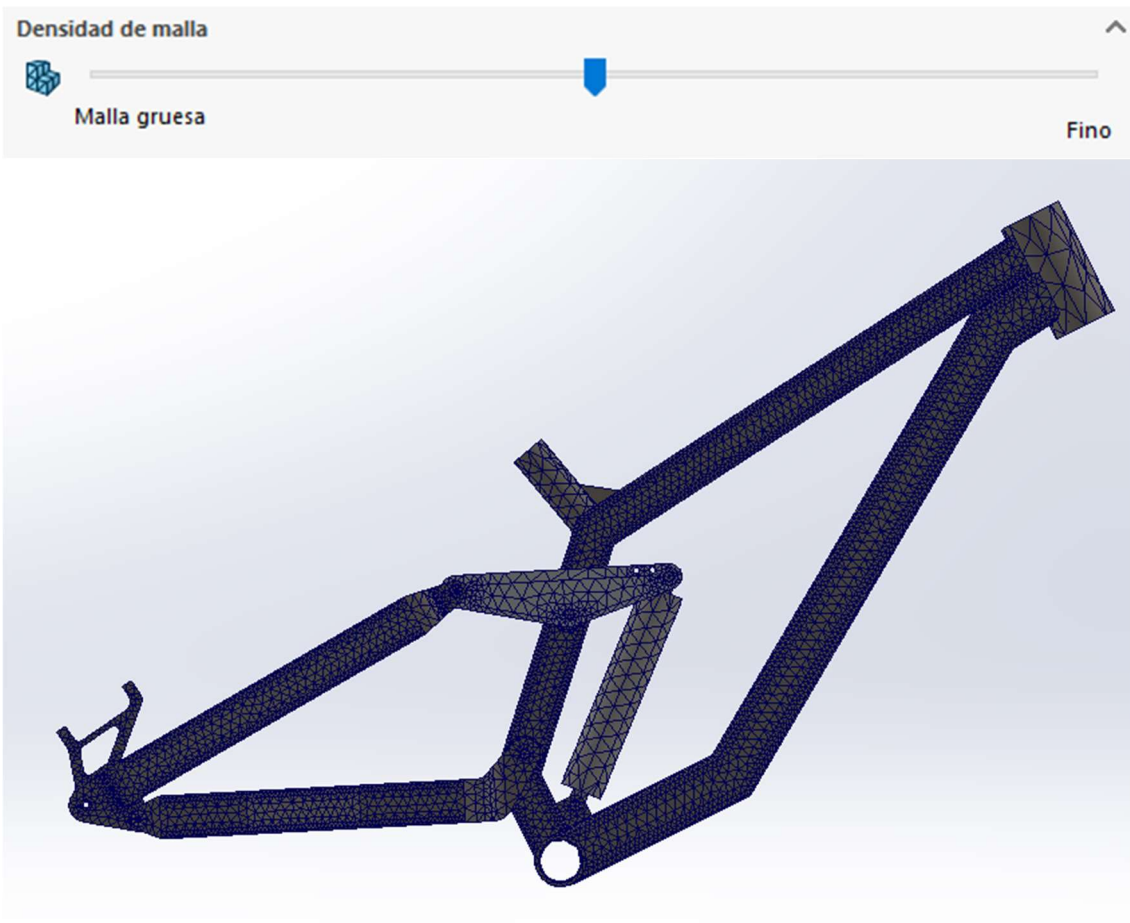


Remark: Rigid restraint on the rear wheel axle attaching points.

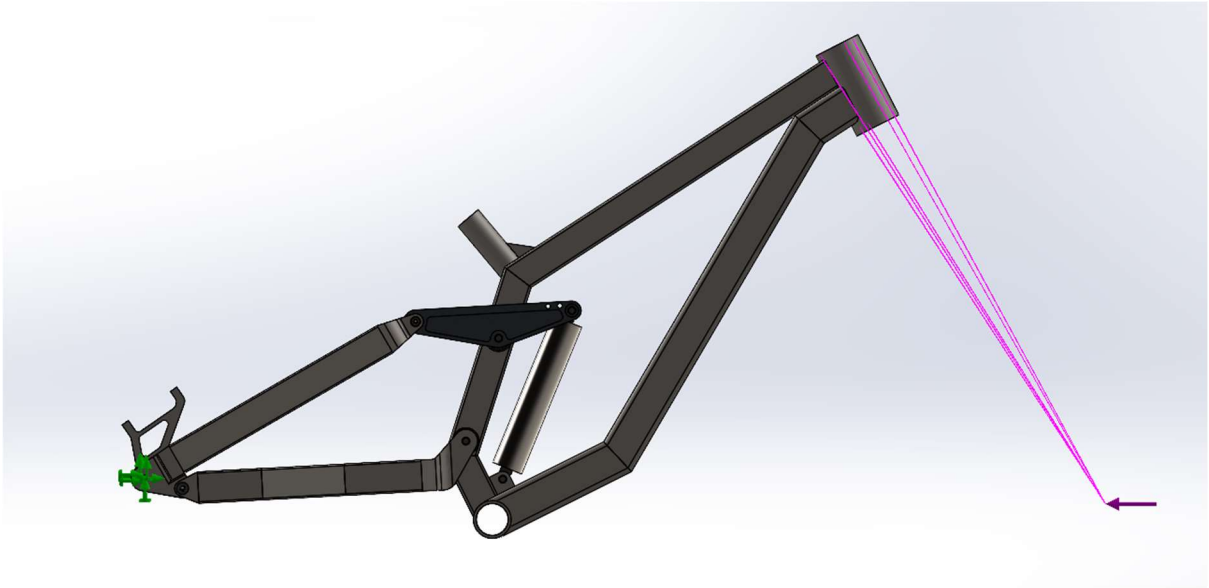
1.1.2. Loads:



1.1.3. Mesh:

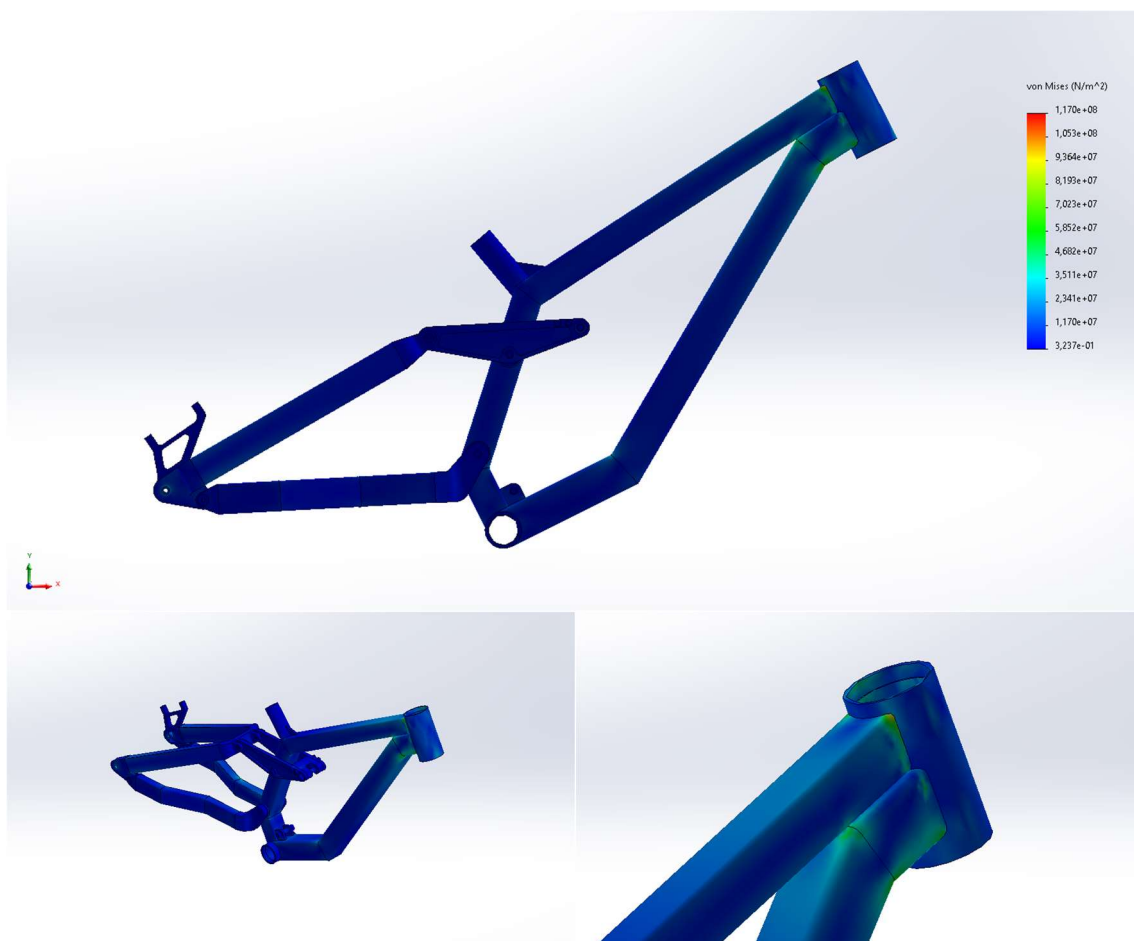


1.1.4. Final model preview:

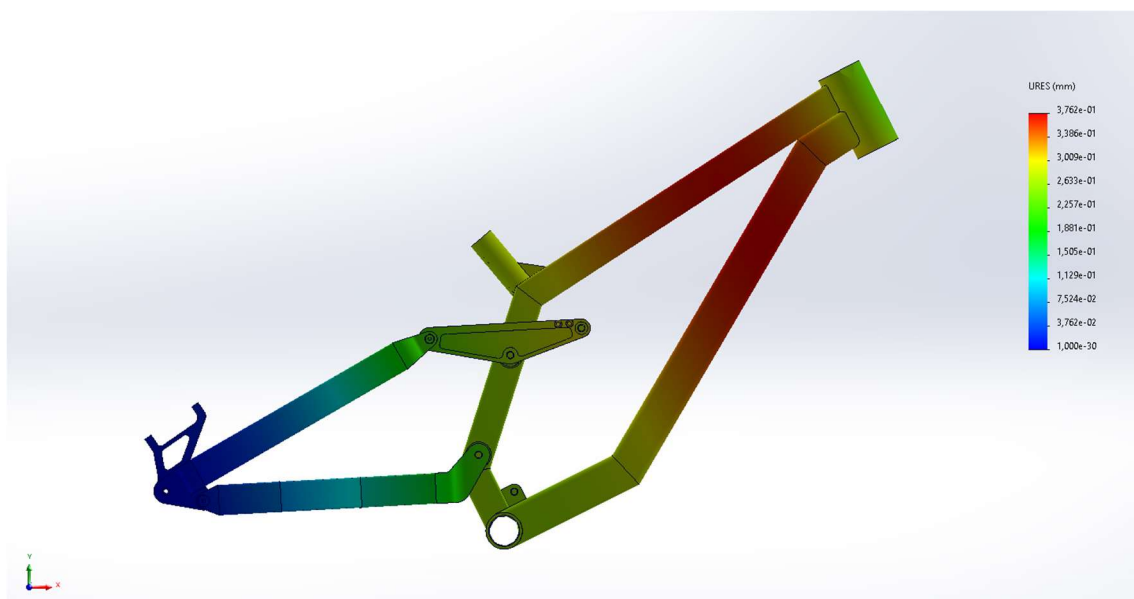


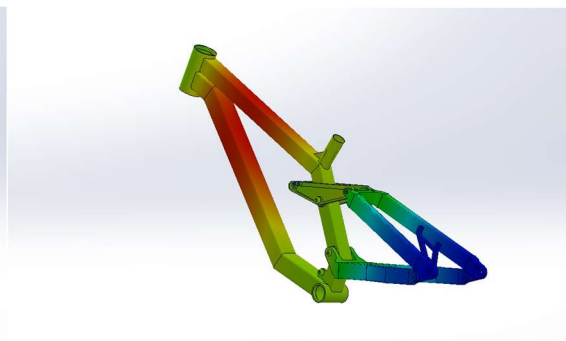
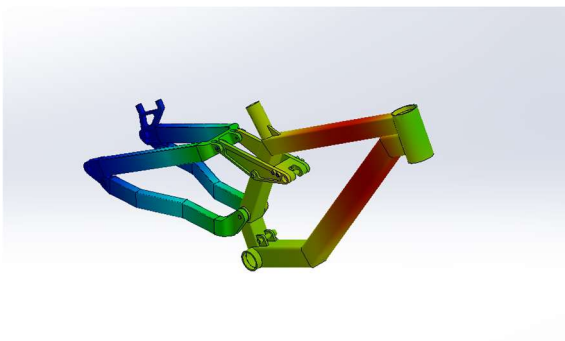
1.2. Test results

1.2.1. Stress analysis:

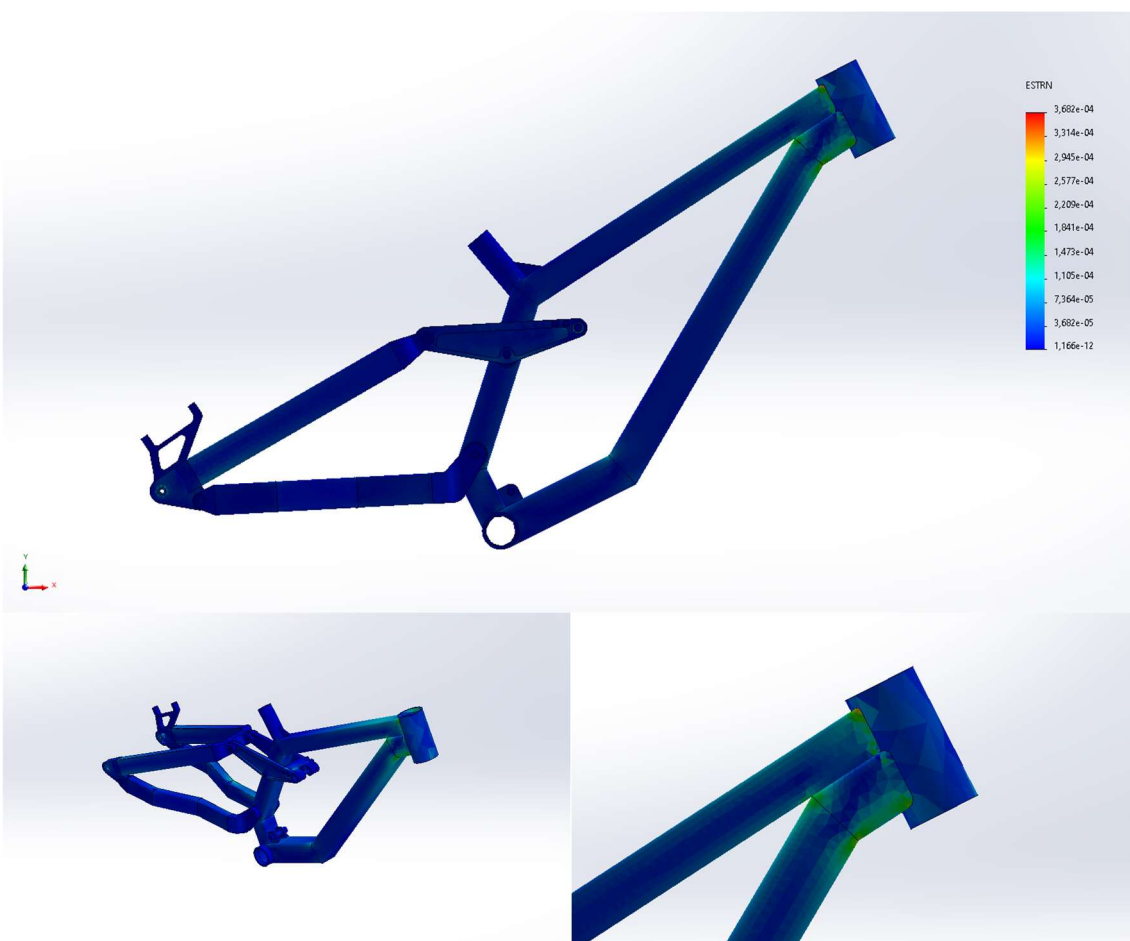


1.2.2. Displacements:



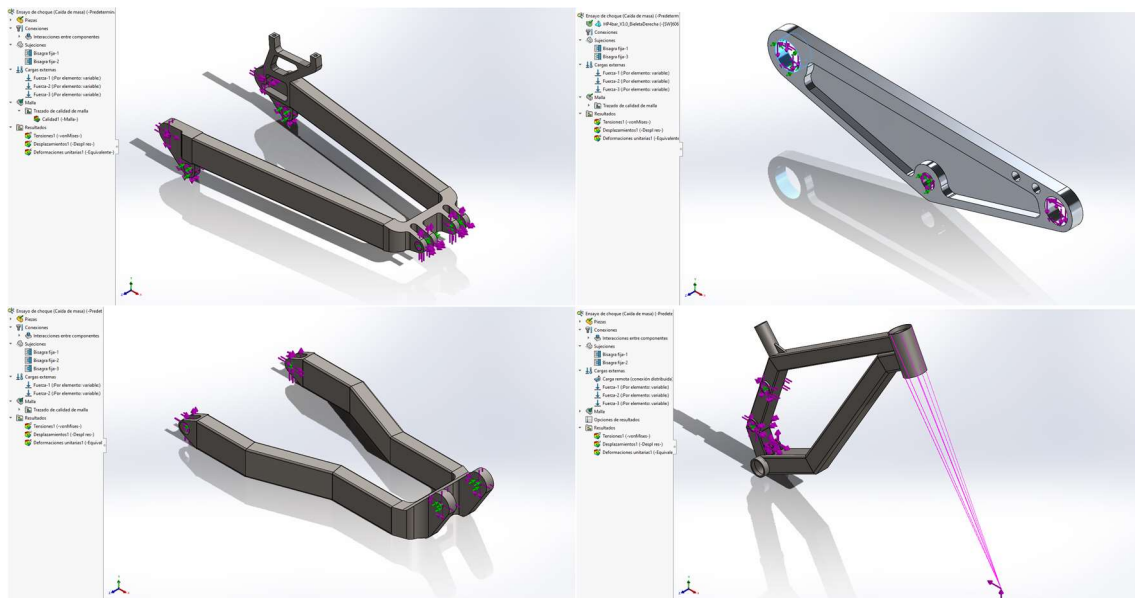


1.2.3. Deformations:

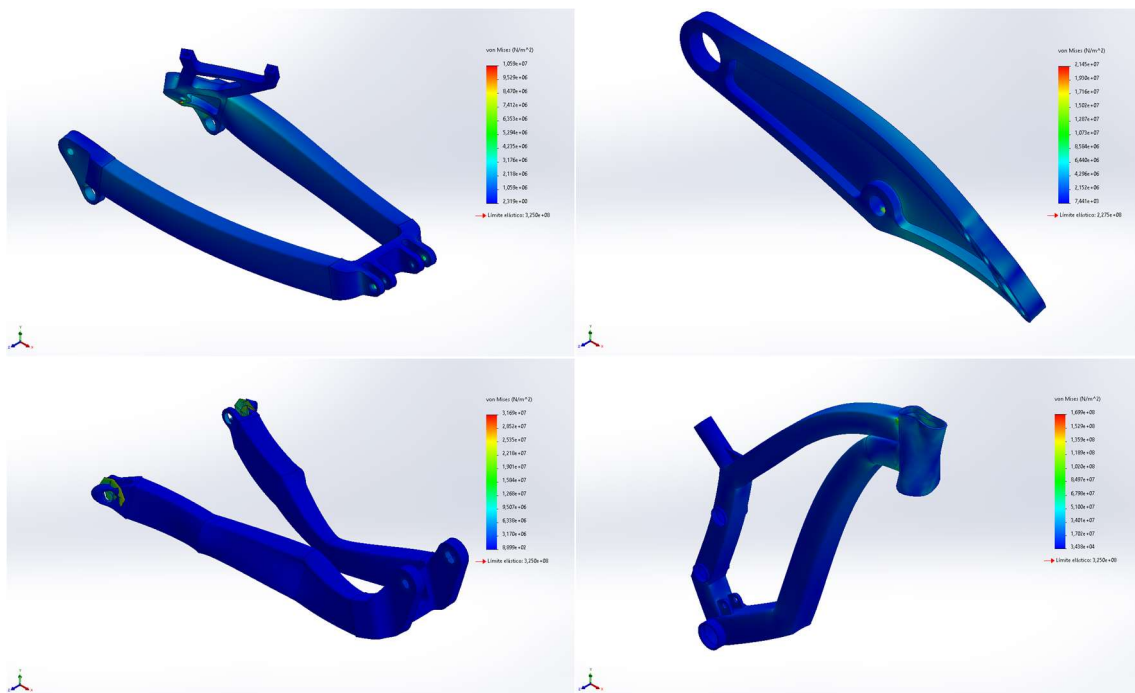


1.2.4. Component's individual analysys:

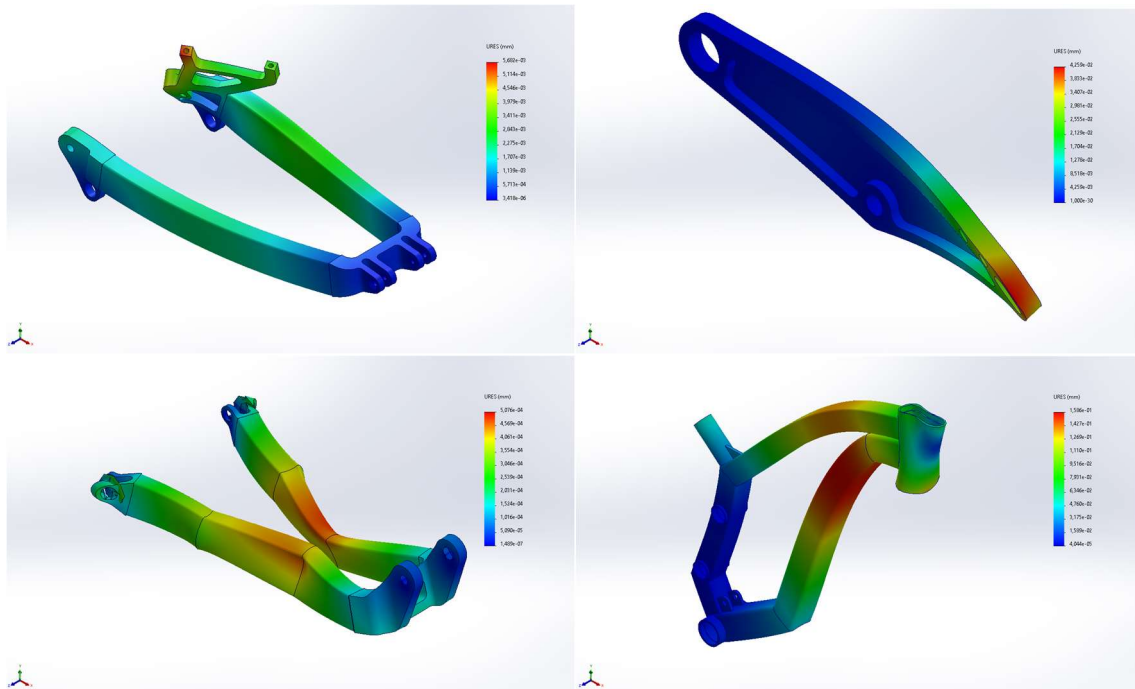
1.2.4.1. Configuration



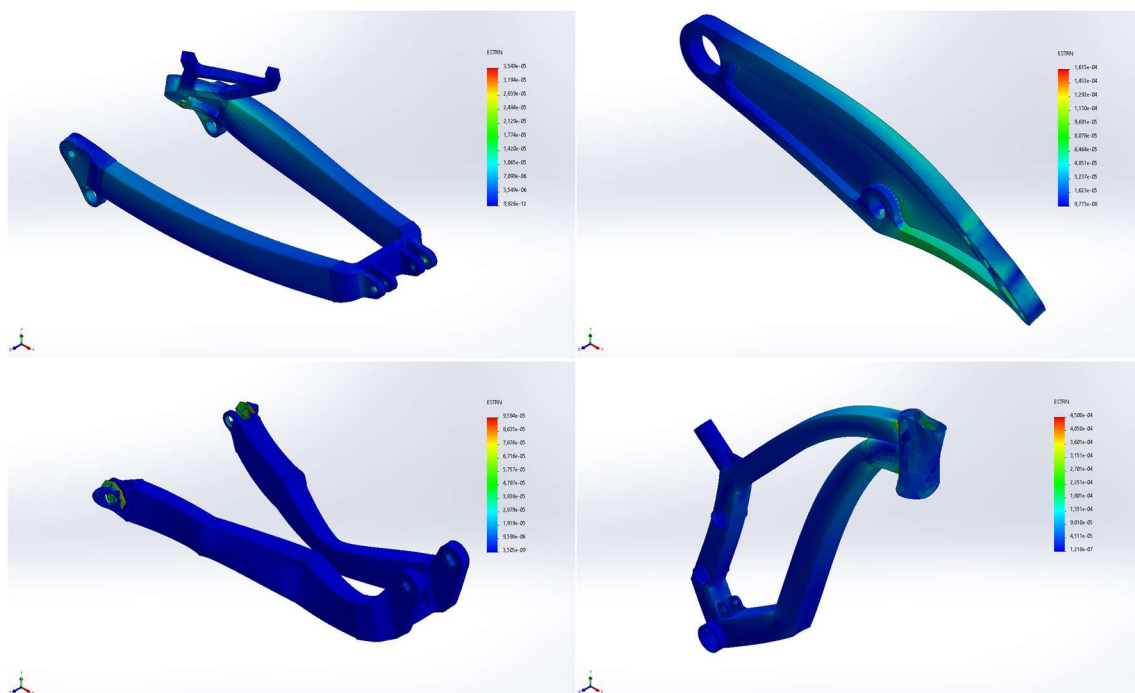
1.2.4.2. Stress analysys:



1.2.4.3. Displacements:



1.2.4.4. Deformations:

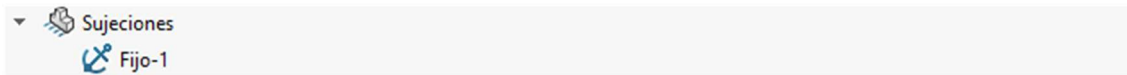


2. FALLING FRAME IMPACT TEST

SIMULATION OF FALLING FRAME IMPACT TEST AS PER ISO 4210-6:2014

2.1. Simulation preparation

2.1.1. Restraints:



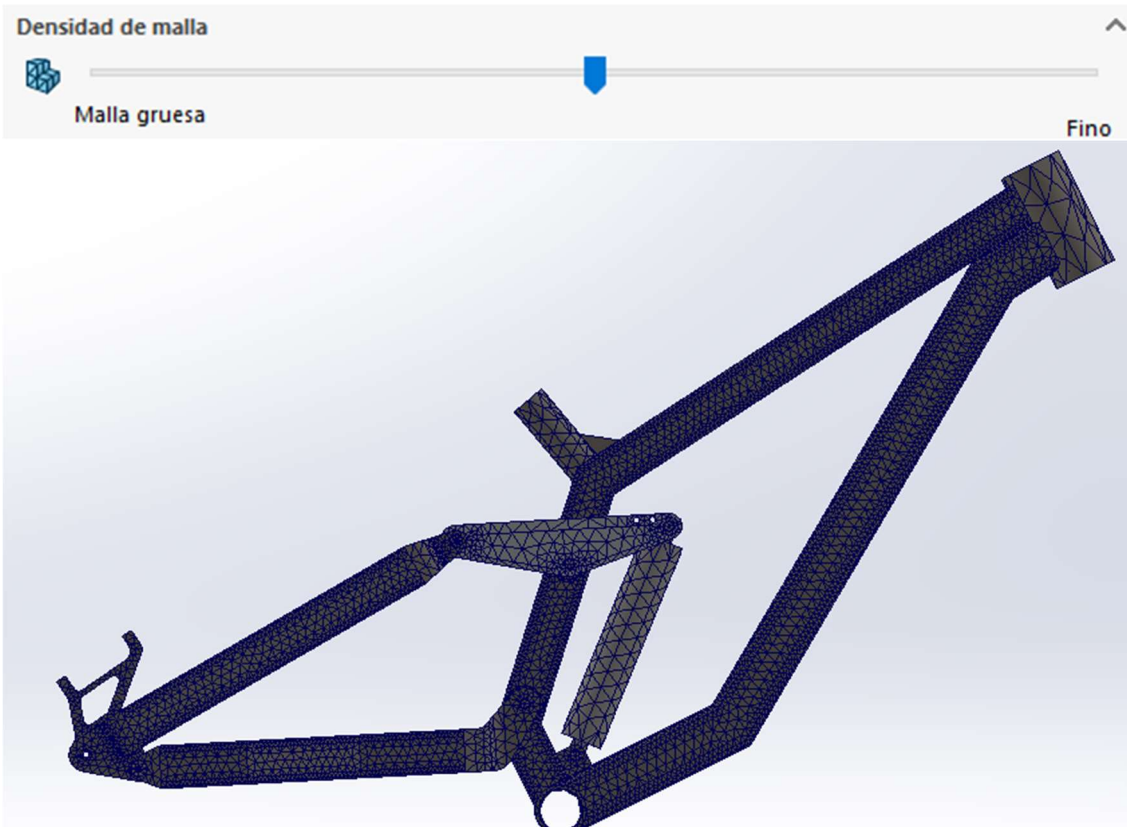
Remark: Rigid restraint on the rear wheel axle attaching points.

2.1.2. Loads:

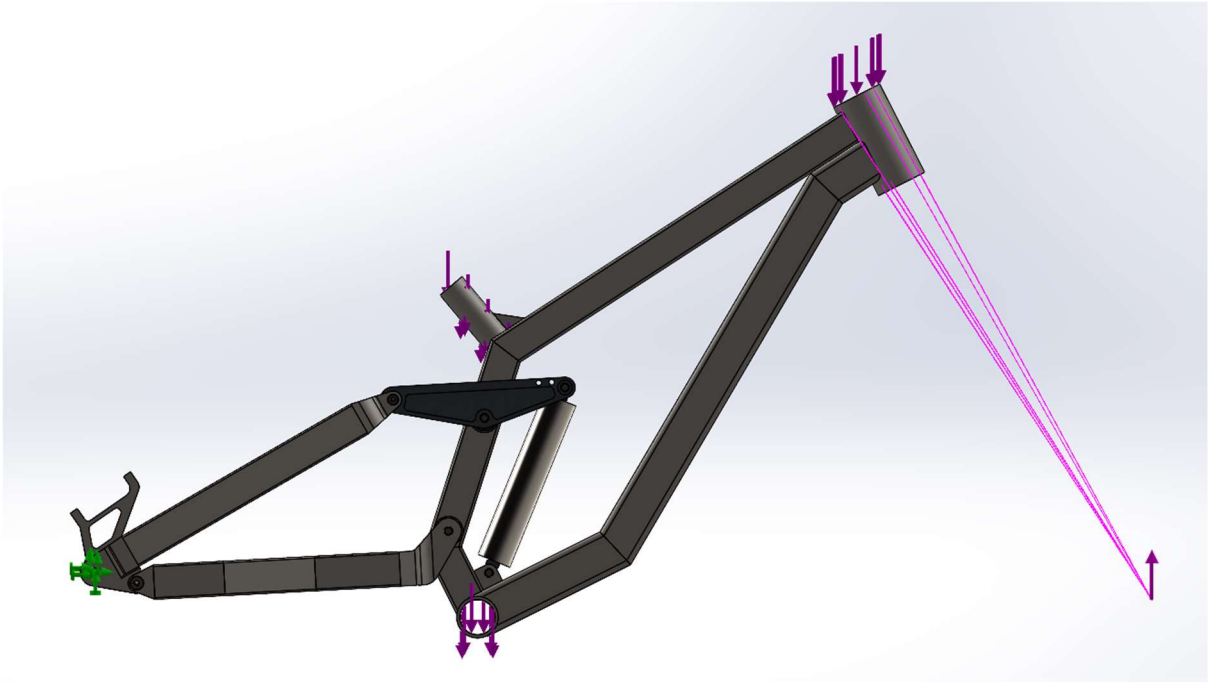


Remark: Remote load – Front wheel reaction
 Load No.1 – Mass on bottom bracket
 Load No. 2 – Mass on headtube
 Load No. 3 – Mass on seat tube

2.1.3. Mesh:

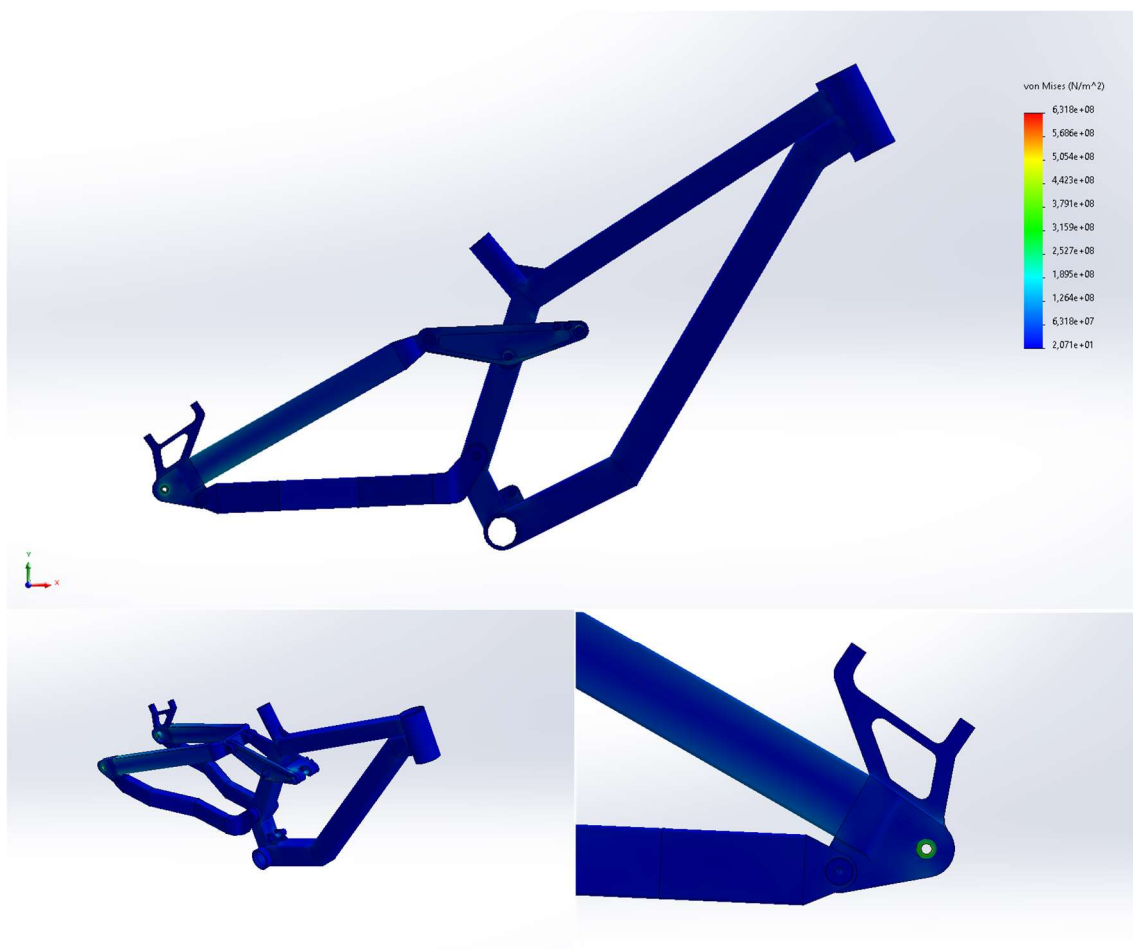


2.1.4. Final model preview:

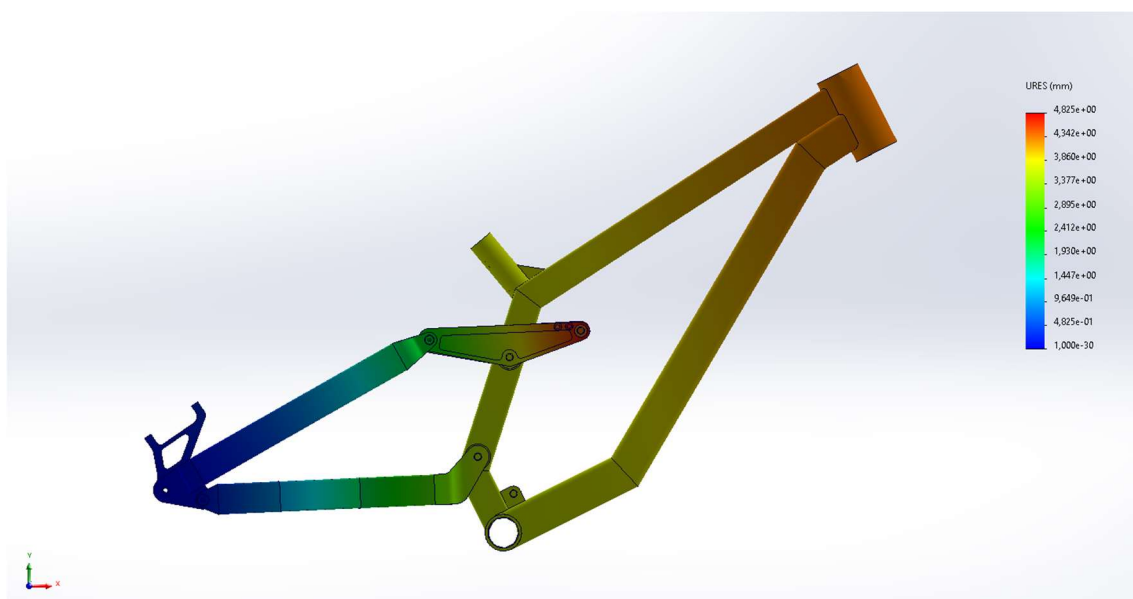


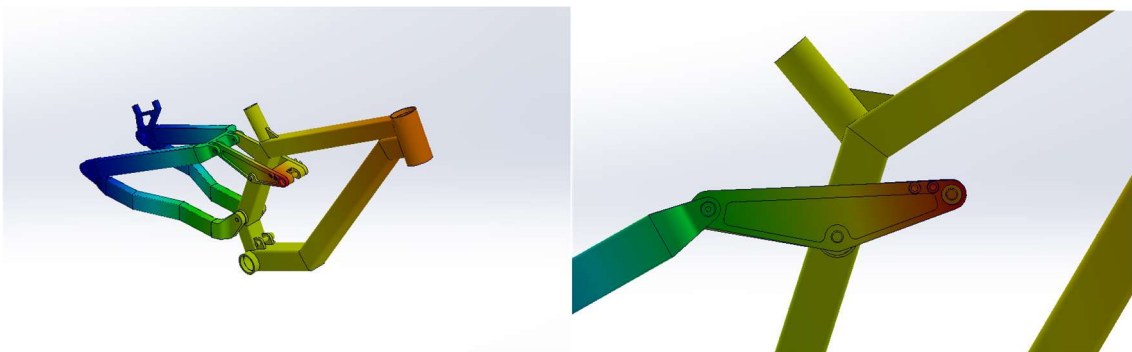
2.2. Test results

2.2.1. Stress analysis:

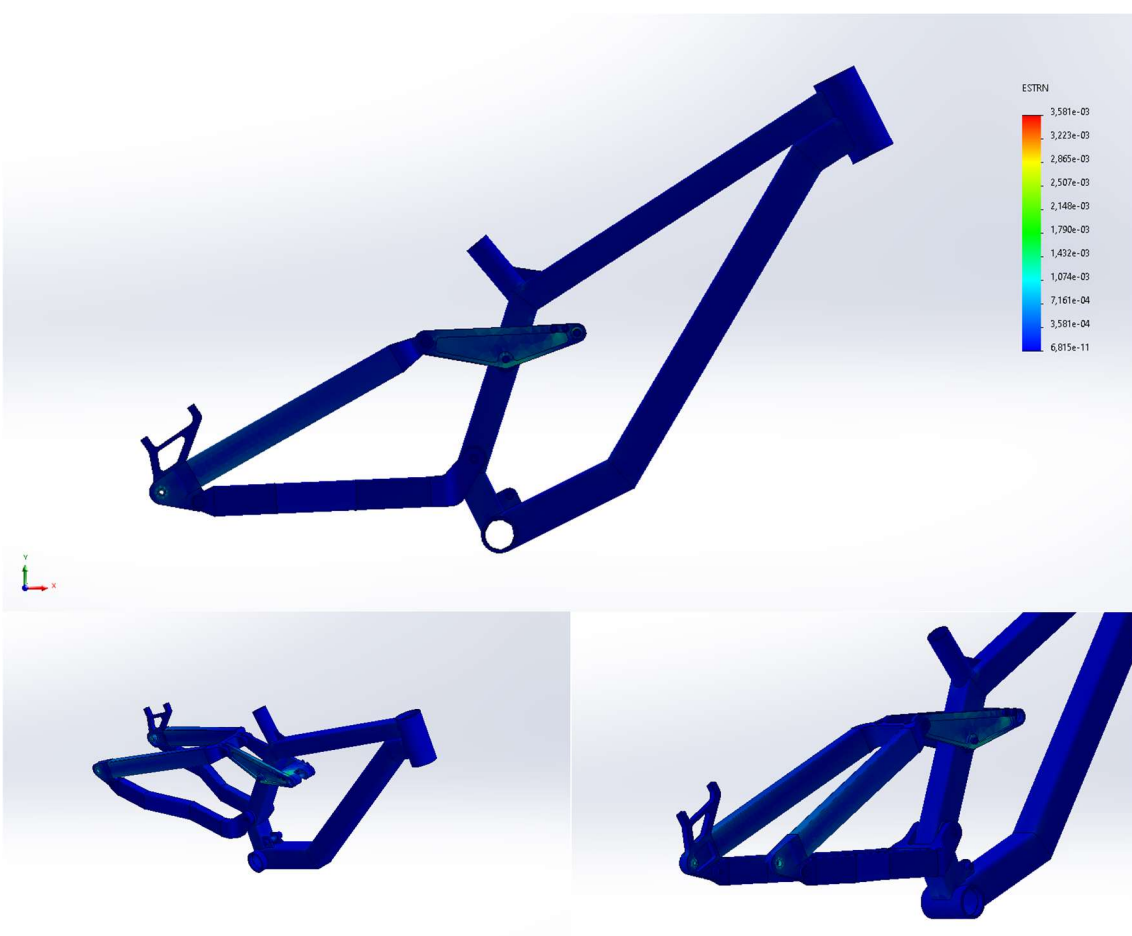


2.2.2. Displacements:



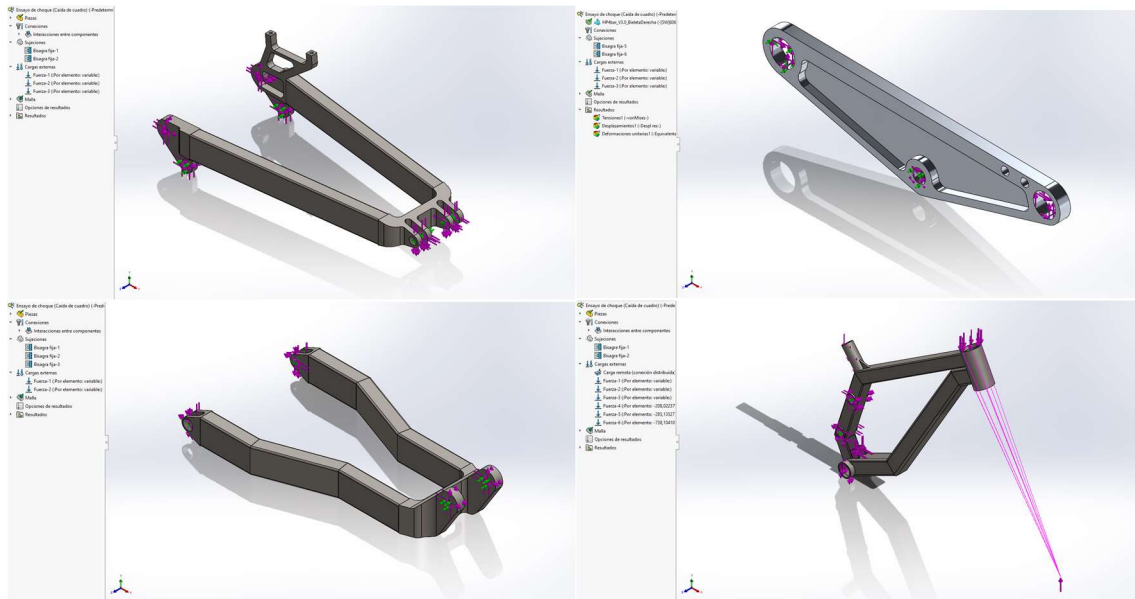


2.2.3. Deformations:

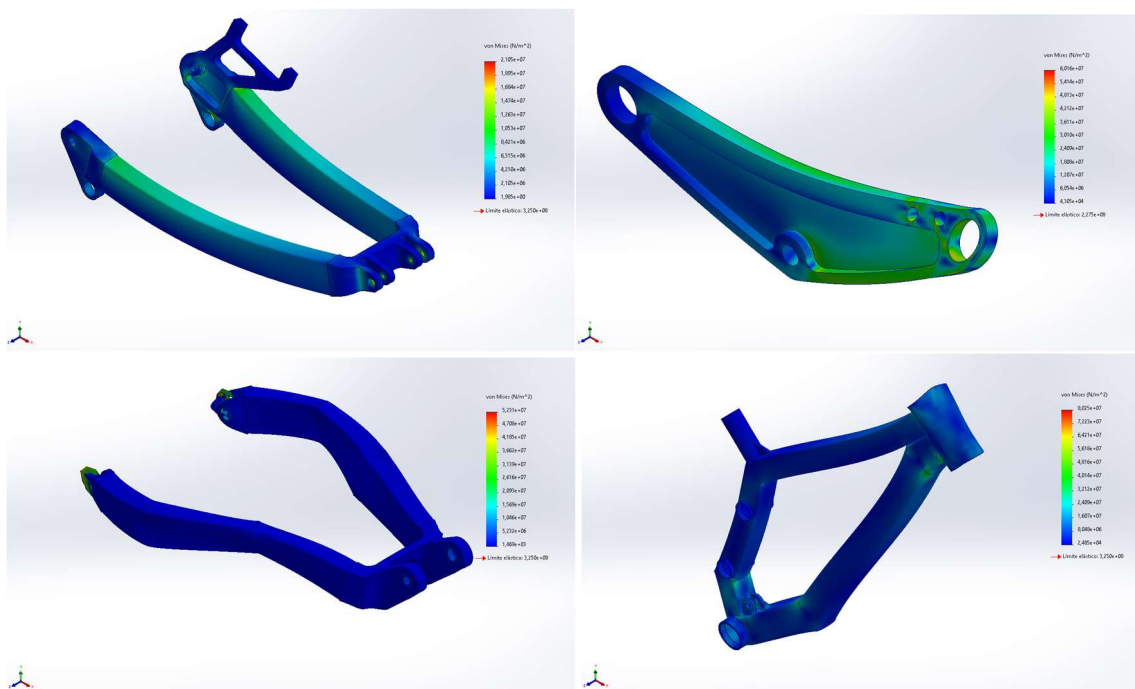


2.2.4. Component's individual analysys:

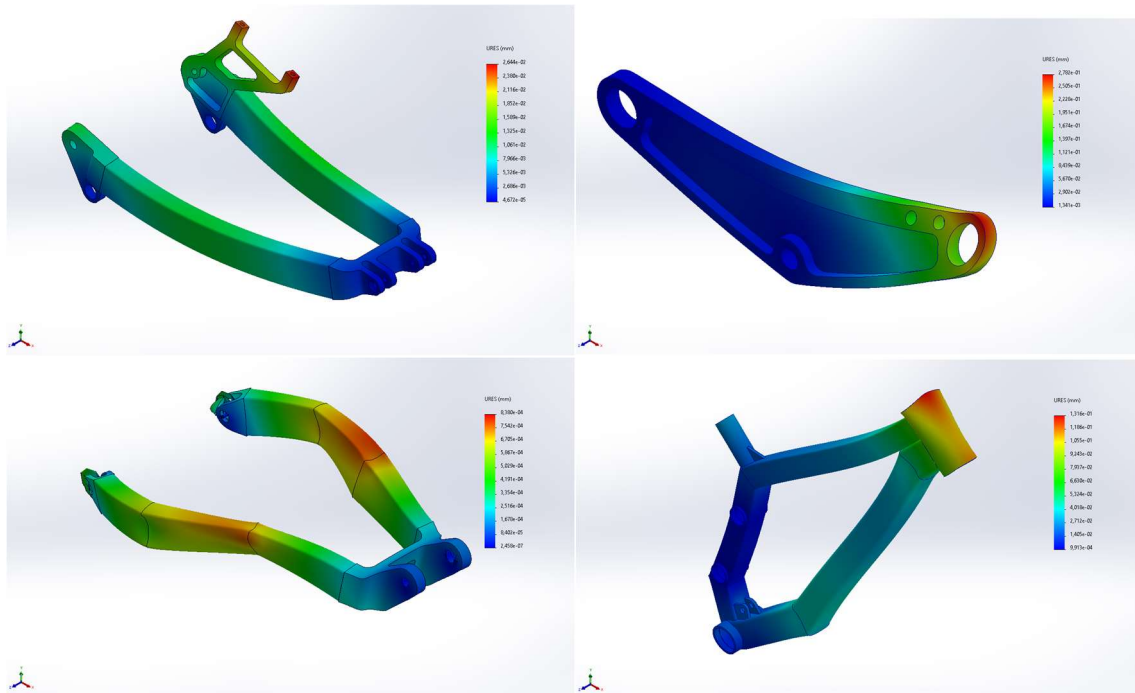
2.2.4.1. Configuration



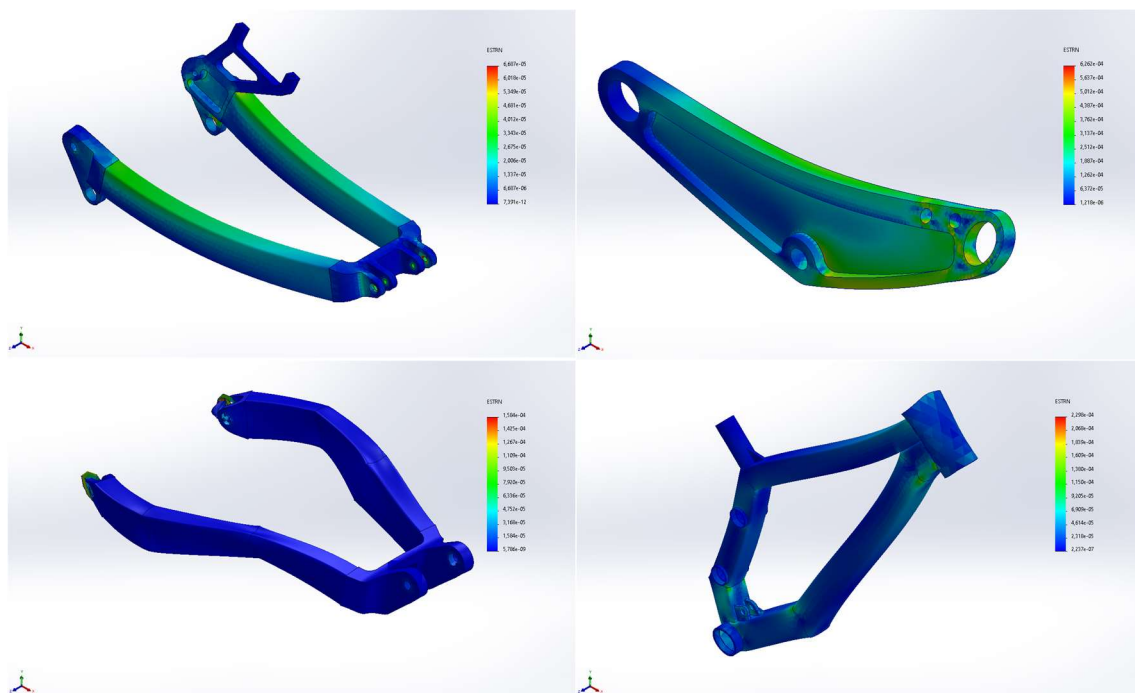
2.2.4.2. Stress analysys:



2.2.4.3. Displacements:



2.2.4.4. Deformations:

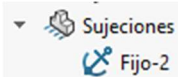


3. FATIGUE TEST WITH PEDALLING FORCES

SIMULATION OF FATIGUE TEST WITH PEDALLING FORCES AS PER ISO 4210-6:2014

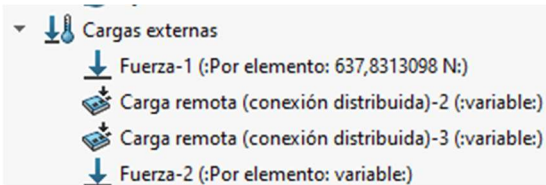
3.1. Simulation preparation

3.1.1. Restraints:



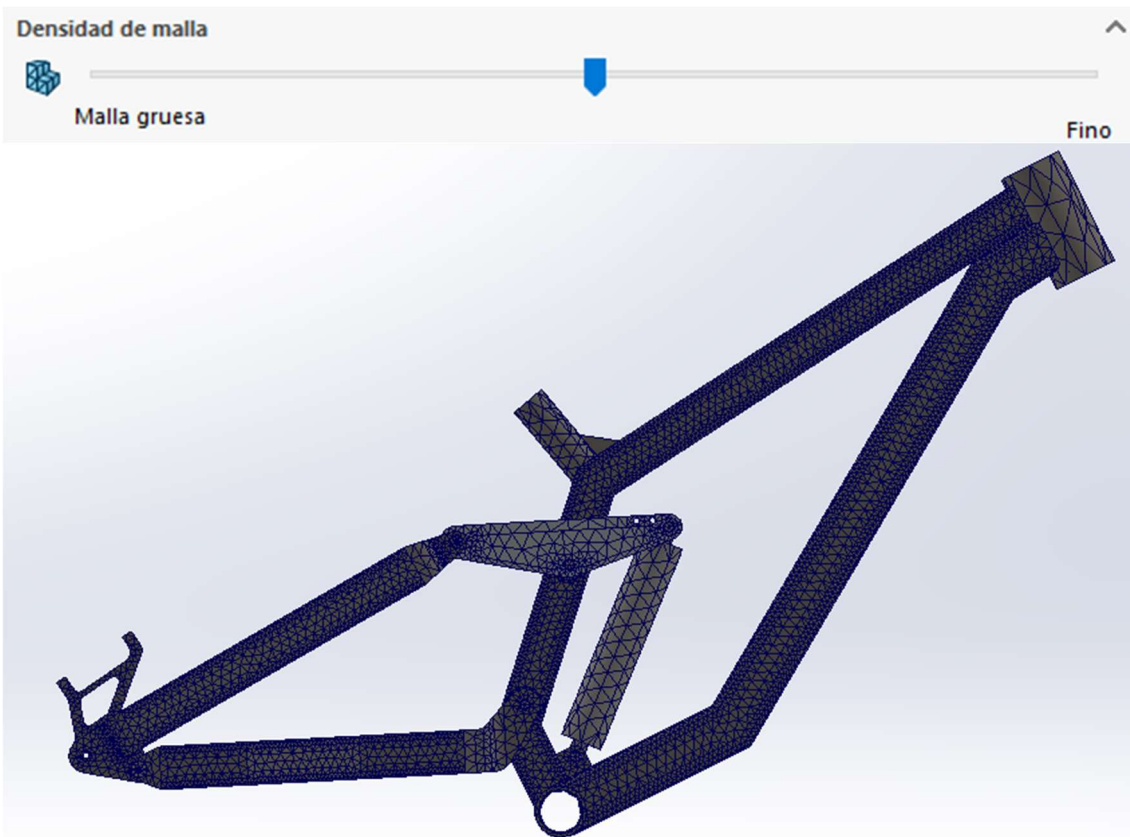
Remark: Rigid restraint on the headtube.

3.1.2. Loads:

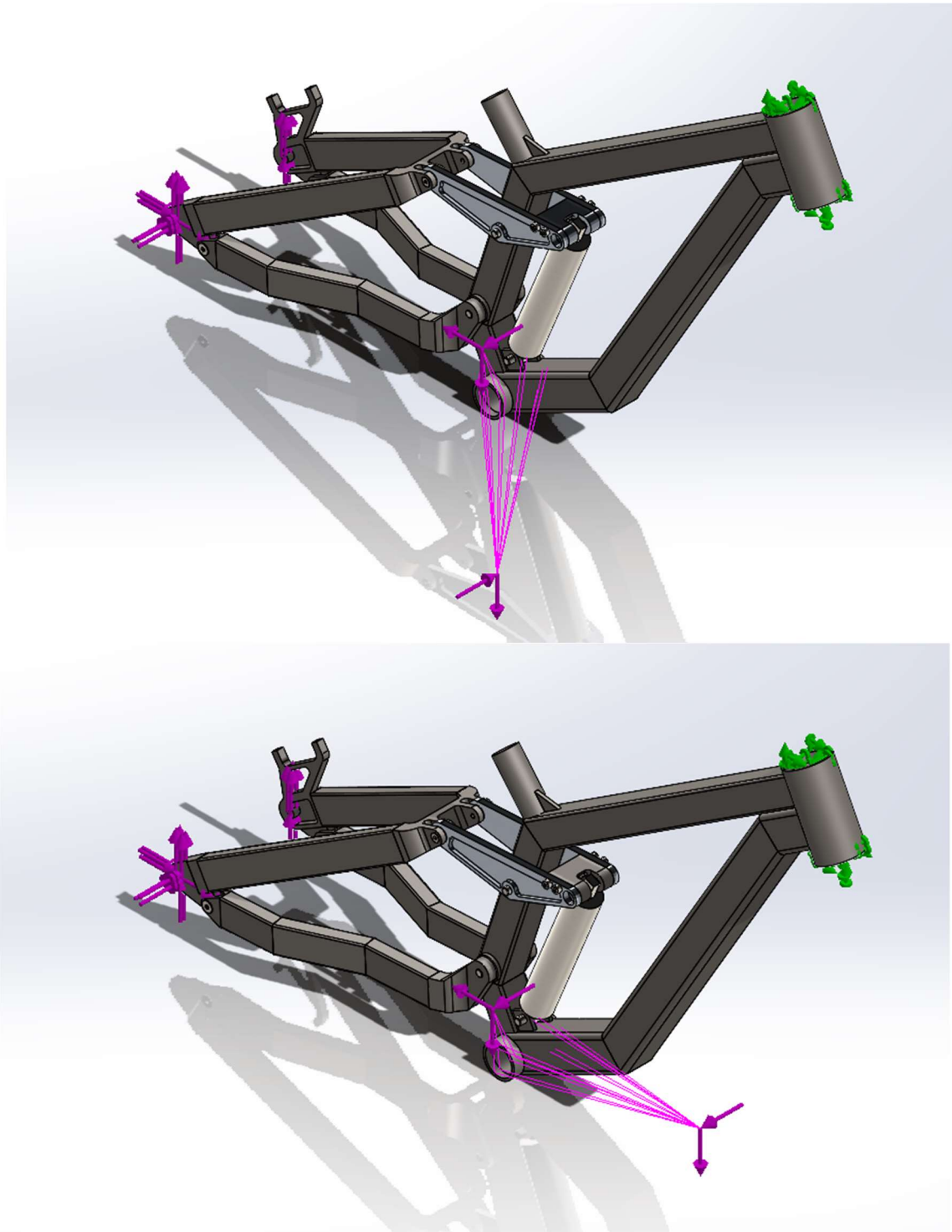


Remark: Remote load No. 2 – Pedal force
 Remote load No. 3 – Chain force on bottom bracket
 Load No. 1 – Vertical rear wheel reaction
 Load No. 3 – Chain force on rear wheel fixing points

3.1.3. Mesh:

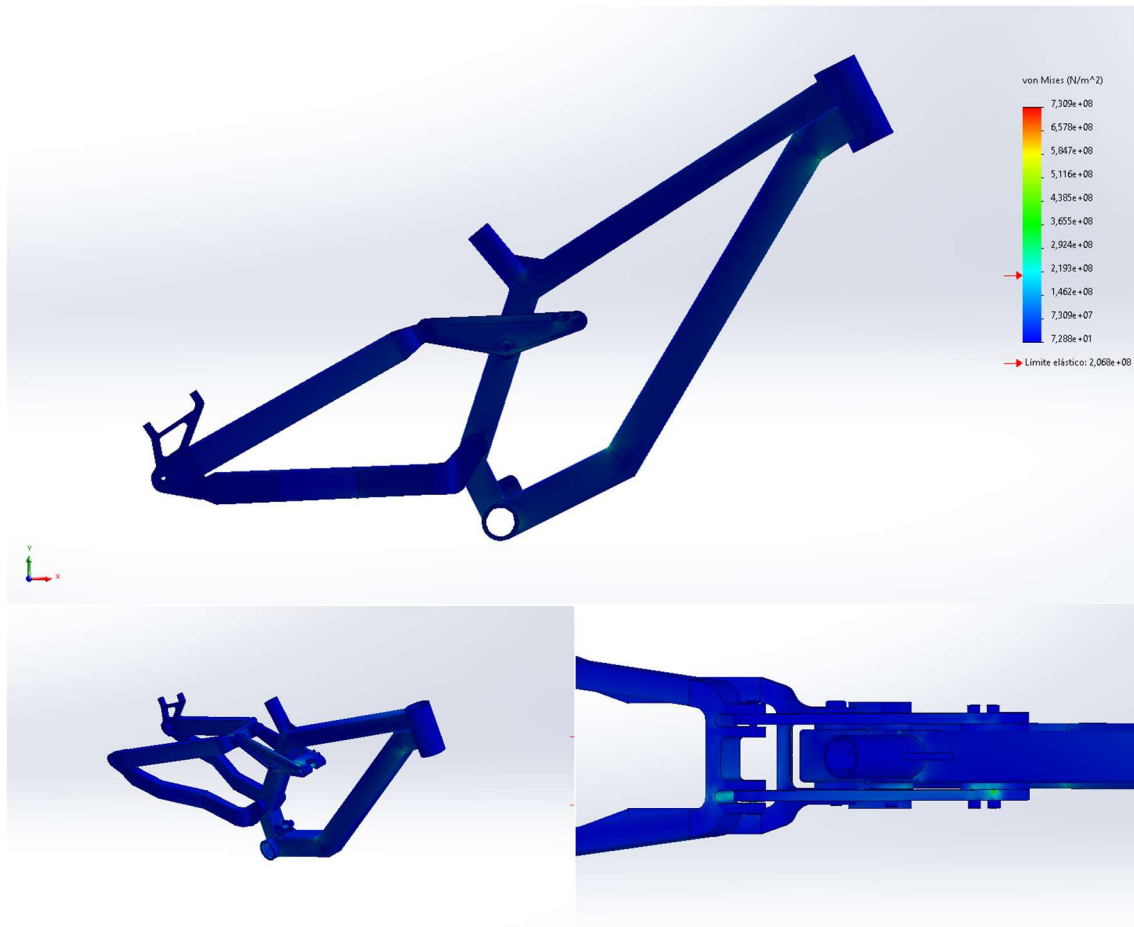


3.1.4. Final model preview:

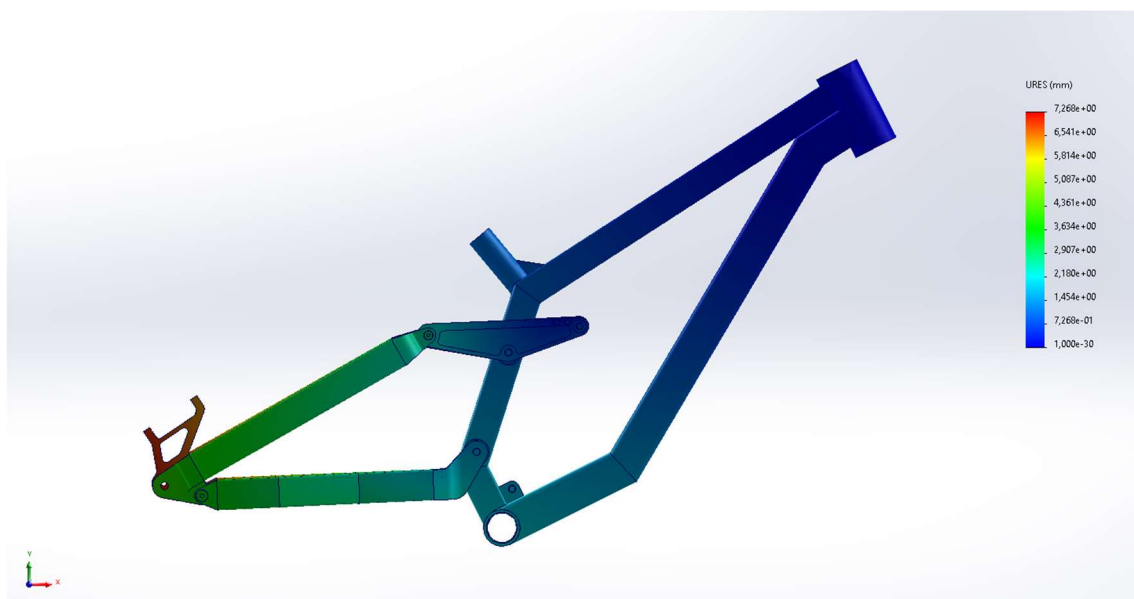


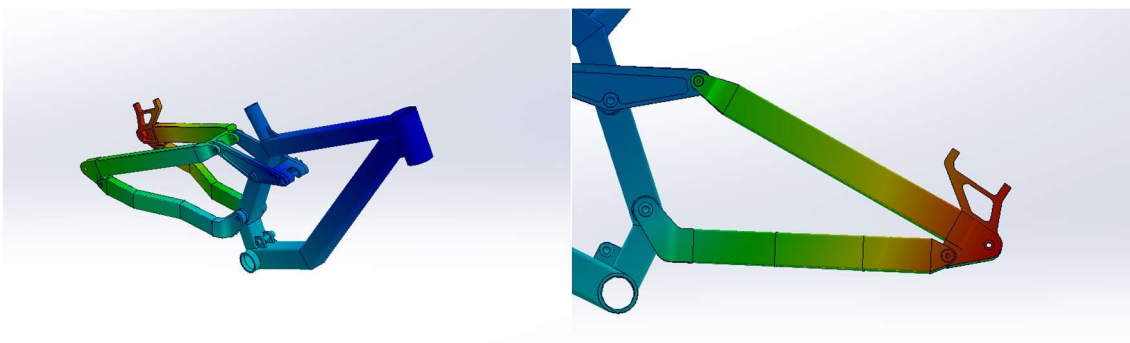
3.2. Test results

3.2.1. Stress analysis: Right pedal

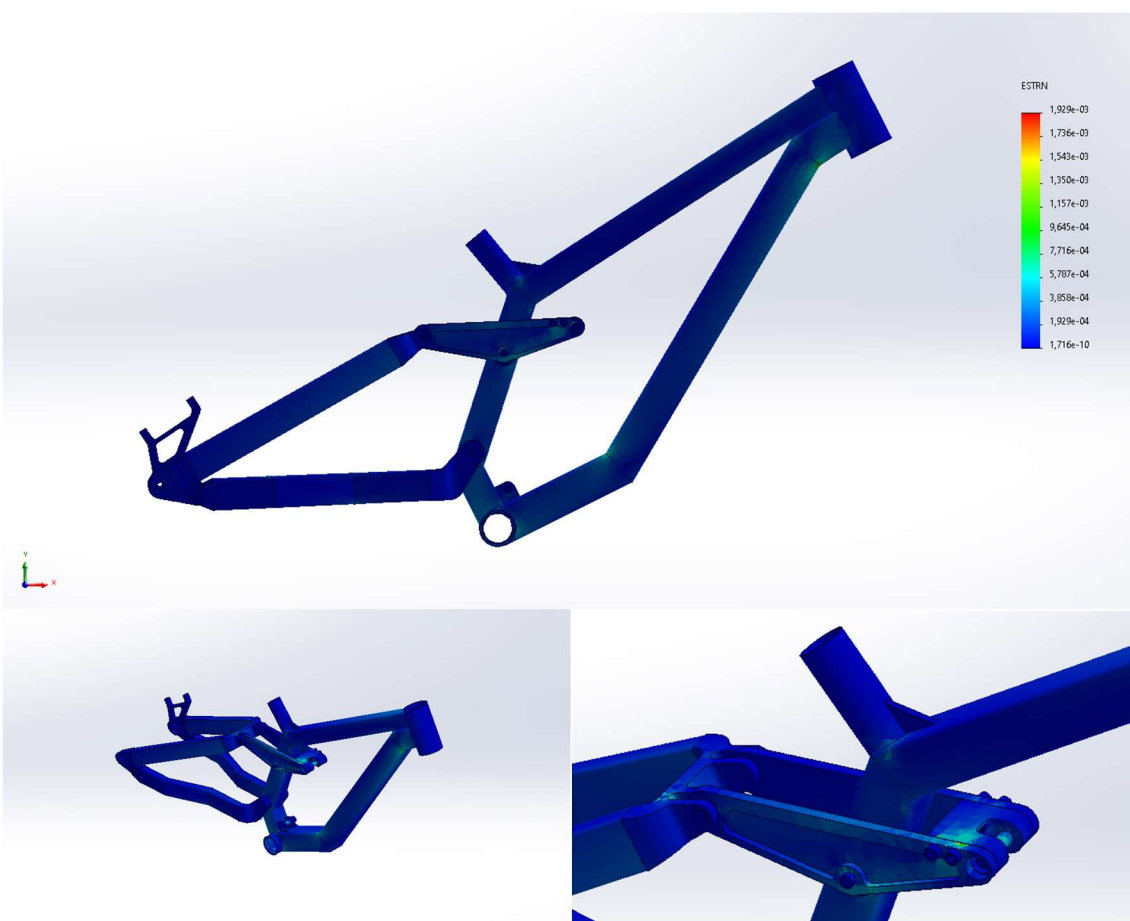


3.2.2. Displacements: Right pedal

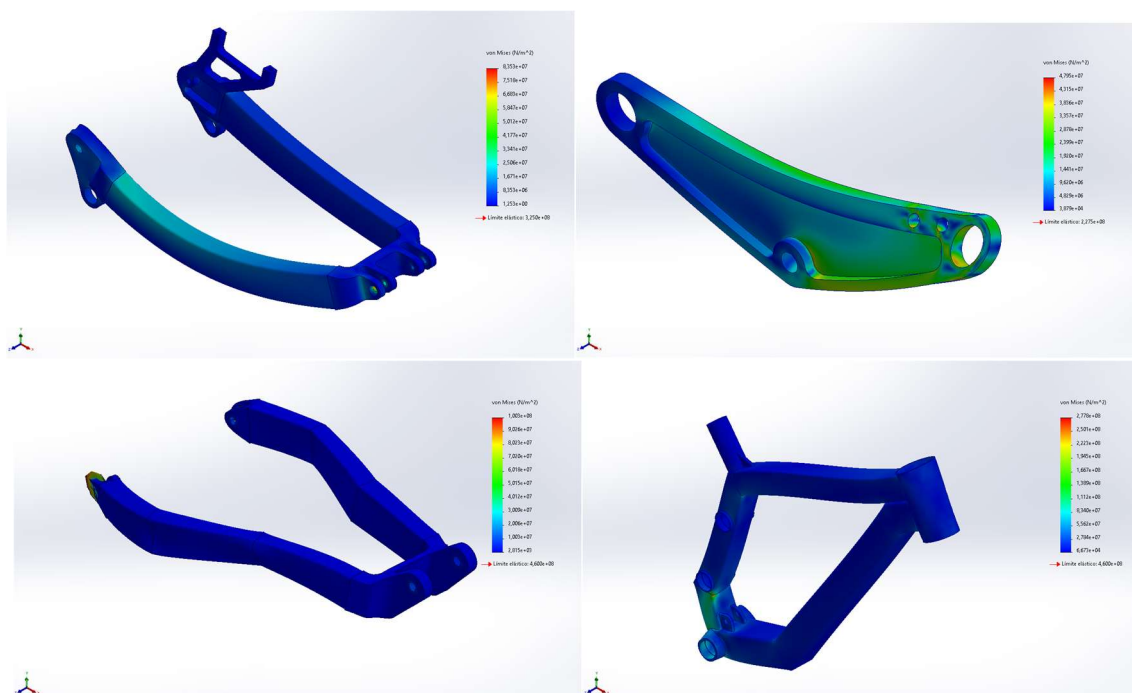
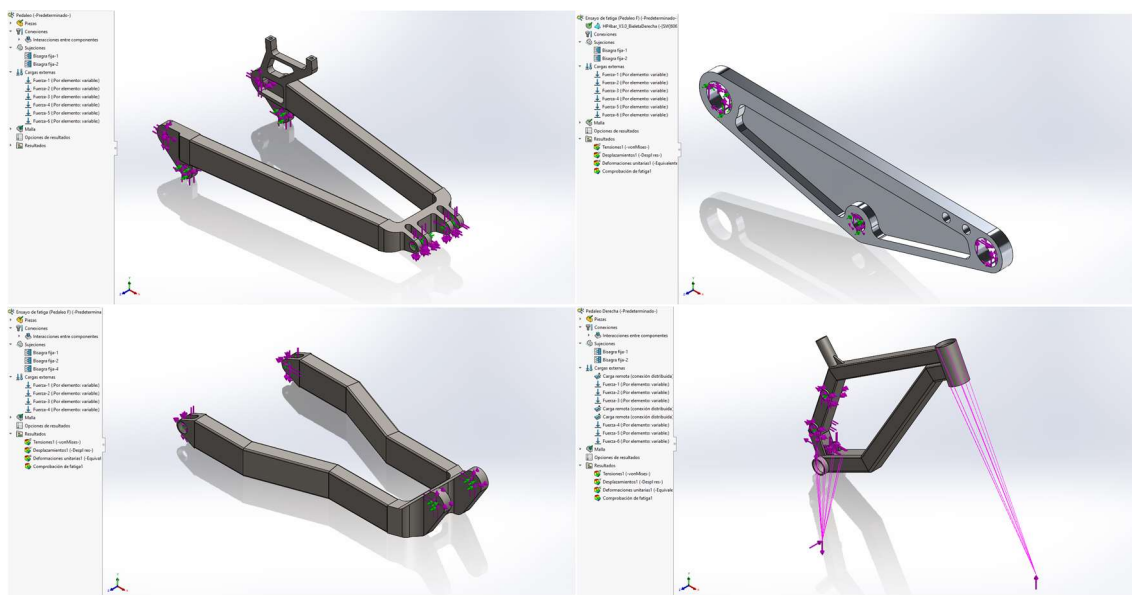




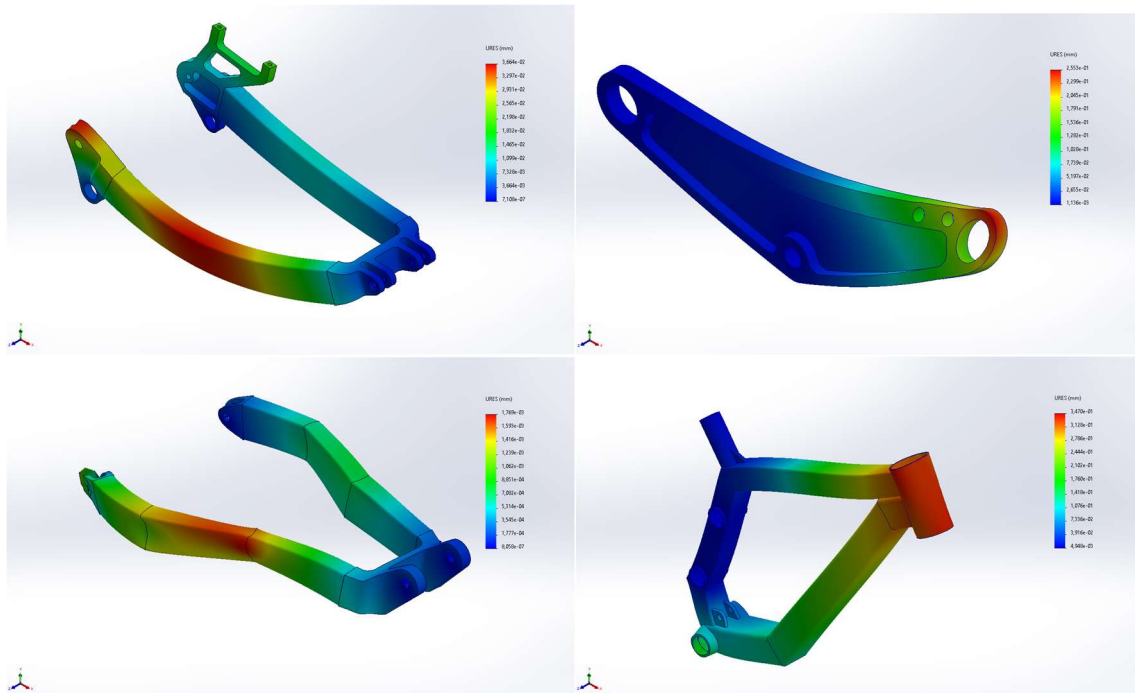
3.2.3. Deformations: Right pedal



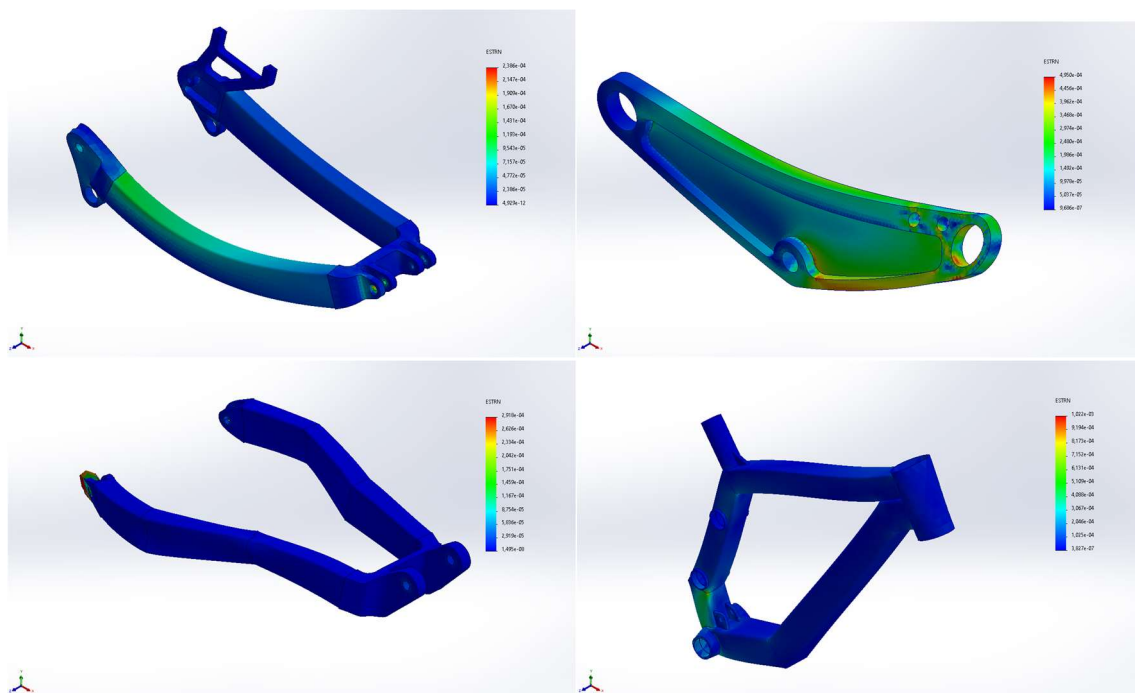
3.2.4.1. Configuration



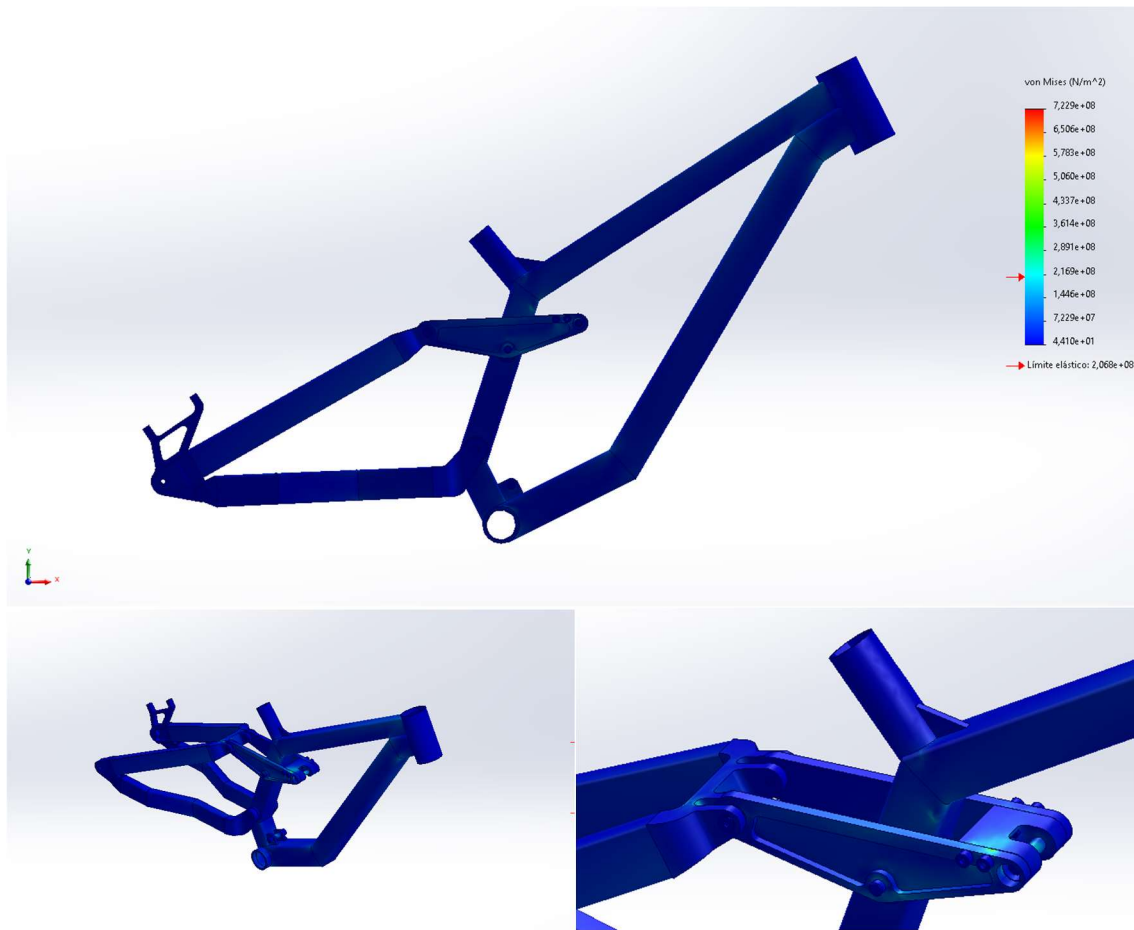
3.2.4.3. Displacements:



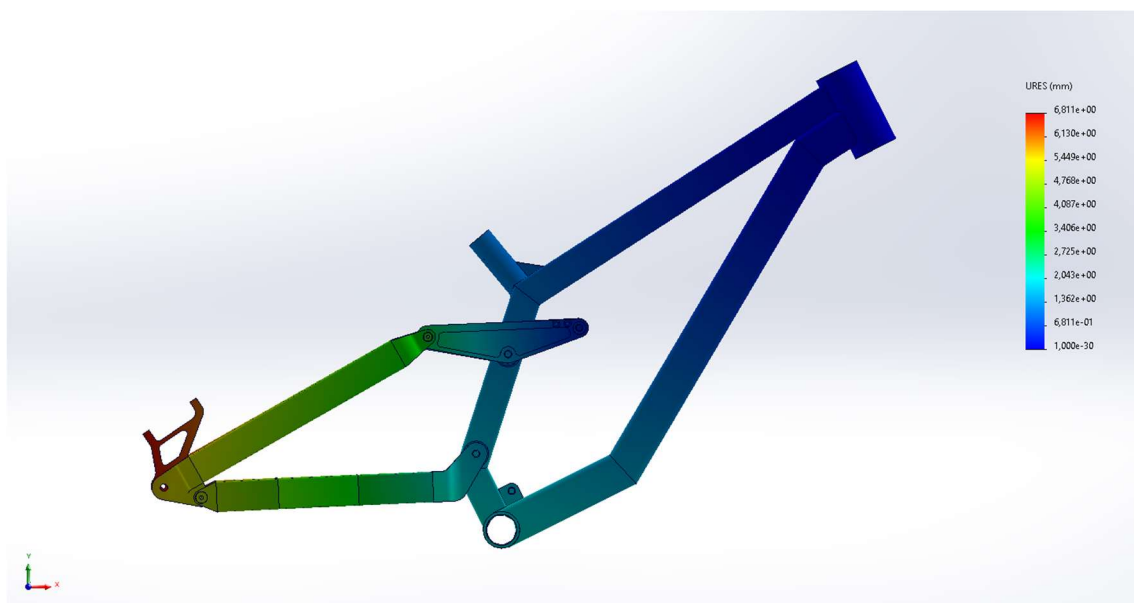
3.2.4.4. Deformations:

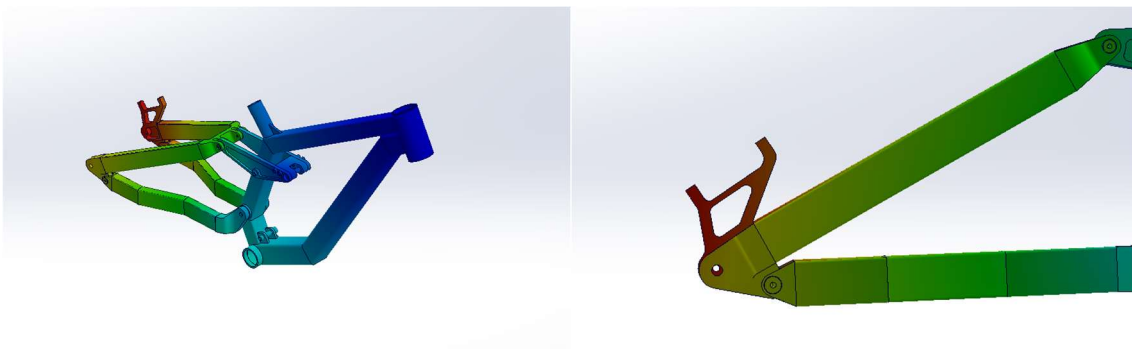


3.2.5. Stress analysis: Left pedal

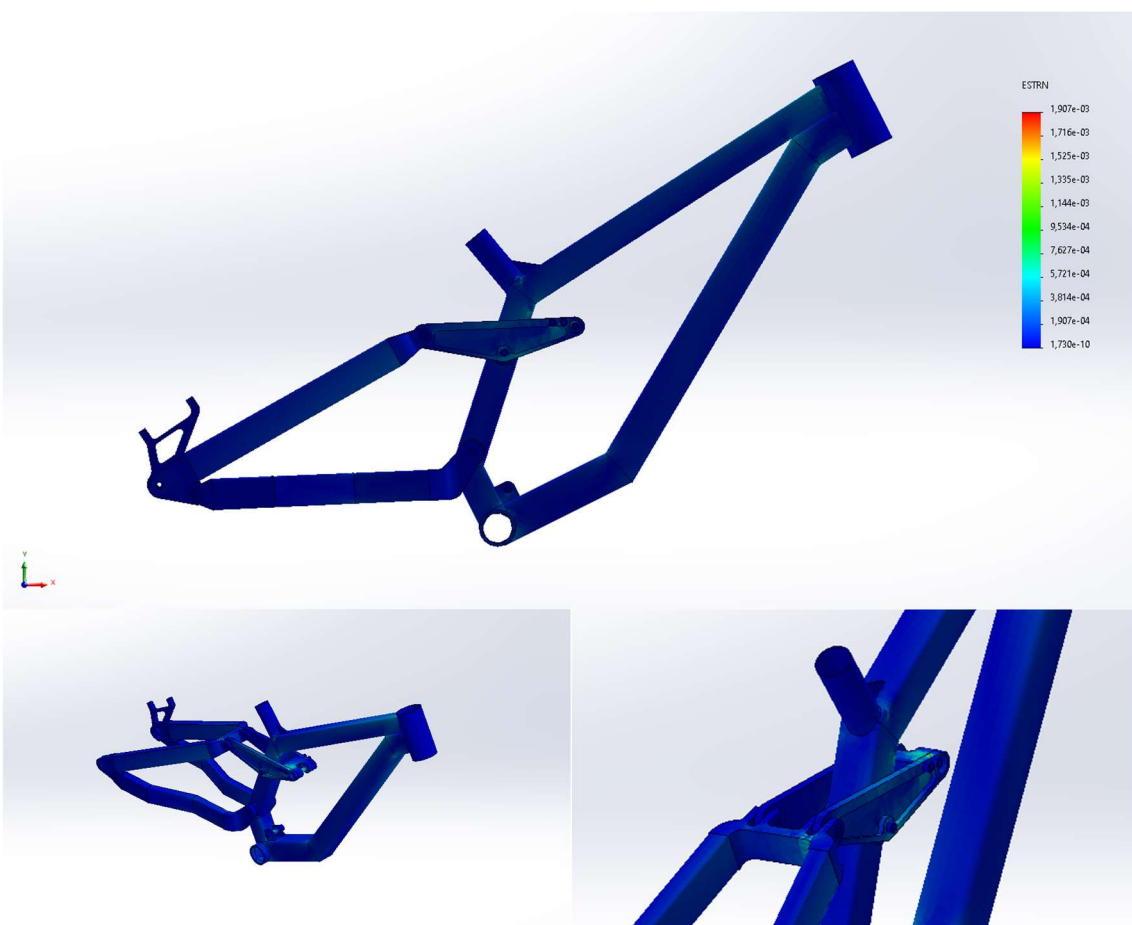


3.2.6. Displacements: Left pedal



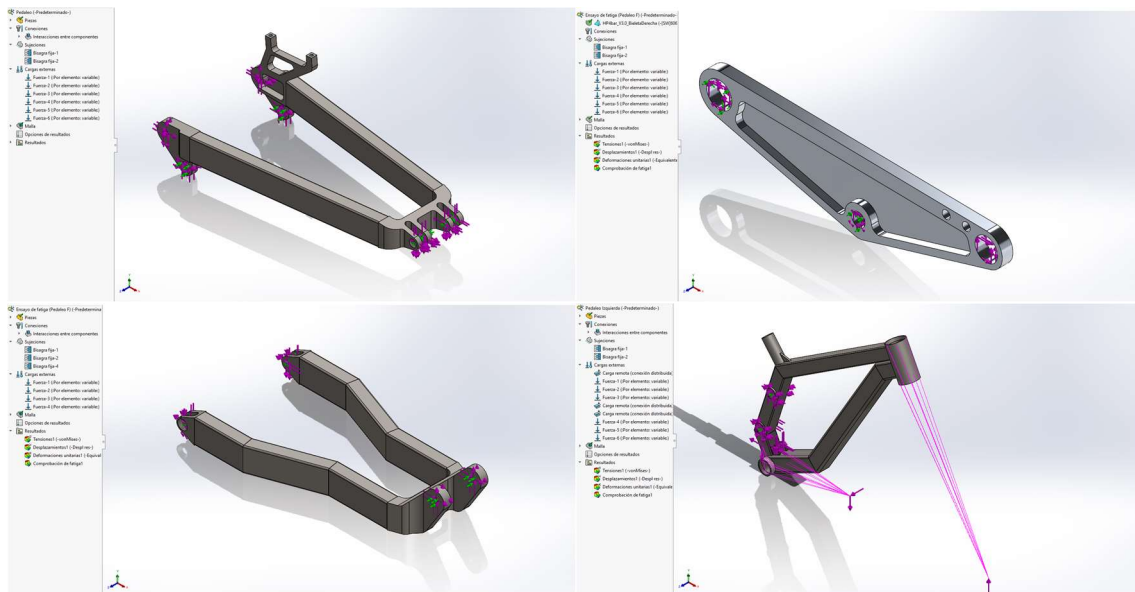


3.2.7. Deformations: Left pedal

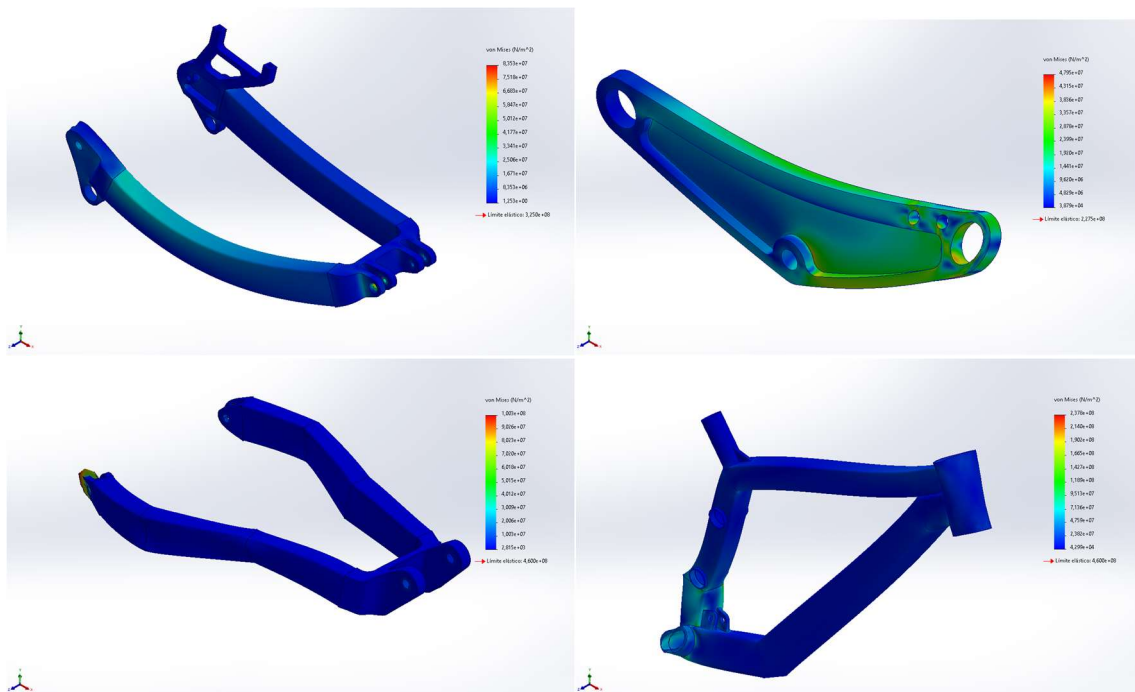


3.2.8. Component's individual analysis: Left pedal

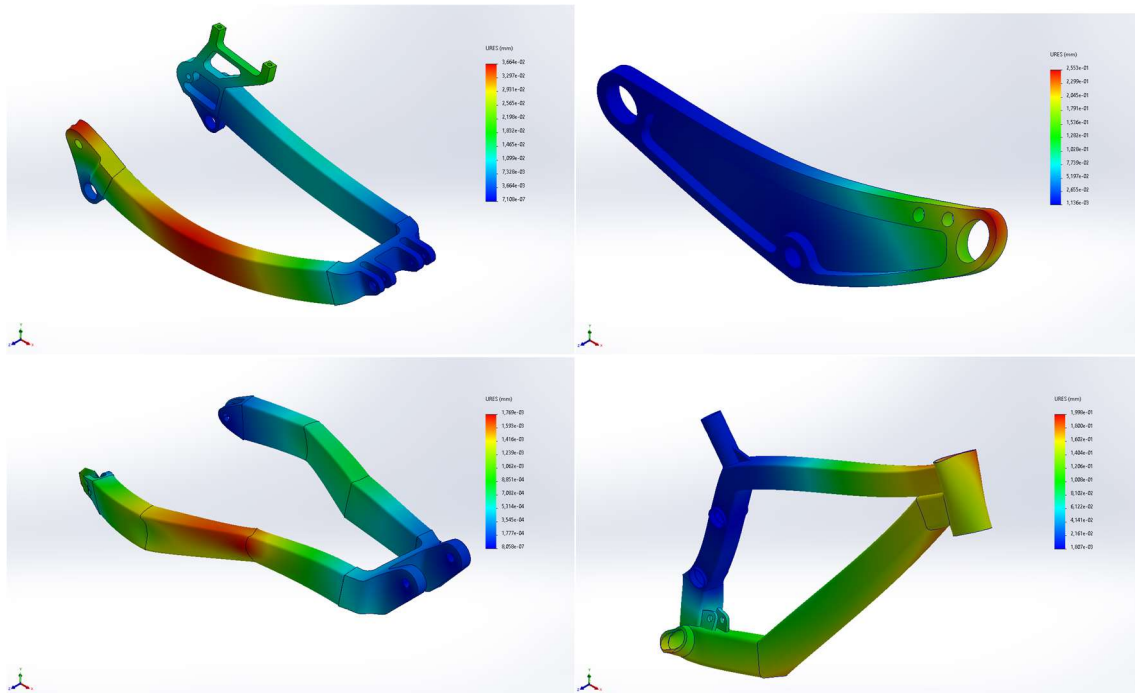
3.2.8.1. Configuration



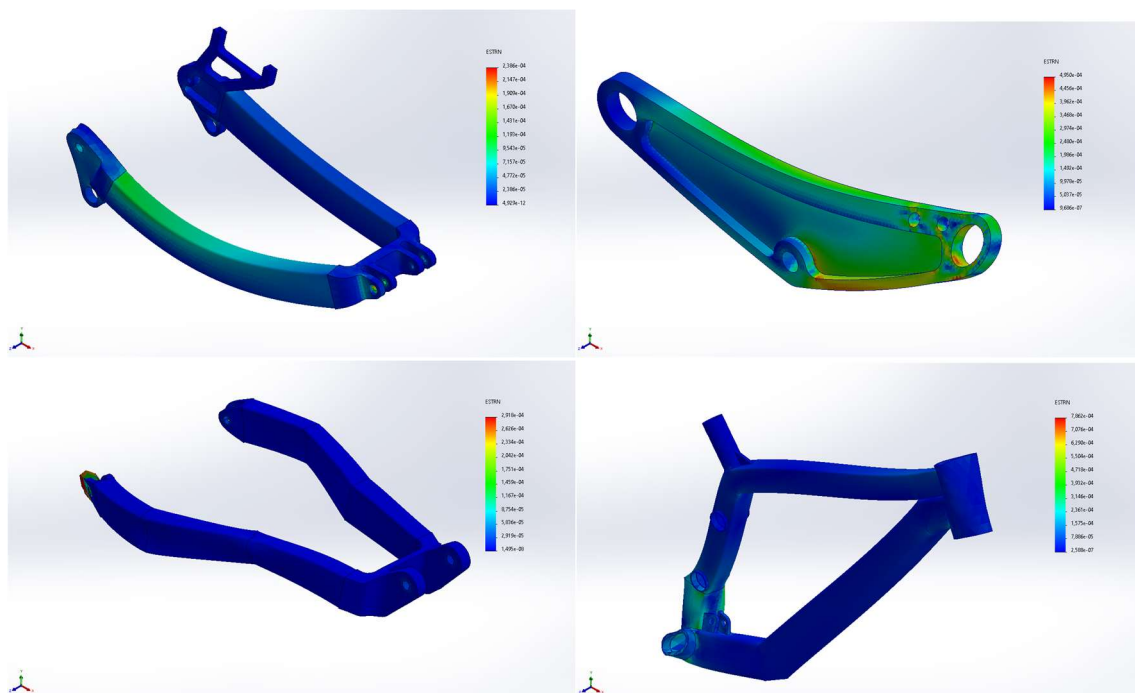
3.2.8.2. Stress analysis:



3.2.8.3. Displacements:

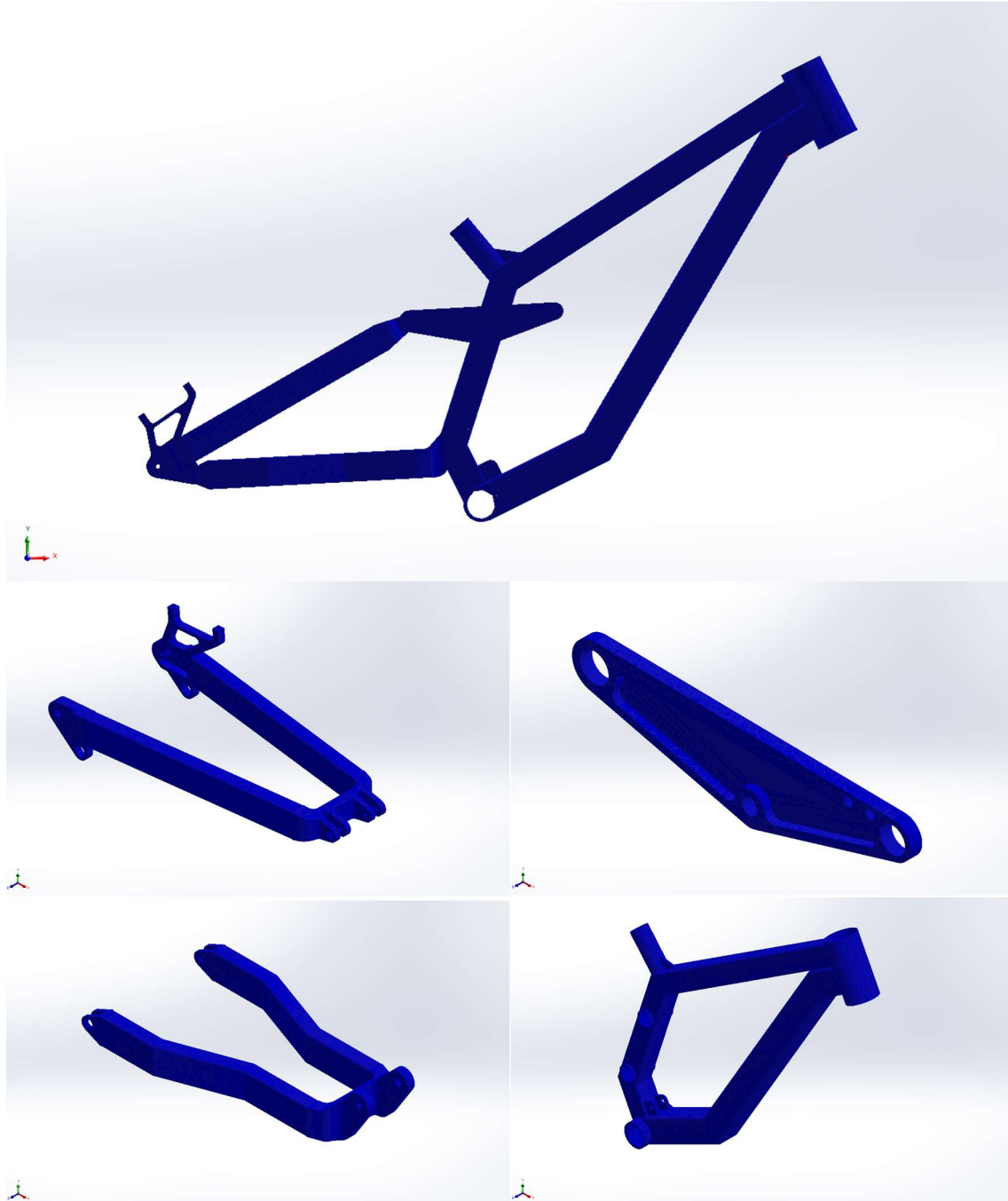


3.2.8.4. Deformations:

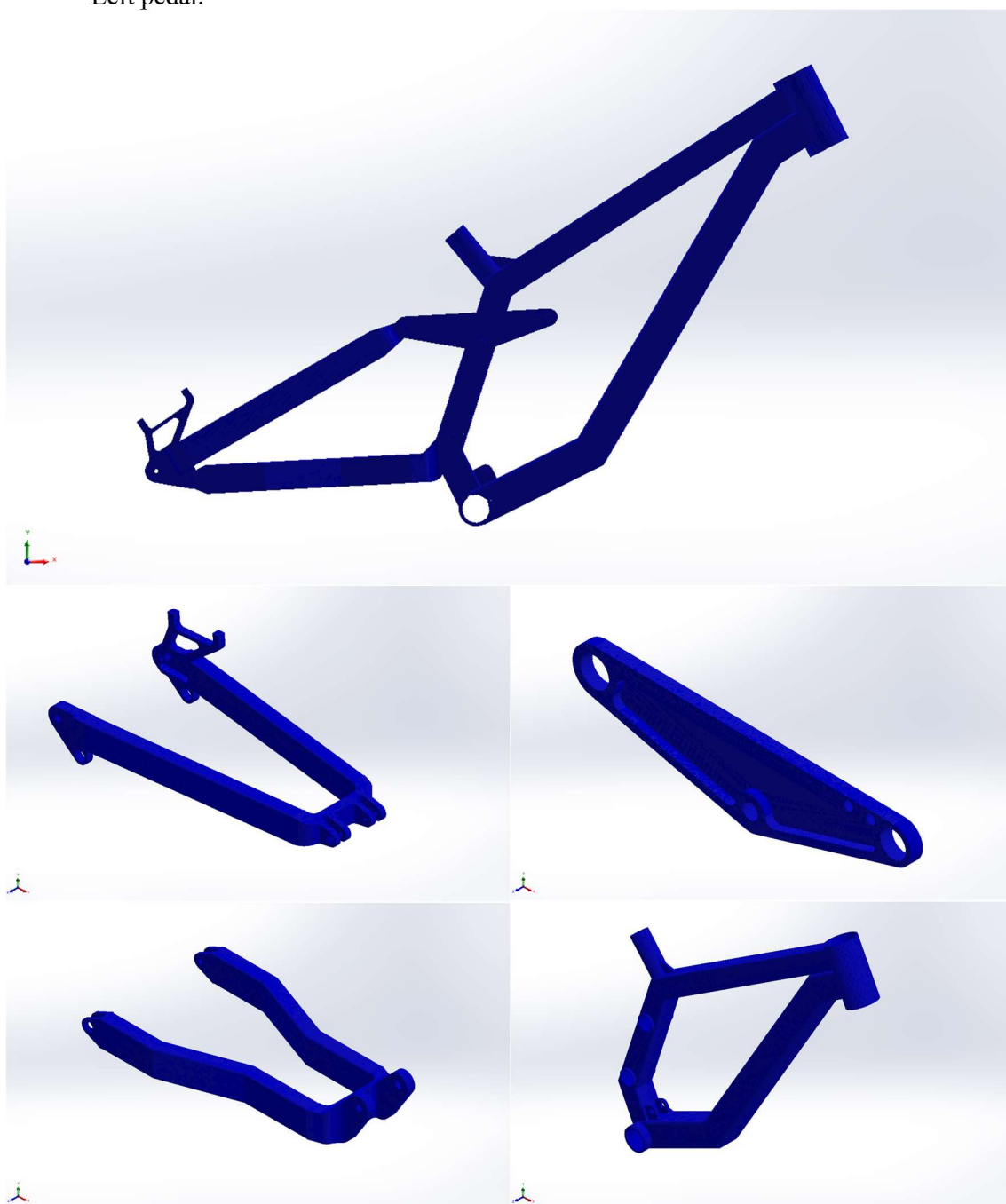


3.2.9. Fatigue verification on static analysis:

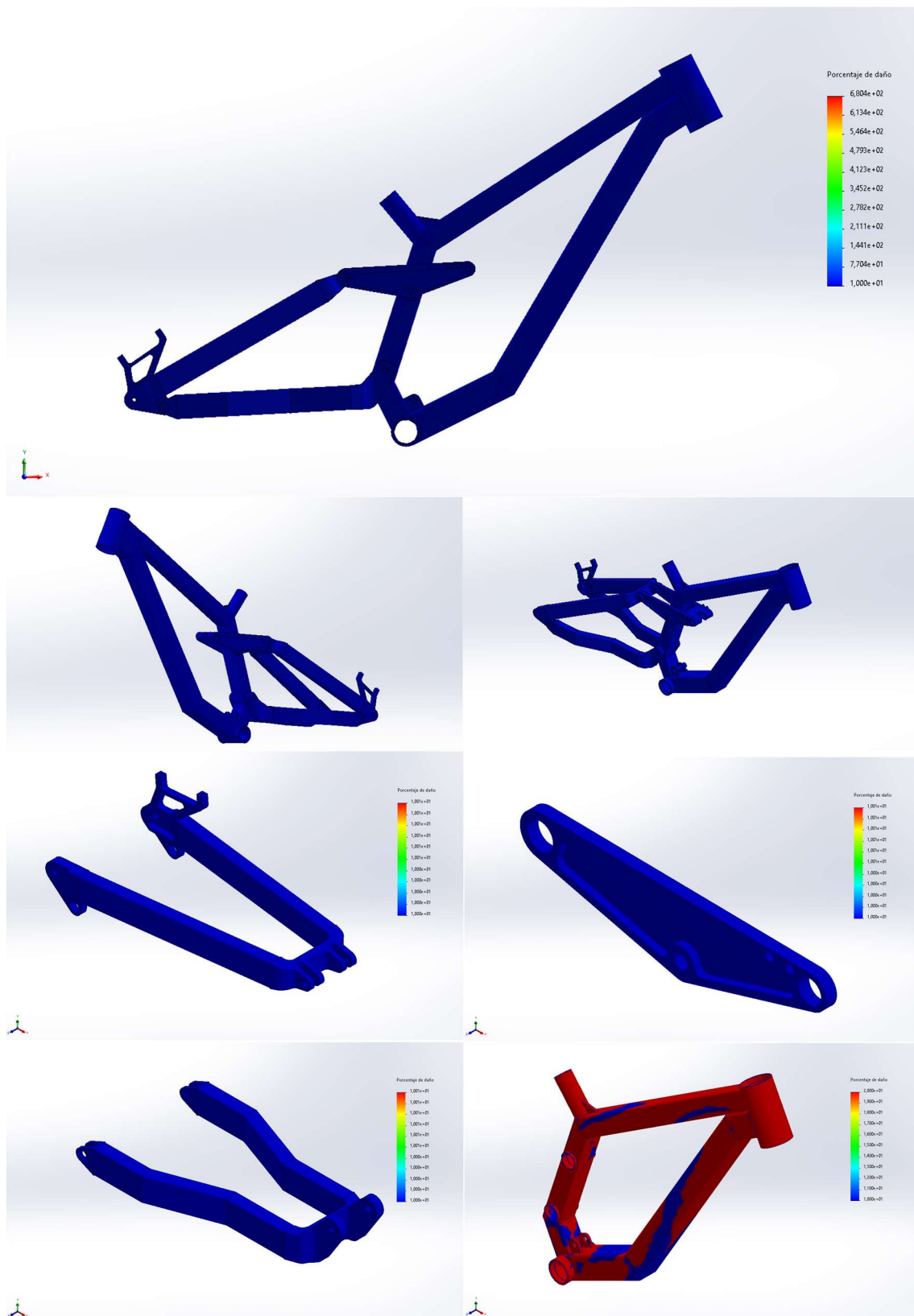
Righth pedal:



Left pedal:



3.2.10. Fatigue damage percentage:

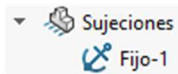


4. FATIGUE TEST WITH HORIZONTAL FORCES

SIMULATION OF FATIGUE TEST WITH HORIZONTAL FORCES AS PER ISO 4210-6:2014

4.1. Simulation preparation

4.1.1. Restraints:

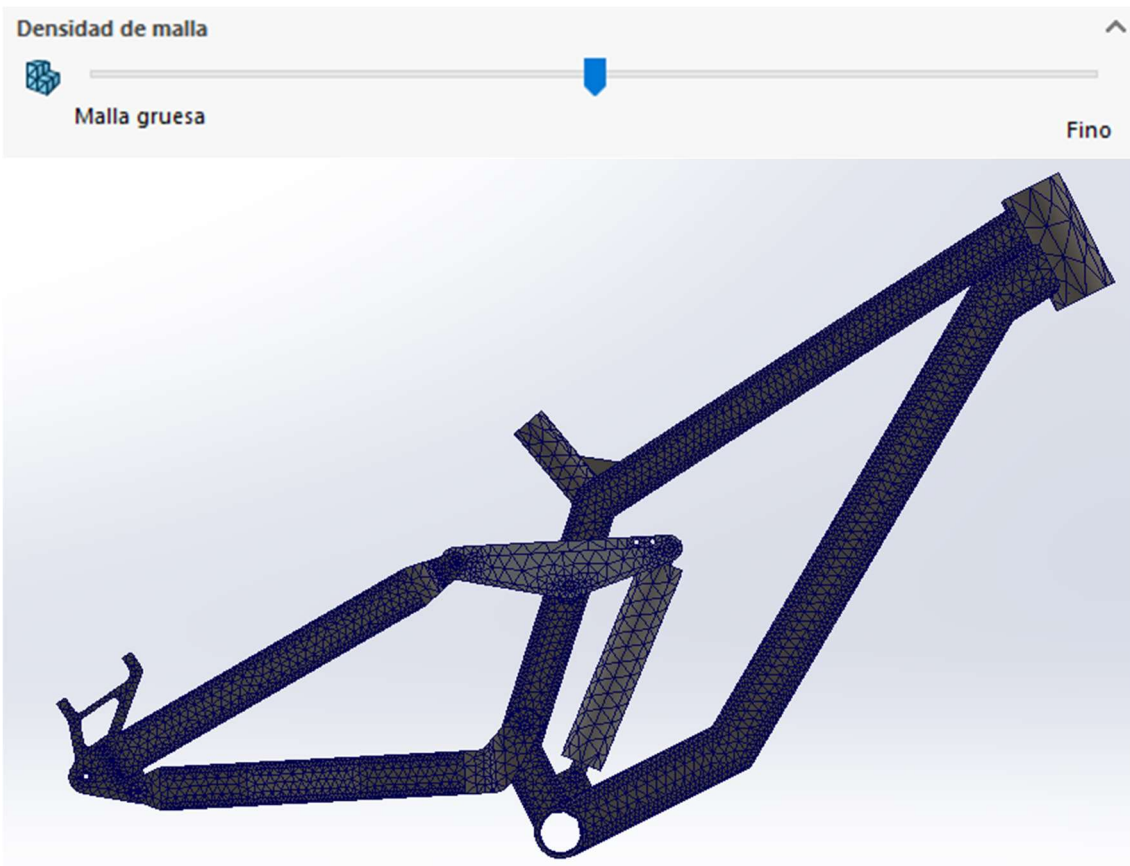


Remark: Rigid restraint on the rear wheel axle attaching points.

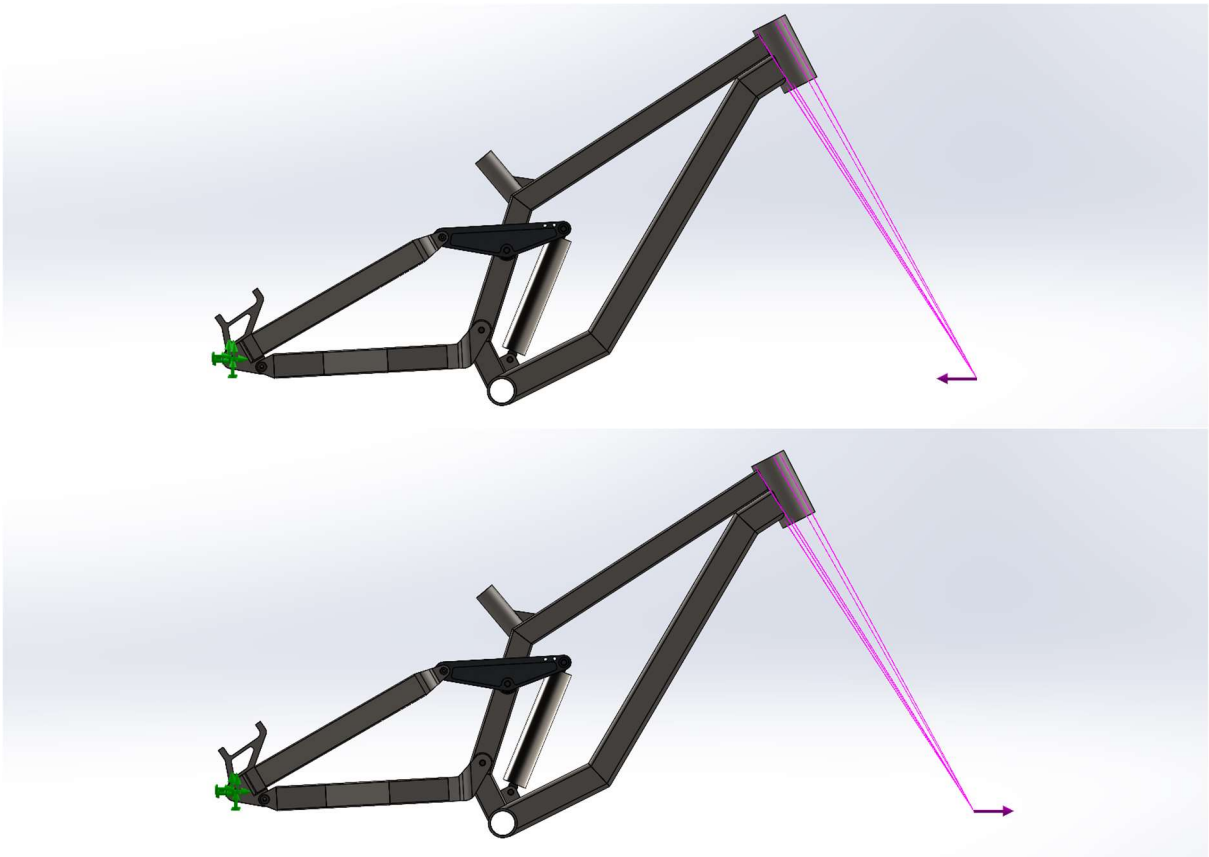
4.1.2. Loads:



4.1.3. Mesh:

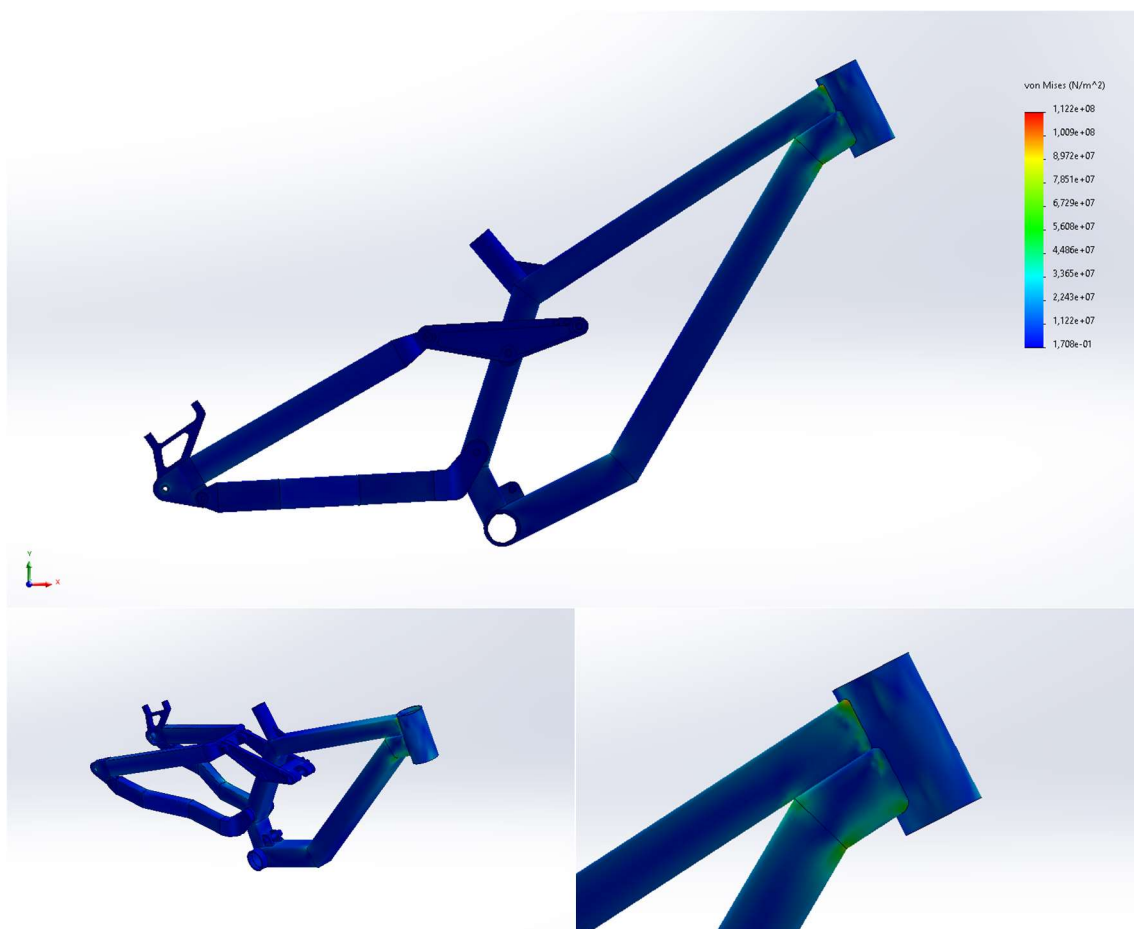


4.1.4. Final model preview:

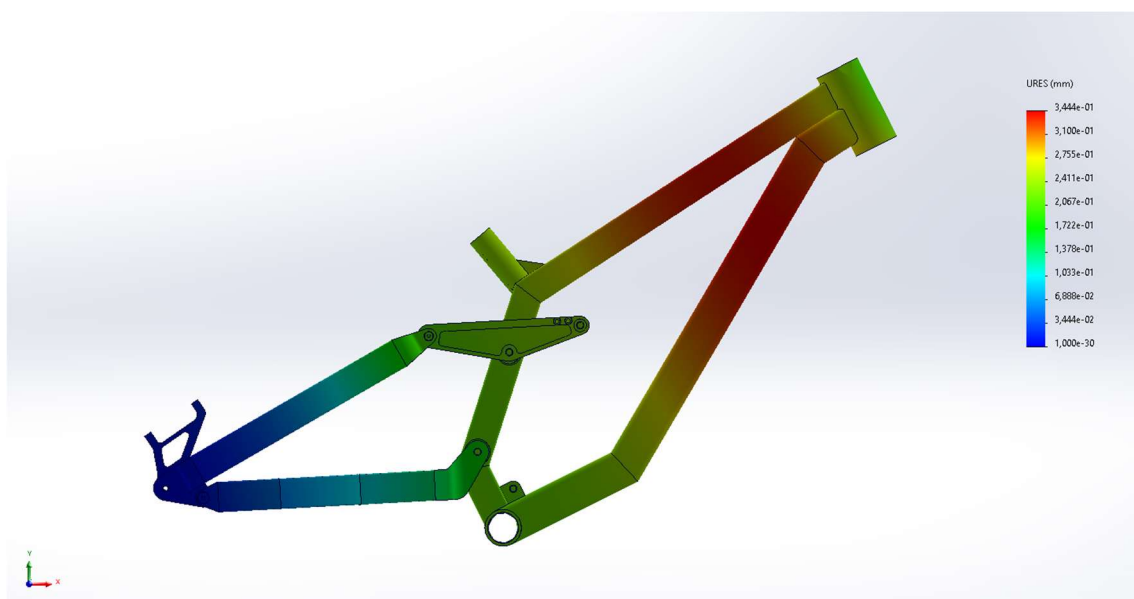


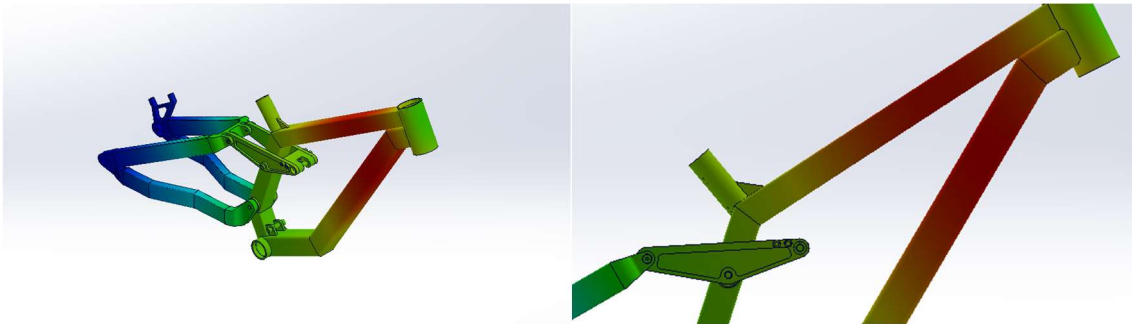
4.2. Test results

4.2.1. Stress analysis: Compression

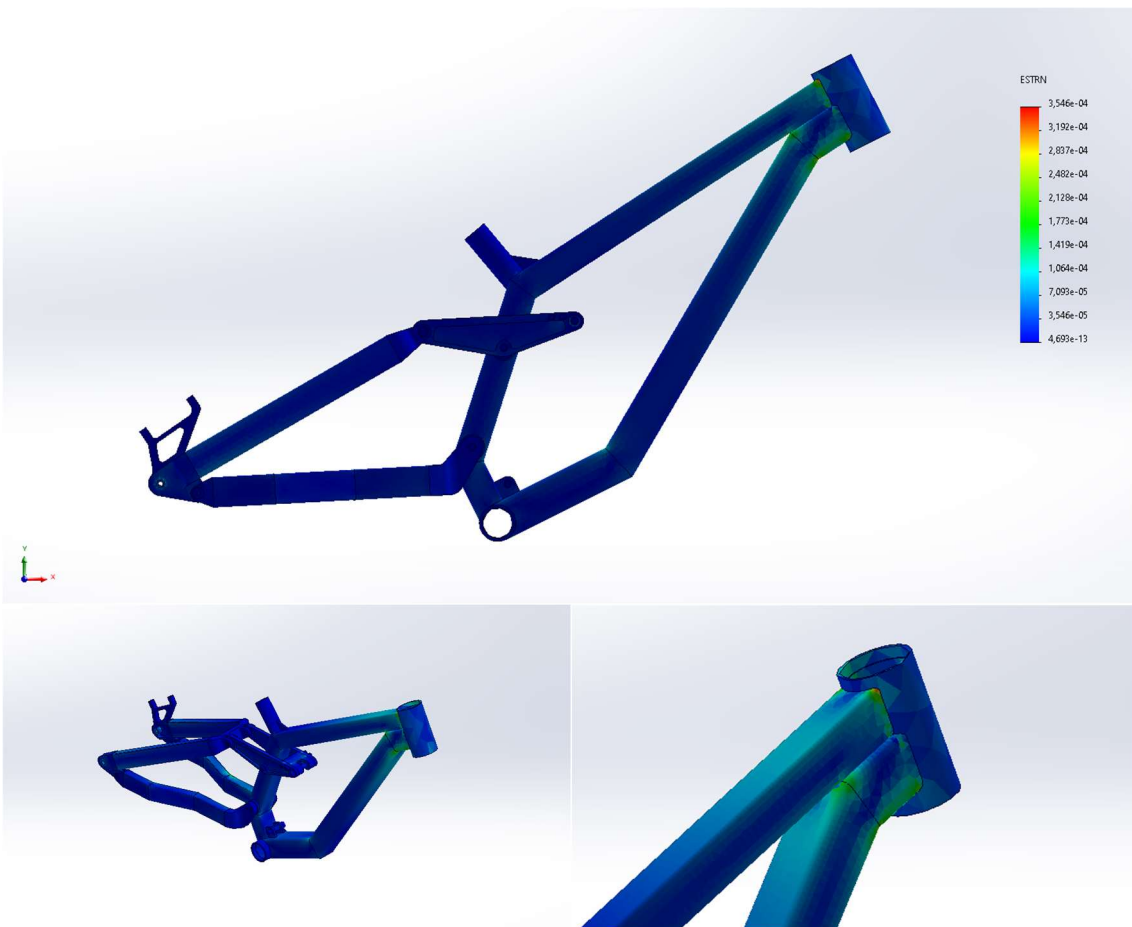


4.2.2. Displacements: Compression



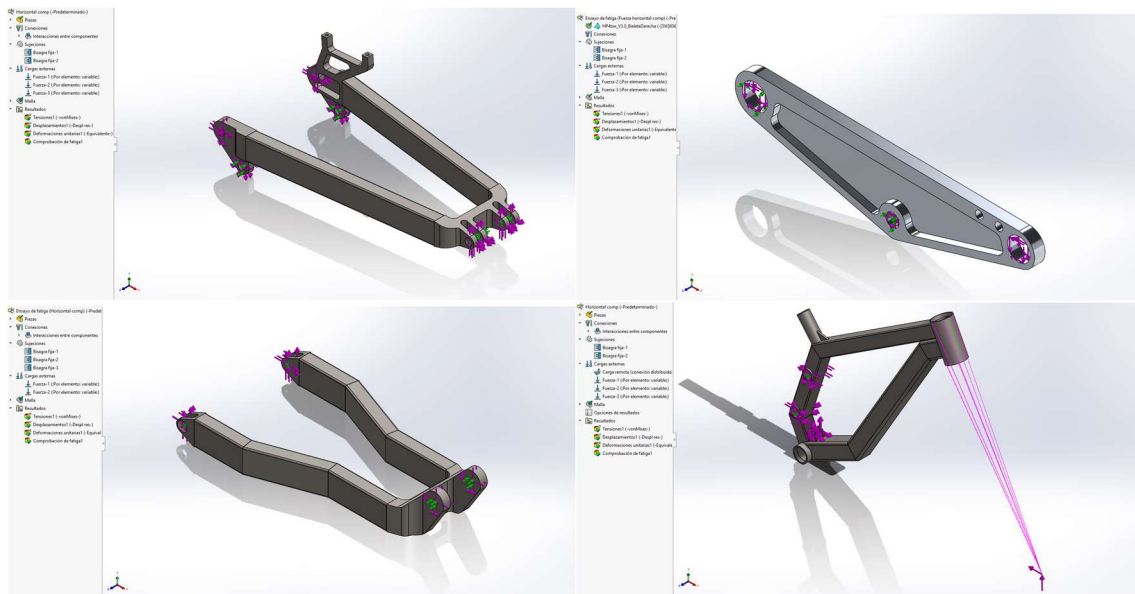


4.2.3. Deformations: Compression

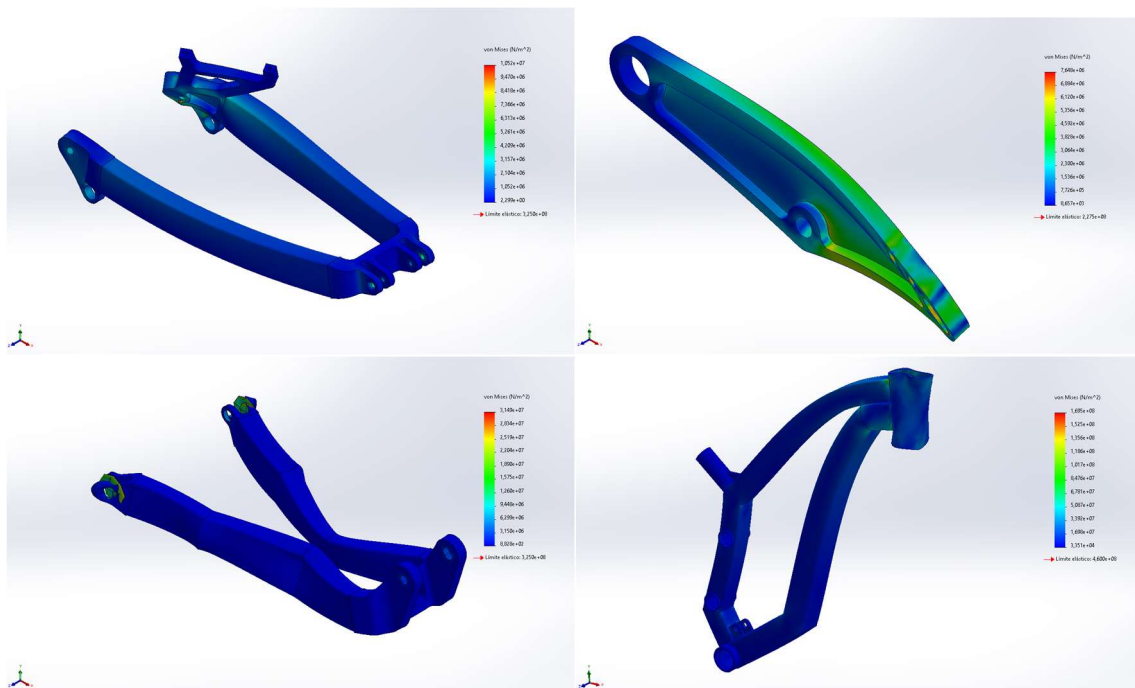


4.2.4. Component's individual analysis: Compression

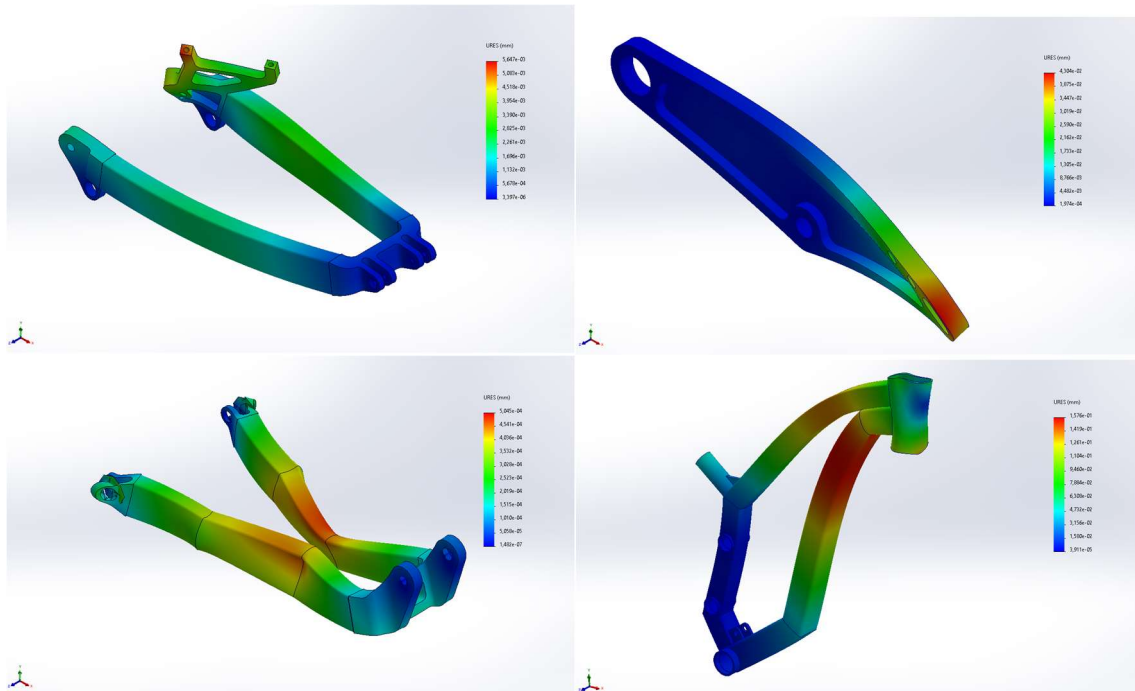
4.2.4.1. Configuration



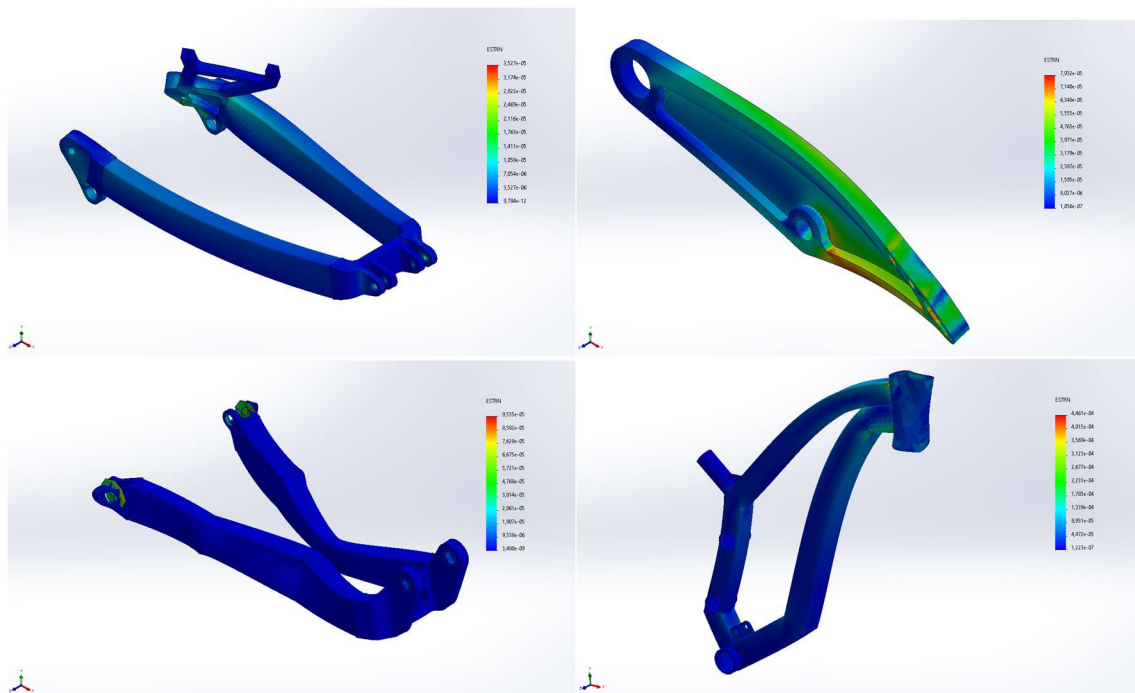
4.2.4.2. Stress analysis:



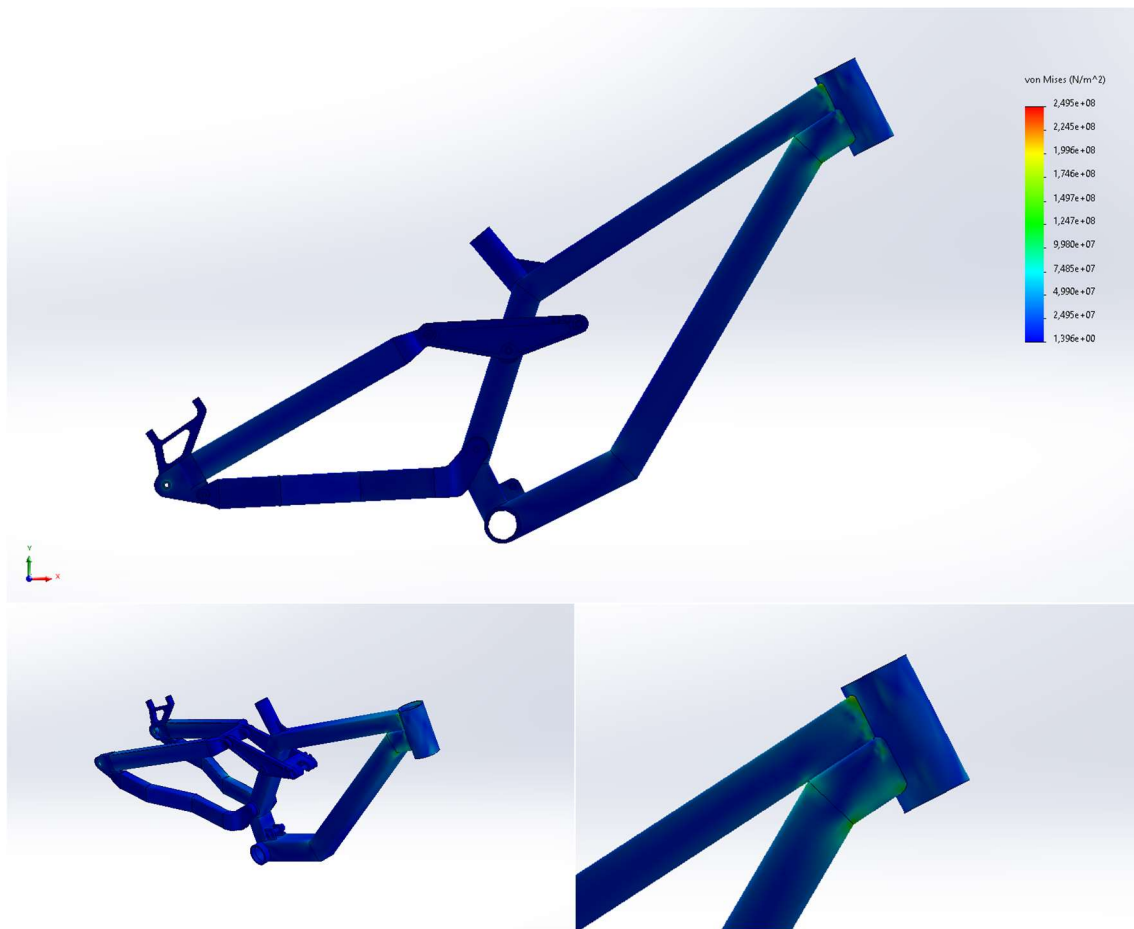
4.2.4.3. Displacements:



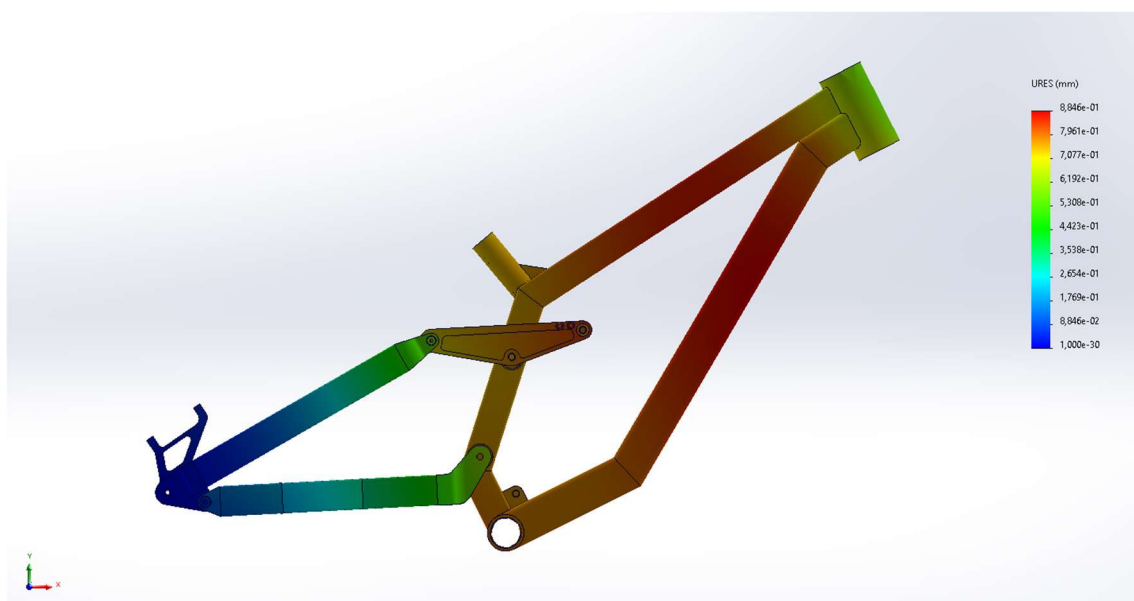
4.2.4.4. Deformations:

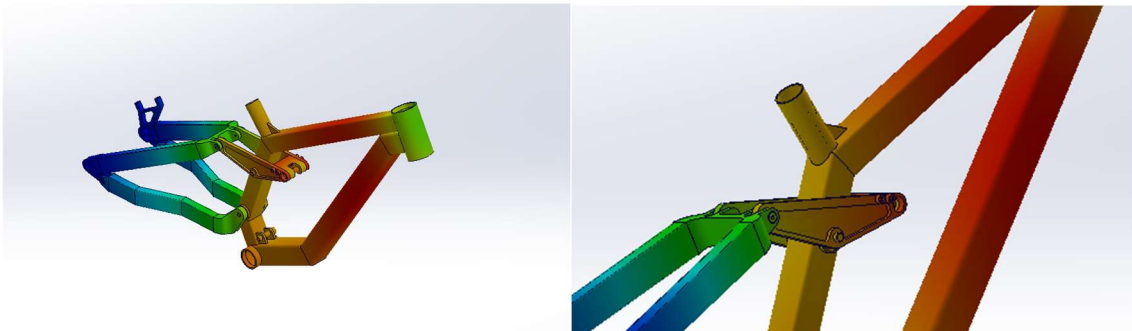


4.2.5. Stress analysis: Traction

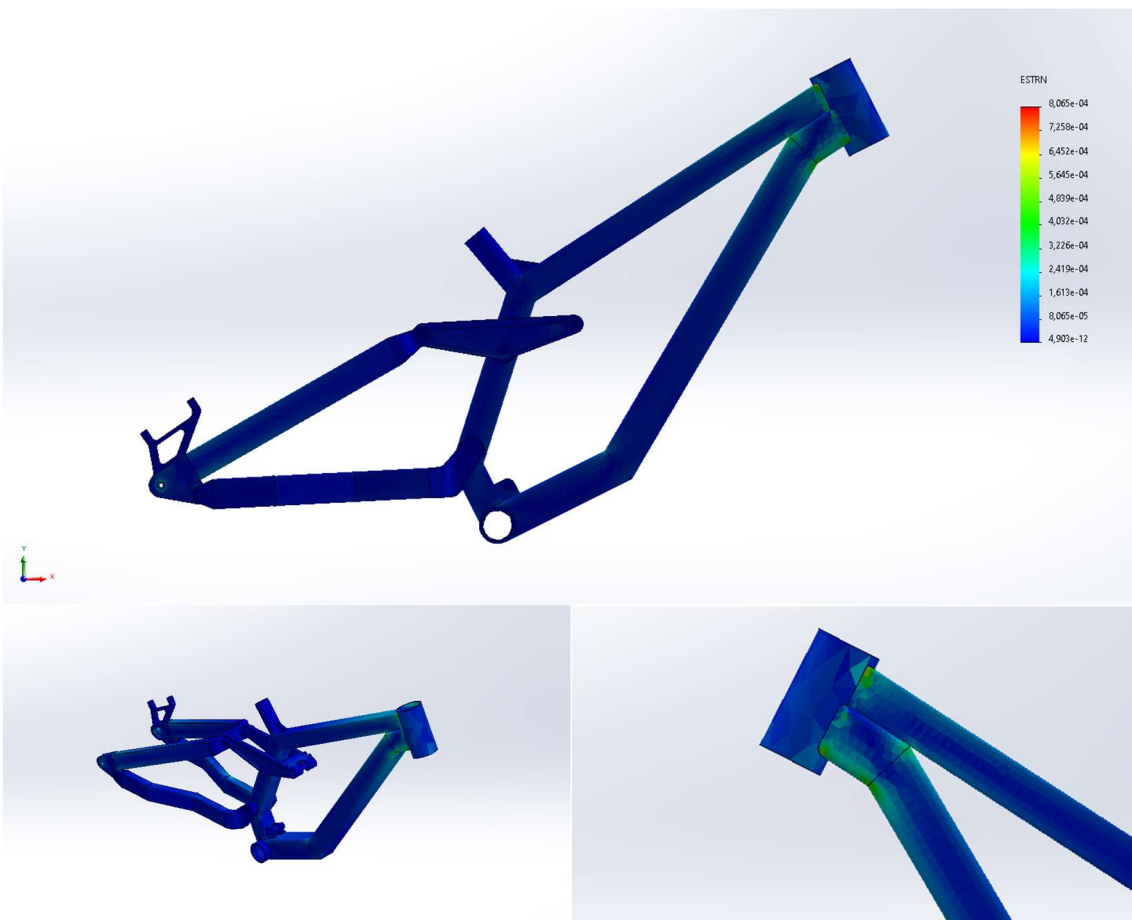


4.2.6. Displacements: Traction



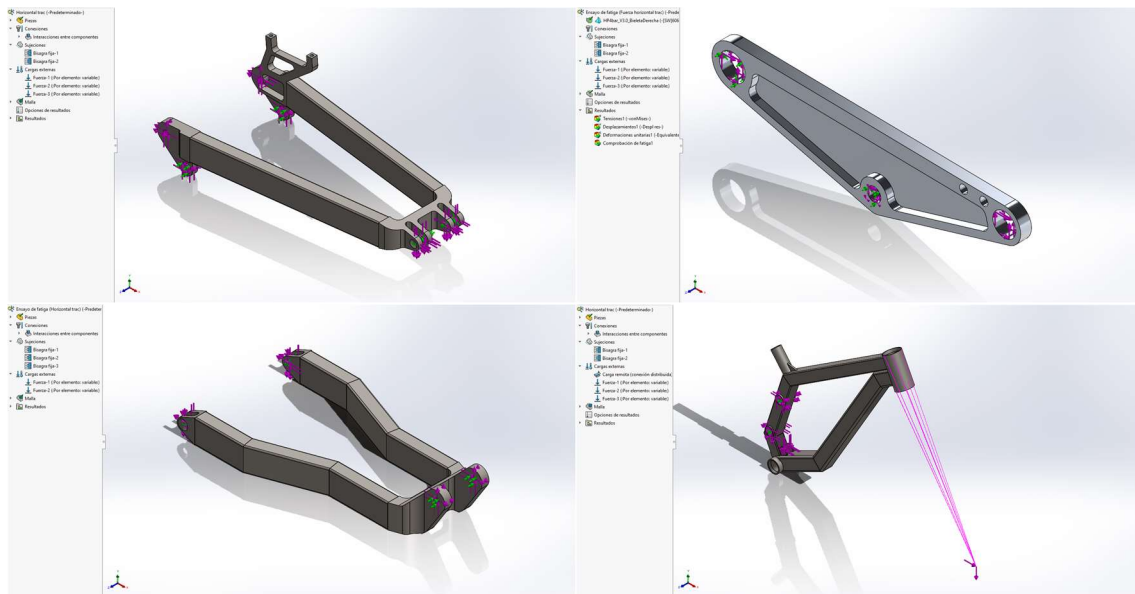


4.2.7. Deformations: Traction

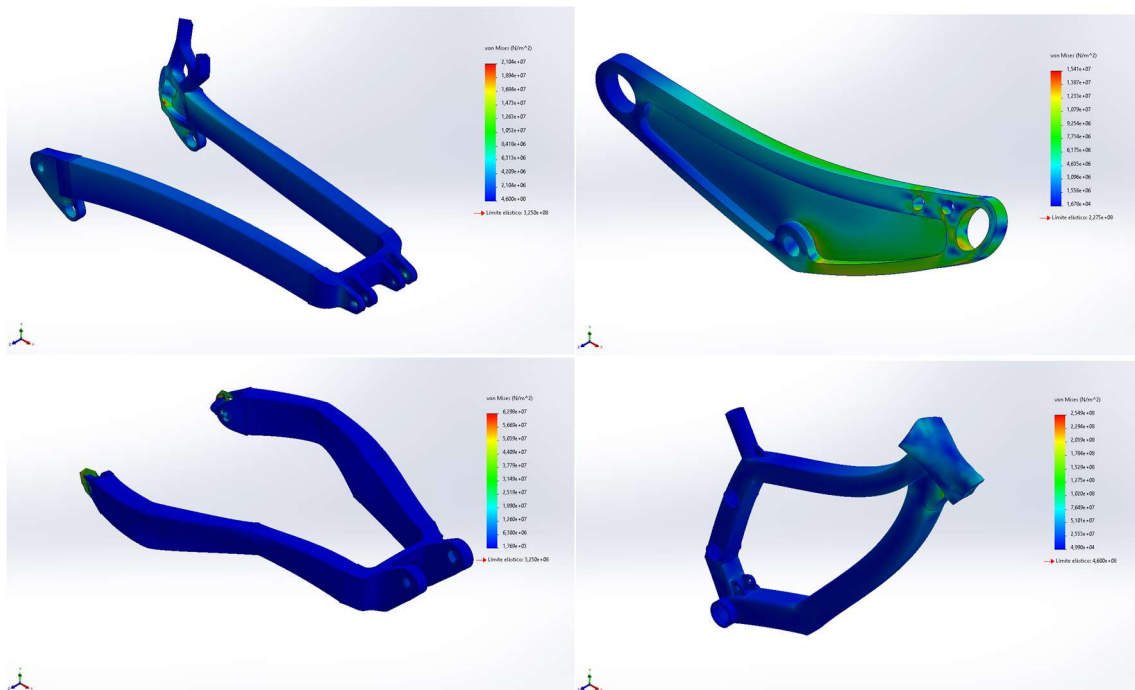


4.2.8. Component's individual analysis: Traction

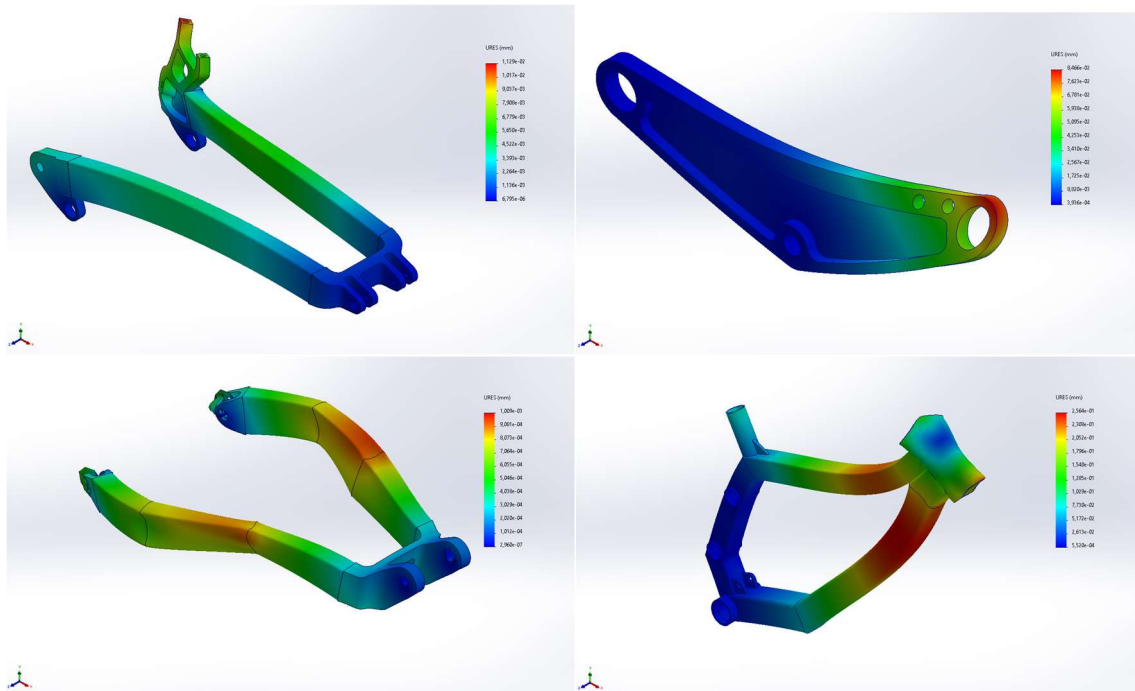
4.2.8.1. Configuration



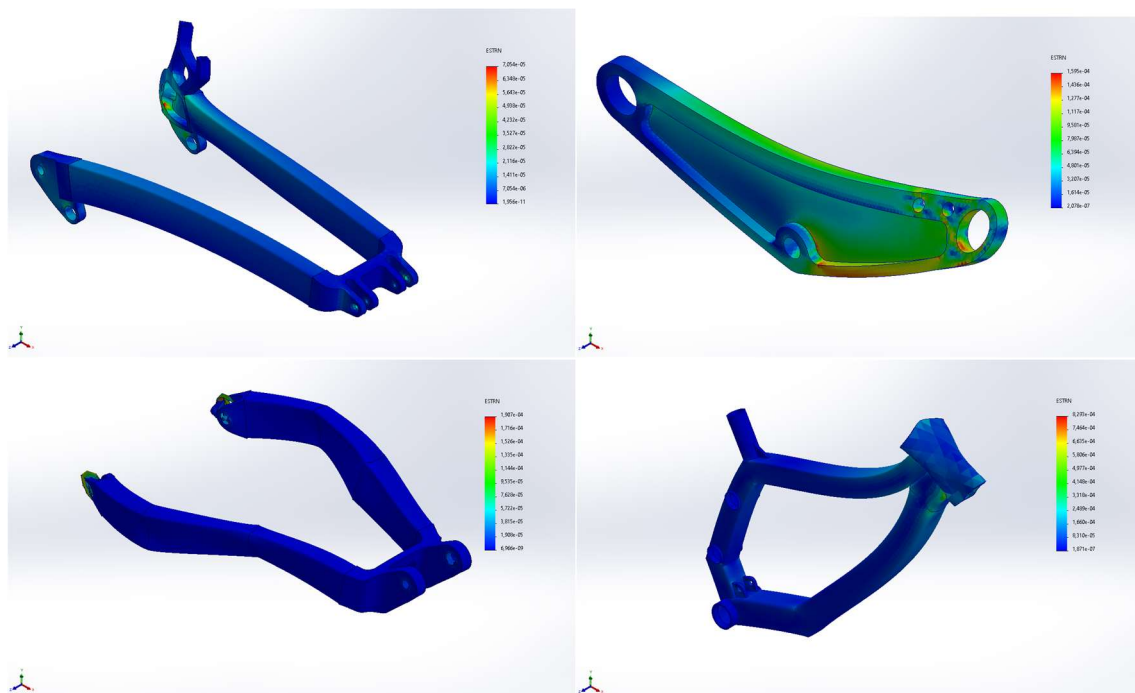
4.2.8.2. Stress analysis:



4.2.8.3. Displacements:

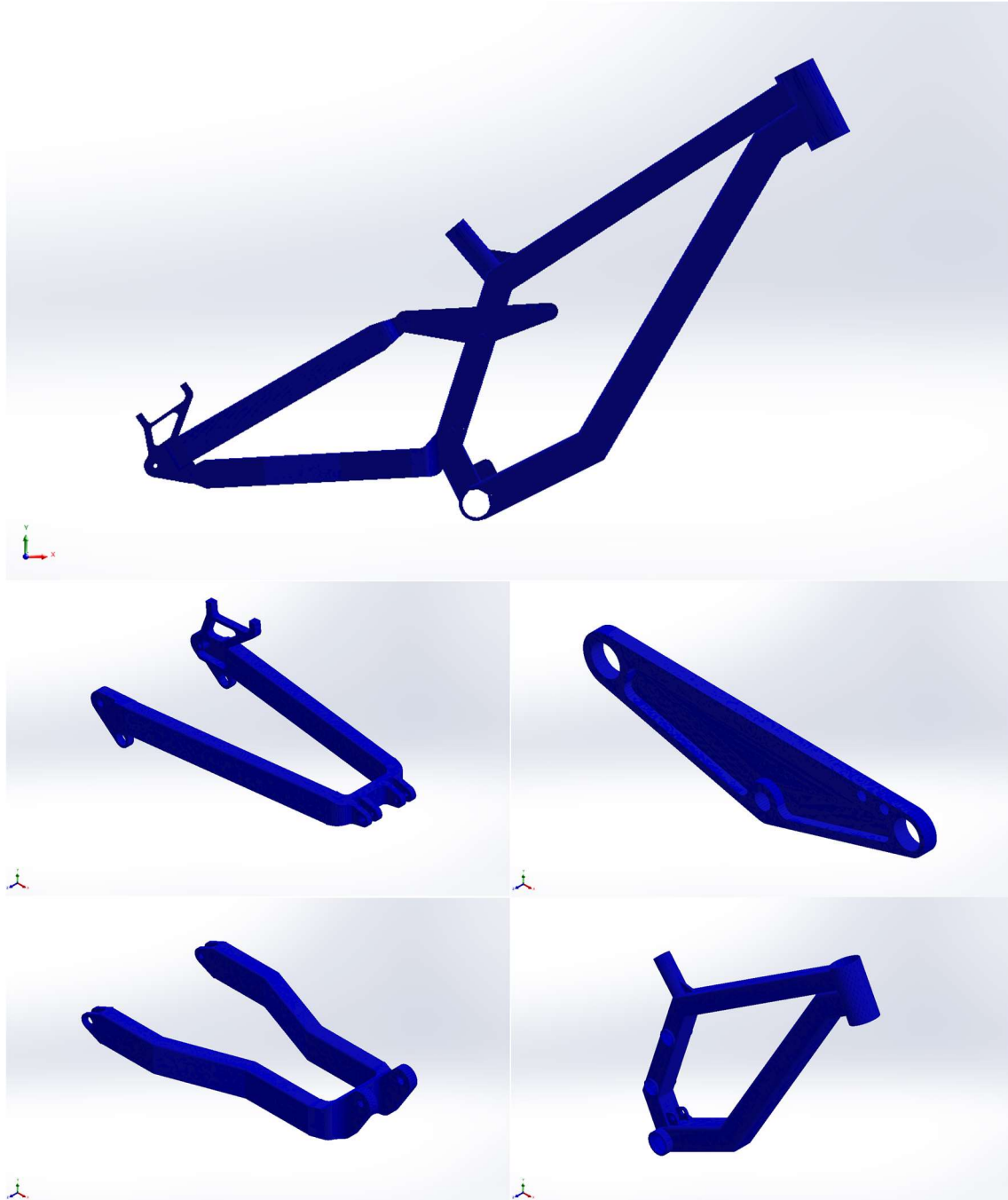


4.2.8.4. Deformations:

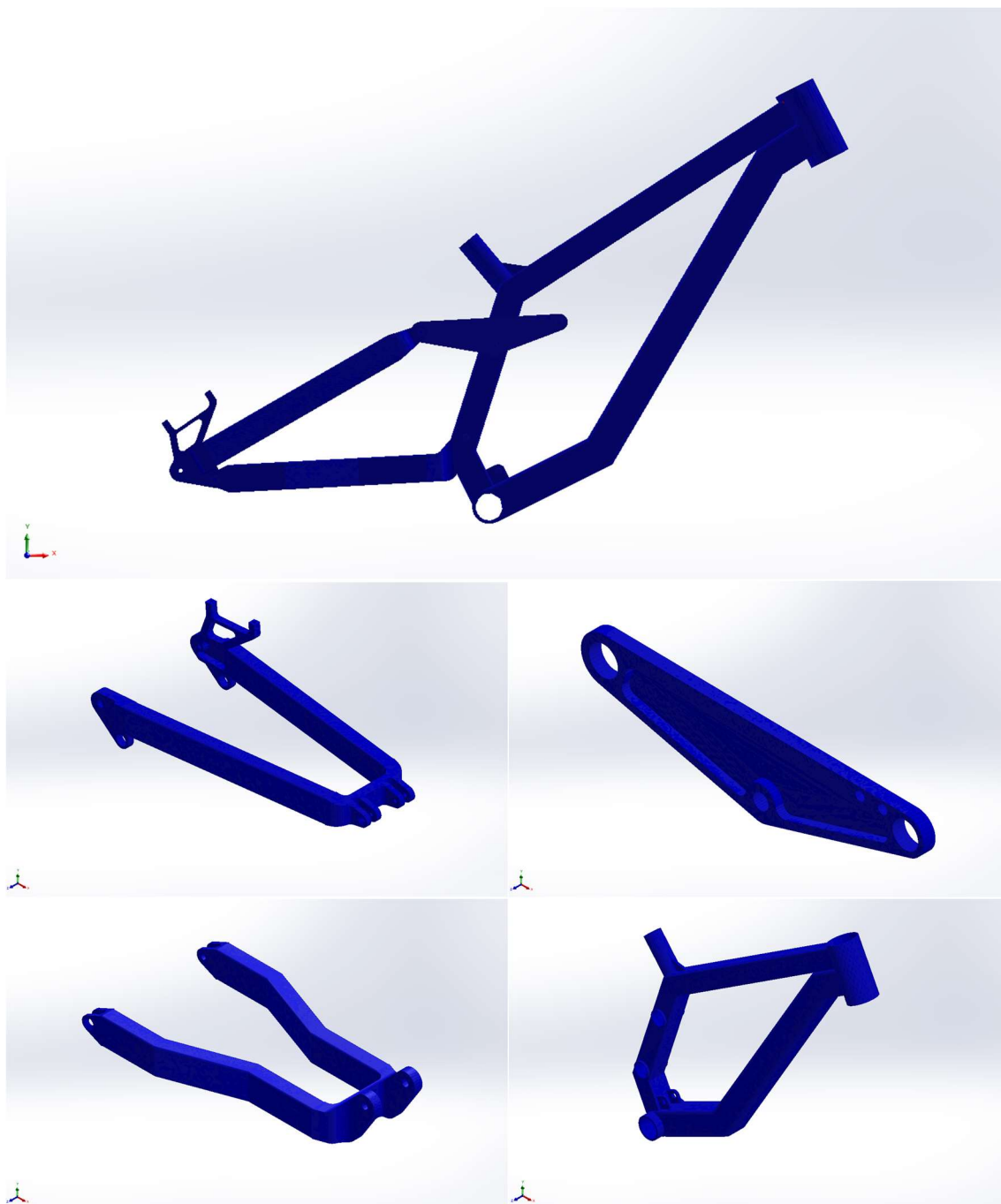


4.2.9. Fatigue verification on static analysis:

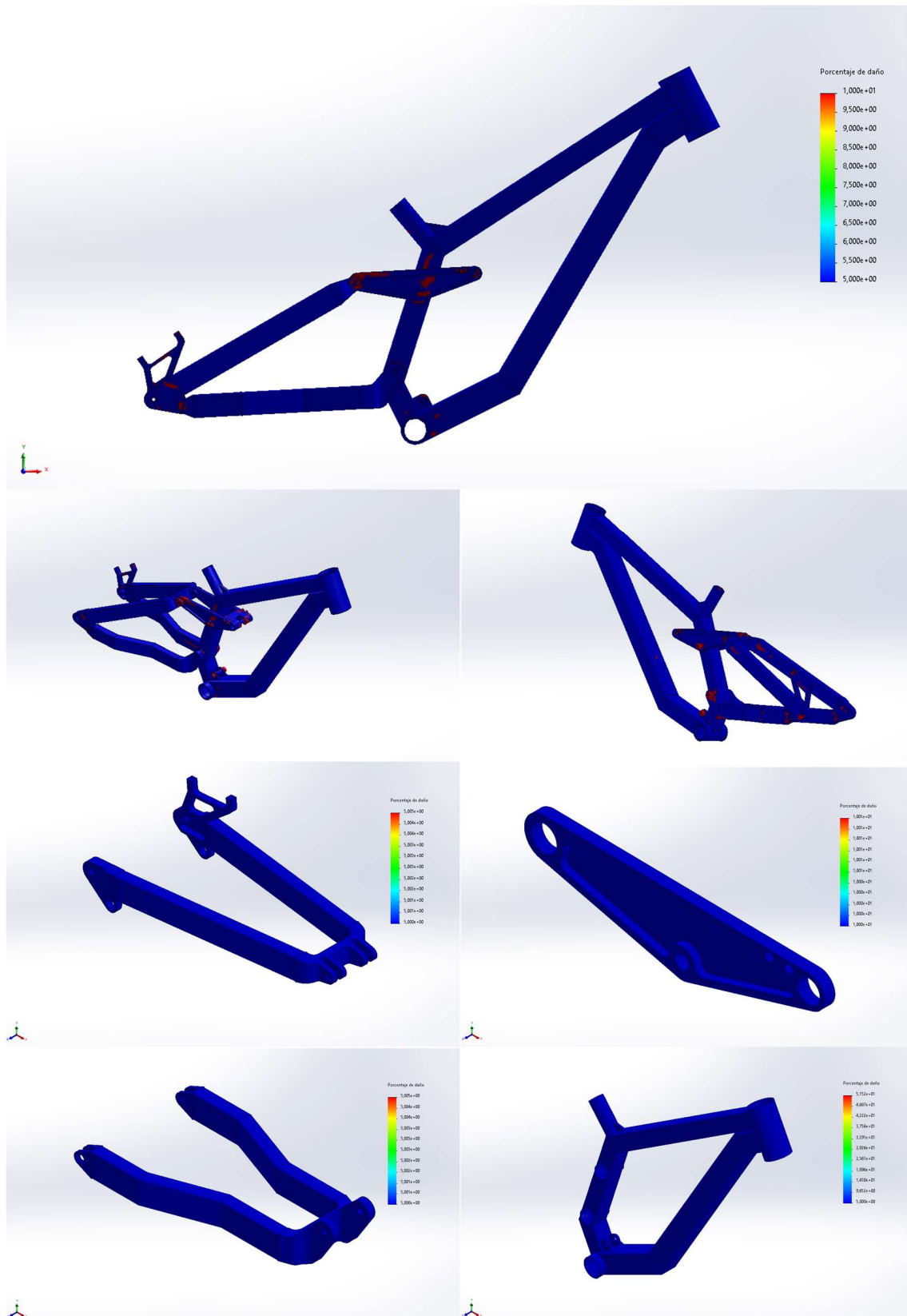
Compression



Traction:



4.2.10. Fatigue damage percentage:

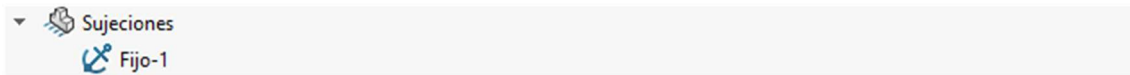


5. FATIGUE TEST WITH A VERTICAL FORCE

SIMULATION OF FATIGUE TEST WITH A VERTICAL FORCE AS PER ISO 4210-6:2014

5.1. Simulation preparation

5.1.1. Restraints:



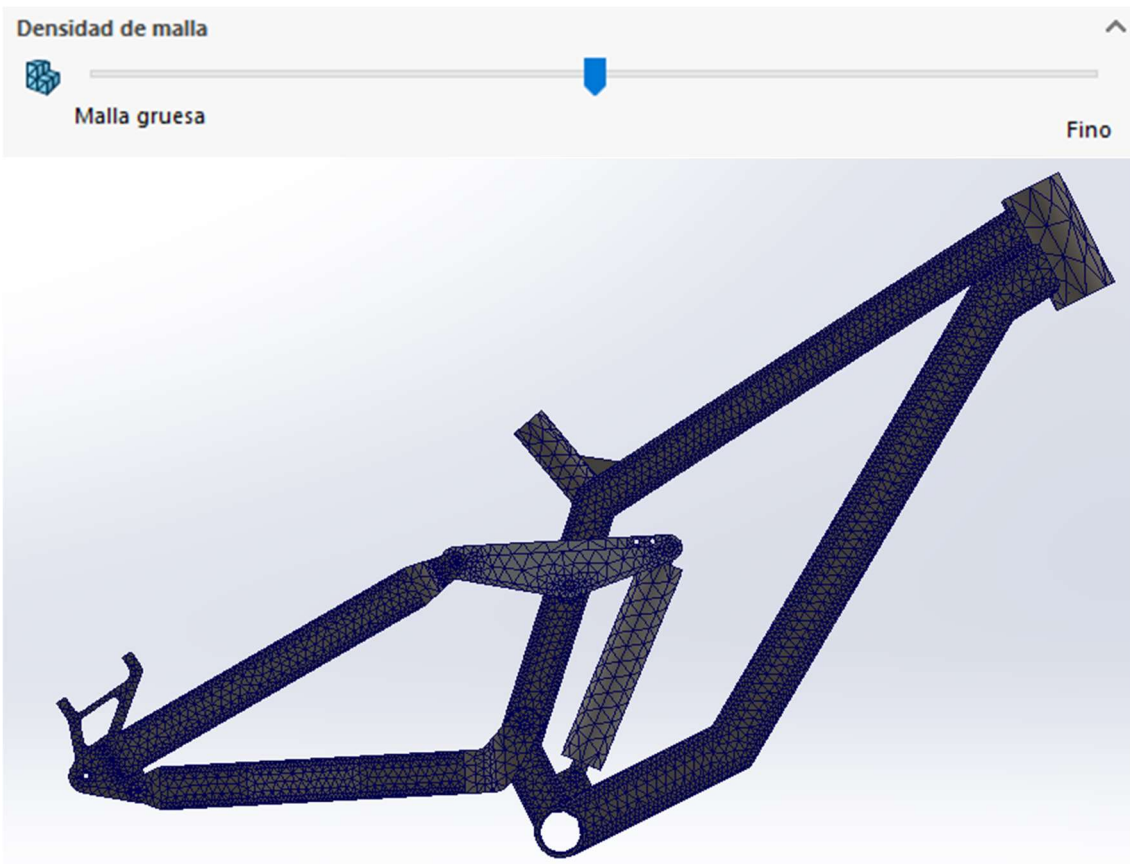
Remark: Rigid restraint on the rear wheel axle attaching points.

5.1.2. Loads:

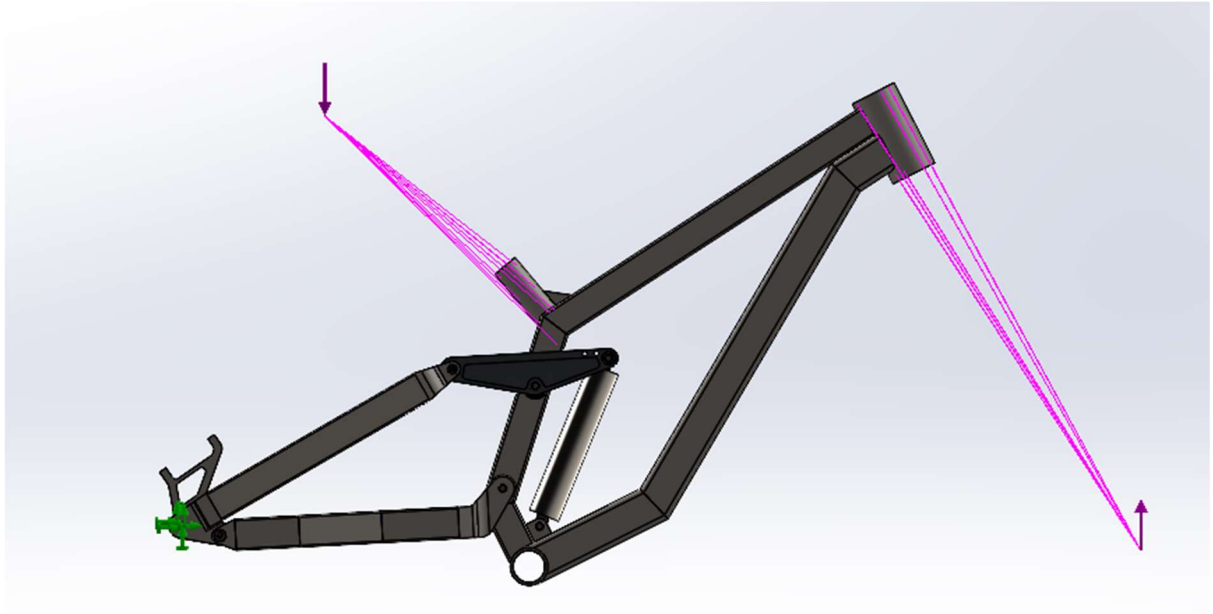


Remark: Remote load No. 1 – Front wheel reaction
 Remote load No. 2 – Force applied on seat post

5.1.3. Mesh:

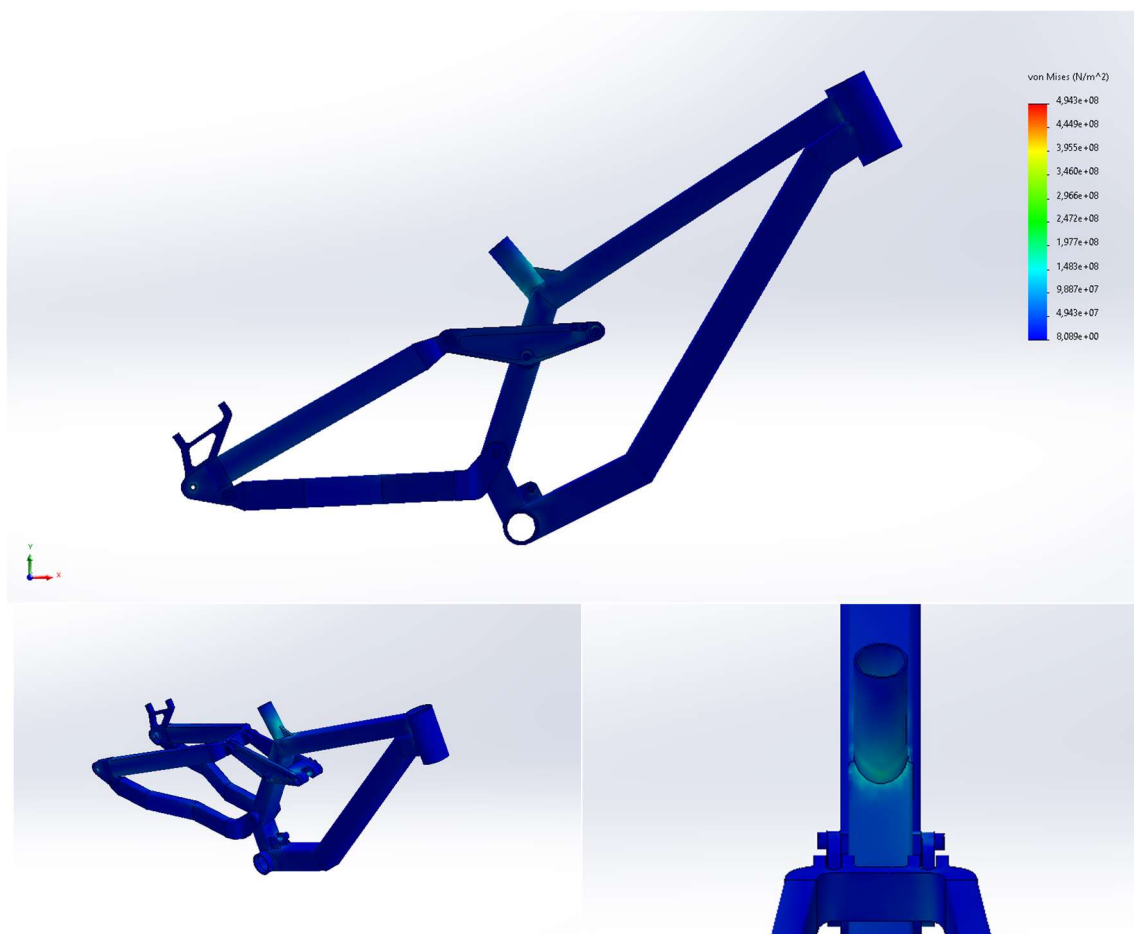


5.1.4. Final model preview:

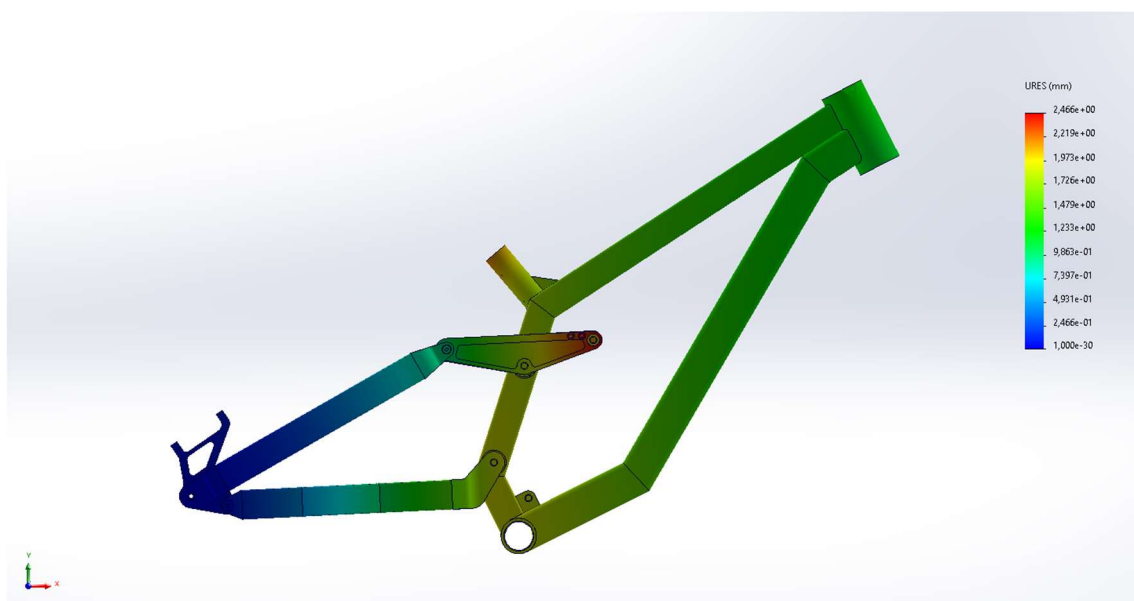


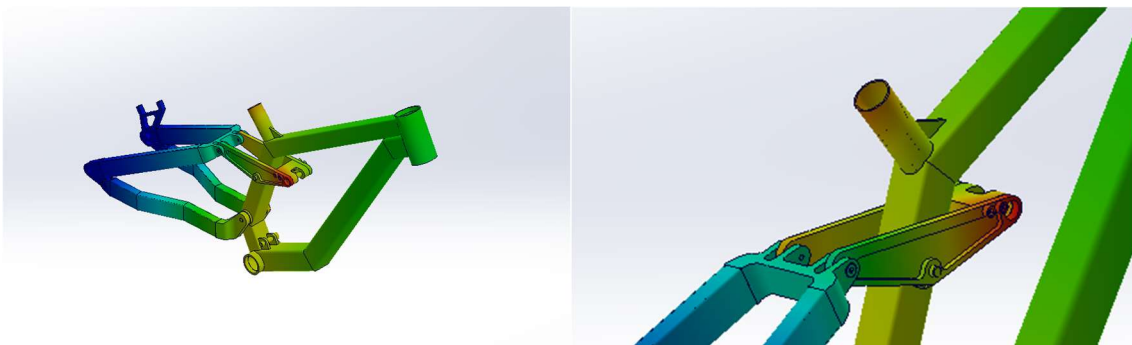
5.2. Test results

5.2.1. Stress analysis:

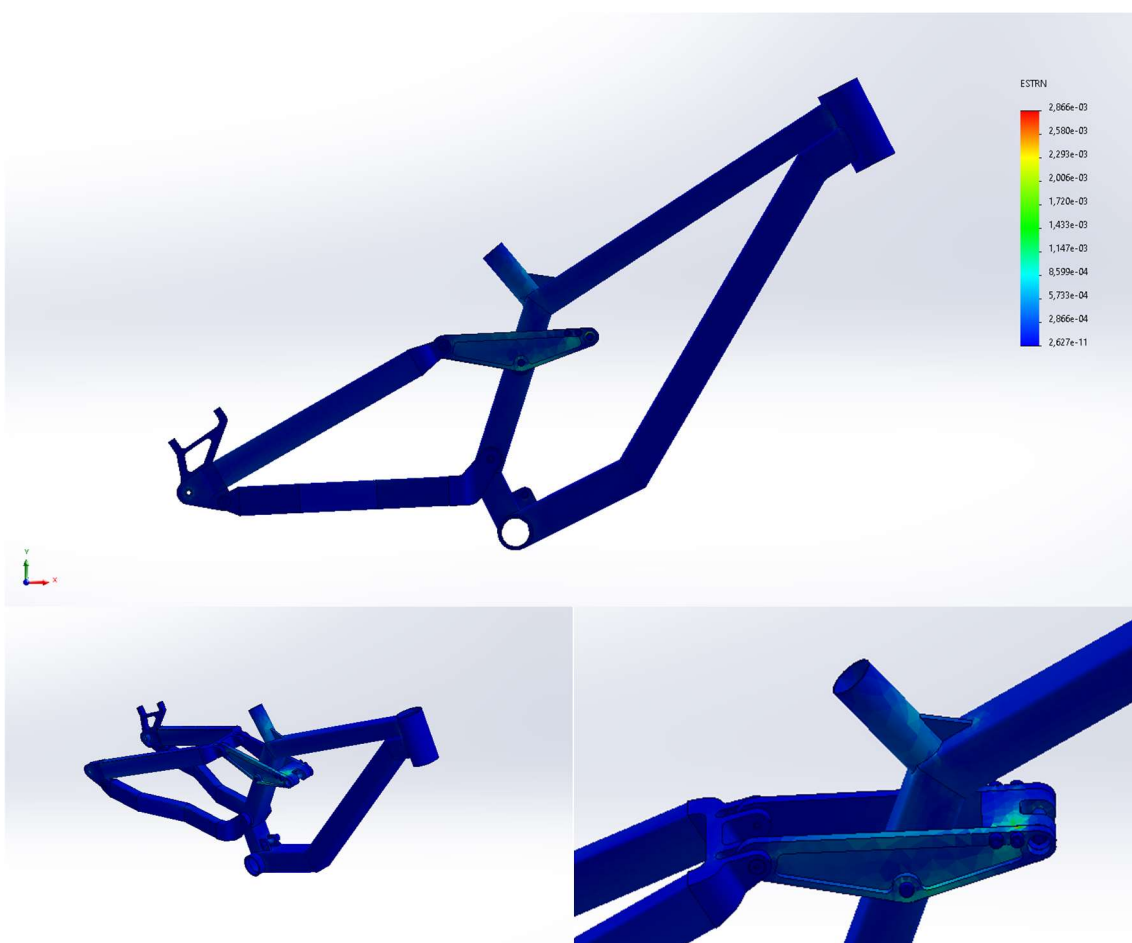


5.2.2. Displacements:



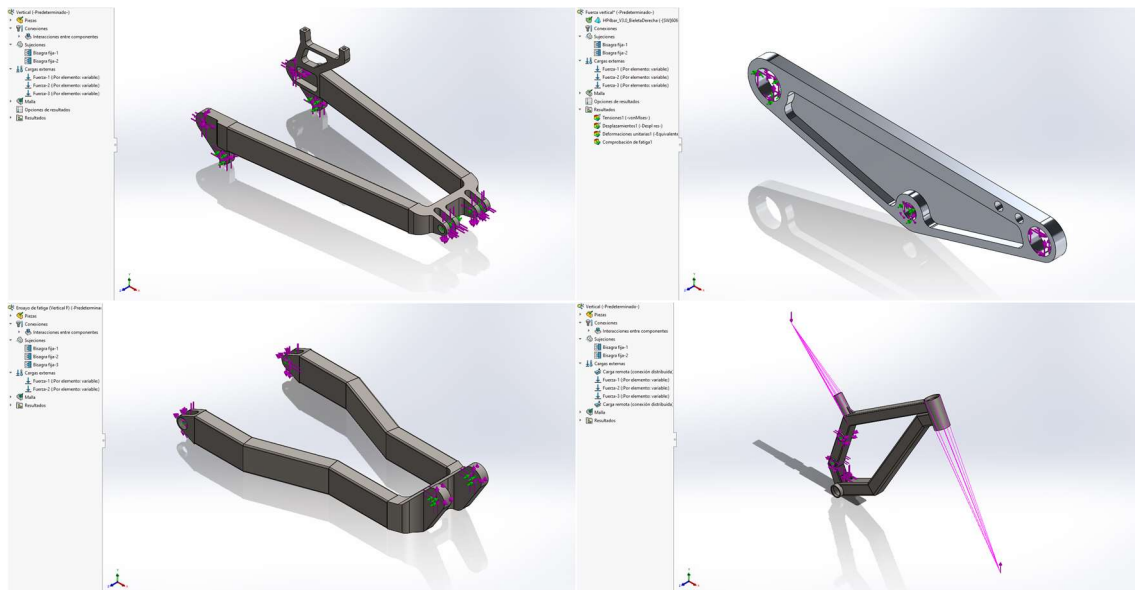


5.2.3. Deformations:

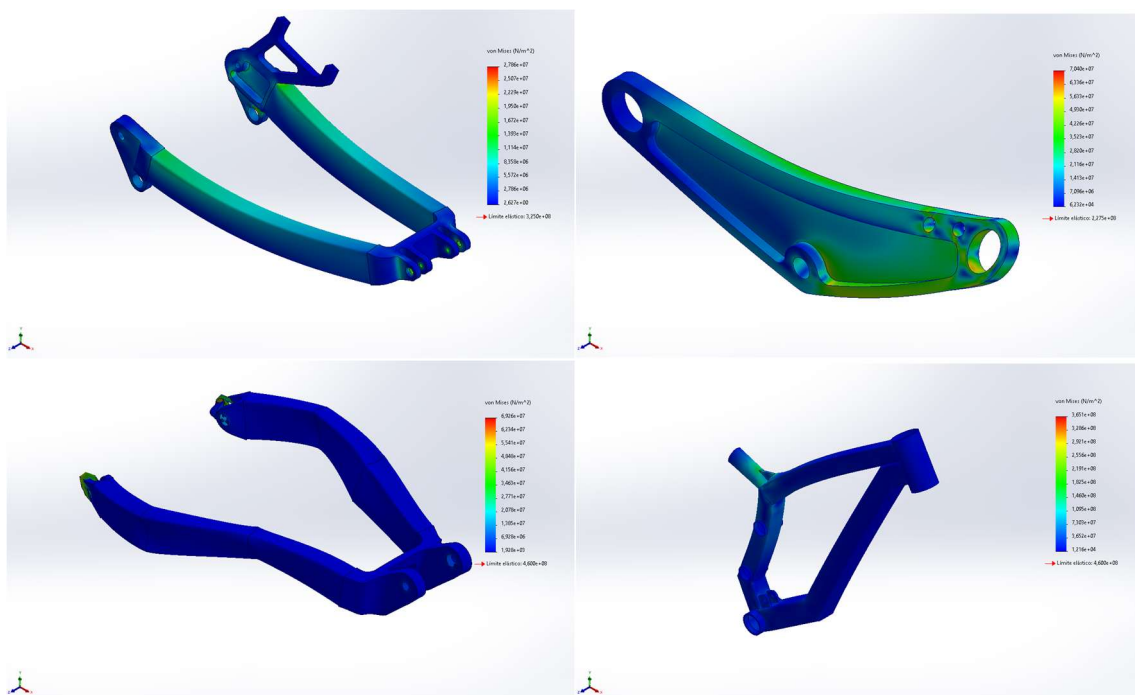


5.2.4. Component's individual analysys:

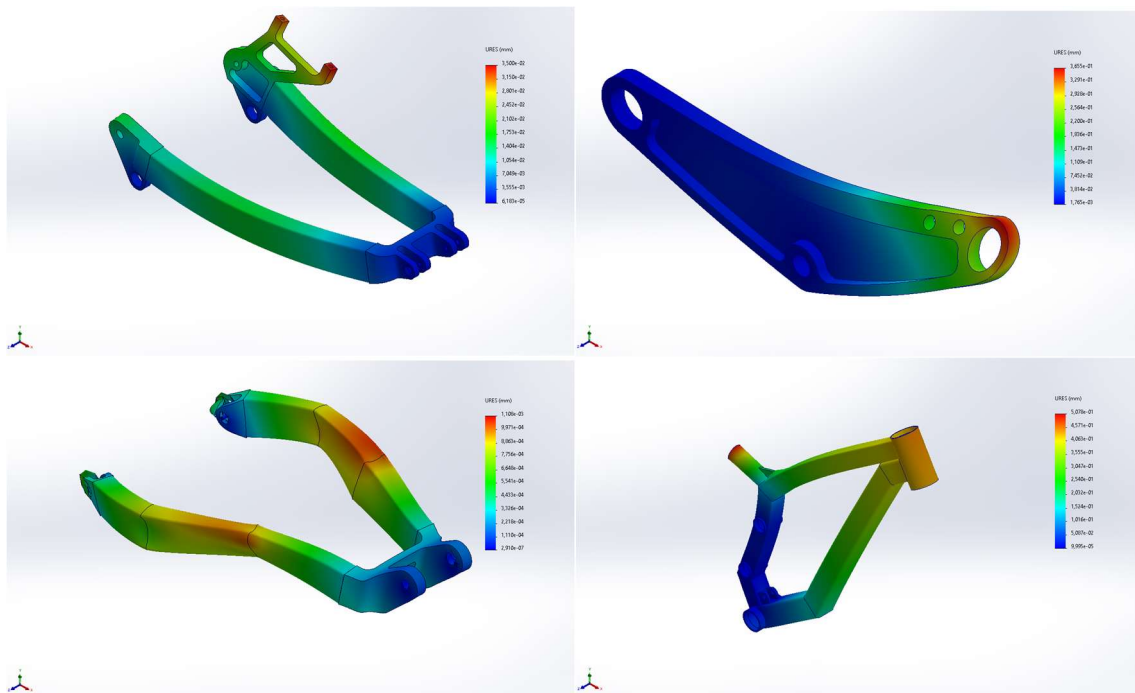
5.2.4.1. Configuration



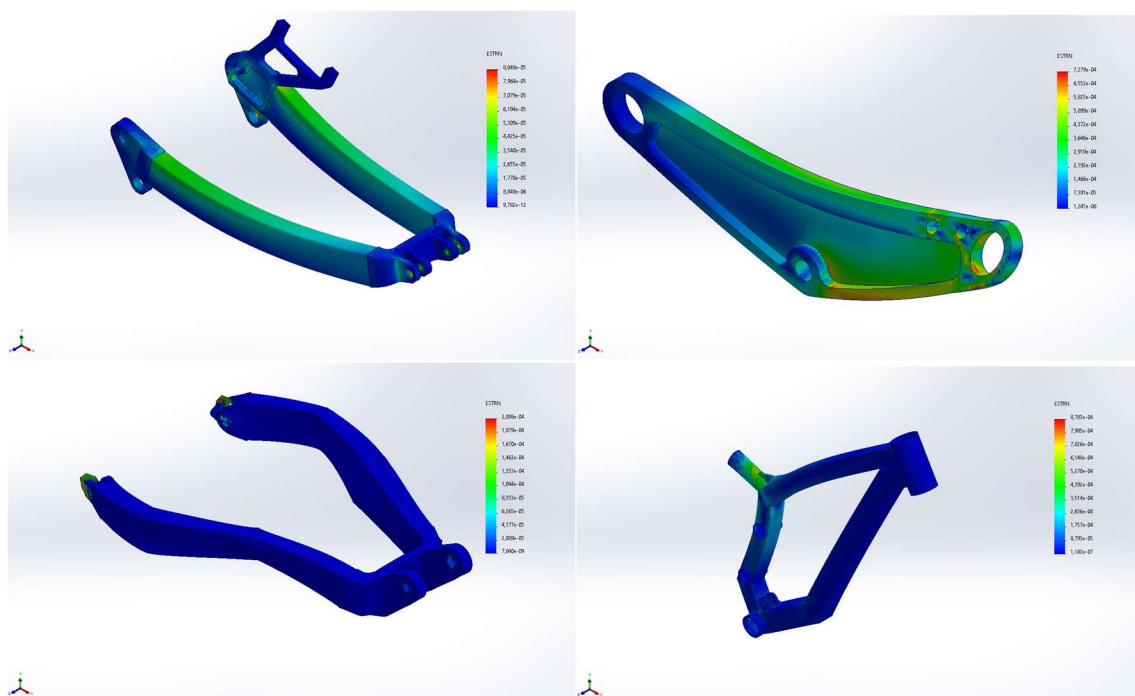
5.2.4.2. Stress analysys:



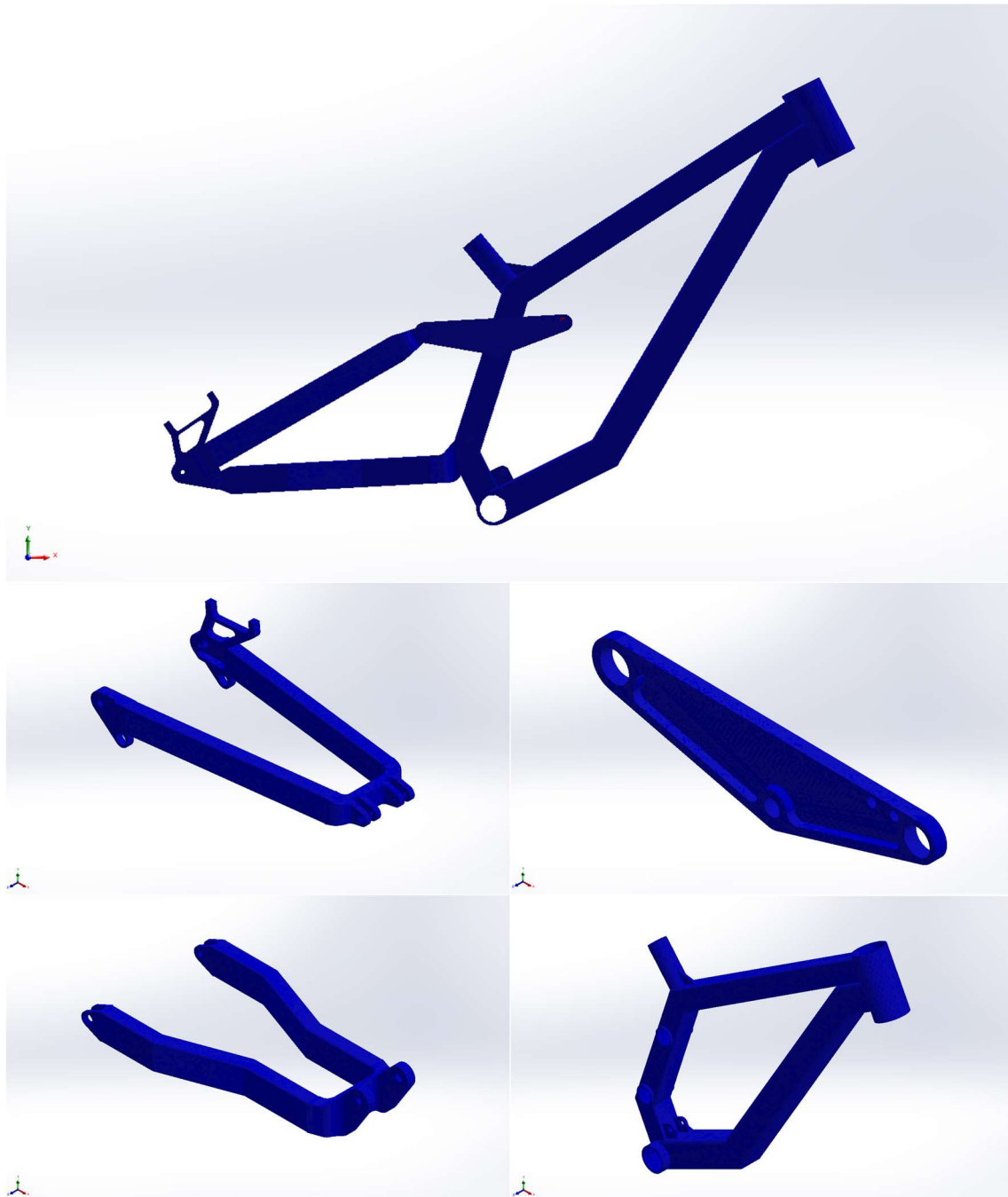
5.2.4.3. Displacements:



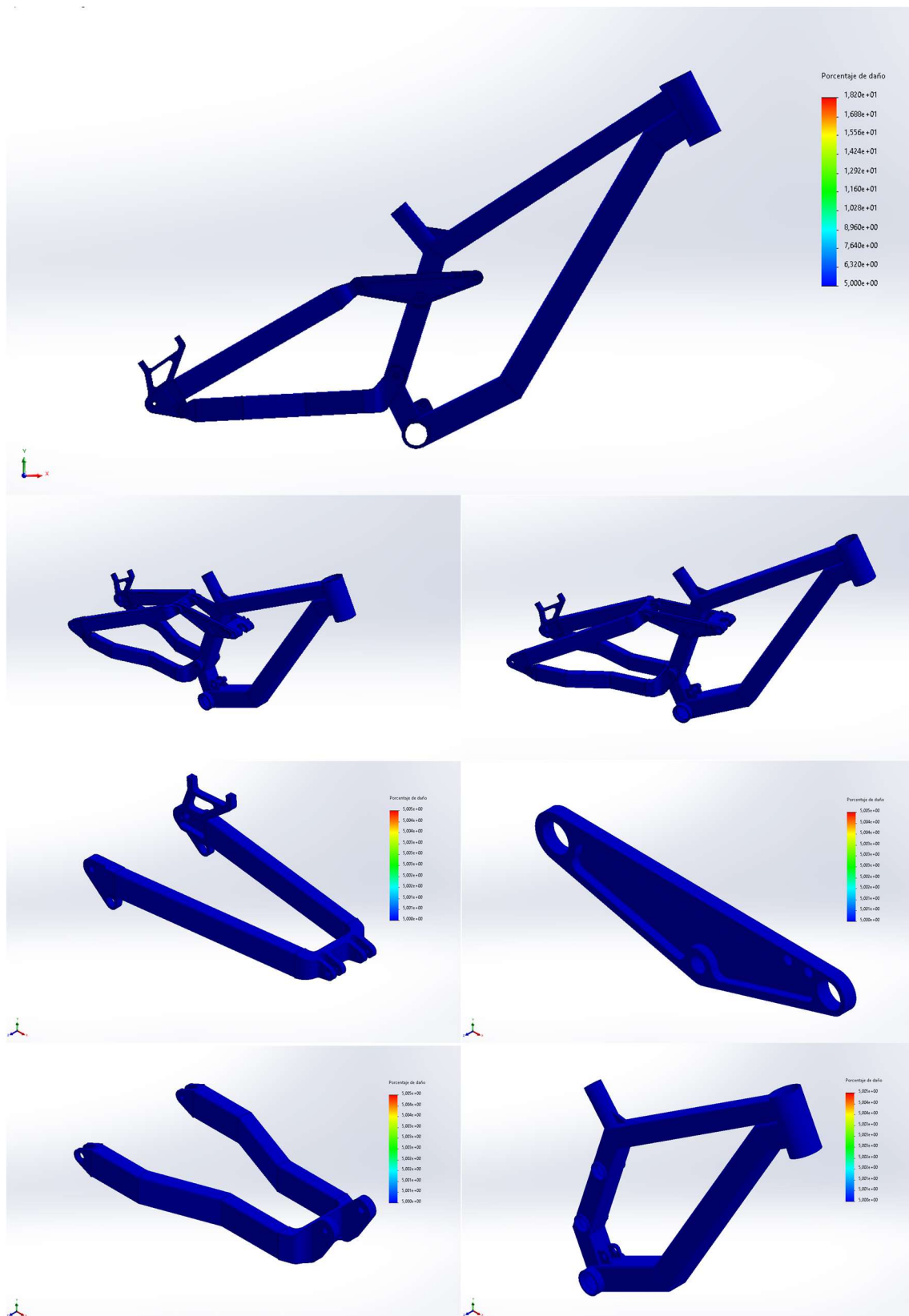
5.2.4.4. Deformations:



5.2.5. Fatigue verification on static analysis:



5.2.6. Fatigue damage percentage:



ANNEX VI: CALCULUS SHEET

[illegible]

F1xt	603,738354
F1yt	-22,0721126
F1xb	-299832,619
F1yb	0
1Fxt	0
1Fyt	0
1Fxb	0
1Fyb	0
12x	0
12y	-299832,619
14x	0
14y	0
15x	0
15y	0
21x	0
21y	0
23x	0
23y	0
32x	-503,738354
32y	22,0721126
34x	-8162,54255
34y	0
41x	0
41y	0
43x	0
43y	0
45x	0
45y	0

Points	x	y
BB	0	0
HT	440	608,47
FW	782,61	20
RW	-446,36	64,93
1F	492,21	506,01
1.2	-33,64	100
1.4	8,07	231,17
1S	13,42	51,43
2.3	-397,11	51,41
3.4	-96,25	259,4
4S	103,64	260,27
SD	-261,3269024	576,01111
P	123,7436867	-123,7436867

Loads	x	y
FW	-603,738354	22,0721126
RW	603,738354	-22,0721126
BB	0	0
HT	0	0
SD	0	0
P	0	0

$$m \cdot g \cdot h = \frac{1}{2} \cdot m \cdot v^2$$

$$v = \sqrt{2 \cdot g \cdot h}$$

$F = m \cdot a$	

t_m	0,1
f_c

Results	
0.36	Fixt -2311.352744
	Fixt 856.2581138
	Fixb 2915.091098
	Fixb -22.07211622
	1Fxt 2311.352744
	1Fxt -856.2581138
	1Fyb 2915.091098
	1Fyb -22.07211622
	12x 836.709506
	12y 111.8543894
	14x -339.9227928
	14y -381.496671
	15x 106.9516407
	15y 1103.828283
	21x 232.9711521
	21y -111.8543894
	23x 836.709506
	23y 111.8543894
	32x -836.709506
	32y -111.8543894
	34x 232.9711521
	34y 139.926502
	41x 339.9227928
	41y -381.496671
	43x -232.9711521
	43y -139.926502
	45x -106.9516407
	45y -247.70169

Rotation						
Chainsatay	Angle:		0,02102554			
x	364,61	0,99977897	-0,02102399	12x'	-834,172943	23x'
y	40,96	0,02102399	0,99977897	12y'	-129,420642	23y'

Rear bar	Angle:	0.50702958							
x	364	0.87419074	-0.48558268	32x'	-677,129152	34x'	138,628835	RWx'	RWy'
y	35,73	0.48558268	0.87419074	32y'	-504,073719	34y'	230,204066	517,064646	-312,460126

Rocker link	Angle:	0,00430927						
x	104,2	0,99999072	-0,00430925	43x'	-232,391866	41x'	338,275671	45x'
y	-28,68	0,00430925	0,99999072	43y'	-134,92919	41y'	382,957942	45y'

FHTx	FHTy	1fx	1fy	HTfx	HTy	1fx	2fy	12x	12y	14x	14y	15x	15y	21x	21y	23x	23y	32x	32y	34x	34y	41x	41y	43x	43y	45x	45y
1	0	0	1	0	0	0	0	0	0	0	0	0	0	0	0	0	0	0	0	0	0	0	0	0	0	0	0
0	0	0	0	1	0	0	0	0	0	0	0	0	0	0	0	0	0	0	0	0	0	0	0	0	0	0	0
0	0	-102.46	52.21	0	0	0	0	0	0	0	0	0	0	0	0	0	0	0	0	0	0	0	0	0	0	0	0
1	0	0	0	1	0	0	0	0	0	0	0	0	0	0	0	0	0	0	0	0	0	0	0	0	0	0	0
0	1	0	0	0	1	0	0	0	0	0	0	0	0	0	0	0	0	0	0	0	0	0	0	0	0	0	0
0	0	0	1	0	0	1	0	0	0	0	0	0	0	0	0	0	0	0	0	0	0	0	0	0	0	0	0
0	0	0	0	1	0	0	1	0	0	0	0	0	0	0	0	0	0	0	0	0	0	0	0	0	0	0	0
0	0	0	0	0	1	0	1	0	1	0	1	0	1	0	0	0	0	0	0	0	0	0	0	0	0	0	0
0	0	0	0	0	0	1	0	1	0	1	0	1	0	0	0	0	0	0	0	0	0	0	0	0	0	0	0
0	0	0	0	-608.47	440	-506.01	492.21	-100	-33.64	-231.17	8.07	-51.43	13.42	0	0	0	0	0	0	0	0	0	0	0	0	0	0
0	0	0	0	0	0	0	0	0	1	0	0	0	0	1	0	0	0	0	0	0	0	0	0	0	0	0	0
0	0	0	0	0	0	0	0	0	1	0	0	0	0	0	0	1	0	0	0	0	0	0	0	0	0	0	0
0	0	0	0	0	0	0	0	0	0	0	0	0	0	0	1	0	1	0	0	0	0	0	0	0	0	0	0
0	0	0	0	0	0	0	0	0	0	0	0	0	0	0	0	1	0	1	0	0	0	0	0	0	0	0	0
0	0	0	0	0	0	0	0	0	0	0	0	0	0	0	0	0	1	0	0	0	0	0	0	0	0	0	0
0	0	0	0	0	0	0	0	0	0	0	0	0	0	-48.59	363.47	0	1	0	0	0	0	0	0	0	0	0	0
0	0	0	0	0	0	0	0	0	0	0	0	0	0	0	0	1	0	0	1	0	0	0	0	0	0	0	0
0	0	0	0	0	0	0	0	0	0	0	0	0	0	0	0	0	1	0	0	1	0	0	0	0	0	0	0
0	0	0	0	0	0	0	0	0	0	0	0	0	0	0	0	0	0	1	0	1	0	0	0	0	0	0	0
0	0	0	0	0	0	0	0	0	0	0	0	0	0	0	0	0	0	0	0	1	0	0	0	0	0	0	0
0	0	0	0	0	0	0	0	0	0	0	0	0	0	0	0	0	0	0	0	0	1	0	0	0	0	0	0
0	0	0	0	0	0	0	0	0	0	0	0	0	0	0	0	0	0	0	0	0	0	1	0	0	0	0	0
0	0	0	0	0	0	0	0	0	0	0	0	0	0	0	0	0	0	0	0	0	0	0	1	0	0	0	0
0	0	0	0	0	0	0	0	0	0	0	0	0	0	0	0	0	0	0	0	0	0	0	0	1	0	0	0
0	0	0	0	0	0	0	0	0	0	0	0	0	0	0	0	0	0	0	0	0	0	0	0	0	1	0	0
0	0	0	0	0	0	0	0	0	0	0	0	0	0	0	0	0	0	0	0	0	0	0	0	0	0	1	0
0	0	0	0	0	0	0	0	0	0	0	0	0	0	0	0	0	0	0	0	0	0	0	0	0	0	0	1
0	0	0	0	0	0	0	0	0	0	0	0	0	0	0	0	0	0	0	0	0	0	0	0	0	0	0	1
0	0	0	0	0	0	0	0	0	0	0	0	0	0	0	0	0	0	0	0	0	0	0	0	0	0	0	1
0	0	0	0	0	0	0	0	0	0	0	0	0	0	0	0	0	0	0	0	0	0	0	0	0	0	0	1
0	0	0	0	0	0	0	0	0	0	0	0	0	0	0	0	0	0	0	0	0	0	0	0	0	0	0	1
0	0	0	0	0	0	0	0	0	0	0	0	0	0	0	0	0	0	0	0	0	0	0	0	0	0	0	1
0	0	0	0	0	0	0	0	0	0	0	0	0	0	0	0	0	0	0	0	0	0	0	0	0	0	0	1
0	0	0	0	0	0	0	0	0	0	0	0	0	0	0	0	0	0	0	0	0	0	0	0	0	0	0	1
0	0	0	0	0	0	0	0	0	0	0	0	0	0	0	0	0	0	0	0	0	0	0	0	0	0	0	1
0	0	0	0	0	0	0	0	0	0	0	0	0	0	0	0	0	0	0	0	0	0	0	0	0	0	0	1
0	0	0	0	0	0	0	0	0	0	0	0	0	0	0	0	0	0	0	0	0	0	0	0	0	0	0	1
0	0	0	0	0	0	0	0	0	0	0	0	0	0	0	0	0	0	0	0	0	0	0	0	0	0	0	1
0	0	0	0	0	0	0	0	0	0	0	0	0	0	0	0	0	0	0	0	0	0	0	0	0	0	0	1
0	0	0	0	0	0	0	0	0	0	0	0	0	0	0	0	0	0	0	0	0	0	0	0	0	0	0	1
0	0	0	0	0	0	0	0	0	0	0	0	0	0	0	0	0	0	0	0	0	0	0	0	0	0	0	1
0	0	0	0	0	0	0	0	0	0	0	0	0	0	0	0	0	0	0	0	0	0	0	0	0	0	0	1
0	0	0	0	0	0	0	0	0	0	0	0	0	0	0	0	0	0	0	0	0	0	0	0	0	0	0	1
0	0	0	0	0	0	0	0	0	0	0	0	0	0	0	0	0	0	0	0	0	0	0	0	0	0	0	1
0	0	0	0	0	0	0	0	0	0	0	0	0	0	0	0	0	0	0	0	0	0	0	0	0	0	0	1
0	0	0	0	0	0	0	0	0	0	0	0	0	0	0	0	0	0	0	0	0	0	0	0	0	0	0	1
0	0	0	0	0	0	0	0	0	0	0	0	0	0	0	0	0	0	0	0	0	0	0	0	0	0	0	1
0	0	0	0	0	0	0	0	0	0	0	0	0	0	0	0	0	0	0	0	0	0	0	0	0	0	0	1
0	0	0	0	0	0	0	0	0	0	0	0	0	0	0	0	0	0	0	0	0	0	0	0	0	0	0	1
0	0	0	0	0	0	0	0	0	0	0	0	0	0	0	0	0	0	0	0	0	0	0	0	0	0	0	1
0	0	0	0	0	0	0	0	0	0	0	0	0	0	0	0	0	0	0	0	0	0	0	0	0	0	0	1
0	0	0	0	0	0	0	0	0	0	0	0	0	0	0	0	0	0	0	0	0	0	0	0	0	0	0	1
0	0	0	0	0	0	0	0	0	0	0	0	0	0	0	0	0	0	0	0	0	0	0	0	0	0	0	1
0	0	0	0	0	0	0	0	0	0	0	0	0	0	0	0	0	0	0	0	0	0	0	0	0	0	0	1
0	0	0	0	0	0	0	0	0	0	0	0	0	0	0	0	0	0	0	0	0	0	0	0	0	0	0	1
0	0	0	0	0	0	0	0	0	0	0	0	0	0	0	0	0	0	0	0	0	0	0	0	0	0	0	1
0	0	0	0	0	0	0	0	0	0	0	0	0	0	0	0	0	0	0	0	0	0	0	0	0	0	0	1
0	0	0	0	0	0	0	0	0	0	0	0	0	0	0	0	0	0	0	0	0	0	0	0	0	0	0	1
0	0	0	0	0	0	0	0	0	0	0	0	0	0	0	0	0	0	0	0	0	0	0	0	0	0	0	1
0	0	0	0	0	0	0	0	0	0	0	0	0	0	0	0	0	0	0	0	0	0	0	0	0	0	0	1
0	0	0	0	0	0	0	0	0	0	0	0	0	0	0	0	0	0	0	0	0	0	0	0	0	0	0	1
0	0	0	0	0	0	0	0	0	0	0	0	0	0	0	0	0	0	0	0	0	0	0	0	0	0	0	1
0	0	0	0	0	0	0	0	0	0	0	0	0	0	0	0	0	0	0	0	0	0	0	0	0	0	0	1
0	0	0	0	0	0	0	0	0	0	0	0	0	0	0	0	0	0	0	0	0	0	0	0	0	0	0	1
0	0	0	0	0	0	0	0	0	0	0	0	0	0	0	0	0	0	0	0	0	0	0	0	0	0	0	1
0	0	0	0	0	0	0	0	0	0	0	0	0	0	0	0	0	0	0	0	0	0	0	0	0	0	0	1
0	0	0	0	0	0	0	0	0	0	0	0	0	0	0	0	0	0	0	0	0	0	0	0	0	0	0	1
0	0	0	0	0	0	0	0	0	0	0	0	0	0	0	0	0	0	0	0	0	0	0	0	0	0	0	1
0	0	0	0	0	0	0	0	0	0	0	0	0	0	0	0	0	0	0	0	0	0	0	0	0	0	0	1
0	0	0	0	0	0	0	0	0	0	0	0	0	0	0	0	0	0	0	0	0	0	0	0	0	0	0	1
0	0	0	0	0	0	0	0	0	0	0																	

FHTx		0
FHTy	-461,038373	0
F1x	-133885,544	0
F1y		0
HTFx		0
HTy		0
1Fx		0
1Fy		0
12x	1231,26176	0
12y	-116869,215	0
14x		0
14y		0
15x		0
15y		0
21x		0
21y		0
23x		0
23y		0
32x	-770,22339	0
32y		0
34x		0
34y		0
41x		0
41y		0
43x		0
43y		0
45x		0
45y		0

Points	x	y
BB	0	0
HT	440	608,47
FW	782,61	20
RW	-446,36	64,93
1F	492,21	506,01
1.2	-33,64	100
1.4	8,07	231,17
15	13,42	51,43
2.3	-397,11	51,41
3.4	-96,25	259,4
45	103,64	260,27
SD	-261,3269024	576,011111
DP	123,7343687	-123,7343687

Loads	x	y
FW	0	461,038373
RW	0	770,22339
BB	0	-738,104109
HT	0	-208,022379
SD	0	-285,135275
P	0	0

$m \cdot g \cdot h = 1/2 \cdot m \cdot v^2$	
$v = \text{SQRT}(2 \cdot g \cdot h)$	
$F = m \cdot a$	$a = v / \text{timepact}$
$\text{timepact} =$	0,1
$a = v / t$	24,4948974
$a = v / t$	0
$a = v / t$	14,7620822
$a = v / t$	20,8022379
$a = v / t$	9,50450917

Results		
0.3	FHTx	-1071.781476
0	FHTy	-168.508561
5954	F1x	1071.781476
6655	F1y	-461.038373
6785	F1x	1071.781476
	HTy	168.508561
	1Fy	-1071.781476
	12x	-461.038373
	12y	-1381.233239
	14x	-168.648315
	14y	202.664994
	15x	-721.4317551
	15y	-1838.466039
	21x	1381.233239
	21y	-168.648315
	23x	-1381.233239
	23y	-168.648315
	32x	1381.233239
	32y	-168.648315
	34x	-1381.233239
	41x	-954.8717054
	41y	202.664994
	43x	-2624.831889
	43y	1381.233239
	49x	-954.8717054
	49y	721.4317551
	45x	1660.90183

Rotation		Angle:					
Chainsatay							
x	364,61	0,99977897	-0,02102399	12x'	1377,0459	23x'	-1377,0459
y	40,96	0,02102399	0,99977897	12y'	213,646542	23y'	-213,646542

Rear bar	Angle:	0.50702958							
x	364	0.87419074	-0.48558268	32x'	1117.79929	34x'	-743.792149	RWx'	RWy'
v	35.73	0.48558268	0.87419074	32v'	832.120789	34v'	-1505.44295	374.00714	673.322159

Rocker link	Angle:	0,00430927							
x	104,2	0,99999072	-0,00430925	43x'	1377,10563	41x'	-2091,33441	45x'	714,228775
y	-28,68	0,00430925	0,99999072	43y'	960,814923	41y'	-2633,86843	45y'	1673,05351

FHTx	600
FHTy	-21,935,441.9
Flx	-297976,052
Fly	0
HFTx	0
HTy	0
1Fx	0
1Fy	0
12x	0
12y	-297976,052
14x	0
15x	0
15y	0
21x	0
21y	0
23x	0
23y	-600
32x	21,935,441.9
34x	-8112
41x	0
41y	0
43x	0
43y	0
45x	0
45y	0

Results	
FHTx	-2297,040825
FHTy	850,956155
FHTx	2897,040825
FHTy	-21,93544187
FHTx	2297,040825
FHTy	-850,956155
1fx	-2897,040825
1fy	21,93544187
12x	831,5285924
12y	111,1617859
14x	-337,8179875
15x	-379,1344398
15y	106,2893951
21x	1096,993637
21y	-831,5285924
23x	-133,072277
23y	831,5285924
32x	111,1617859
32y	-831,5285924
34x	-111,1617859
34y	231,5285924
41x	337,8179875
41y	379,1344398
43x	-231,5285924
43y	-133,072277
45x	-106,2893951
45y	-246,0372121

Rocker link	Angle:	0,00430927							
x	104,2	0,99999072	-0,00430925	43x'	-230,952893	41x'	336,181065	45x'	-105,228172
y	-28,68	0,00430925	0,99999072	43y'	-134,093707	41y'	380,586663	45y'	-246,492956

FHTx	0
FHTy	-180,671389
Flx	-52466,9714
Fly	0
HFTx	0
HTy	0
1Fx	0
1Fy	0
12x	1200
12y	-366059,254
14x	0
14y	0
15x	0
15y	0
21x	0
21y	0
23x	0
23y	0
32x	-1019,32861
32y	0
34x	0
34y	0
41x	0
41y	0
43x	0
43y	0
45x	0
45y	0

Feature	Value	Significance
FHTx	0	
FHTy	-551,902524	
F1x	-160272,493	
F1y	0	
HTTx	0	
HTTy	0	
1Fx	0	
1Fy	0	
12x	0	
12y	-13050,4422	
14x	0	
14y	0	
15x	0	
15y	0	
21x	0	
21y	0	
23x	0	
23y	0	
32x	-637,83131	
32y	0	
34x	0	
34y	0	
41x	0	
43x	0	
43y	0	
45x	0	
45y	0	

Loads	x	y
FW	0	551,902524
RW	0	637,83131
BB	0	0
HT	0	0
SD	0	0
P	0	-1189,73383

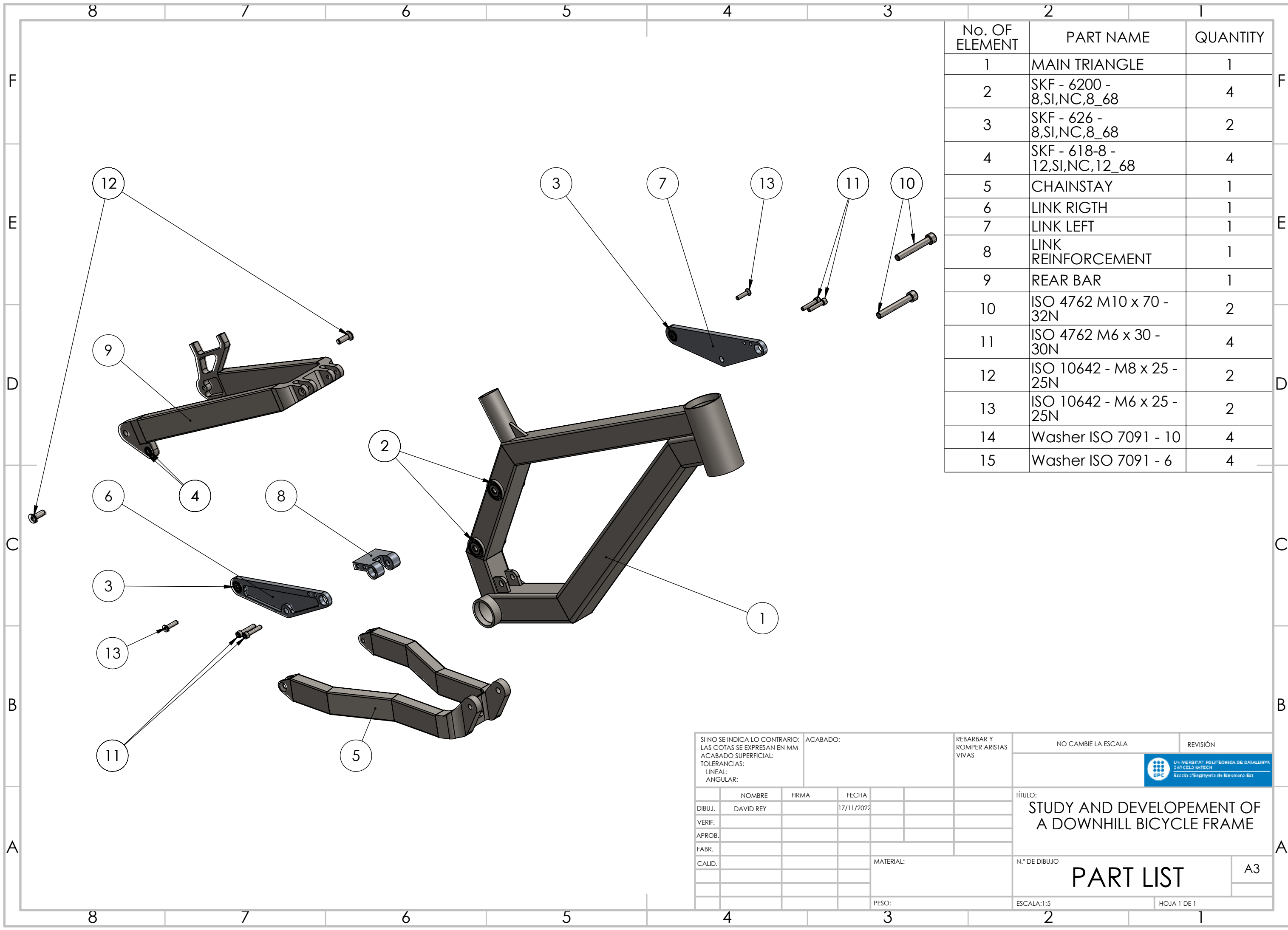
Results	
PHTx	-1283.014466
FHTx	-171.9553148
FTx	1283.014466
FTy	-551.9025239
HTFx	1283.014466
1Ftx	-171.9553148
1Fy	551.9025239
12x	-152.909504
12y	1741.242325
14x	1723.655049
15x	-597.4263661
21x	-2844.603384
21y	1143.815959
23x	-152.909504
23y	-1143.815959
32x	-152.909504
32y	1143.815959
34x	-152.909504
34y	-1143.815959
41x	-1741.242325
41y	-2173.655049
43x	1143.815959
43y	790.7408138
45x	597.4263661
45y	1382.914235

Rotation	Angle: 0,02102554					
Chainsatay						
x	364,61	0,99977897	-0,02102399	12x'	1140,34837	23x'
y	40,96	0,02102399	0,99977897	12y'	176,923287	23y'
						-1140,34837
						-176,923287


Rear bar	Angle:	0.50702958							
x	364	0.87419074	-0.48558268	32x'	925,663118	34x'	-615,943279	RWx'	RWy'
y	35,73	0.48558268	0.87419074	32y'	689,089295	34y'	-1246,67552	309,719839	557,586228

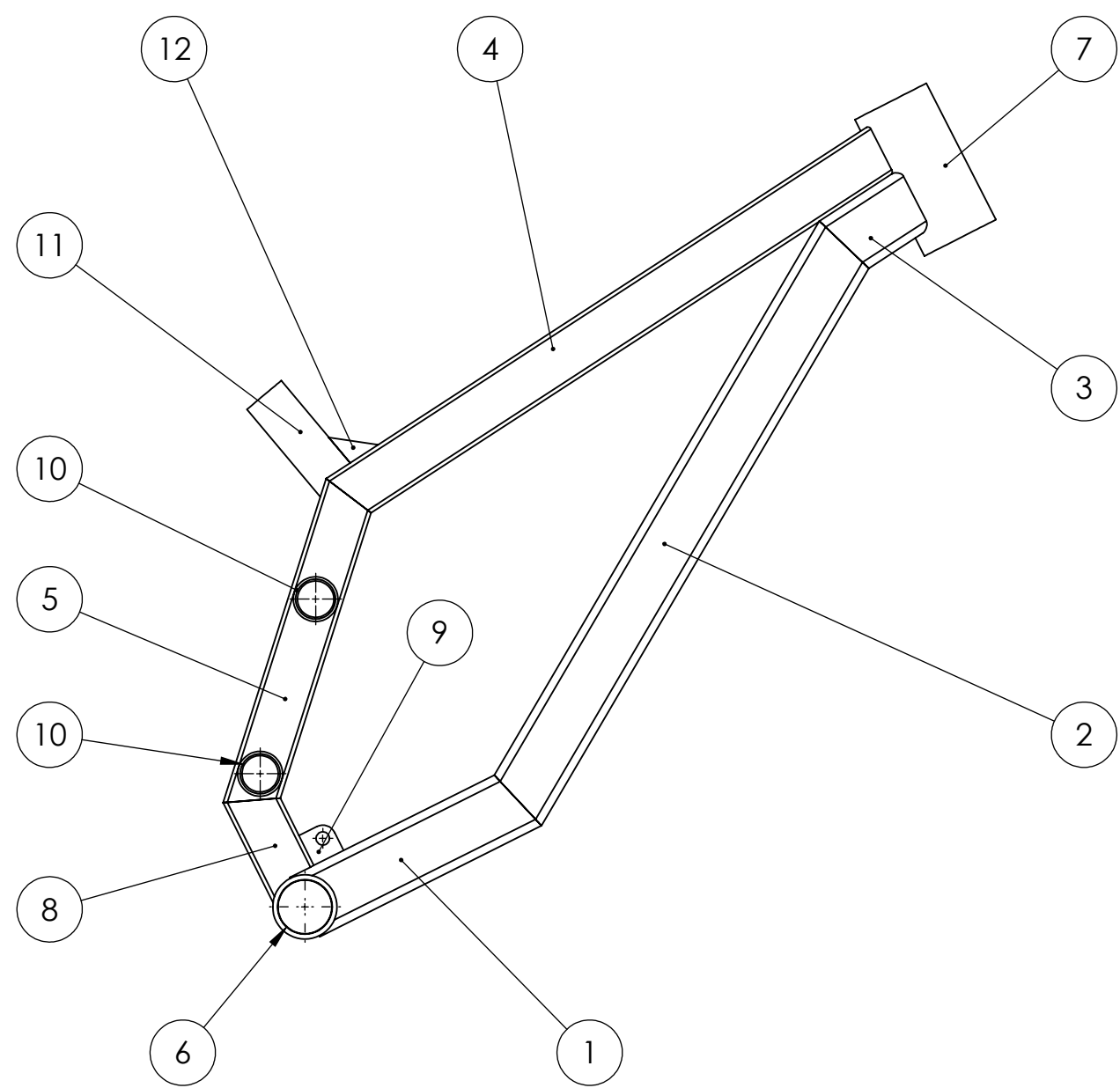
Rocker link	Angle:	0,00430927							
x	104,2	0,99999072	-0,00430925	43x'	1140,39784	41x'	-1731,85933	45x'	591,461491
y	-28,68	0,00430925	0,99999072	43y'	795,662465	41y'	-2181,13832	45y'	1385,47586

ANNEX VII: DIMENSIONAL DRAWINGS




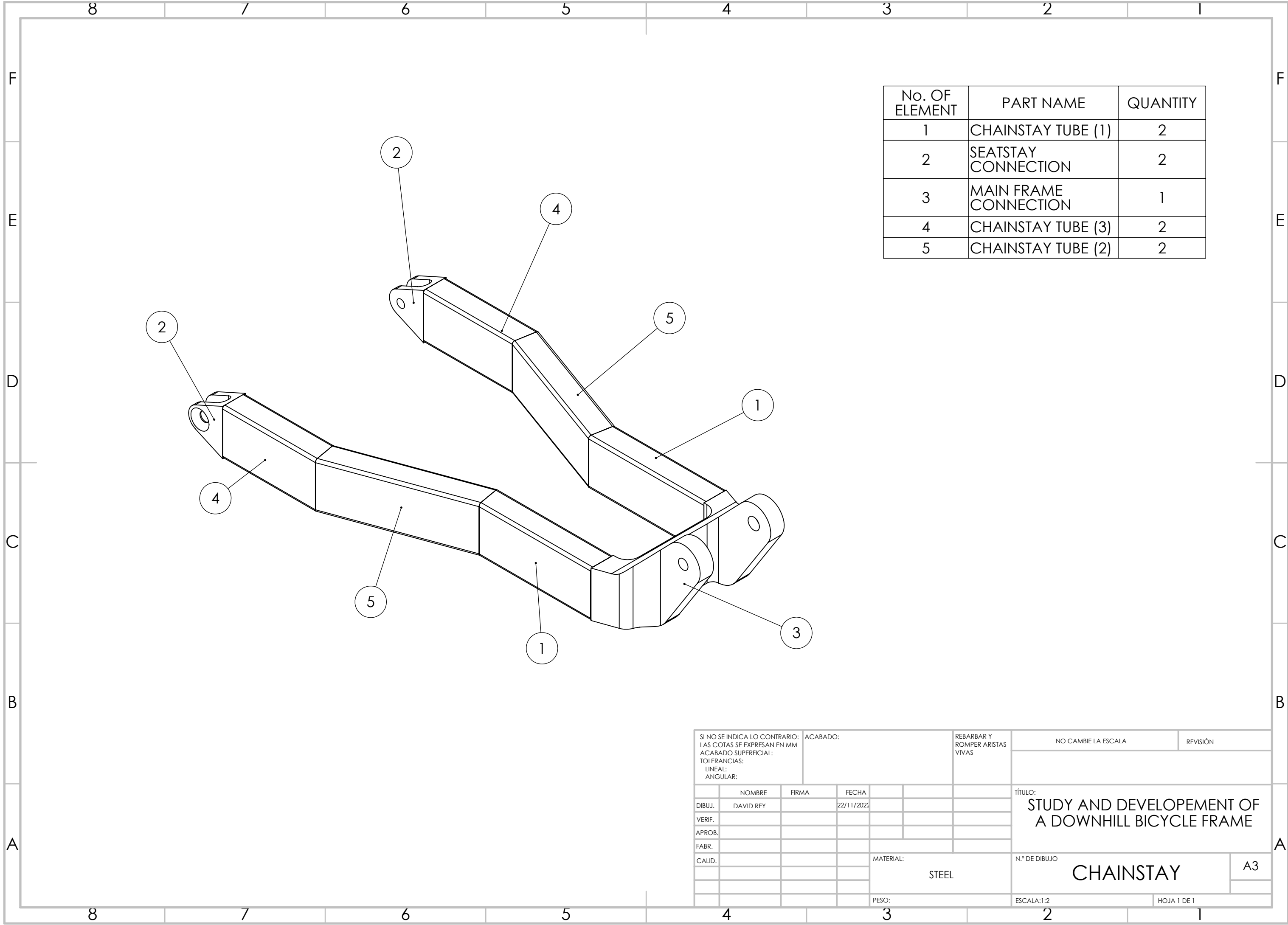
No. OF ELEMENT	PART NAME	QUANTITY
1	MAIN TRIANGLE	1
2	SKF - 6200 - 8,SI,NC,8_68	4
3	SKF - 626 - 8,SI,NC,8_68	2
4	SKF - 618-8 - 12,SI,NC,12_68	4
5	CHAINSTAY	1
6	LINK RIGTH	1
7	LINK LEFT	1
8	LINK REINFORCEMENT	1
9	REAR BAR	1
10	ISO 4762 M10 x 70 - 32N	2
11	ISO 4762 M6 x 30 - 30N	4
12	ISO 10642 - M8 x 25 - 25N	2
13	ISO 10642 - M6 x 25 - 25N	2
14	Washer ISO 7091 - 10	4
15	Washer ISO 7091 - 6	4

SI NO SE INDICA LO CONTRARIO: LAS COTAS SE EXPRESAN EN MM ACABADO SUPERFICIAL: TOLERANCIAS: LINEAL: ANGULAR:				ACABADO:		REBARBAR Y ROMPER ARISTAS VIVAS		NO CAMBIE LA ESCALA		REVISIÓN		
												
DIBUJ.				NOMBRE		FIRMA		FECHA		TÍTULO:		
VERIF.				DAVID REY				17/11/2022		STUDY AND DEVELOPEMENT OF A DOWNHILL BICYCLE FRAME		
APROB.												
FABR.												
CALID.												
								MATERIAL:		N.º DE DIBUJO		
										PART LIST		
								PESO:		ESCALA:1:5		
										HOJA 1 DE 1		



N.º DE ELEMENTO	N.º DE PIEZA	DESCRIPCIÓN	CANTIDAD
1	DOWN TUBE (3)	50 x 50 x 2	1
2	DOWN TUBE (2)	50 x 50 x 2	1
3	DOWN TUBE (1)	50 x 50 x 2	1
4	UPPER TUBE (1)	40 x 40 x 3.2	1
5	UPPER TUBE (2)	40 x 40 x 3.2	1
6	BOTTOM BRACKET	48.3 x 4.0	1
7	HEAD TUBE	60.3 x 3.2	1
8	UPPER TUBE (3)	40 x 40 x 3.2	1
9	SHOCK SUPPORT		2
10	LINK SUPPORT	33.7 x 3.2	2
11	SEAT TUBE	33.7 x 2.6	1
12	SEAT POST REINFORCEMENT		1

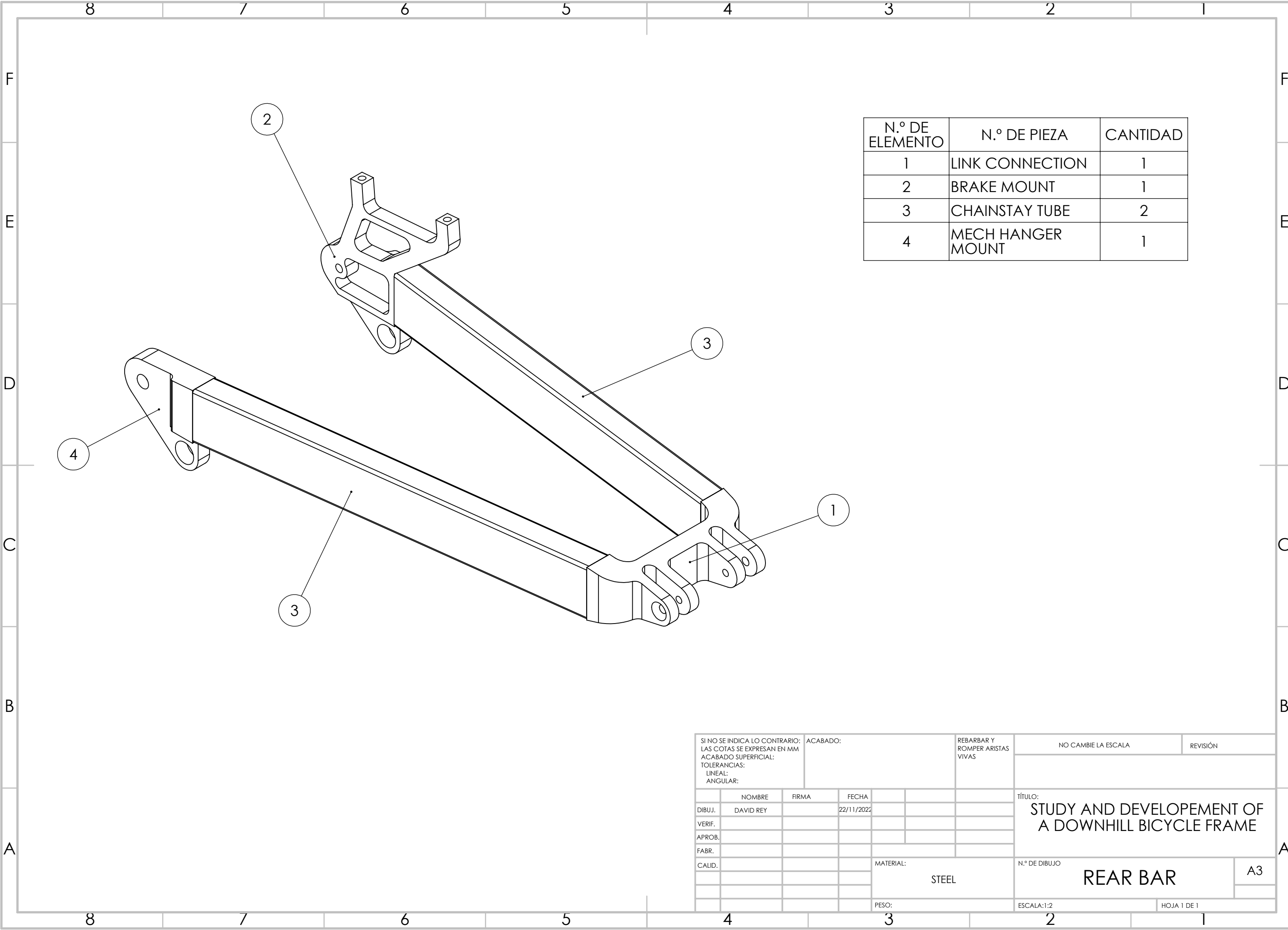
SI NO SE INDICA LO CONTRARIO: LAS COTAS SE EXPRESAN EN MM ACABADO SUPERFICIAL: TOLERANCIAS: LINEAL: ANGULAR:				ACABADO:		REBARBAR Y ROMPER ARISTAS VIVAS		NO CAMBIE LA ESCALA		REVISIÓN		
												
DIBUJ.				NOMBRE		FIRMA		FECHA		TÍTULO:		
VERIF.				DAVID REY				10/11/2022		STUDY AND DEVELOPEMENT OF A DOWNHILL BICYCLE FRAMEASSEMBLY		
APROB.										N.º DE DIBUJO		
FABR.										MAIN TRIANGLE		
CALID.										A3		
								MATERIAL:		ESCALA:1:5		
								STEEL		HOJA 1 DE 1		
								PESO:				



No. OF ELEMENT	PART NAME	QUANTITY
1	CHAINSTAY TUBE (1)	2
2	SEATSTAY CONNECTION	2
3	MAIN FRAME CONNECTION	1
4	CHAINSTAY TUBE (3)	2
5	CHAINSTAY TUBE (2)	2

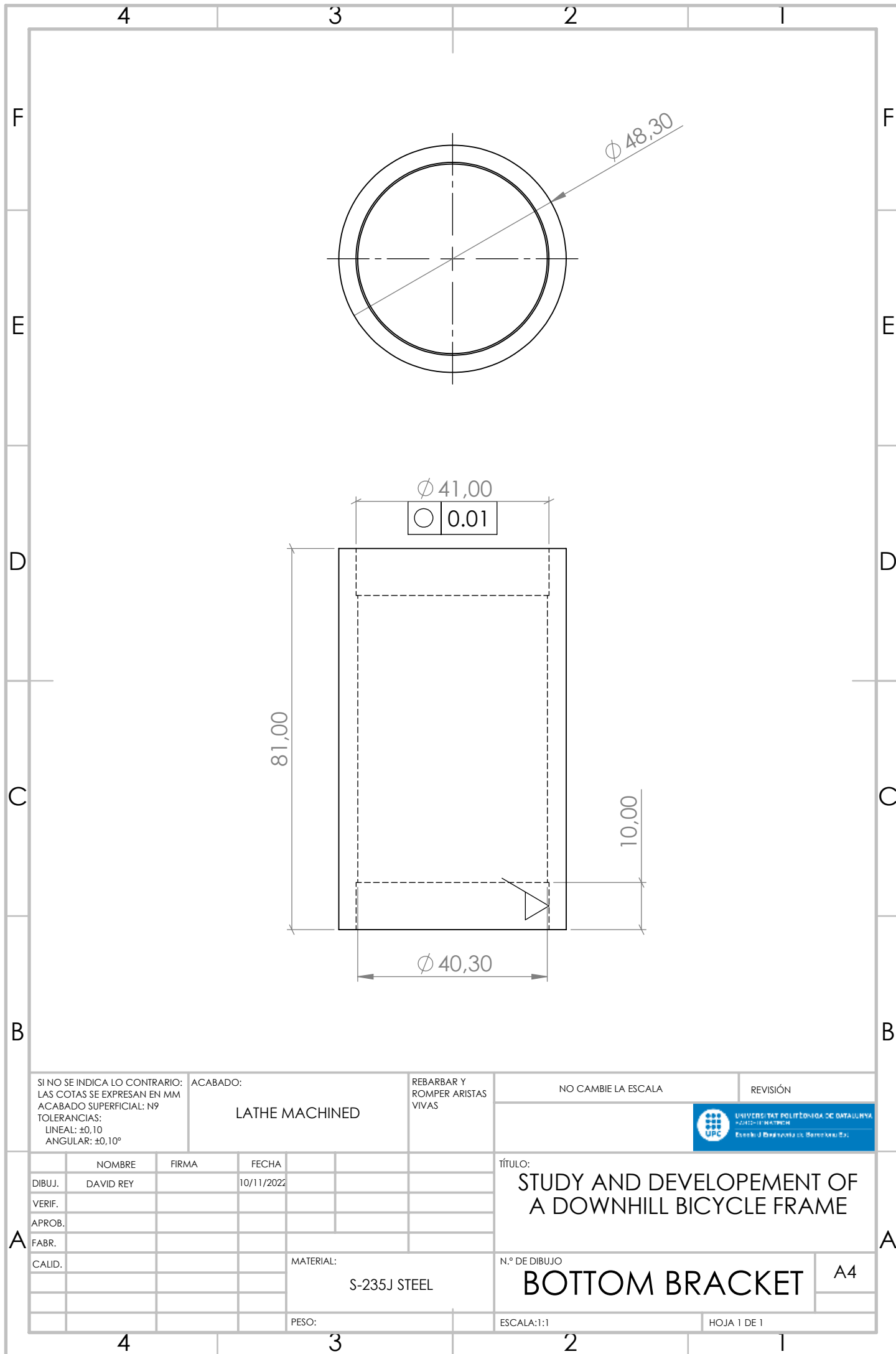
SI NO SE INDICA LO CONTRARIO: LAS COTAS SE EXPRESAN EN MM ACABADO SUPERFICIAL: TOLERANCIAS: LINEAL: ANGULAR:	ACABADO:	REBARBAR Y ROMPER ARISTAS VIVAS	NO CAMBIE LA ESCALA		REVISIÓN
	NOMBRE	FIRMA	FECHA	TÍTULO: STUDY AND DEVELOPEMENT OF A DOWNHILL BICYCLE FRAME	
DIBUJ.	DAVID REY		22/11/2022		
VERIF.					
APROB.					
FABR.					
CALID.				MATERIAL: STEEL	
				PESO:	ESCALA:1:2
					HOJA 1 DE 1

N.º DE DIBUJO
CHAINSTAY
A3



N.º DE ELEMENTO	N.º DE PIEZA	CANTIDAD
1	LINK CONNECTION	1
2	BRAKE MOUNT	1
3	CHAINSTAY TUBE	2
4	MECH HANGER MOUNT	1

SI NO SE INDICA LO CONTRARIO: LAS COTAS SE EXPRESAN EN MM ACABADO SUPERFICIAL: TOLERANCIAS: LINEAL: ANGULAR:				ACABADO:		REBARBAR Y ROMPER ARISTAS VIVAS		NO CAMBIE LA ESCALA		REVISIÓN	
		NOMBRE		FIRMA		FECHA					
DIBUJ.		DAVID REY				22/11/2022					
VERIF.											
APROB.											
FABR.											
CALID.											



SI NO SE INDICA LO CONTRARIO:
LAS COTAS SE EXPRESAN EN MM
ACABADO SUPERFICIAL: N9
TOLERANCIAS:
LINEAL: $\pm 0,10$
ANGULAR: $\pm 0,10^\circ$

ACABADO:

LATHE MACHINED

REBARBAR Y
ROMPER ARISTAS
VIVAS

NO CAMBIE LA ESCALA

REVISIÓN



UNIVERSITAT POLITÈCNICA DE CATALUNYA
BARCELONA
Escuela de Ingeniería de Diseño y Fabricación

	NOMBRE	FIRMA	FECHA		
DIBUJ.	DAVID REY		10/11/2022		
VERIF.					
APROB.					
FABR.					
CALID.					

MATERIAL:

S-235J STEEL

PESO:

TÍTULO:

STUDY AND DEVELOPEMENT OF
A DOWNHILL BICYCLE FRAME

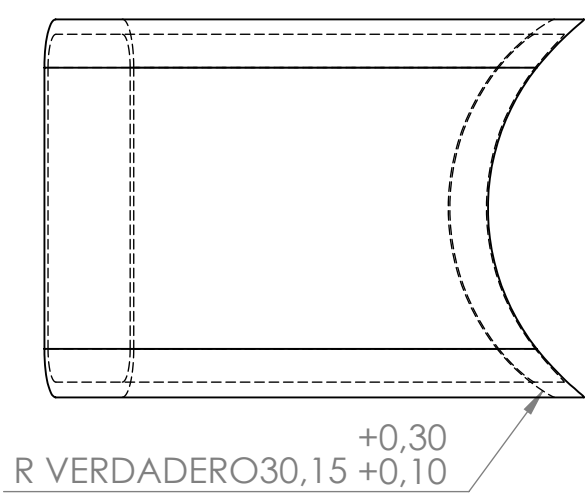
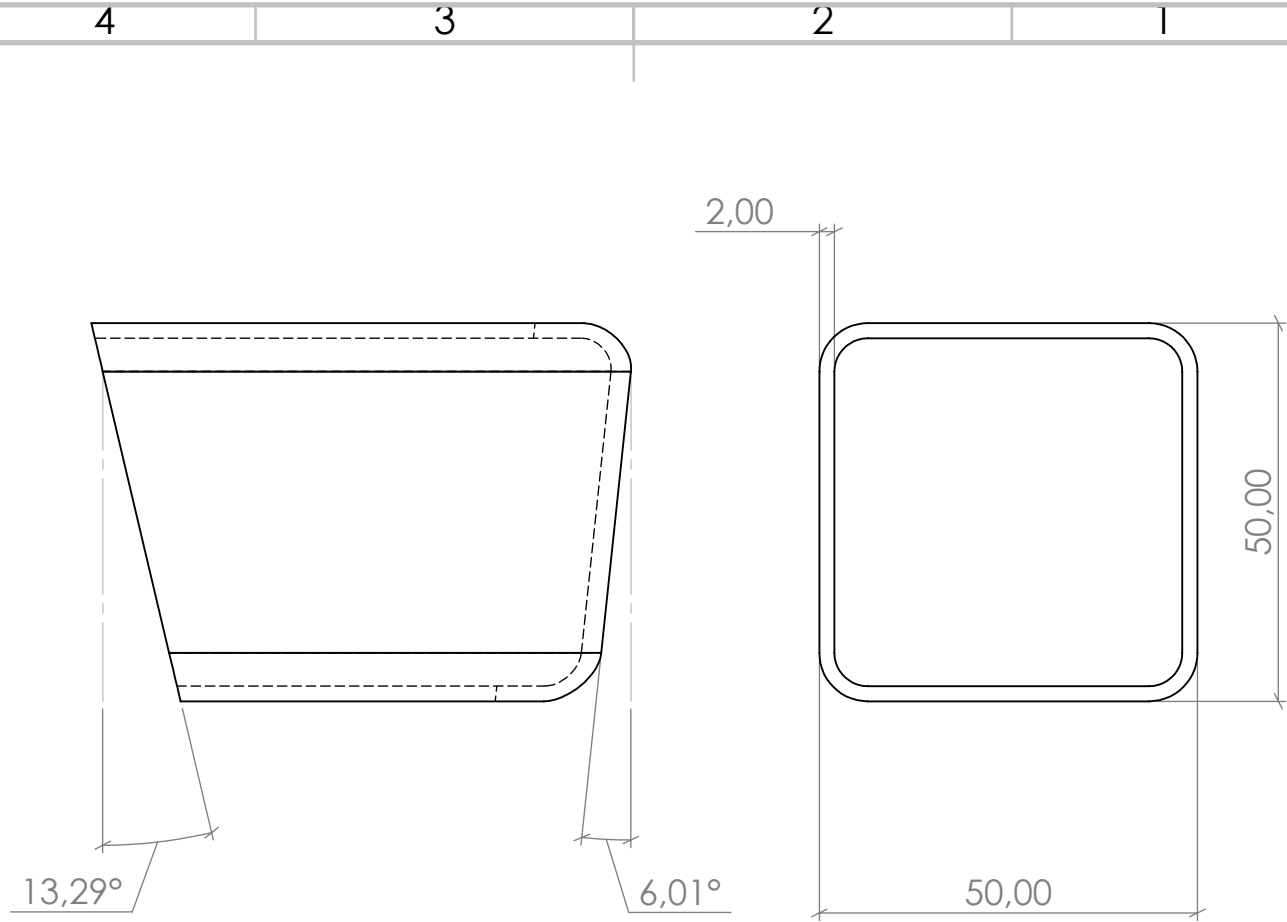
N.º DE DIBUJO


BOTTOM BRACKET

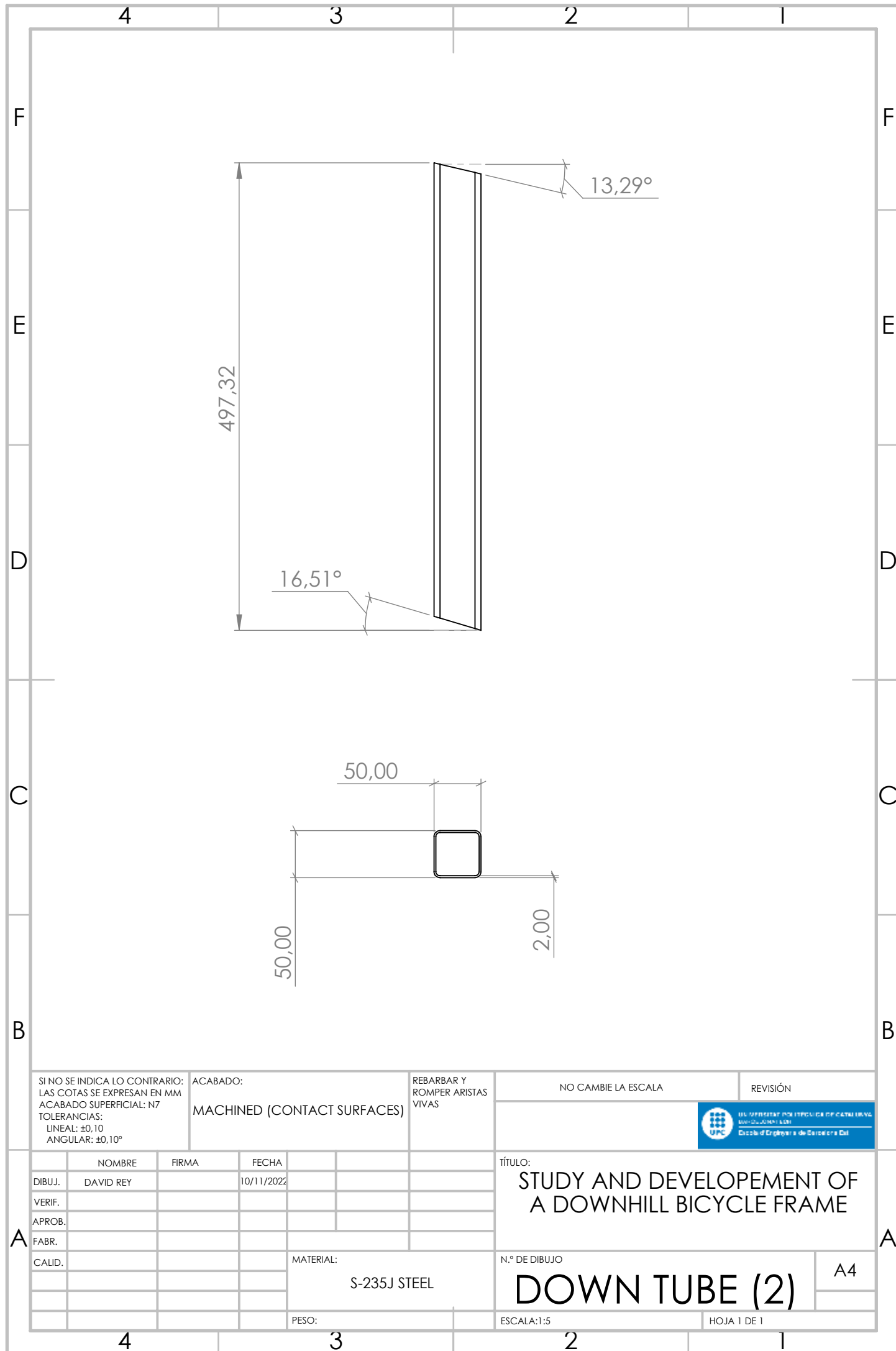
A4

ESCALA:1:1

HOJA 1 DE 1



SI NO SE INDICA LO CONTRARIO: LAS COTAS SE EXPRESAN EN MM ACABADO SUPERFICIAL: N7 TOLERANCIAS: LINEAL: ±0,10 ANGULAR: ±0,10°		ACABADO: MACHINED (CONTACT SURFACES)		REBARBAR Y ROMPER ARISTAS VIVAS		NO CAMBIE LA ESCALA		REVISIÓN	
								 UNIVERSITAT POLITÈCNICA DE CATALUNYA BARCELONATECH Escuela Ingeniería de Barcelona Esp	
NOMBRE		FIRMA		FECHA		TÍTULO:			
DIBUJ.		DAVID REY		10/11/2022		STUDY AND DEVELOPEMENT OF A DOWNHILL BICYCLE FRAME			
VERIF.									
APROB.									
FABR.									
CALID.									
						N.º DE DIBUJO			
						DOWN TUBE (1)			
						A4			
						ESCALA:1:1			
						HOJA 1 DE 1			



SI NO SE INDICA LO CONTRARIO:
LAS COTAS SE EXPRESAN EN MM
ACABADO SUPERFICIAL: N7
TOLERANCIAS:
LINEAL: $\pm 0,10$
ANGULAR: $\pm 0,10^\circ$

ACABADO:
MACHINED (CONTACT SURFACES)

REBARBAR Y
ROMPER ARISTAS
VIVAS

NO CAMBIE LA ESCALA

REVISIÓN



	NOMBRE	FIRMA	FECHA		
DIBUJ.	DAVID REY		10/11/2022		
VERIF.					
APROB.					
FABR.					
CALID.					
				MATERIAL:	
				S-235J STEEL	
				PESO:	

TÍTULO:
**STUDY AND DEVELOPEMENT OF
A DOWNHILL BICYCLE FRAME**

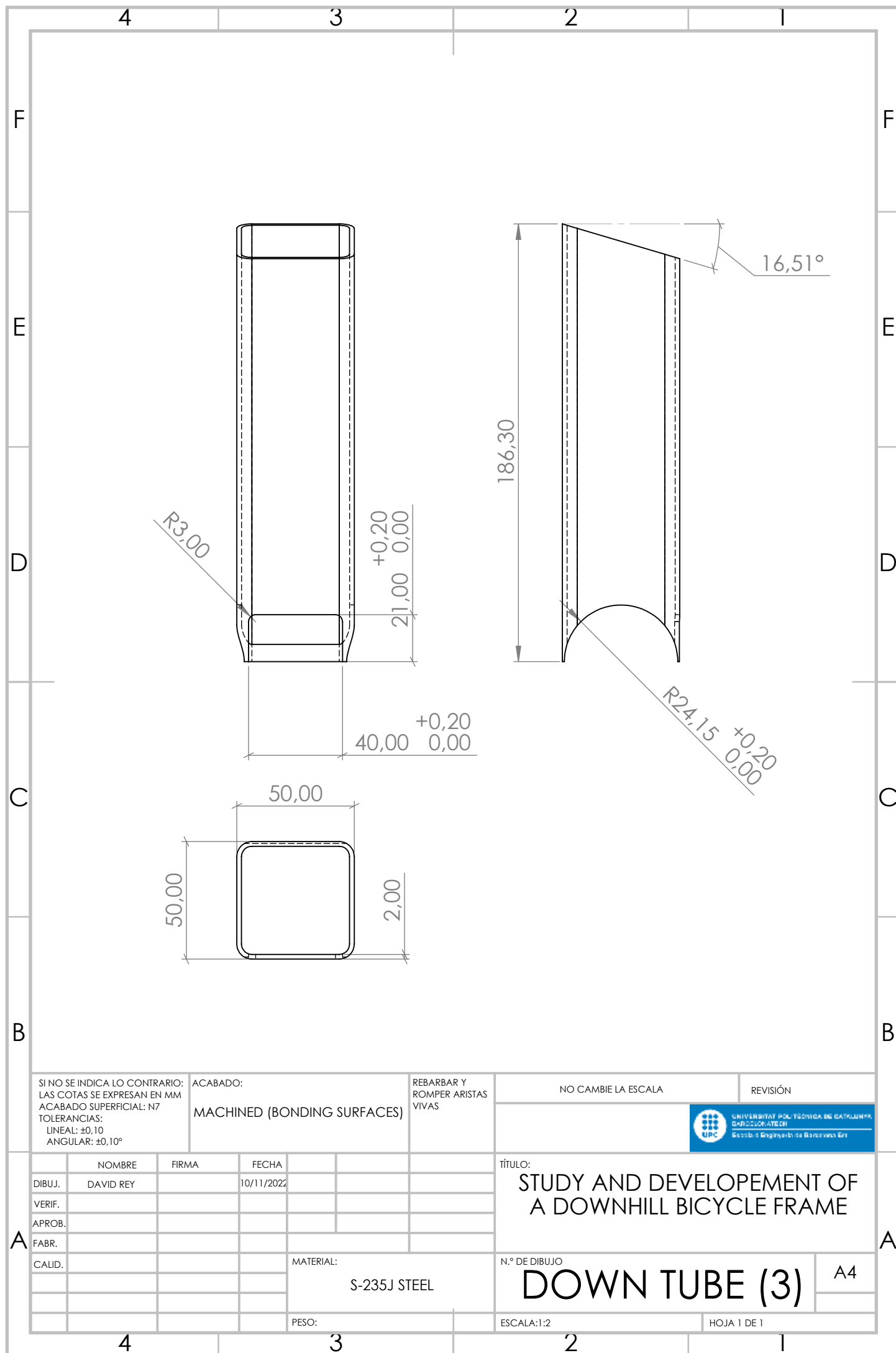
N.º DE DIBUJO

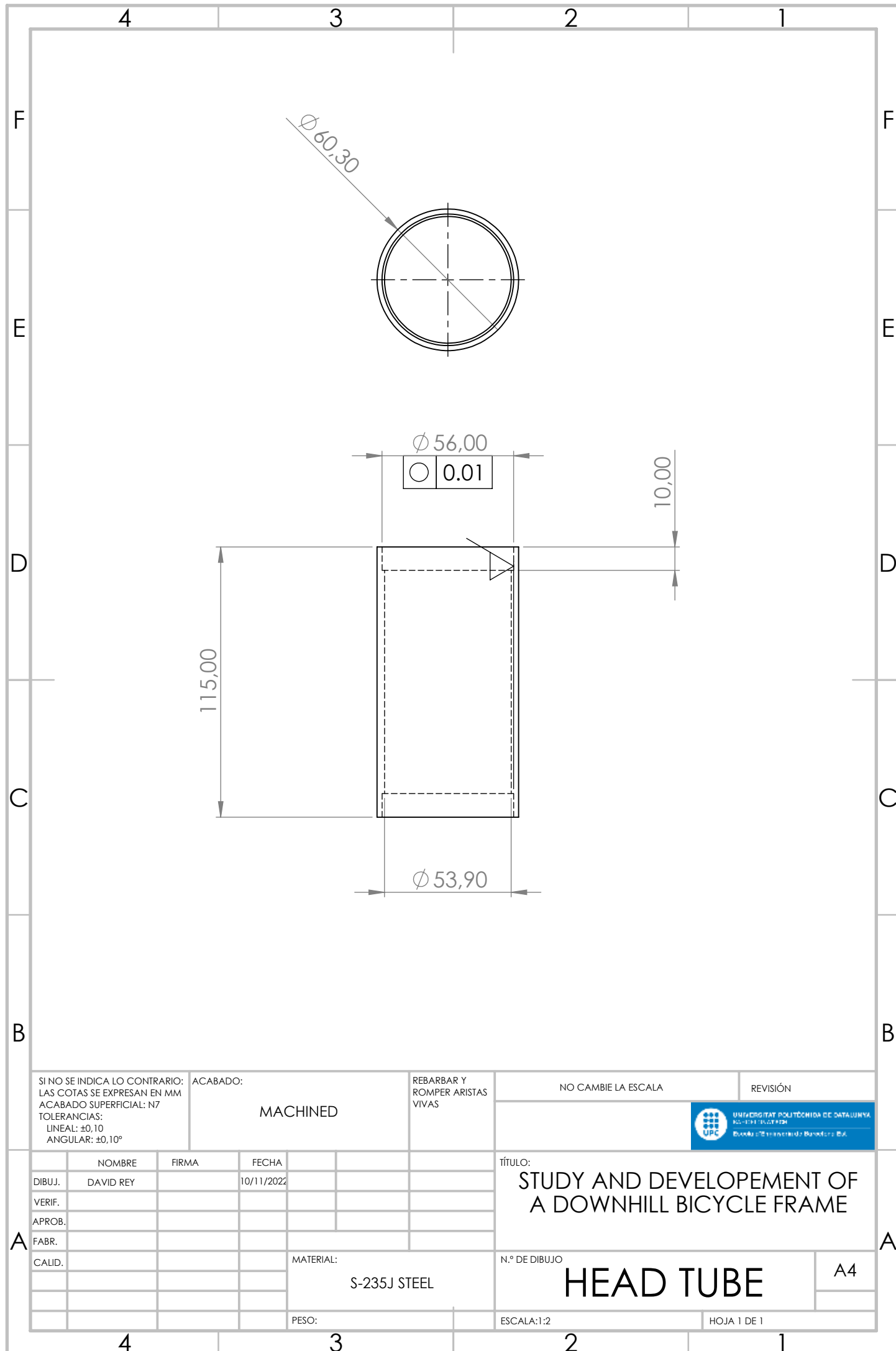
DOWN TUBE (2)

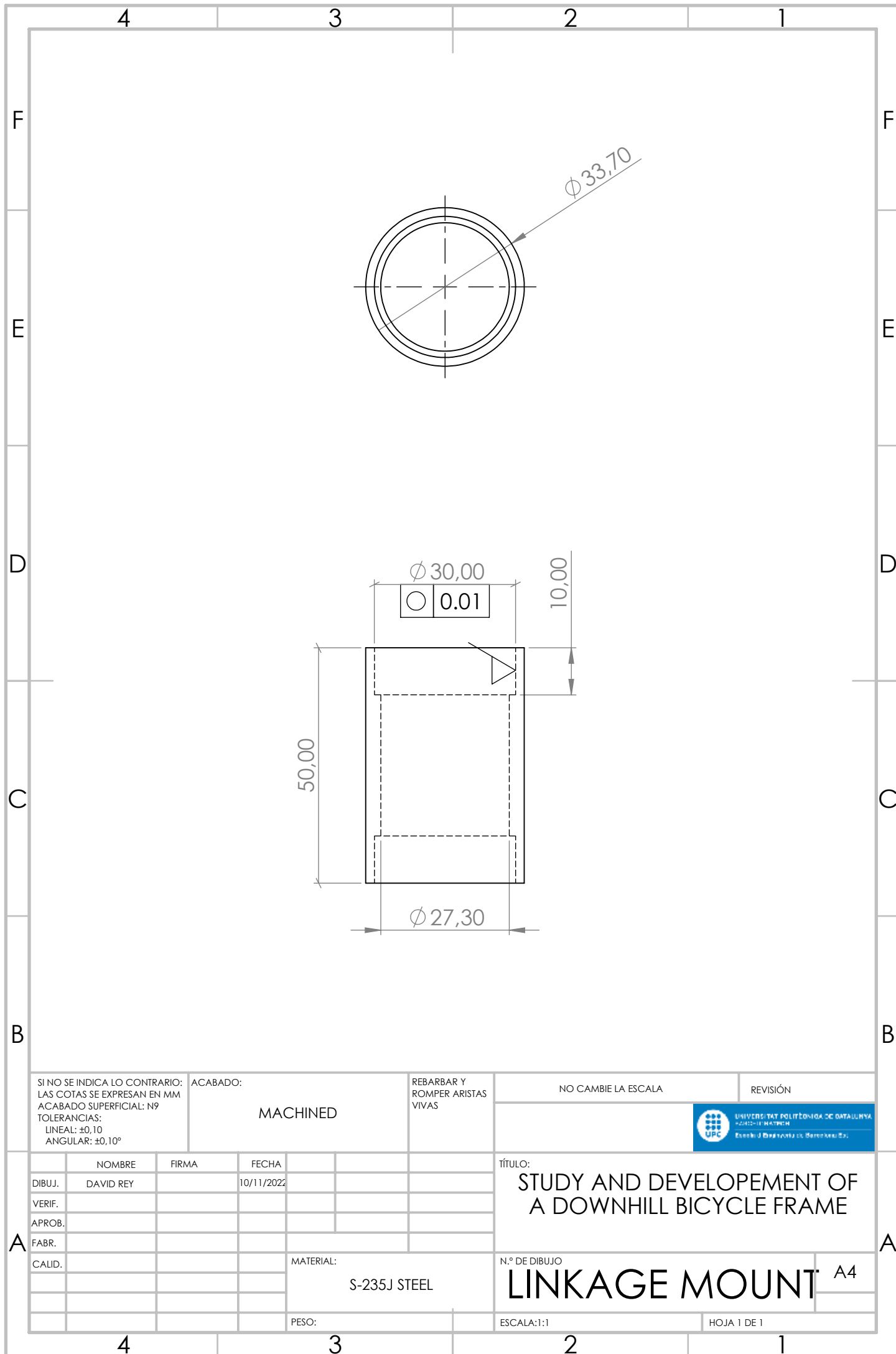
A4


ESCALA:1:5

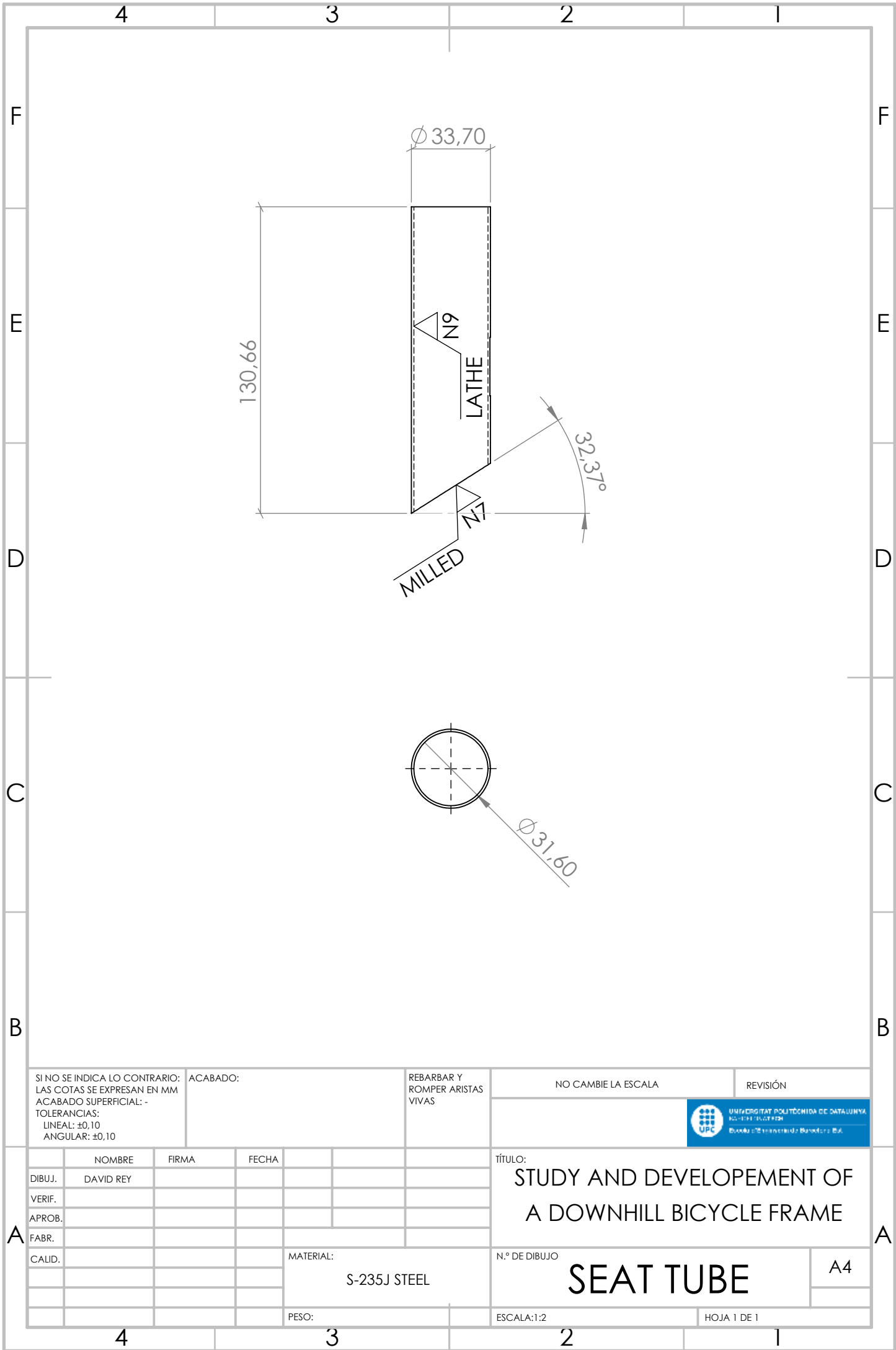
HOJA 1 DE 1




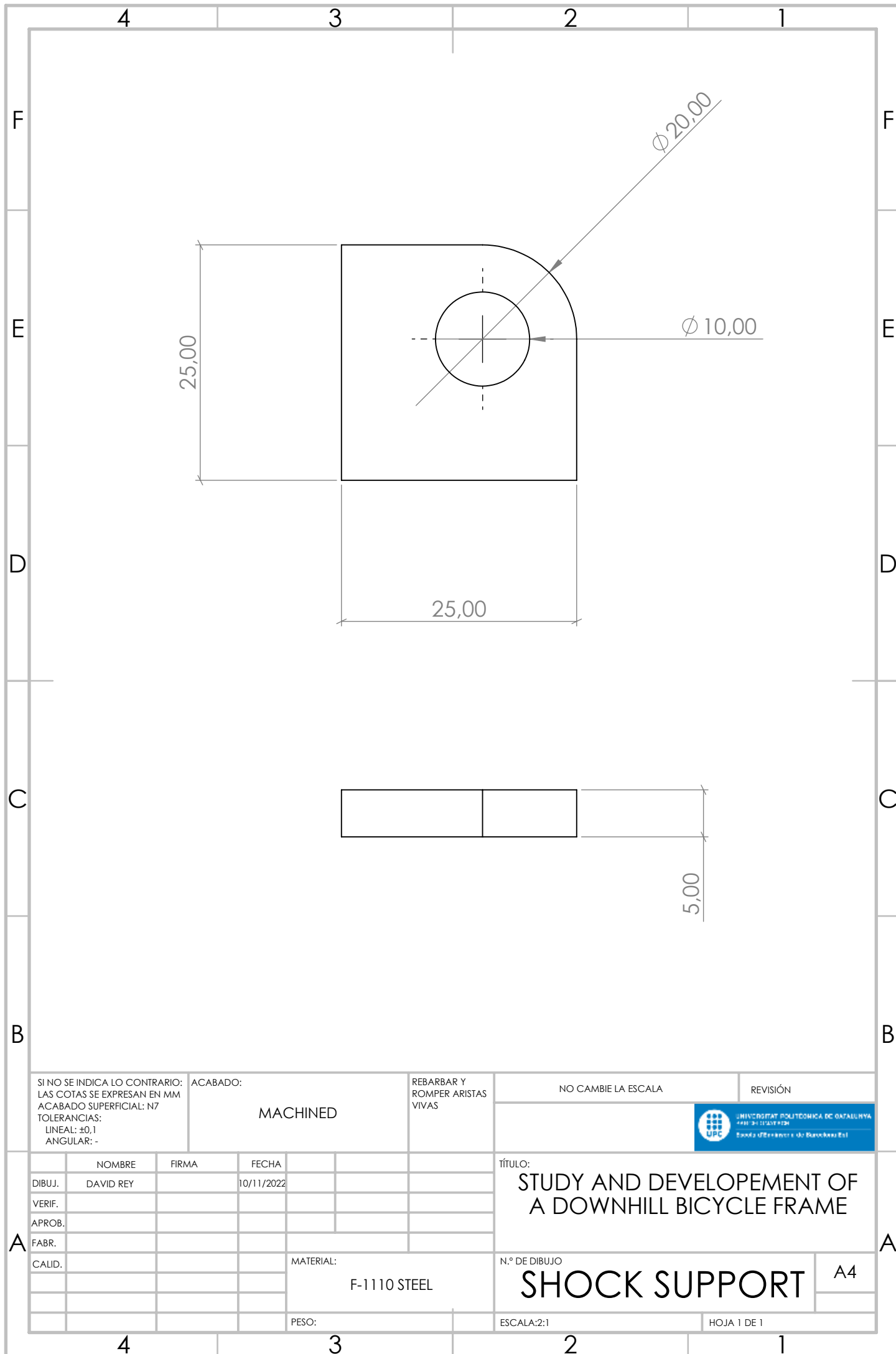





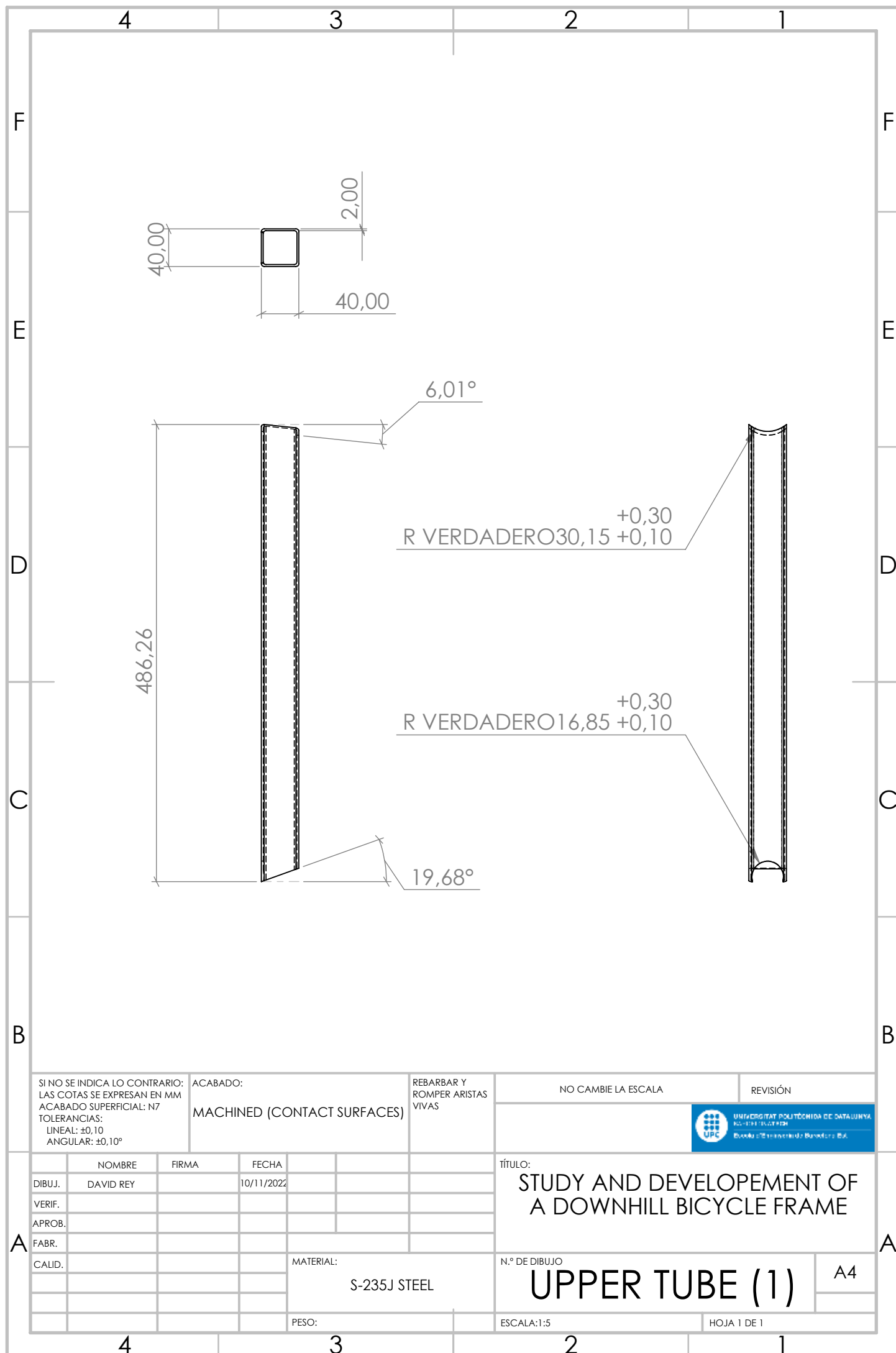
SI NO SE INDICA LO CONTRARIO: LAS COTAS SE EXPRESAN EN MM ACABADO SUPERFICIAL: N9 TOLERANCIAS: LINEAL: $\pm 0,10$ ANGULAR: $\pm 0,10^\circ$		ACABADO: MACHINED		REBARBAR Y ROMPER ARISTAS VIVAS		NO CAMBIE LA ESCALA		REVISIÓN	
								 UNIVERSITAT POLITÈCNICA DE CATALUNYA ADICIONAT TÈCNIC Escola d'Enginyeria de Barcelona Est.	
NOMBRE		FIRMA		FECHA		TÍTULO:			
DIBUJ.		DAVID REY		10/11/2022		STUDY AND DEVELOPEMENT OF A DOWNHILL BICYCLE FRAME			
VERIF.									
APROB.									
FABR.									
CALID.									
						N.º DE DIBUJO			
						LINKAGE MOUNT A4			
						MATERIAL:			
						S-235J STEEL			
						PESO:			
						ESCALA:1:1			
						HOJA 1 DE 1			



SI NO SE INDICA LO CONTRARIO: LAS COTAS SE EXPRESAN EN MM ACABADO SUPERFICIAL: - TOLERANCIAS: LINEAL: ±0,10 ANGULAR: ±0,10				ACABADO:		REBARBAR Y ROMPER ARISTAS VIVAS		NO CAMBIE LA ESCALA		REVISIÓN		
								<div> UNIVERSITAT POLITÈCNICA DE CATALUNYA RS-TECHNICAL Barcelonà 08034 Barcelona, ES</div>				
	NOMBRE		FIRMA		FECHA				TÍTULO: STUDY AND DEVELOPEMENT OF A DOWNHILL BICYCLE FRAME			
DIBUJ.	DAVID REY											
VERIF.												
APROB.												
FABR.												
CALID.												
					MATERIAL:			N.º DE DIBUJO SEAT TUBE			A4	
					S-235J STEEL							
					PESO:			ESCALA:1:2			HOJA 1 DE 1	



SI NO SE INDICA LO CONTRARIO: LAS COTAS SE EXPRESAN EN MM ACABADO SUPERFICIAL: N7 TOLERANCIAS: LINEAL: ±0,1 ANGULAR: -		ACABADO: MACHINED		REBARBAR Y ROMPER ARISTAS VIVAS		NO CAMBIE LA ESCALA		REVISIÓN	
								 UNIVERSITAT POLITÈCNICA DE CATALUNYA FACULTAT D'ENGINYERIA ENGINYERIA DE DISENY I DISENY DE PRODUCTES	
						TÍTULO:			
						STUDY AND DEVELOPEMENT OF A DOWNHILL BICYCLE FRAME			
						N.º DE DIBUJO			
						SHOCK SUPPORT			
						A4			
						ESCALA:2:1			
						HOJA 1 DE 1			



SI NO SE INDICA LO CONTRARIO:
LAS COTAS SE EXPRESAN EN MM
ACABADO SUPERFICIAL: N7
TOLERANCIAS:
LINEAL: $\pm 0,10$
ANGULAR: $\pm 0,10^\circ$

ACABADO:
MACHINED (CONTACT SURFACES)

REBARBAR Y
ROMPER ARISTAS
VIVAS

NO CAMBIE LA ESCALA

REVISIÓN



UNIVERSITAT POLITÈCNICA DE CATALUNYA
BARCELONA

Barrada de Transmissió de Bases de D.A.

	NOMBRE	FIRMA	FECHA		
DIBUJ.	DAVID REY		10/11/2022		
VERIF.					
APROB.					
FABR.					
CALID.					

MATERIAL:
S-235J STEEL

PESO:

TÍTULO:
STUDY AND DEVELOPEMENT OF
A DOWNHILL BICYCLE FRAME

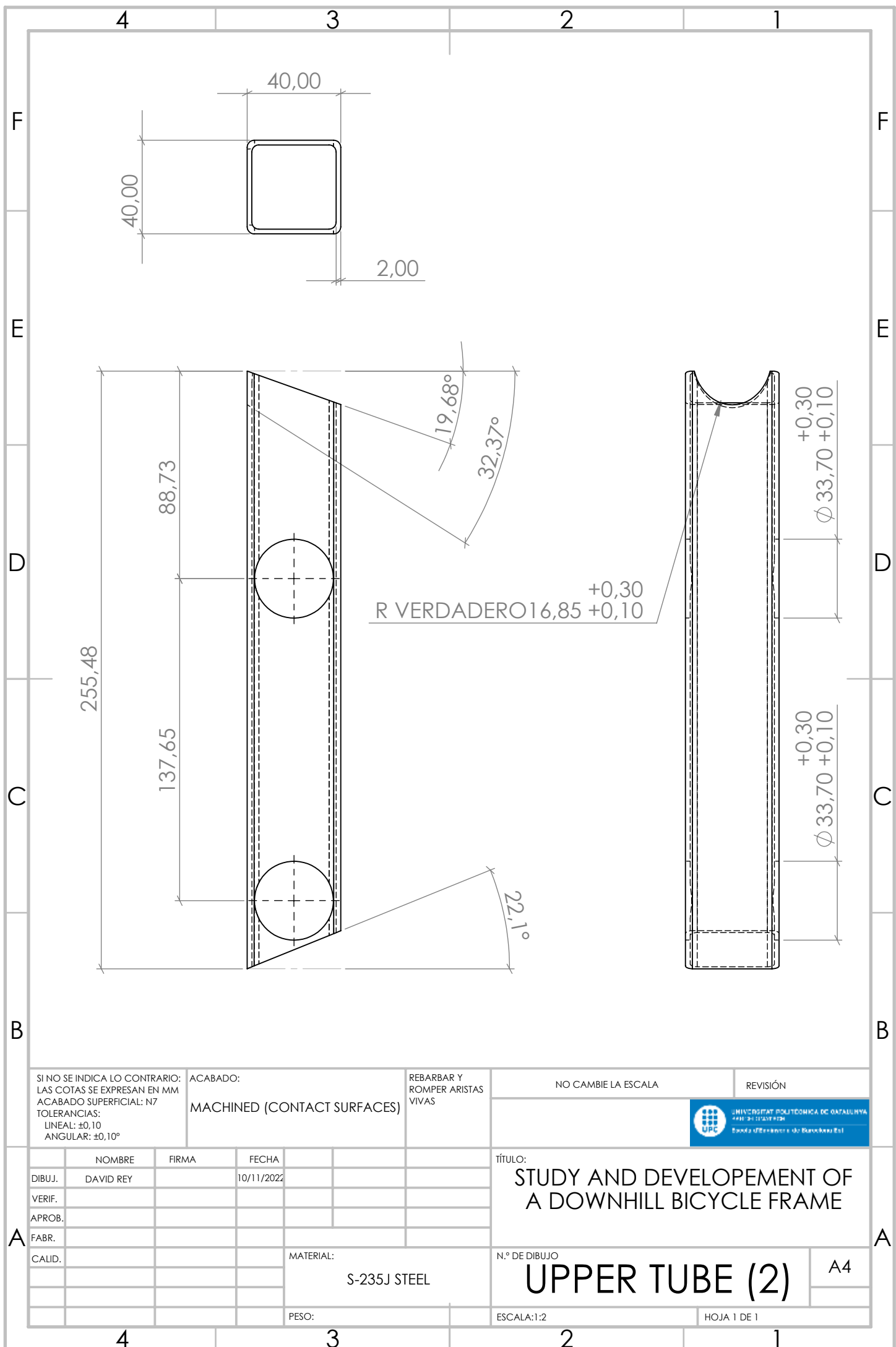
N.º DE DIBUJO

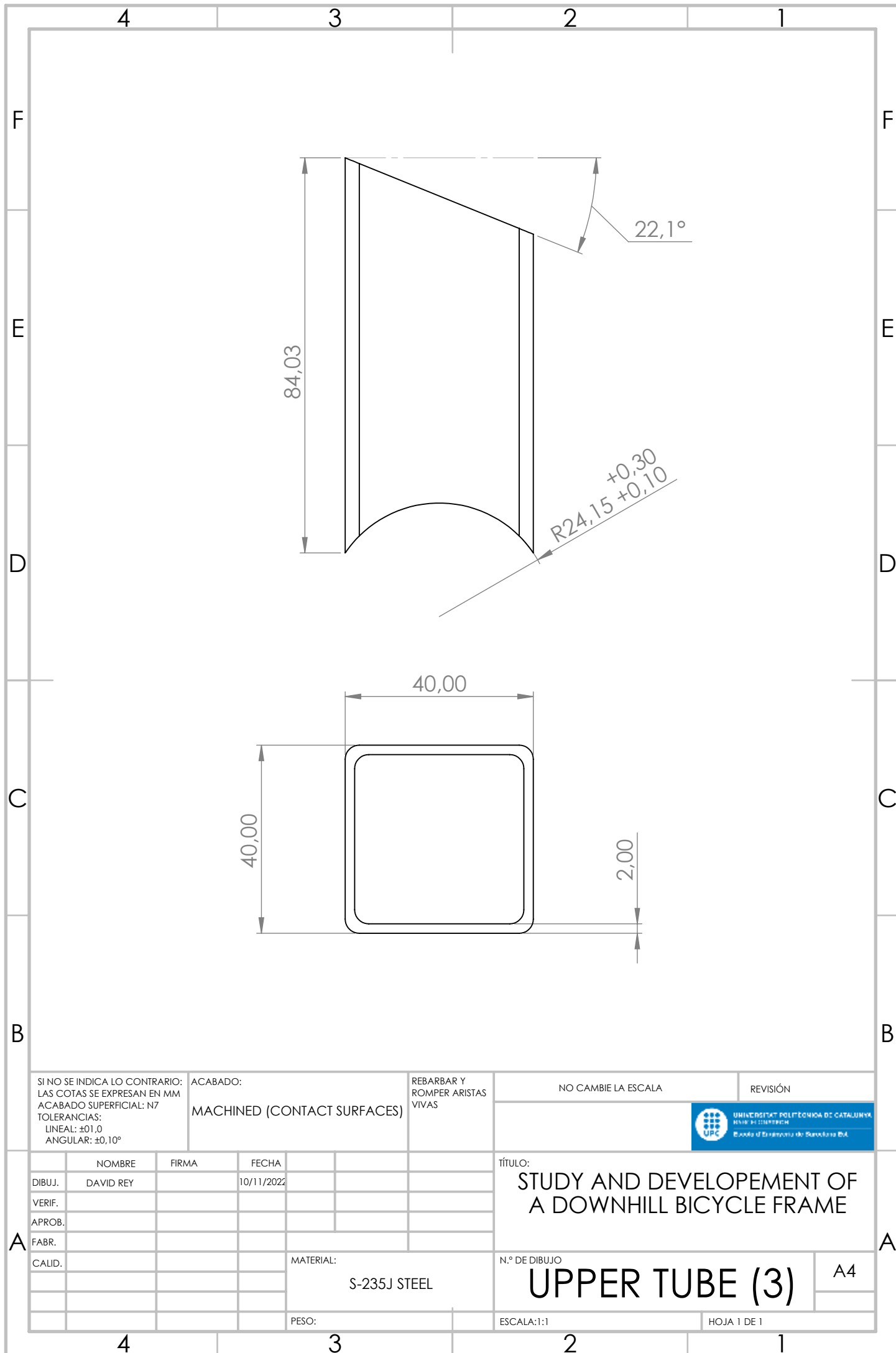
UPPER TUBE (1)

A4

ESCALA:1:5

HOJA 1 DE 1





SI NO SE INDICA LO CONTRARIO:
LAS COTAS SE EXPRESAN EN MM
ACABADO SUPERFICIAL: N7
TOLERANCIAS:
LINEAL: $\pm 0,10$
ANGULAR: $\pm 0,10^\circ$

ACABADO:
MACHINED (CONTACT SURFACES)

REBARBAR Y
ROMPER ARISTAS
VIVAS

NO CAMBIE LA ESCALA

REVISIÓN



	NOMBRE	FIRMA	FECHA		
DIBUJ.	DAVID REY		10/11/2022		
VERIF.					
APROB.					
FABR.					
CALID.					

MATERIAL:
S-235J STEEL

PESO:

TÍTULO:
STUDY AND DEVELOPEMENT OF
A DOWNHILL BICYCLE FRAME

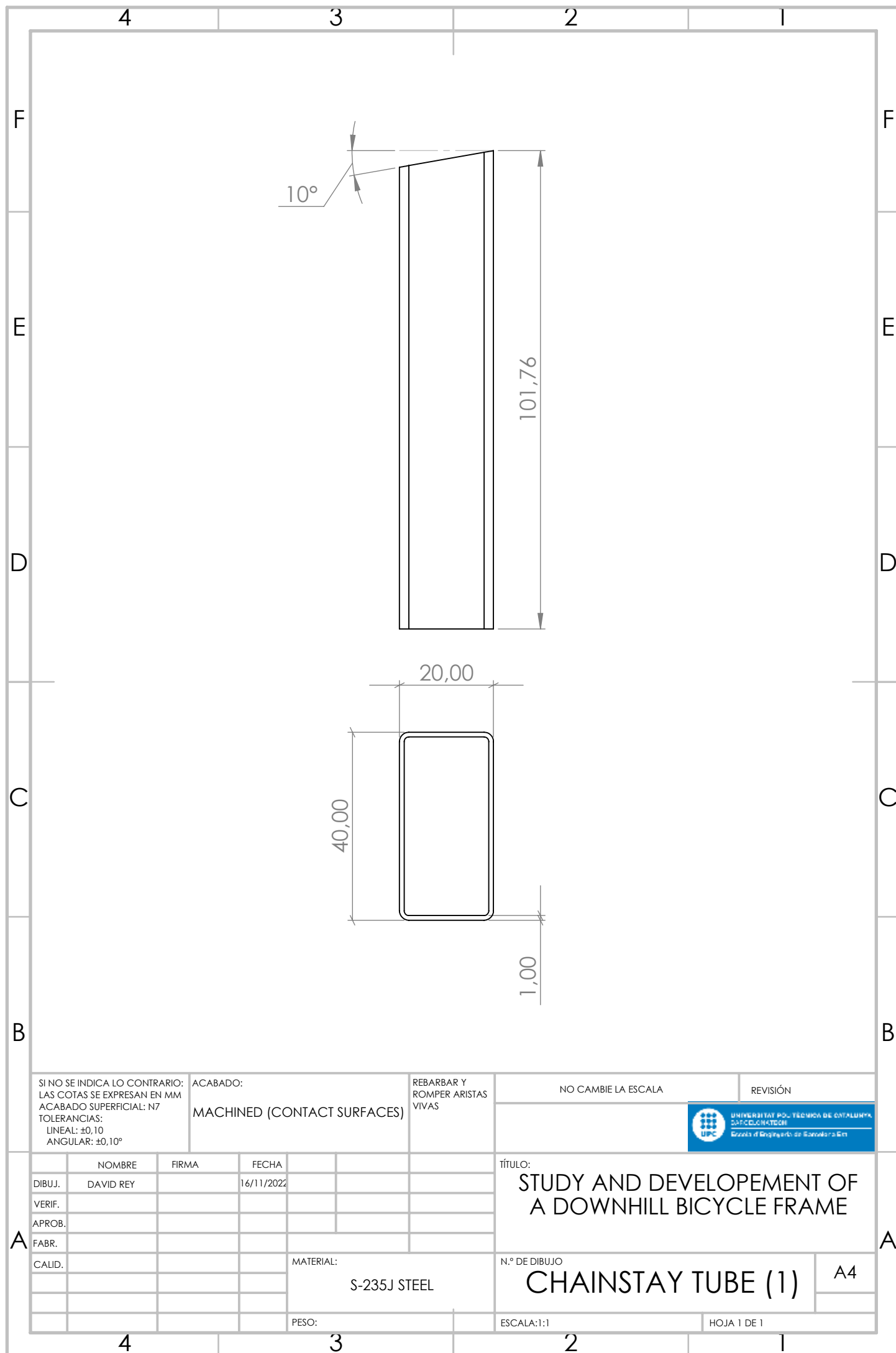
N.º DE DIBUJO

UPPER TUBE (3)

A4

ESCALA:1:1

HOJA 1 DE 1



SI NO SE INDICA LO CONTRARIO:
LAS COTAS SE EXPRESAN EN MM
ACABADO SUPERFICIAL: N7
TOLERANCIAS:
LINEAL: $\pm 0,10$
ANGULAR: $\pm 0,10^\circ$

ACABADO:
MACHINED (CONTACT SURFACES)

REBARBAR Y
ROMPER ARISTAS
VIVAS

NO CAMBIE LA ESCALA

REVISIÓN



	NOMBRE	FIRMA	FECHA		
DIBUJ.	DAVID REY		16/11/2022		
VERIF.					
APROB.					
FABR.					
CALID.					

MATERIAL:
S-235J STEEL

PESO:

TÍTULO:
STUDY AND DEVELOPEMENT OF
A DOWNHILL BICYCLE FRAME

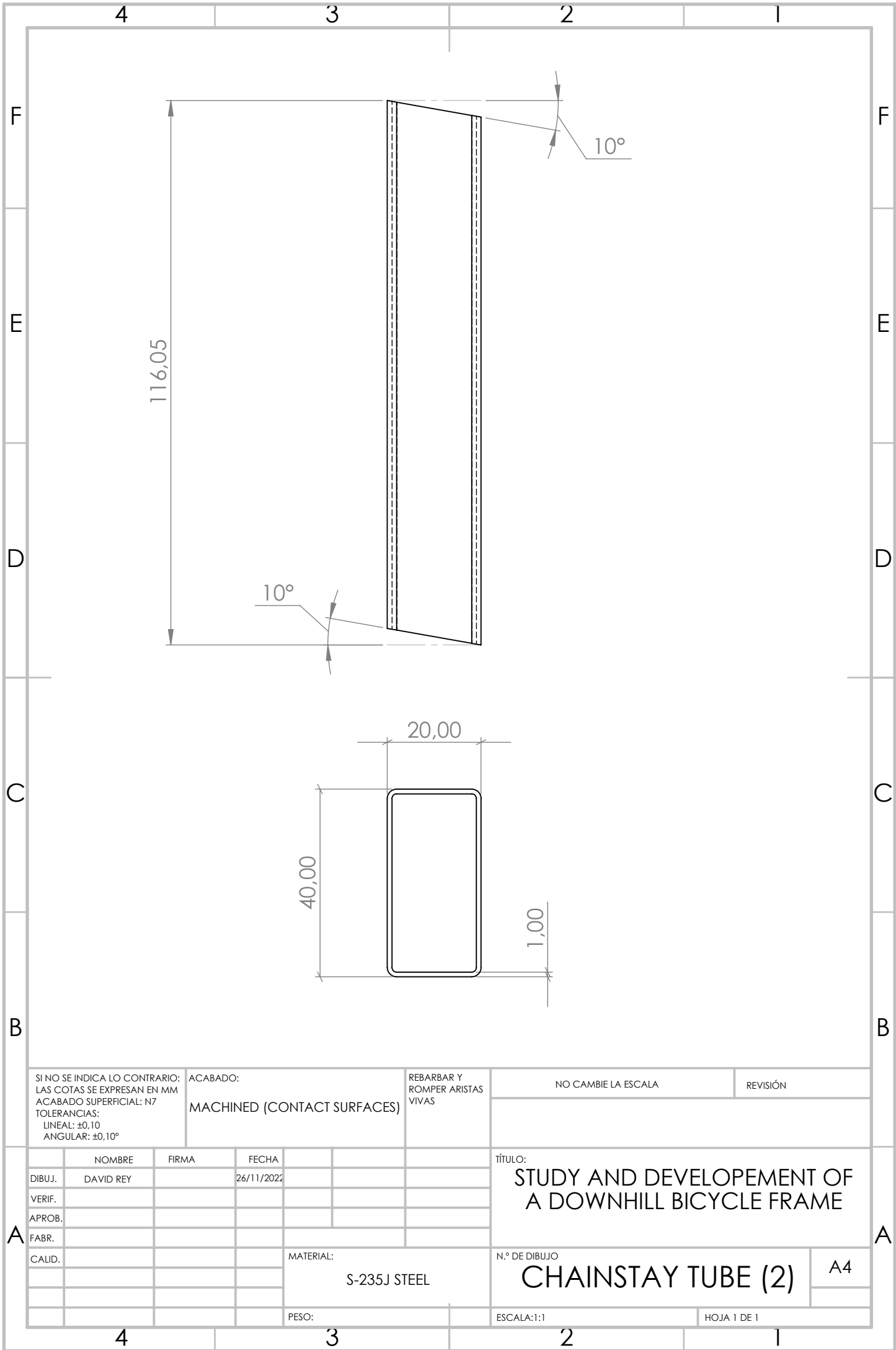
N.º DE DIBUJO

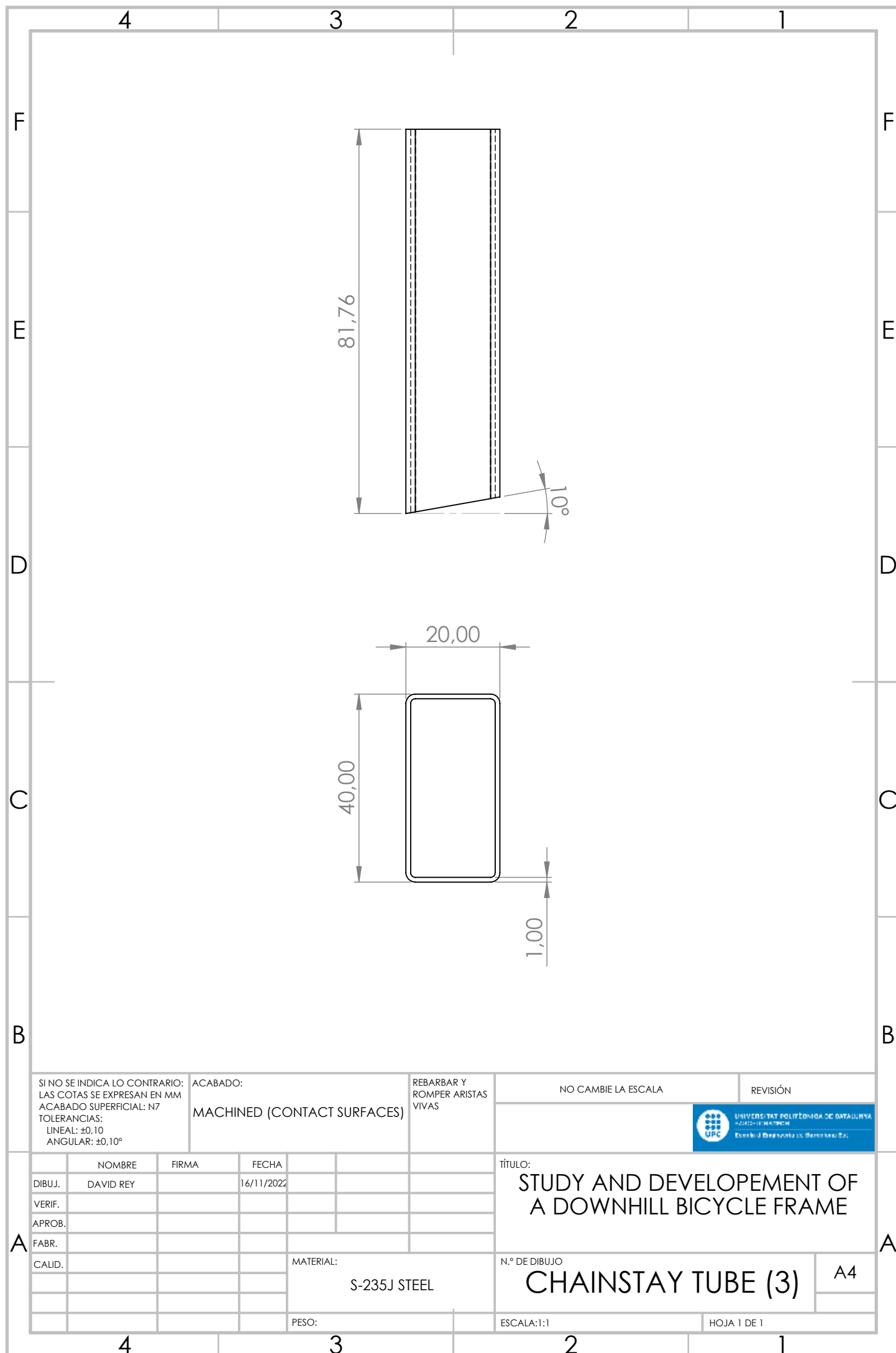
CHAINSTAY TUBE (1)

A4

ESCALA:1:1

HOJA 1 DE 1





SI NO SE INDICA LO CONTRARIO:
LAS COTAS SE EXPRESAN EN MM
ACABADO SUPERFICIAL: N7
TOLERANCIAS:
LINEAL: $\pm 0,10$
ANGULAR: $\pm 0,10^\circ$

ACABADO:
MACHINED (CONTACT SURFACES)

REBARBAR Y
ROMPER ARISTAS
VIVAS

NO CAMBIE LA ESCALA

REVISIÓN



	NOMBRE	FIRMA	FECHA		
DIBUJ.	DAVID REY		16/11/2022		
VERIF.					
APROB.					
FABR.					
CALID.					

MATERIAL:
S-235J STEEL

PESO:

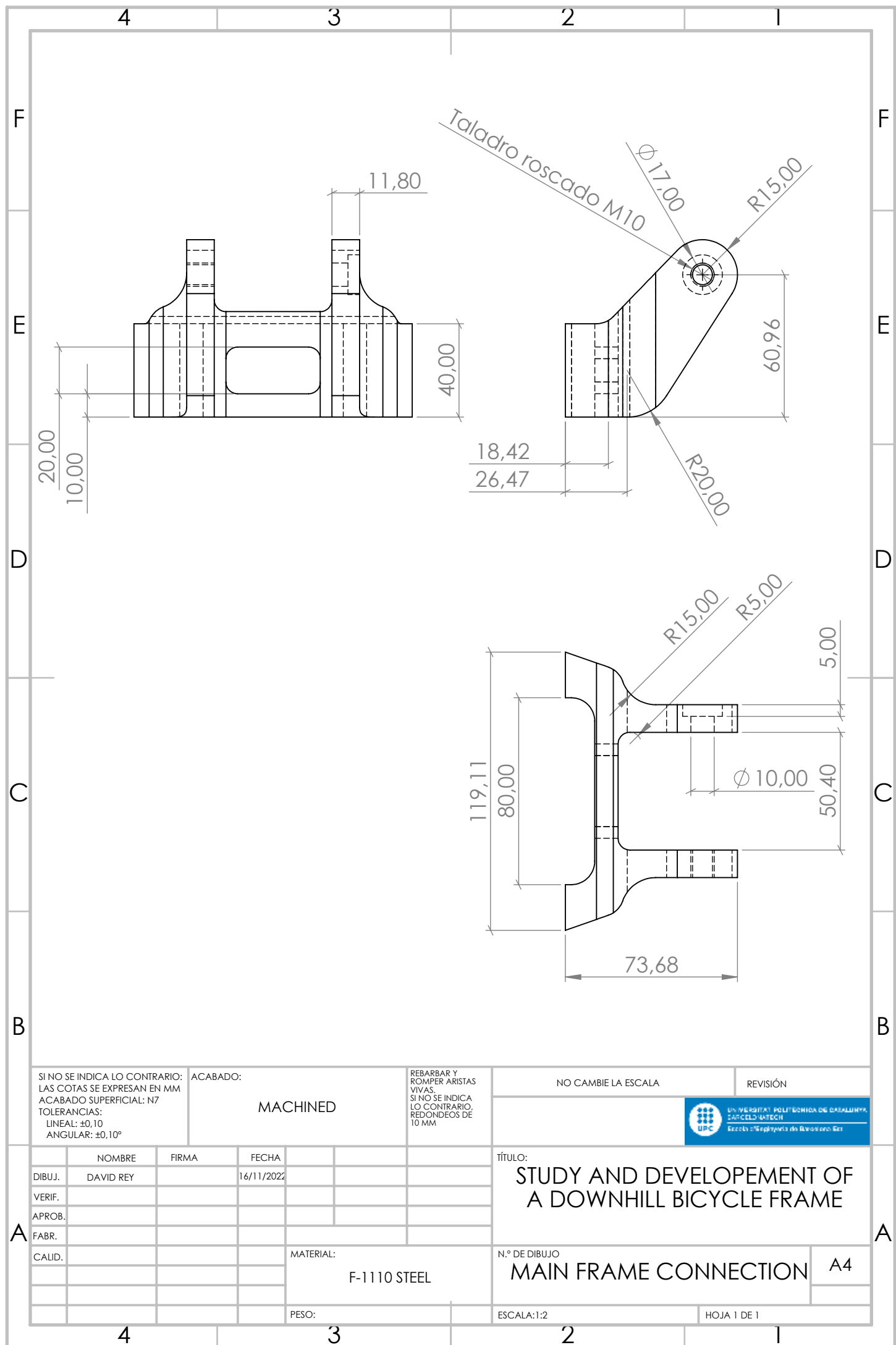
TÍTULO:
STUDY AND DEVELOPEMENT OF
A DOWNHILL BICYCLE FRAME

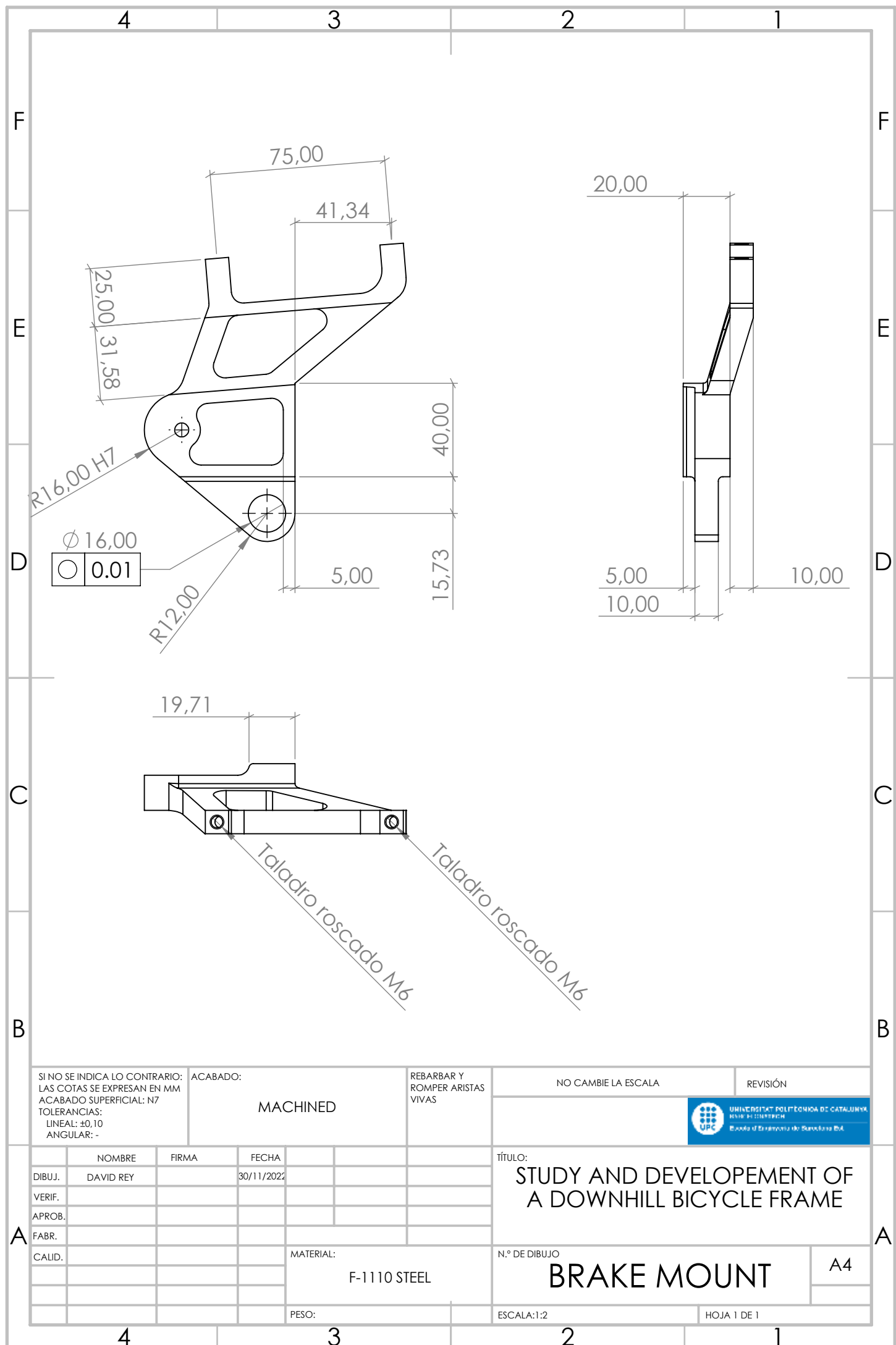
N.º DE DIBUJO
CHAINSTAY TUBE (3)

A4

ESCALA:1:1

HOJA 1 DE 1





SI NO SE INDICA LO CONTRARIO:
LAS COTAS SE EXPRESAN EN MM
ACABADO SUPERFICIAL: N7
TOLERANCIAS:
LINEAL: $\pm 0,10$
ANGULAR: -

ACABADO:

MACHINED

REBARBAR Y
ROMPER ARISTAS
VIVAS

NO CAMBIE LA ESCALA

REVISIÓN



UNIVERSITAT POLITÈCNICA DE CATALUNYA
BARCELONA
Escuela de Ingeniería de Barcelona IBEL

	NOMBRE	FIRMA	FECHA	
DIBUJ.	DAVID REY		30/11/2022	
VERIF.				
APROB.				
FABR.				
CALID.				

MATERIAL:

F-1110 STEEL

PESO:

TÍTULO:

STUDY AND DEVELOPEMENT OF
A DOWNHILL BICYCLE FRAME

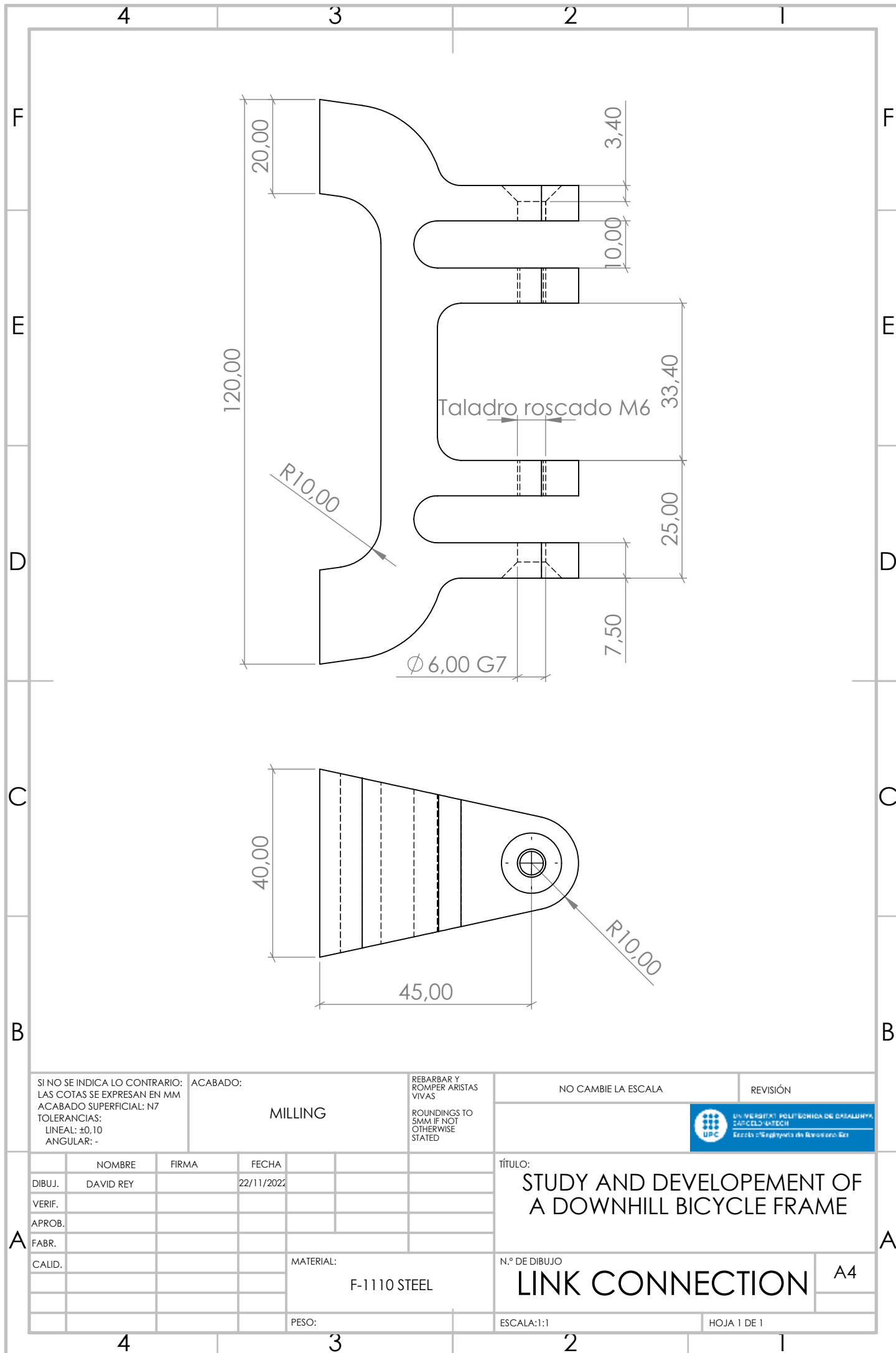
N.º DE DIBUJO


BRAKE MOUNT

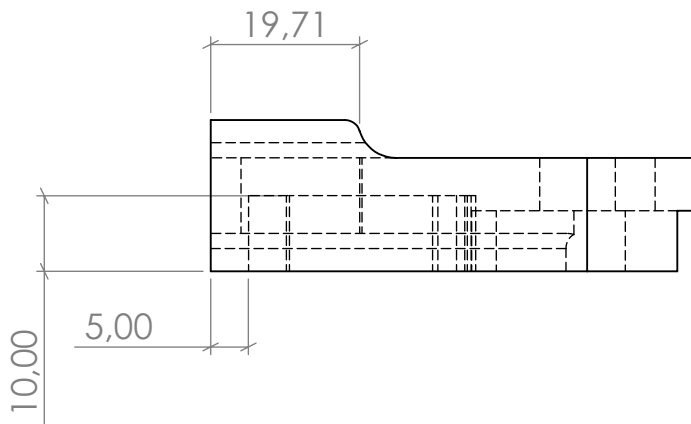
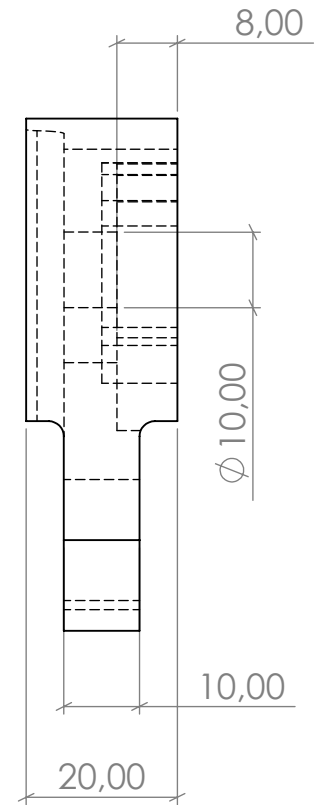
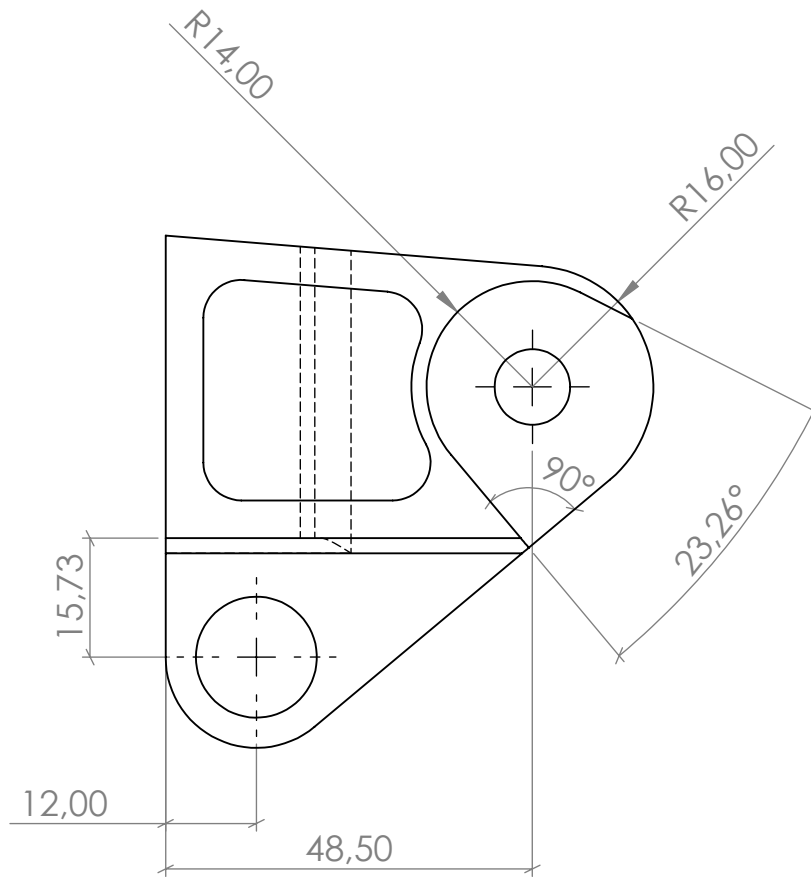
A4

ESCALA:1:2

HOJA 1 DE 1



SI NO SE INDICA LO CONTRARIO: LAS COTAS SE EXPRESAN EN MM ACABADO SUPERFICIAL: N7 TOLERANCIAS: LINEAL: ±0,10 ANGULAR: -		ACABADO: MILLING		REBARBAR Y ROMPER ARISTAS VIVAS ROUNDINGS TO 5MM IF NOT OTHERWISE STATED		NO CAMBIE LA ESCALA		REVISIÓN	
								 UNIVERSITAT POLITÈCNICA DE CATALUNYA BARCELONA TECH Escuela d'Enginyeria de Barcelona Est	
NOMBRE		FIRMA		FECHA		TÍTULO:			
DIBUJ.		DAVID REY		22/11/2022		STUDY AND DEVELOPEMENT OF A DOWNHILL BICYCLE FRAME			
VERIF.									
APROB.									
FABR.									
CALID.									
						N.º DE DIBUJO			
						LINK CONNECTION			
						A4			
						ESCALA:1:1			
						HOJA 1 DE 1			



SI NO SE INDICA LO CONTRARIO:
LAS COTAS SE EXPRESAN EN MM
ACABADO SUPERFICIAL: N7
TOLERANCIAS:
LINEAL: $\pm 0,10$
ANGULAR: $\pm 0,10^\circ$

ACABADO:

MILLING

REBARBAR Y
ROMPER ARISTAS
VIVAS

NO CAMBIE LA ESCALA

REVISIÓN



	NOMBRE	FIRMA	FECHA
DIBUJ.	DAVID REY		22/11/2022
VERIF.			
APROB.			
FABR.			
CALID.			

MATERIAL:

F-1110 STEEL

PESO:

TÍTULO:

STUDY AND DEVELOPEMENT OF
A DOWNHILL BICYCLE FRAME

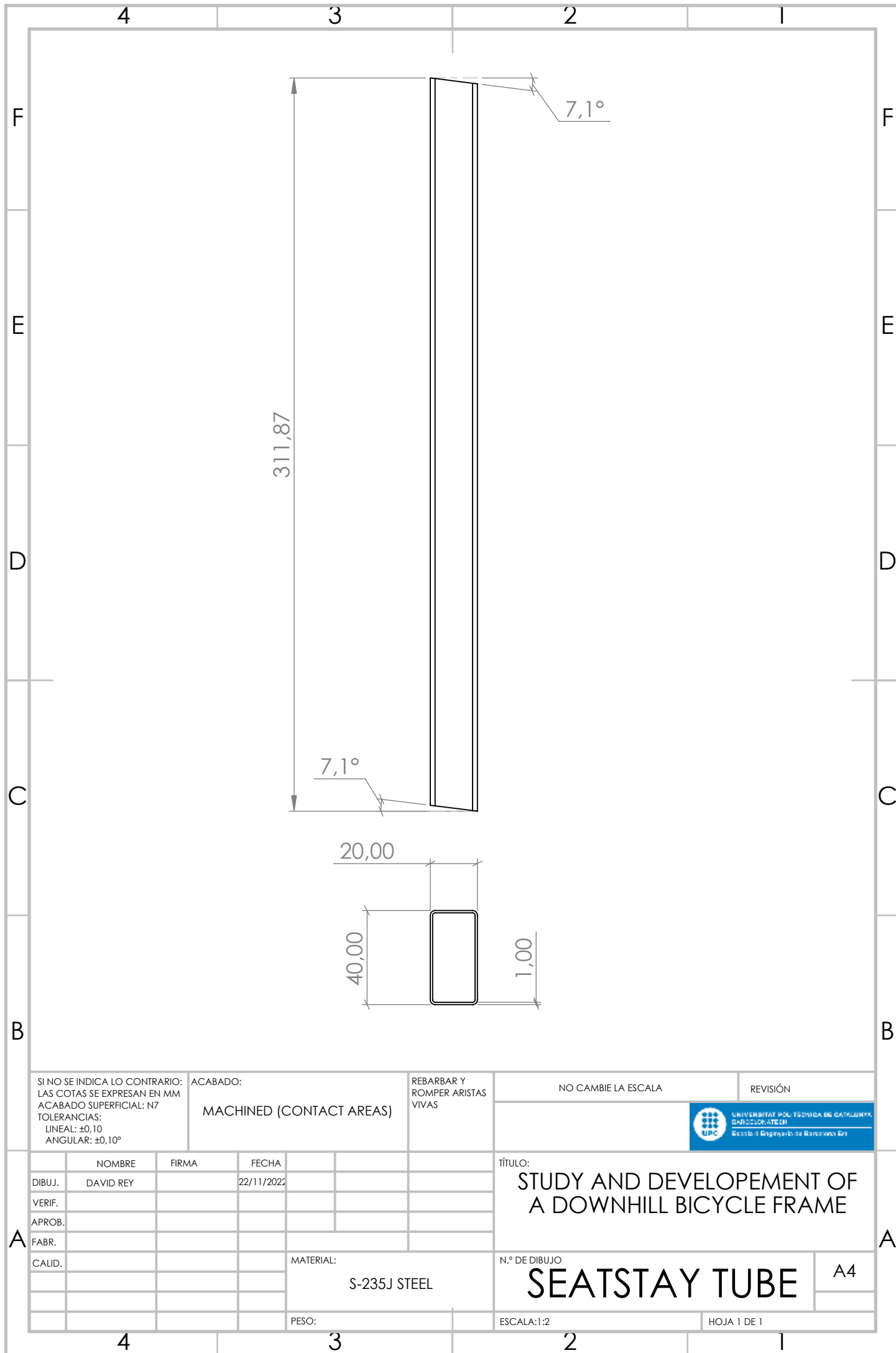
N.º DE DIBUJO

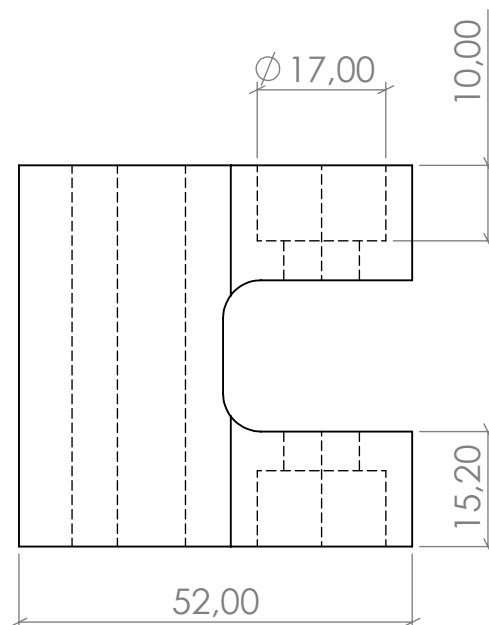
MECH HANGER MOUNT


A4

ESCALA:1:1

HOJA 1 DE 1





SI NO SE INDICA LO CONTRARIO: LAS COTAS SE EXPRESAN EN MM ACABADO SUPERFICIAL: N7 TOLERANCIAS: LINEAL: ±0,10 ANGULAR: -				ACABADO: MACHINED				REBARBAR Y ROMPER ARISTAS VIVAS				NO CAMBIE LA ESCALA				REVISIÓN							
												 UNIVERSITAT POLITECNICA DE CATALUNYA BARCELONA-ATEM Escola d'Enginyeria de Barcelona Est											
												TÍTULO:											
												STUDY AND DEVELOPEMENT OF A DOWNHILL BICYCLE FRAME											
DIBUJ.				DAVID REY				22/11/2022															
VERIF.																							
APROB.																							
FABR.																							
CALID.																							
												MATERIAL:											
												5083 ALUMINUM ALLOY											
												PESO:											
												ESCALA:1:1											
												HOJA 1 DE 1											
												N.º DE DIBUJO											
												LINK REINFORCEMENT											
												A4											

